A Genomic Screen for the Identification of Novel Components of the S-phase Checkpoint

Emma Bowen

PhD Thesis

Department of Biomedical Science

Supervisor Prof. Carl Smythe

September 2014

Abstract

Checkpoints function to help cells to cope with DNA damage by activating a range of mechanisms preventing cell death and genome instability. The S-phase checkpoint, activated by replication stress or DNA damage, inhibits origin firing, stabilises the replisome, prevents mitosis and degrades histone mRNA. Identification of the components involved in the S-phase checkpoint has the potential to identify novel tumour suppressor genes, as well as potential novel targets for the development of new therapeutics. Such therapeutics might be expected to act as sensitisers by preventing cancer cells mounting a successful response to DNA damage and replication stress, and thus lead to their destruction.

In this work I sought to identify novel components of the S-phase checkpoint using RNAi screening. In order to perform a genome-wide screen, a robust, reproducible assay was required in which knockdown of known components of the checkpoint gave a positive result. Initial work in *Drosophila* S2R+ cells showed that responses to the S-phase checkpoint were conserved in these cells but were not robust or long lasting meaning that they couldn't be used in an RNAi screen. Work in human HCT116 cells did show a reliable response and a genome-wide RNAi screen was performed assessing the effectiveness of the S-M checkpoint in this cell line.

After secondary screening of 100 hits from the original screen, four hits were taken forward for further analysis: C12orf66, CCDC149, SCD and S1PR2. Knockdown of these genes was confirmed and their effect on mitotic components assessed. Knockdown of CCDC149 or SCD decreased cyclin B1 and CDK1 levels after checkpoint activation even though they overcame the S-M checkpoint. Knockdown of C12orf66 resulted in prematurely mitotic cells with decreased levels of CDK1. S1PR2 knockdown had no effect on CDK1 or Cyclin B1 but did give rise to some prematurely mitotic cells.

In conclusion I have identified four novel components of the S-phase checkpoint which could potentially be therapeutic targets for cancer.

Table of Contents

Abstract i
Table of Contents ii
List of figures v
List of Tables vi
Abbreviations vii
Acknowledgments ix
1. Introduction 1
1.1 Cell cycle 1
1.2 DNA damage 2
1.3 Replication stress 2
1.4 DNA damage response 3
1.4.1 Cancer and the DDR 4
1.4.2 Key DDR components 5
1.4.2.1 ATR and CHK1 5
1.4.2.2 ATM and CHK2 7
1.4.2.3 Cross talk between ATR-CHK1 and ATM-CHK2 pathways 8
1.4.3 G1/S Checkpoint 8
1.4.4 G2/M Checkpoint 10
1.4.5 S-phase Checkpoint 12
1.4.5.1 Inhibition of late origin firing 12
1.4.5.2 Stabilisation of replisome 15
1.4.5.3 S-M Checkpoint 16
1.4.5.4 Histone mRNA decay 19
1.4.6 Checkpoints in *Drosophila* 22
1.5 RNA interference 23
1.5.1 miRNA 23
1.5.2 siRNA 25
1.5.3 Using RNAi Experimentally 25
1.5.4 Genome-wide RNAi screening 26
1.6 Aim 27
2. Materials and Methods 28
2.1 Materials 28
2.1.1 Solutions 28
2.1.2 Primers 28
2.1.3 siRNA 30
2.1.4 High-throughput equipment 31
2.1.5 Graphs and analysis 31
2.2 General Protocols 31
2.2.1 DNA Work 31
2.2.1.1 Processing of Whatman disc 31
2.2.1.2 Transformation 31
2.2.1.3 PCR 32
2.2.1.4 DNA extraction and purification 32
2.2.1.5 Agarose Gel 32
2.2.1.6 Restriction digest 32
2.2.1.7 Ligation 33
2.2.1.8 DNA sequencing 33
2.2.2 RNA Work 33
2.2.2.1 RNA extraction 33
2.2.2.2 DNaseI treatment 33
2.2.2.3 Reverse transcription 34
2.2.2.4 QPCR 34

2.2.2.5 Analysis of QPCR....34
2.2.2.6 Synthesis of dsRNA....35
2.2.3 Cell Culture....35
2.2.3.1 Growth conditions....35
2.2.3.2 Addition of chemicals....36
2.2.3.3 Transfection of S2R+ cells with dsRNA....36
2.2.3.4 Transfection of S2R+ cells with plasmid DNA....37
2.2.3.5 Transfection of HCT116 cells with siRNA....37
2.2.4 Protein extraction and Analysis....37
2.2.4.1 S2R+ cell lysis....37
2.2.4.2 HCT116 cell lysis....37
2.2.4.3 SDS-PAGE....38
2.2.4.4 Western Blotting....38
2.2.4.5 Luciferase assay....39
2.2.5 Imaging cells....40
2.2.5.1 Imaging cells on microscope slide....40
2.2.5.2 Imaging cells on 384-well plate....40
2.2.5.3 Analysis of images on 384-well plate....40
2.2.6 Analysis of high-throughput data....40
2.2.6.1 Normalisation of screen data....40
2.2.6.2 Analysis of protein interactions....41
2.3 Experiment protocols....41
2.3.1 Histone mRNA decay assay....41
2.3.2 Creation of Ren-PEST-UTR and Ren-PEST-CON....41
2.3.3 Measuring the half-life of Renilla....42
2.3.4 Dual-pulse replication assay....42
2.3.4.1 Microscope slide format....42
2.3.4.2 384-well plate format....43
2.3.5 S-M Checkpoint assay....44
2.3.5.1 In S2R+ cells....44
2.3.5.2 In Human cells....44
2.3.6 Flow cytometry to identify premature mitosis....45
3. Histone mRNA decay in *Drosophila* cells....47
3.1 Introduction....47
3.2 Results....47
3.2.1 Histone mRNA decay....47
3.2.2 Creation of destabilised luciferase histone mRNA reporter....49
3.2.3 Luciferase mRNA decay....50
3.2.4 Luciferase protein levels and activity....50
3.3 Conclusions....54
4. Other S-phase checkpoint responses in *Drosophila* cells....57
4.1 Introduction....57
4.2 Results....58
4.2.1 Dual Pulse replication assay in S2R+ cells....58
4.2.1.1 Replication Patterns in S2R+ cells....58
4.2.1.2 S-phase checkpoint replication effects in S2R+ cells....60
4.2.1.3 Inhibiting the S-phase checkpoint in S2R+ cells....62
4.2.2 S-M checkpoint in S2R+ cells....65
4.3 Conclusions....67
5. S-M checkpoint assay optimisation in a human cell line....69
5.1 Introduction....69
5.2 Results....69
5.2.1 S-M checkpoint in human cell lines....69
5.2.2 Optimisation of conditions for screening....71

5.2.3 Assay Plate 74
5.2.4 Kinome-Phosphatome screen 77
5.3 Conclusions 80
6. Genome-wide screening and Secondary screening 83
6.1 Introduction 83
6.2 Results 83
6.2.1 Genome-wide screening 83
6.2.2 Hits 86
6.2.3 Secondary screening 86
6.2.3.1 HU secondary screen 90
6.2.3.2 Aph secondary screen 93
6.2.3.3 No replication stress secondary screen 93
6.2.3.4 Conclusions from the secondary screens 94
6.3 Conclusions 94
7. Validation of hits 100
7.1 Introduction 100
7.2 Results 101
7.2.1 Confirmation of knockdown 101
7.2.2 Deconvolution of siRNAs 101
7.2.3 Further investigation of role of hits in S-M checkpoint 107
7.2.3.1 Premature mitosis 107
7.2.3.2 CDK1 and Cyclin B1 110
7.3 Conclusions 113
8. Discussion and Future Perspectives 115
8.1 Introduction 115
8.2 How do *Drosophila* culture cells survive with a weak checkpoint? 115
8.3 Mitotic regulation 117
8.3.1 How do cells enter mitosis with high CDK1 phosphorylation? 117
8.3.2 How do cells enter mitosis with low cyclin B1 levels? 118
8.3.3 How does knockdown of CCDC149 or SCD decrease cyclin B1 levels? 119
8.3.4 How do cells enter mitosis with low CDK1 levels? 119
8.3.5 How does knockdown of CCDC149, SCD or C12orf66 decrease CDK1 levels? 120
8.4 What function are the hits playing in the S-phase checkpoint? 121
8.4.1 C12orf66 121
8.4.2 CCDC149 122
8.4.3 SCD 123
8.4.4 S1PR2 123
8.5 What other information can be obtained from the genome-wide RNAi screening data? 124
8.6 Final conclusions 125
9. Bibliography 126

List of figures

Figure 1-1. ATR Activation 6
Figure 1-2. G1/S Checkpoint. 9
Figure 1-3. G2/M Checkpoint. 11
Figure 1-4. S-phase Checkpoint. 13
Figure 1-5. S-M checkpoint in different cell types. 18
Figure 1-6. Model of histone mRNA degradation. 21
Figure 1-7. RNAi pathways 24
Figure 3-1. Histone mRNA decay in S2R+ and HeLa cells. 48
Figure 3-2. Strategy for the creation of Ren-PEST-UTR and Ren-PEST-CON. 51
Figure 3-3. Renilla luciferase is destabilised by the addition of a PEST sequence 52
Figure 3-4. Addition of the stem-loop causes replication dependent decay of Renilla mRNA 53
Figure 3-5. Addition of the stem-loop doesn't cause replication dependent decay of Renilla protein or activity. 55
Figure 4-1. Replication patterns in S2R+ cells. 59
Figure 4-2. Replication stress causes stalling of S-phase progression 61
Figure 4-3. Knockdown of Grp has only a slight effect on the replication checkpoint. 63
Figure 4-4. Caffeine doesn't override the replication checkpoint in S2R+ cells. 64
Figure 4-5. S-M checkpoint in S2R+ cells. 66
Figure 5-1. S-M checkpoint in human cell lines. 70
Figure 5-2. Optimisation of S-M checkpoint assay in HCT116 cells. 73
Figure 5-3. Assay plate controls for S-M checkpoint screen. 76
Figure 5-4. Kinome-Phosphatome screen results 79
Figure 6-1. Genome-wide RNAi screen of S-M checkpoint. 85
Figure 6-2. Hits from the genome-wide RNAi screen 89
Figure 6-3. Secondary screening 92
Figure 6-4. Summary of hits performance in primary and secondary screens. 95
Figure 6-5. Identified components in the S-M checkpoint. 98
Figure 7-1. mRNA levels after hit gene knockdown with pooled siRNA 102
Figure 7-2. mRNA levels after knockdown of hits with deconvolved siRNA 104
Figure 7-3. Protein levels after knockdown of hits. 105
Figure 7-4. Effect of knockdown with deconvolved siRNAs on S-M checkpoint assay 106
Figure 7-5. Effect of knockdown of hits on premature mitosis. 109
Figure 7-6. Knockdown of hits affects CDK1/cyclin B1. 111

List of Tables

Table 2-1. Primers 28
Table 2-2. siRNA 30
Table 2-3. PCR Conditions 32
Table 2-4. dsRNA synthesis 35
Table 2-5. Chemicals added to cells. 36
Table 2-6. Antibodies used in Western blotting. 39
Table 2-7. S-M Checkpoint conditions in HCT116 cells 45
Table 6-1. Genes that crossed the initial threshold and were taken forward for secondary screening. 87
Table 6-2. Genes that crossed the initial threshold but were not taken forward 88
Table 6-3. Weaker hits selected for secondary screening. 91
Table 6-4. Summary of hits from primary and secondary screens 96

Abbreviations

9-1-1 complex	Rad9-Rad1-Hus1 complex
Ago	Argonaute protein
APC/C	Anaphase promoting complex/cyclosome
Aph	Aphidicolin
ATM	Ataxia-telangiectasia mutated
ATR	ATM and Rad3-related
ATRIP	ATR-interacting protein
Bp	Base pair
BrdU	5-bromo-2'-deoxyuridine
C. elegans	*Caenorhabditis elegans*
C12orf66	Chromosome 12 open reading frame 66
CCDC149	Coiled-coil domain containing protein 149
CCT complex	Chaperonin containing TCP complex
CDK	Cyclin-dependent kinase
CHX	Cycloheximide
CldU	5-chloro-2'-deoxyuridine
DDR	DNA damage response
DNA-PK	DNA-activated protein kinase
Drosophila	*Drosophila melanogaster*
DSB	Double strand break
dsRNA	Double-stranded RNA
EMSA	Electrophoretic mobility shift assay
Exo1	Exonuclease 1
G1	Gap phase 1
G2	Gap phase 2
GPCR	G-protein coupled receptor
GSK-3β	Glycogen synthase kinase-3β
HU	Hydroxyurea
IdU	5-iodo-2'-deoxyuridine
IR	Ionising radiation
Kd	Kinase-dead
MAPK	Mitogen-activated protein kinase
MI	Mitotic index
miRISC	miRNA-induced silencing complex
miRNA	Micro RNA
M-phase	Mitosis
MRN complex	Mre11-Rad50-Nbs1 complex
NMD	Nonsense mediated decay
NT	Non-targeting
ORC	Origin recognition complex
OTP	ON-TARGETplus
Phospho	Phosphorylated
Phospho-H3	Phosphorylated histone H3 (S10)
PIKK	Phosphoinositide 3-kinase related kinase

PLK1	Polo-like kinase 1
QPCR	Quantitative PCR
RAN	Ras-related nuclear protein
Rb	Retinoblastoma protein
RNAi	RNA interference
ROS	Reactive oxygen species
RPA	Replication protein A
S	Serine
S1P	Sphingosine-1-phosphate
S1PR2	Sphingosine-1-phosphate receptor 2
SCD	Stearoyl-CoA desaturase
shRNA	Small-hairpin RNA
siRISC	siRNA-induced silencing complex
siRNA	Small interfering RNA
SLBP	Stem-loop binding protein
SMC1	Structural maintenance of chromosome 1
S-phase	DNA synthesis phase
SSB	Single strand break
ssDNA	Single-stranded DNA
T	Threonine
TUTase	Terminal uridyl transferase
UTR	Untranslated region
UV	Ultra-violet
Xenopus	*Xenopus laevis*
Y	Tyrosine

Acknowledgments

Firstly, I would like to thank Carl Smythe for all he has done in supervising me through this project. For constructing the idea of the work, guiding me when I hit rocks and allowing me to take ownership of the project and take it where I wished. I am also very grateful to all the members of the Smythe lab who have supported me with techniques, troubleshooting and tea. Steve Brown and his collegues Amy Taylor, Carly Lynsdale and Lucie Nkoy in the Sheffield RNAi Screening Facility have helped immensely and I would like to thank them too. For making the screen possible and also for their help with assay development and screen analysis. Further thanks goes to David Strutt and Guiseppe Battaglia for their advice and the BBSRC for funding.

I am also very grateful for the support on many friends and family who have listened to problems, prayed with me and reminded me that there is life outside the lab. In particular I am thankful to my parents for their unwavering confidence in me and interest in what I was doing even when they didn't understand it. Finally I want to thank my husband, Chris, for all his support. For putting up with weekends where I was in the lab, rants about cells and frustrations with science. I am grateful for all the love, support and encouragement he has given me.

1. Introduction

As cells progress through the cell cycle, the quality and integrity of the genome needs to be maintained. Fundamental to an organism's survival is the ability of cells to accurately pass on the information content contained in their DNA to daughter cells. If DNA is highly mutated or lost between generations, the daughter cells' survival may be compromised as essential genes may lose function or gain unwanted functions. As DNA can be damaged in multiple ways, cells operate a DNA damage response (DDR) pathway to limit the loss of genome information and protect an organism's survival.

1.1 Cell cycle

The cell cycle is made up of four distinct phases: Gap phase 1 (G1), DNA synthesis phase (S), Gap phase 2 (G2) and mitosis (M). Progression through these phases is highly regulated by cyclins and cyclin-dependent kinases (CDKs). Cyclin levels oscillate throughout the cell cycle and therefore only allow activation of their cognate kinases in precise phases (Alberts et al., 2008). The commitment to duplicate the genome and subsequently to segregate each copy are critical events in the life cycle of a cell, and it is not surprising therefore that complex regulatory mechanisms control these major events.

Mitotic entry is particularly important to regulate due to its irreversible nature and requirement for complex reorganisation of the cell architecture. It is controlled predominantly by CDK1 (also called CDC2) and cyclin B1 (Lee and Nurse, 1987). In mammalian cells, CDK1 is constitutively expressed but cyclin B1 levels rise during S-phase and peak at late G2 (Pines and Hunter, 1989). In order that mitosis is initiated quickly and at the correct time, the CDK1/cyclin B1 complex is kept inactive until the end of G2. This is achieved by two main mechanisms. Firstly, cyclin B1 is excluded from the nucleus as a consequence of efficient export by exportin 1 (Hagting et al., 1998; Pines and Hunter, 1991; Toyoshima et al., 1998). When mitosis is initiated, cyclin B1 is phosphorylated blocking the exportin 1 binding site and CDK1/cyclin B1 accumulates in the nucleus (Li et al., 1995; Yang et al., 2001). Inhibition is also achieved by phosphorylation of CDK1 at threonine (T) 14 (by PKMYT1) and tyrosine (Y) 15 (by WEE1 and PKMYT1) (Gould and Nurse, 1989; Liu et al., 1997; McGowan and Russell, 1993; Norbury et al., 1991). This blocks the ATP-binding site and inhibits CDK1's activity. When mitosis is initiated these inhibitory phosphorylations are

removed by the CDC25 phosphatases and CDK1 is activated (Gautier et al., 1991; Kumagai and Dunphy, 1991; Strausfeld et al., 1991). Multiple feedback mechanisms (including the inhibition of WEE1 and the activation of CDC25 by CDK1; reviewed in Lindqvist et al., 2009) operate in the system ensuring a rapid activation of CDK1.

1.2 DNA damage

The DNA in cells is under constant attack from a range of sources. Normal metabolism produces reactive oxygen species (ROS) which can react with DNA and produce a variety of different lesions. One of the most common is the production of 8-oxoguanine by the reaction of ROS with guanine. This modified base is able to pair with adenine meaning that after replication what was originally a guanine base is substituted with a thymidine (Jena, 2012). This endogenous DNA damage alone has been predicted to occur 100-500 times per day in a human cell (Maynard et al., 2009).

Exogenous agents also damage DNA. Ultra-violet (UV) radiation causes the formation of cyclobutane pyrimidine dimers and 6-4 photoproducts which distort the shape of the DNA helix. This restricts the binding of regulatory proteins to the affected DNA with an impact on transcription and replication (Sinha and Häder, 2002). Ionising radiation (IR) also causes a range of lesions including base damage, single strand breaks (SSBs) and double strand breaks (DSBs)(Lomax et al., 2013). Many chemicals also damage DNA. For example, the mechanisms of action of the anti-cancer drugs cisplatin and bleomycin are dependent on their DNA damaging capability, with the former causing intra- and inter-strand crosslinking, while the latter induces SSBs (Poirier, 2004). The principal mutagenic substance in cigarette smoke, benzo[a]pyrene, is converted into a highly reactive epoxide derivative that creates bulky mutagenic adducts by covalently reacting with the N2 position on guanine (Cheng et al., 1989).

1.3 Replication stress

DNA damage is particularly problematic when cells are undergoing DNA replication as many lesions can cause replication stress as well as replication stress resulting in more DNA damage. Replication stress is defined as 'the slowing or stalling of replication fork progression and/or DNA synthesis' (Zeman and Cimprich, 2014). As well as DNA lesions, replication stress can also be caused by a limited supply of replication factors, repetitive DNA sequences, fragile sites, secondary structure in

DNA, ribonucleotide incorporation and transcription complexes (Zeman and Cimprich, 2014). Experimentally, replication stress can be induced by limiting the nucleotide pool (for example by addition of hydroxyurea (HU) which inhibits ribonucleotide reductase), inhibiting topoisomerases (by addition of camptothecin or etoposide) or directly inhibiting DNA polymerase (by addition of aphidicolin (Aph))(Allen et al., 2011).

Once replication forks have stalled/slowed due to problems with replication, there is often an uncoupling of the replicative helicase from the DNA polymerase. This results in the continuation of the helicase and a large stretch of single stranded DNA (ssDNA) is formed (Pacek and Walter, 2004; Walter and Newport, 2000). If unrepaired or not stabilised stalled forks can also collapse and form DSB causing further damage to DNA (Michel et al., 1997).

1.4 DNA damage response

In order for cells to survive DNA damage and replication stress, they have evolved a complex network of response pathways. Collectively called the DNA damage response (DDR), these sense lesions and activate a network of transducers and effectors. A wide range of effects can occur in the cell dependent on type of DNA damage, type of cell and the stage of the cell cycle. These include delay of cell cycle progression, activation of DNA repair processes and/or initiation of apoptosis. These networks act in co-ordination to limit the amount of damage passed on to future generations of cells. (Zhou and Elledge, 2000).

One of the earliest identified responses to DNA damage was the stalling of the cell cycle. This gave rise to the term 'checkpoint', defined as a mechanism which delayed cell cycle progression to allow time for DNA repair (Hartwell and Weinert, 1989). Many checkpoint components were originally identified in yeast (Al-Khodairy and Carr, 1992; Enoch et al., 1992; Weinert and Hartwell, 1988) but identification of homologs in mammalian systems have shown that they are well conserved mechanisms. Multiple checkpoint pathways have now been discovered which operate to delay cell cycle progression, but the upstream components also play a role in activating other DNA damage responses.

1.4.1 Cancer and the DDR

An understanding of checkpoints and the DDR is important, not least because of their two-fold role in cancer. Firstly, the DDR protects cells from mutations which can lead to genome instability and cancer development. Cancer results from an accumulation of mutations that activate proliferation and inhibit cell death (Hanahan and Weinberg, 2000). These mutations can arise when damaged DNA is not repaired effectively. If the majority of damaged DNA is repaired correctly, the chances of developing mutations in oncogenes and tumour-suppressor genes is reduced. It follows that defects in DDR genes will increase the mutational load and may pre-dispose to cancer. Consistent with this notion, a number of inherited syndromes involving defective DDR components give rise to inherited cancer predisposition syndromes. Examples include ataxia telangiectasia, Li-Fraumeni syndrome and Fanconi's Anaemia (Kastan and Bartek, 2004).

Secondly, the DDR provides cancer cells with a degree of protection from the radio- and chemo-therapies used to treat a spectrum of cancers and therefore can be used to sensitise them. DNA damaging agents are used against a wide range of cancers and remain the most effective type of treatment. Limitations include severe side-effects arising from a lack of selectivity for cancer cells and thus unavoidable damage and cell death in normal tissue. In addition, the micro-evolutionary nature of cancer inevitably results in tumour cells that have acquired specific resistance to the therapy. Increasing the effectiveness of these DNA damaging agents could help alleviate these problems. (Zhou and Bartek, 2004).

After DNA damage, cells are very dependent on the DDR to survive. In many cancer cells, the G1/S checkpoint is abrogated by mutations in the retinoblastoma protein (RB1) and p53 (Massagué, 2004) which has the effect of increasing the dependency of such cells on the S and G2/M checkpoints for survival. A strategy involving the inhibition of these checkpoints together with DNA damaging agents might be expected to have a higher therapeutic index; such an approach might lead to selective cancer cell elimination as normal cells would be protected by their intact G1/S checkpoint. Therefore the identification and analysis of mechanism components of the S-phase checkpoints can contribute to novel approaches for target identification and in the longer term, novel cancer treatments (Chen et al., 2012).

1.4.2 Key DDR components

The initial DDR is largely mediated by the phosphoinositide 3-kinase related kinases (PIKKs) ataxia-telangiectasia mutated (ATM) and ataxia-telangiectasia and Rad3-related (ATR). These large serine/threonine kinases are activated by DNA damage or replication stress and initiate a wide range of cellular responses. These responses are primarily via ATR's activation of checkpoint kinase 1 (CHK1) and ATM's activation of checkpoint kinase 2 (CHK2).

1.4.2.1 ATR and CHK1

ATR is an essential protein in cells (Brown and Baltimore, 2000; de Klein et al., 2000) and is activated by a wide range of chromatin-associated perturbations, including replication stress, DNA adducts and cross-links. This is most likely due to the fact that all of these generate ssDNA, which is the DNA structure proposed to activate ATR. Though there are still many unanswered questions about ATR activation, the current model in mammalian cells is shown in Figure 1-1 and described below. (Cimprich and Cortez, 2008).

Once generated, ssDNA is rapidly coated in replication protein A (RPA) to protect it from nucleases and hairpin formation. This heterotrimeric protein complex also functions to recruit ATR to sites of ssDNA (Fanning et al., 2006). This recruitment occurs via the ATR interacting protein (ATRIP) which binds ATR (Cortez et al., 2001) and the basic cleft domain of RPA1 (Ball et al., 2007; Zou and Elledge, 2003). ATRIP is a key component of ATR activation and loss of ATRIP gives a similar phenotype to loss of ATR (Cortez et al., 2001).

Independent of ATR and ATRIP localisation, but necessary for ATR's activation, is the recruitment of the RAD9-RAD1-HUS1 (9-1-1) complex to ssDNA. This ring structure is loaded on to the junctions of ssDNA with double-stranded DNA (possibly formed by DNA polymerase α primers (Yan and Michael, 2009a)) by the clamp loader complex RAD17-RFC (Bermudez et al., 2003; Ellison and Stillman, 2003). This recruitment is also dependent on RPA (Zou et al., 2003), and in *Xenopus laevis* has been shown to require DNA Polymerase α and topoisomerase 2-binding protein 1 (TOPBP1) (Yan and Michael, 2009b).

TOPBP1, which interacts with RAD9 (Delacroix et al., 2007; Lee et al., 2007), ATR and ATRIP (Mordes et al., 2008), is necessary for ATR activation (Delacroix et al.,

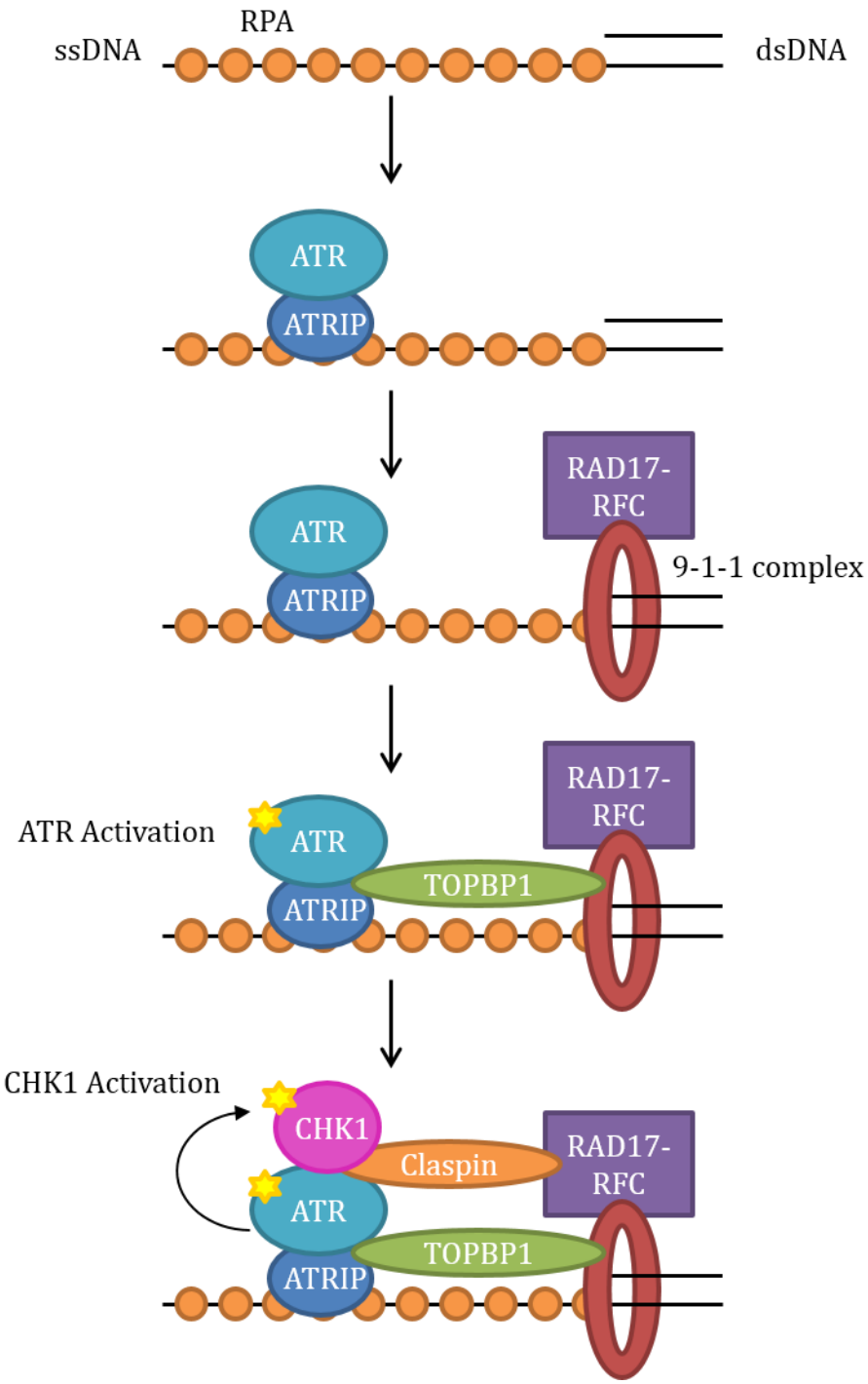

Figure 1-1. ATR Activation

Model of current understanding of ATR and CHK1 activation in mammalian cells.

2007; Kumagai et al., 2006). The details of how and when it is recruited to sites of damage are still under investigation (Parrilla-Castellar and Karnitz, 2003; Wang et al., 2011; Yan and Michael, 2009b) as is the mechanism of ATR activation (Liu et al., 2011). One theory is that binding of TOPBP1 to ATR's PIKK regulatory domain causes a conformational change in ATR resulting in an increased affinity for substrates (Nam and Cortez, 2011).

Once activated, ATR can phosphorylate hundreds of targets (Matsuoka et al., 2007; Mu et al., 2007; Stokes et al., 2007) but one of the key substrates is CHK1. ATR phosphorylates CHK1 on serine (S) residues 317 and 345 (Liu et al., 2000; Zhao and Piwnica-Worms, 2001) resulting in its increased activity as a serine/threonine kinase (Feijoo et al., 2001; Walker et al., 2009). This phosphorylation is dependent on the presence of the mediator protein Claspin, which brings ATR and CHK1 together (Chini and Chen, 2003; Kumagai and Dunphy, 2000; Lin et al., 2004). Claspin is located at replication forks (Lee et al., 2003a) and binds phosphorylated RAD17 (Wang et al., 2006a). It itself is phosphorylated upon DNA damage or replication stress (by casein kinase 1 (Meng et al., 2011)) which permits its interaction with CHK1 (Chini and Chen, 2003; Kumagai and Dunphy, 2000). A second mediator, BRCA1, may also be involved in CHK1 phosphorylation (Lin et al., 2004; Sato et al., 2012; Yarden et al., 2012) and additional new components involved in ATR activation and signalling are still being discovered (Nam and Cortez, 2011).

1.4.2.2 ATM and CHK2

In contrast to ATR activation, ATM is activated predominantly by DSBs (Nakagawa et al., 1999). These can arise from DNA damaging agents (Veatch and Okada, 1969), collapsed replication forks (Michel et al., 1997) or uncapped telomeres (Lange, 2009). One of the first complexes recruited to the DSB is the MRE11-RAD50-NBS1 (MRN) complex (Carney et al., 1998; Dolganov et al., 1996; Mirzoeva and Petrini, 2001). This forms a physical bridge across the break and is involved in DSB repair (Stracker and Petrini, 2011). Through an interaction between NBS1 and ATM, the MRN complex is also involved in the recruitment of ATM to DSB sites (Falck et al., 2005; You et al., 2005). Crucial for its activation is the autophosphorylation of ATM on S1981 after DNA damage (Bakkenist and Kastan, 2003). Combined with other modifications (Bensimon et al., 2010; Kozlov et al., 2006; Sun et al., 2007), this results in the dissociation of ATM homodimers to monomers increasing the activity of the kinase (Bakkenist and Kastan, 2003). Full and prolonged activation is dependent on multiple

mediators including the MRN complex (Lee and Paull, 2004; Uziel et al., 2003), MDC1 (Stewart et al., 2003), 53BP1, and BRCA1 (Lee et al., 2010). Once activated, ATM phosphorylates a wide range of substrates including histone H2A.X, CHK2, and p53 (Banin et al., 1998; Burma et al., 2001; Canman et al., 1998; Friesner et al., 2005; Matsuoka et al., 2000).

1.4.2.3 Cross talk between ATR-CHK1 and ATM-CHK2 pathways

Though historically the ATR-CHK1 and ATM-CHK2 pathways have been seen as separate pathways responding to different forms of damage, there is recently more evidence of their overlapping functions. ATM is known to be activated by DBS and ATR by ssDNA, but these lesions are often both present after DNA damage. When a DSB occurs, ATM activates the resection of one strand to produce ssDNA-RPA which can activate ATR (Jazayeri et al., 2006). Conversely when replication forks encounter single-strand nicks, DSB can form leading to ATM activation (Smith et al., 2010; Stiff et al., 2006).

Their downstream signalling can also be more intertwined. Evidence has been seen that CHK2 can be phosphorylated independently of ATM, probably by ATR (Pabla et al., 2008; Wang et al., 2006b) as well as by DNA-activated protein kinase (DNA-PK) (Müller et al., 2007). ATM may also phosphorylate CHK1 as CHK1 phosphorylation after IR is defective in ATM-null cells (Gatei et al., 2003). This defect may though be caused by the lack of resection in ATM-null cells, preventing ATR activation and its phosphorylation of CHK1.

1.4.3 G1/S Checkpoint

When DNA damage is detected during G1, the G1/S checkpoint is activated and prevents cells entering S-phase to allow time for DNA repair. This checkpoint operates via two pathways: one gives a rapid but short lived delay to replication, whereas the other results in a more long-lasting delay but takes longer to operate (see Figure 1-2; Lukas et al., 2004)

The fast mechanism responds to the DNA damage by activation of ATR or ATM. Subsequent activation of CHK1 or CHK2 leads to phosphorylation of the phosphatase CDC25A. This modification (in particular the phosphorylation of S76 by CHK1) promotes CDC25A's ubiquitination by SCF-βTRCP and results in the rapid

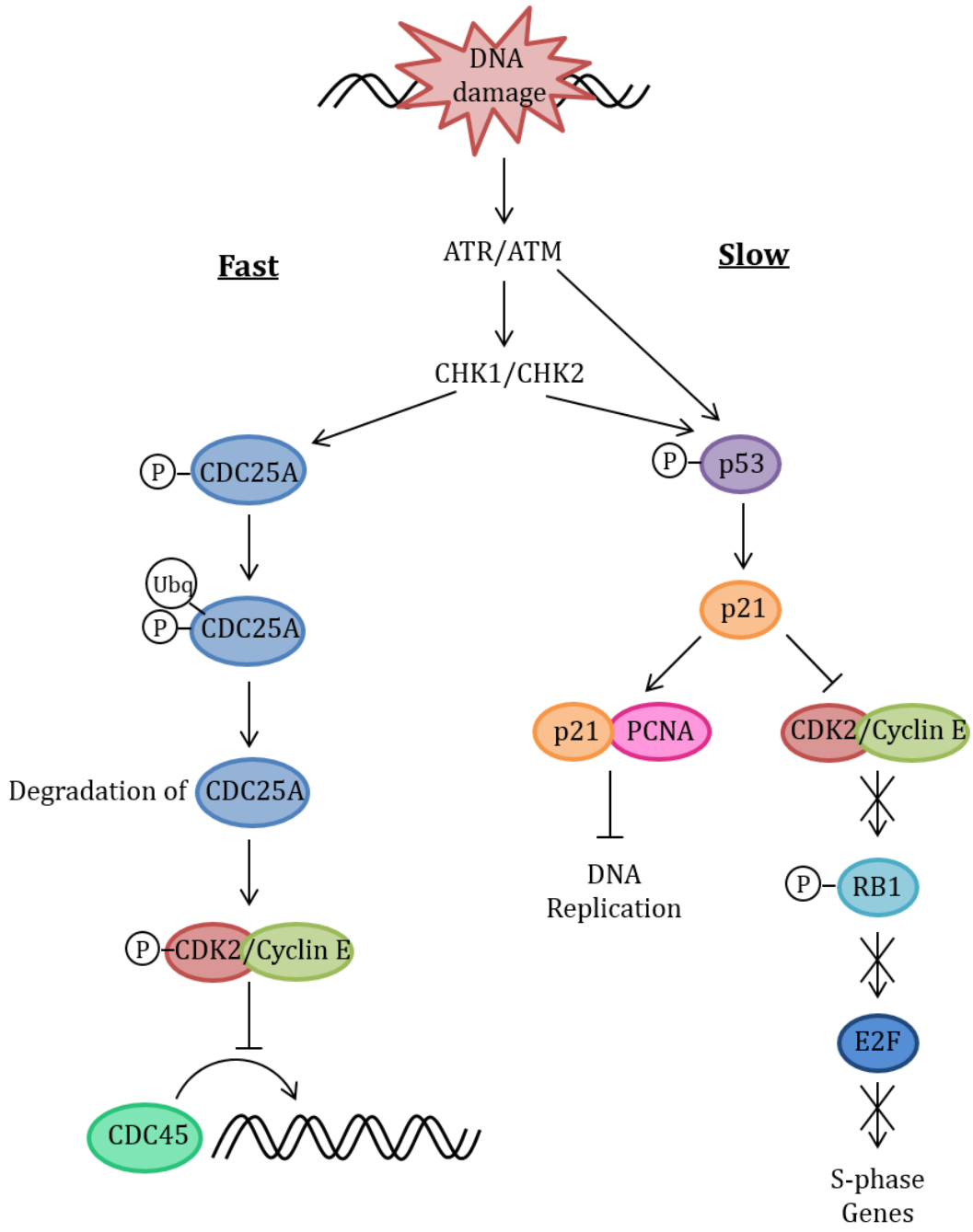

Figure 1-2. G1/S Checkpoint.

After DNA damage in G1, fast and slow checkpoint pathways operate to inhibit entry into, and progression through, this S-phase. P = phosphorylation Ubq= ubiquitination.

proteasome-mediated degradation of CDC25A (Busino et al., 2003; Jin et al., 2008). CDC25A is then unable to remove the inhibitory phosphate from CDK2 preventing CDK2/cyclin E activation. CDK2/cyclin E normally promotes the loading onto DNA of the polymerase recruiting factor, CDC45, (Costanzo et al., 2000). Therefore the activation of this pathway prevents the initiation of DNA replication.

The slow mechanism is also activated by ATR/ATM and CHK1/CHK2 but is additionally dependent on the transcription factor p53. In unstressed cells p53 has a low binding affinity for DNA and has a short half-life (principally due to regulation by MDM2; reviewed in Moll and Petrenko, 2003). Phosphorylation of p53 by ATR, ATM, CHK1 and CHK2 at multiple sites causes an increase in its stabilisation, nuclear accumulation and activity as a transcription factor (Appella and Anderson, 2001). This enables the transcription of multiple targets including p21 (also known as Cip1 or WAF1). p21 can associate with PCNA and prevent its binding to DNA polymerase, inhibiting replication (Abbas and Dutta, 2009). p21 is also an inhibitor of CDK2/cyclin E (Poon et al., 1996). Depending on the precise timing of p21 expression, this inhibition can prevent entry into S-phase as well as S-phase progression. In unstressed cells, CDK2/cyclin E -mediated phosphorylation of RB1 releases the transcription factor E2F and allows the transcription of S-phase genes (Blagosklonny and Pardee, 2002). This transcription is blocked by elevated levels of p21. DNA damage also results in a rapid increase in p21 by activating the degradation of cyclin D1. As p21 is found associated with cyclin D1 and CDK4/6 this degradation enables the release of p21, increasing its availability for CDK2/cyclin E inhibition (Agami and Bernards, 2000).

1.4.4 G2/M Checkpoint

The G2/M checkpoint functions to prevent cells from entering mitosis when DNA damage is present. By preventing activation of CDK1/cyclin B1, the cell is stalled in G2 to allow time for DNA repair or, if severe damage is present, programmed cell death. The basic checkpoint is conserved in most eukaryotes and the first components were discovered in budding yeast (Weinert and Hartwell, 1988). The key features of the mammalian G2/M checkpoint are described below and shown in Figure 1-3.

Activation of CHK1 and CHK2 by ATR or ATM (depending on the nature of the initial lesion) results in the phosphorylation and inhibition of CDC25C (Matsuoka et al., 1998; Peng et al., 1997; Sanchez et al., 1997). This is one of the phosphatases

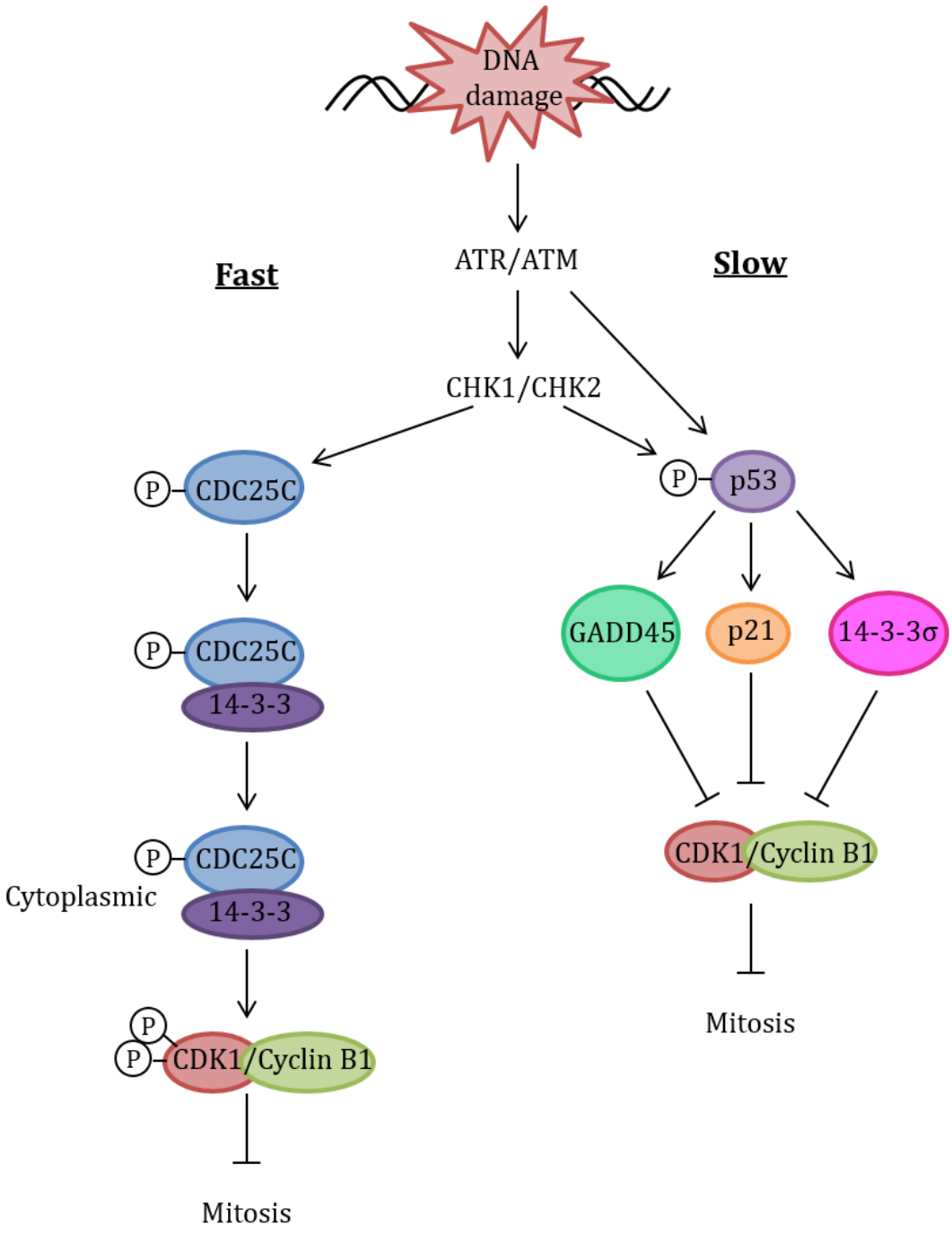

Figure 1-3. G2/M Checkpoint.

DNA damage during G2 causes inhibition of mitosis by fast (CDC25C-dependent) and slow (p53-dependent) mechanisms.

required to remove the inhibitory phosphate from Y15 and T14 on CDK1, (see section 1.1). Phosphorylation of CDC25C on S216 by CHK1 or CHK2 creates a binding site for 14-3-3 proteins (Peng et al., 1997). This binding sequesters CDC25C in the cytoplasm resulting in it being unable to dephosphorylate and activate nuclear CDK1/cyclinB1(Graves et al., 2001).

The pathway is further reinforced by CHK1's inhibitory phosphorylation of polo-like kinase 1 (PLK1) (Tsvetkov and Stern, 2005) (which normally activates CDC25C (Roshak et al., 2000) and CHK1's activation of WEE1 (Lee et al., 2001) (which normally inhibits CDK1 (McGowan and Russell, 1995; Parker and Piwnica-Worms, 1992)). CDC25A and CDC25B also play a role in dephosphorylating CDK1 and are targets of the checkpoint. CDC25A can be phosphorylated by CHK1 and subsequently degraded (as in the G1/S checkpoint) and CDC25B is phosphorylated by p38 and bound to 14-3-3 proteins after UV treatment (Donzelli and Draetta, 2003).

As with the G1/S checkpoint, there is also a slower, longer-lasting mechanism which is dependent on p53. Multiple p53 transcription targets (p21, GADD45, 14-3-3σ) inhibit CDK1/cyclin B1 preventing mitosis initiation. (Taylor and Stark, 2001)

1.4.5 S-phase Checkpoint

S-phase is one of the most crucial stages for the genomic integrity of the cell. As well as cells being subject to DNA damage, as in other stages of the cell cycle, they are also susceptible to replication stress. In order to cope with this, the S-phase checkpoint activates a wide range of different cellular processes to protect the cell. These include inhibition of late origin firing, replication fork stabilisation, inhibition of mitosis and histone mRNA decay (reviewed in Bartek et al., 2004). Historically these have often been described as separate checkpoints (intra-S-phase, replication and S-M), though as they have many overlapping mechanisms I will refer to them as one checkpoint network (see Figure 1-4).

1.4.5.1 Inhibition of late origin firing

DNA replication in eukaryotes is undertaken by thousands of replication forks across the genome that emanate from replication origins. All origins do not fire at the same time as there is a temporal sequence of origin firing throughout S-phase which is linked to transcription (reviewed in Gilbert, 2002). All origins are licensed during G1 when the origin recognition complex (ORC), CDC6 and CDT1 recruit the helicase

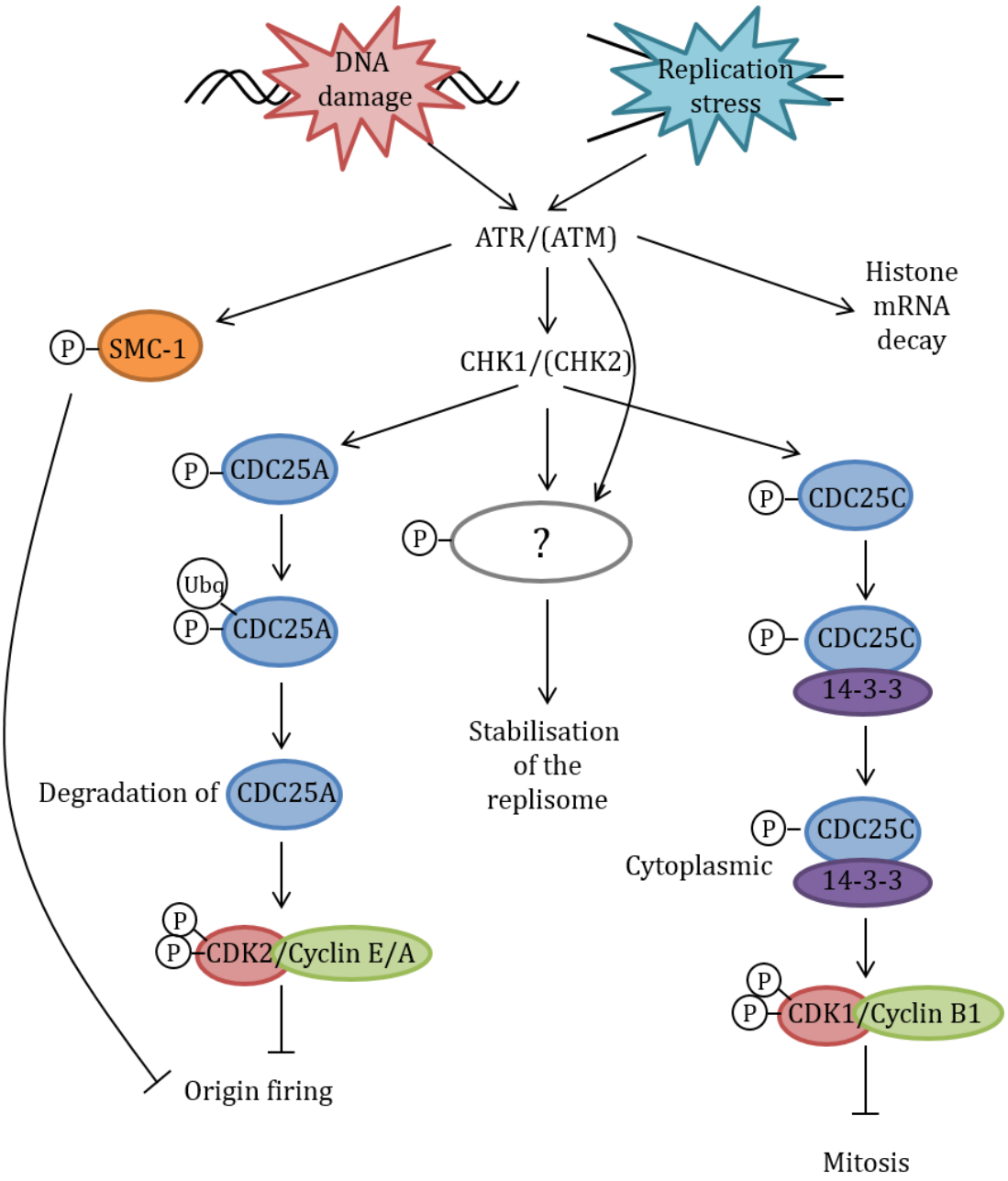

Figure 1-4. S-phase Checkpoint.

Replication stress and DNA damage can activate at least 4 responses in S-phase cells: inhibition of origin firing, stabilisation of the replisome, inhibition of mitosis (S-M checkpoint) and histone mRNA decay. P = phosphorylation. Ubq = ubiquitination

MCM2-7 to replication origins. As cells progress into S-phase, replication is initiated by the activation of S-phase specific kinases, CDK2/cyclin A and CDC7/DBF4 (DBF4 dependent kinase). Phosphorylation of various targets causes the recruitment of a number of proteins including CDC45, TOPBP1, Treslin and GINS to allow for helicase activation. PCNA, RPA and DNA polymerases are then able to bind to start replication. (Bell and Dutta, 2002).

When cells encounter DNA damage or replication stress during S-phase, the rate of DNA synthesis is reduced. This has been shown to be mainly due to a checkpoint response inhibiting origin firing at unfired, late origins (Merrick et al., 2004; Painter and Young, 1980; Santocanale and Diffley, 1998). The mechanisms involved in regulating origin firing are not completely understood but there are at least four different pathways that may play a role in mammals.

CDC25A is degraded after activation of the G1/S checkpoint but also after activation of the S-phase checkpoint (Mailand et al., 2000; Molinari et al., 2000). The mechanism is similar to the G1/S checkpoint with phosphorylation of CDC25A by CHK1 (Zhao et al., 2002) and possibly CHK2 (Falck et al., 2001; Jin et al., 2008), at multiple sites. These phosphorylation events prime it for phosphorylation in the DSG degron sequence by NEK11 (Melixetian et al., 2009). This phosphorylation acts as a site for the recruitment of the SCF-βTRCP ubiquitin ligase which targets CDC25A for proteasomal degradation (Busino et al., 2003; Jin et al., 2003). Without high levels of CDC25A, the inhibitory phosphates on CDK2 are not removed and CDK2/cyclin A cannot activate CDC45 loading and replication initiation (Falck et al., 2001). In some prolonged S-phase checkpoint responses, a p53-dependent mechanism may also decrease CDC25A by preventing its transcription (Demidova et al., 2009).

As well as activating the above pathway, ATM and ATR have also been shown to phosphorylate structural maintenance of chromosome 1 (SMC1) after DNA damage (Kim et al., 2002; Tomimatsu et al., 2009; Yazdi et al., 2002). Mutations at S957 and S966 preventing phosphorylation, results in cells which continue to synthesise DNA after radiation implying that phosphorylation of SMC1 is important for the inhibition of late origin firing. The mechanism downstream of SMC1 that impacts on replication is unknown.

In budding yeast (which does not use the CDC25A-CDK2 inhibition pathway), Rad53 (CHK2 homolog) phosphorylates Dbf4 and Sld3 after a range of DNA damage/replication stress treatments (Lopez-Mosqueda et al., 2010; Zegerman and

Diffley, 2010). This interferes with Sld3's interaction with Dpb11 (TOPBP1 homolog) and Cdc45, and mutations in the phosphorylation sites prevented the inhibition of origin firing after checkpoint activation. Treslin (TICRR) has been identified as the vertebrate homolog of Sld3 (Kumagai et al., 2010; Sanchez-Pulido et al., 2010; Sansam et al., 2010) and although it has not been shown to be phosphorylated by CHK1, its interaction with TOPBP1 is decreased after HU treatment in a CHK1-dependent manner (Boos et al., 2011). Whether Treslin plays a functional role in inhibiting late origin firing in mammalian cells is still to be determined.

In yeast, there is also evidence of the S-phase checkpoint targeting the Cdc7/Dbf4 kinase activity to inhibit replication (Jares et al., 2000). There is some evidence for a similar response in *Xenopus* extracts and after low doses of UV in human cells but evidence in other human cell lines indicates otherwise (Costanzo et al., 2003; Heffernan et al., 2007; Lee et al., 2012a; Yamada et al., 2013).

1.4.5.2 Stabilisation of replisome

The stabilisation of components of replication (the replisome) at the replication fork, after DNA damage or replication stress, is vital for the resumption of replication after the hindrance is removed. This has been shown to be part of the checkpoint response as loss of CHK1 or ATM and ATR causes the dissociation of the replisome and a failure to restart replication at stalled forks (Feijoo et al., 2001; Trenz et al., 2006; Zachos et al., 2003). Indeed it is likely that the inability of checkpoint mutant cells to stabilise the replisome, plays a major role in their loss of viability (Tercero et al., 2003).

The molecular mechanisms which are targeted by the checkpoint kinases to stabilise the replisome are far from understood, particularly in mammalian cells. Lee et al. showed that knockdown of DBF4 or CDC7 caused an increase in phosphorylated H2AX after short HU treatments, an indication of DSBs originating from collapsed replication forks, (Lee et al., 2012a). ATR and ATM are also known to phosphorylate many components of the replisome (ORC, RFC, MCM2-7) which may be a cause or consequence of replisome stability (Cortez et al., 2004; Ishimi et al., 2003; Matsuoka et al., 2007; Shi et al., 2007; Yoo et al., 2004).

In budding yeast, experiments have shown that other replication components (Sgs1, Mrc1, RPA and DNA pol α) may be involved, although an exact mechanism of action is yet to be revealed (Cobb et al., 2005, 2003; Katou et al., 2003; Lucca et al., 2004). Other experiments utilising yeast as a model organism have indicated that there may be a

role for chromatin structure in replisome stability, as loss of Ino80 (a chromatin remodelling complex) causes the dissociation of DNA pol α from stalled replication forks and impairs the resumption of replication after HU (Papamichos-Chronakis and Peterson, 2008; Shimada et al., 2008). A key role for exonuclease 1 (Exo1) was found in a budding yeast screen (Segurado and Diffley, 2008). Loss of Exo1 increased the viability of Δrad53 mutants after HU, UV, MMS or IR. These double mutants were still unable to resume replication after HU treatment but could after MMS treatment, implying a complex checkpoint response depending on the nature of the DNA damage lesion.

1.4.5.3 S-M Checkpoint

The S-M checkpoint blocks entry into mitosis if replication is not complete. The initial evidence for the existence of this checkpoint emerged from classic experiments undertaken by Rao and Johnson in 1970, who noted, using HeLa cells, that fusion of a G2 cell with an S-phase cell resulted in delayed mitosis until both nuclei were replicated (Rao and Johnson, 1970). Genetic work in budding yeast also showed that mutants unable to complete DNA synthesis were prevented from entering cell division (Hartwell, 1971). Genetic screens in fission yeast (Al-Khodairy and Carr, 1992; Enoch et al., 1992) and work with chemical inhibitors (in particular caffeine) in a number of model systems (Schlegel and Pardee, 1986; Smythe and Newport, 1992) established conditions where mitosis occurred even though replication was inhibited or incomplete. These and other studies have led to the identification of components of the S-M checkpoint which has a similar mechanism to the G2/M checkpoint and the two can often be hard to distinguish experimentally.

In fission yeast, *Xenopus* and some mammalian cells, the activation of CHK1 by ATR (activation of Cds1 by Rad3 in fission yeast) after replication inhibition is crucial for the S-M checkpoint (Al-Khodairy and Carr, 1992; Enoch et al., 1992; Guo et al., 2000; Kumagai et al., 1998; Murakami and Okayama, 1995; Nghiem et al., 2001; Zachos et al., 2005). ATR's role is also demonstrated in the fact that it is a target (along with ATM; Blasina et al., 1999) of caffeine, which uncouples the dependence of mitosis on the completion of S-phase (Hall-Jackson et al., 1999; Sarkaria et al., 1999). As in the G2/M checkpoint, activated CHK1 phosphorylates CDC25C at S216, promoting the binding of 14-3-3 proteins and CDC25C's nuclear exclusion (Peng et al., 1997; Zeng et al., 1998). CHK1 may also phosphorylate CDC25A leading to its degradation as in the G1/S checkpoint (Molinari et al., 2000). The multiple routes that suppress CDC25

phosphatase activity prevents the removal of inhibitory phosphorylations on CDK1, and thus entry into mitosis is prevented.

There is evidence that the picture is more complex in some mammalian cells (see Figure 1-5). An ATR-independent mechanism has been observed in some rodent and human cell lines (Brown and Baltimore, 2003; Florensa et al., 2003; Steinmann et al., 1991). In the human cervical cancer cell line, HeLa, the S-M checkpoint is not sensitive to caffeine unlike in colorectal cancer cells lines (e.g. HCT116) and Baby Hamster Kidney cells (Florensa et al., 2003; Schlegel and Pardee, 1986). Further investigation into the S-M checkpoint mechanism in HeLa cells showed that addition of a CHK1 selective inhibitor (UCN-01) did abrogate the checkpoint, implying the checkpoint is still dependent on CHK1, but suggests that the cells have an ATR-independent mechanism for activating CHK1 (Rodríguez-Bravo et al., 2006).

The S-M checkpoint in non-transformed rodent cell lines is insensitive to ATR and CHK1 inhibition indicating that these cells have a further mechanism to prevent mitosis (Llopis et al., 2012; Rodríguez-Bravo et al., 2007). In those cells, the checkpoint can be inhibited by the combination of CHK1 and p38 or JNK inhibitors. These data indicate that the mitogen-activated protein kinase (MAPK) pathway operates as another component of the checkpoint mechanism. The MAPK pathway is activated following environmental stress, inflammation and DNA damage (Zarubin and Han, 2005). MK-2 (downstream of p38) has been previously shown to phosphorylate CDC25B and C and this pathway may contribute to the S-M checkpoint via this mechanism (Lemaire et al., 2006; Manke et al., 2005).

The differences in the detailed mechanisms by which different cell types operate the S-M checkpoint may be due to differences in cyclin B1 accumulation throughout S-phase. Caffeine-insensitive cell lines do not accumulate cyclin B1 during S-phase arrest unlike caffeine-sensitive cells (Florensa et al., 2003; Steinmann et al., 1991). Abrogating the checkpoint in HeLa cells with UCN-01 also allows cyclin B1 accumulation (Rodríguez-Bravo et al., 2006). Cyclin B1 over-expression in HT1080 cells (caffeine-insensitive human cells) leads to a caffeine sensitive S-M checkpoint (Tam et al., 1995). Therefore there may be a further mechanism in some cells preventing CDK1/cyclin B1 activation by inhibiting cyclin B1 via an ATR/ATM independent mechanism. However, in non-transformed cells that enter mitosis after HU, CHK1 inhibition and p38 inhibition, cyclin B1 levels remain low (Rodríguez-Bravo et al., 2007).

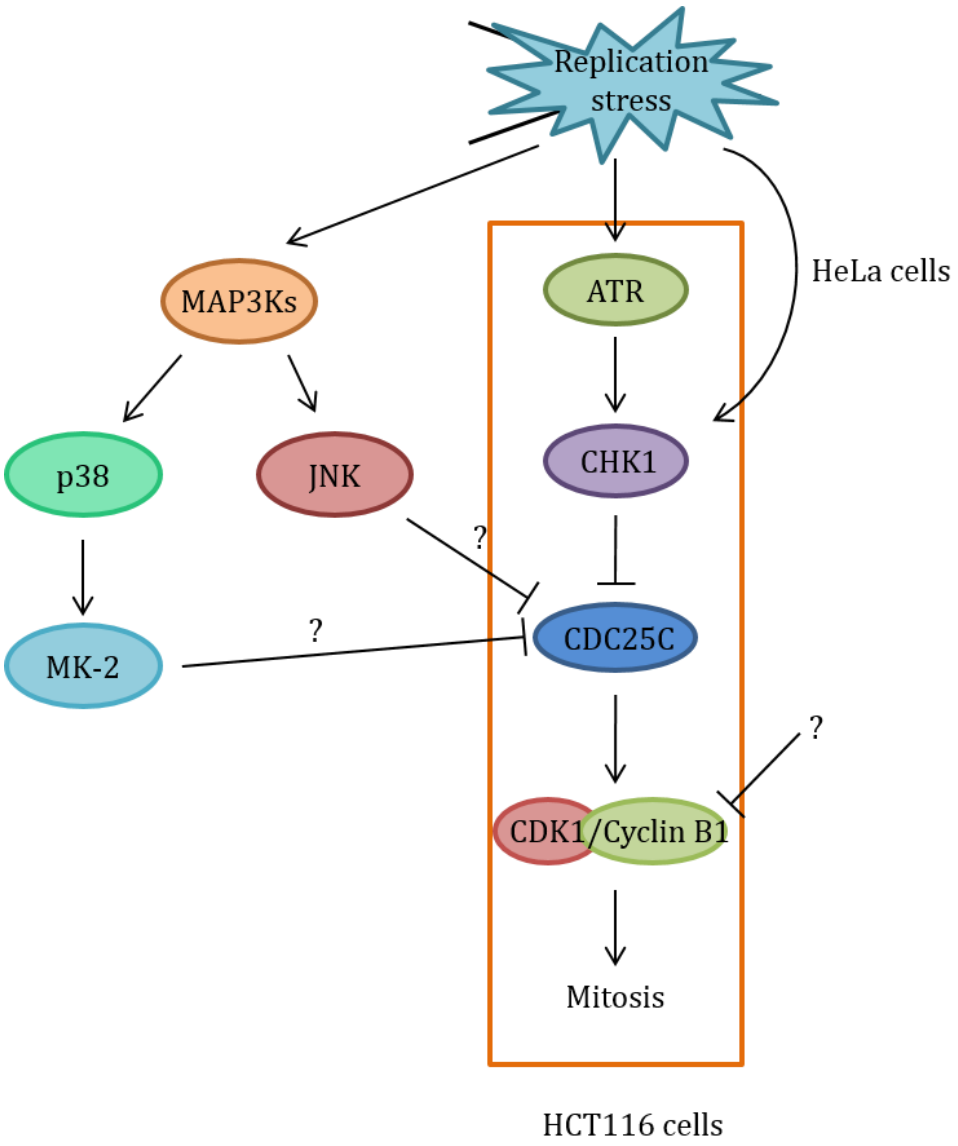

Figure 1-5. S-M checkpoint in different cell types.

The S-M checkpoint has been shown to have different mechanisms in different cell types. The orange box represents the core pathway which yeast, Xenopus, and colorectal cancer cell lines (e.g. HCT116 cells) are solely dependent on. HeLa cells have an additional activation of CHK1 and non-transformed cell lines have an additional MAPK pathway. The end point of the MAPK pathway is unknown though may affect CDC25C. In some cell lines activation of the checkpoint also affects cyclin B1 levels through an unknown mechanism.

It is also interesting to note that many of the caffeine-insensitive cell lines are derived from rodent species, in which the CHK1 phosphorylation site on CDC25C is not conserved (Donzelli and Draetta, 2003). Therefore these alternative pathways may be specific to rodents and not non-transformed lines

1.4.5.4 Histone mRNA decay

Histone mRNA decay does not directly affect cell cycle progression, and therefore is traditionally not seen as part of the S-phase checkpoint. It is, however, a replication-stress response dependent on some DDR kinases and is therefore here included in the S-phase checkpoint network.

Histones are alkaline proteins required to form nucleosomes, needed to package DNA into chromatin. There are multiple clustered histone genes in eukaryotes and their transcription is co-ordinated (Hentschel and Birnstiel, 1981). Some histone genes are expressed throughout the cell cycle at a low level but the majority are only expressed during late G_1 and S phase (Wu and Bonner, 1981), when triggered by CDK2/cyclin activity (Ma et al., 2000; Zhao et al., 2000). Replication-dependent histone gene expression is tightly coupled to DNA synthesis, and when uncoupled transcription can be affected (Eriksson et al., 2005), DNA can be damaged (Meeks-Wagner and Hartwell, 1986; Ye et al., 2003) and cells can arrest in mitosis (Nelson et al., 2002).

In yeast, when DNA replication stops (either due to the end of S-phase or induced by inhibitors), free histones accumulate as they are no longer deposited onto DNA by relevant chaperones (Bonner et al., 1988). To protect the cell from the consequences of an overabundance of unbound histone, Rad53 (homolog of CHK2) regulates the degradation of free histones when replication is inhibited (Gunjan and Verreault, 2003).

In contrast, in higher organisms histones are primarily regulated at the mRNA level. Replication-dependent histones are the only metazoan mRNAs that do not contain a poly(A) tail. Instead they have a conserved stem-loop in the 3' untranslated region (UTR) (Birnstiel et al., 1985). This 6 base pair (bp) stem – 4bp loop is bound by the stem-loop binding protein (SLBP) and this interaction is vital for all histone mRNA metabolism (Williams et al., 1994).

After the addition of replication inhibitors, there is a dramatic decrease in steady-state histone mRNA levels as a consequence of an increase in mRNA degradation

coupled with down-regulation of transcription (Baumbach et al., 1984; Borun et al., 1975; DeLisle et al., 1983; Graves and Marzluff, 1984; Heintz et al., 1983; Sittman et al., 1983a). The mechanism of histone mRNA degradation is partially understood with the current model shown in Figure 1-6 and described below.

mRNA degradation requires ongoing translation (Graves et al., 1987), in particular the terminating ribosome needs to be within 300nt of the stem-loop for degradation to occur (Kaygun and Marzluff, 2005a). This has led to the model that histone mRNA decay occurs whilst in complex with ribosomes by a similar mechanism to nonsense mediated decay (NMD). NMD degrades mRNAs with premature stop codons via recognition of the exon junction complex downstream of a stop codon. It is thought that histone mRNA degradation is initiated by the recruitment of UPF1 (an NMD factor) to the histone mRNA via an interaction with SLBP (Kaygun and Marzluff, 2005b). UPF1 then recruits terminal uridyl transferases (TUTases) which oligouridylate the 3' end of the histone mRNA (Mullen and Marzluff, 2008; Su et al., 2013). This creates a binding site for LSM 1-7 complex which is also present in normal mRNA degradation and is able to recruit decapping enzymes, e.g. DCP2, to inhibit further translation. Degradation of the mRNA then occurs 5' to 3' by XRN1 and simultaneously 3' to 5' by the exosome (Mullen and Marzluff, 2008).

The upstream mechanisms that signals from replication inhibition (in the nucleus) to the histone mRNA (at translation complexes in the cytoplasm) are less well understood. Work by Marzluff's group (Kaygun and Marzluff, 2005b) showed that replication stress-induced histone mRNA decay was reduced by the addition of caffeine or over-expression of kinase-dead (kd) ATR, suggesting a role for ATR in the regulation of replication stress-induced histone mRNA decay. Work by Muller et al. contradicted this showing no effect on histone mRNA either in siRNA-mediated ATR-deficient cells, or in cells overexpressing kdATR, or ATM null cells (Müller et al., 2007). They also showed no necessary role for CHK1 or CHK2 though they did confirm the partial inhibitory effect of caffeine. mRNA decay could be further inhibited by adding the DNA-PK inhibitor LY294002.

DNA-PK is another PIKK involved in the DNA damage response, in particular in non-homologous end-joining after DSBs. This implies that there are at least two separate DDR pathways involved in histone mRNA decay, one involving ATM/ATR (caffeine sensitive) and one requiring DNA-PK (LY294002 sensitive).

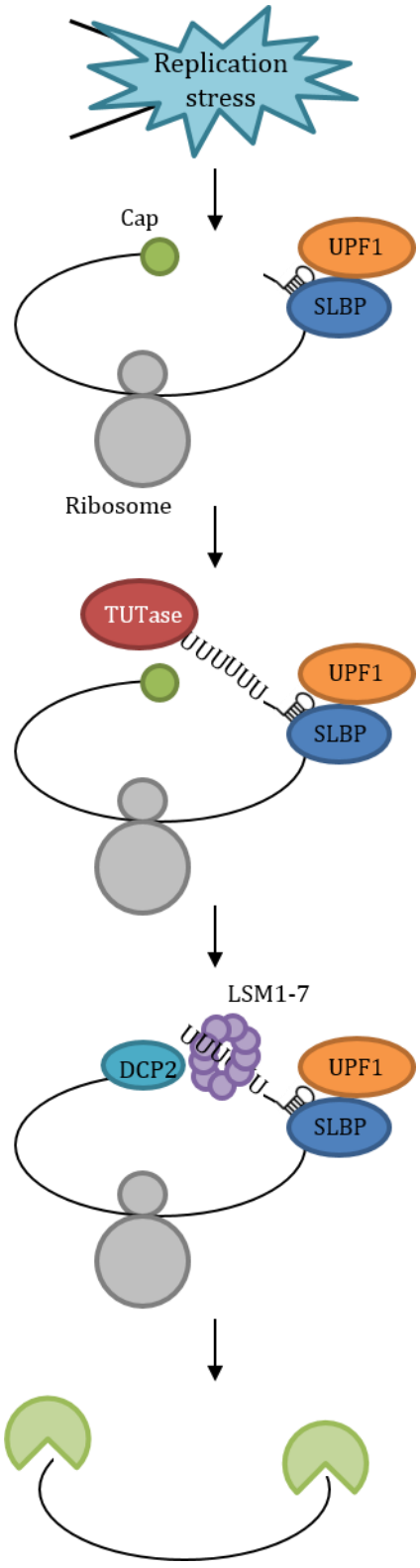

Figure 1-6. Model of histone mRNA degradation.

Model, based on Mullen and Marzluff, 2008, of translation-dependent degradation. After replication stress UPF1 binds SLBP and recruits TUTases which oligouridylate the 3' mRNA end. The LSM1-7 complex binds this tail and recruits decapping enzymes. The mRNA is then degraded from the 5' and 3' ends.

1.4.6 Checkpoints in *Drosophila*

Although checkpoints have primarily been investigated in yeast, *Xenopus* and mammalian systems, some work has also been done in the fruit fly *Drosophila melanogaster*. This model organism has been used due to its genetic tractability and ease of study in whole organisms. Many of the previously described components of checkpoints are conserved in *Drosophila* but there are some distinct differences.

During development, *Drosophila* go through many different stages and their constituent cells can have non-typical cell cycles. After fertilisation, there are 13 rapid syncytial cycles that occur without any gap phases. Then cells develop individual membranes and a G2 phase is introduced (cellular blastoderm embryos). After the 16th nuclear division, many cells enter G1 and arrest except the central nervous system (CNS) and imaginal disc cells. These continue to divide with a normal G1-S-G2-M cell cycle. (Song, 2005).

Checkpoints operate differently throughout these stages. In syncytial embryos when cells are treated with Aph or IR they delay mitosis at metaphase preventing chromosome segregation (Fogarty et al., 1997; Sibon et al., 1997). This delay is dependent on the CHK1 homologue Grapes (Grp), but only occurs transiently as treated cells do eventually undergo mitosis. Cells in the cellular blastoderm respond to radiation by delaying entry into mitosis and stalling in G2, like mammalian cells (Su et al., 2000). This delay appears to occur via the inhibition of Cdk1, as a mutant than cannot be phosphorylated at Thr14 or Tyr15 fails to show a delay comparable to that of the wild-type. Like syncytial embryos though, cells do not remain arrested indefinitely, but ultimately undergo mitosis despite the unrepaired DNA damage, with consequent abnormalities (Su and Jaklevic, 2001).

During late embryogenesis, the imaginal discs and CNS continue to divide and show a robust response to Aph, HU, UV and IR in preventing entry into mitosis. This response is dependent on Mei-41 (ATR), Grp, Mus304 (ATRIP), 14-3-3ε and Claspin (Brodsky et al., 2000; Krause et al., 2001; Lee et al., 2012b).

A similar response is also seen in tissue culture cells derived from late embryos (S2R+ and S2 cells). De Vries and colleagues showed that Grp and Mei-41, but not Dmnk (CHK2), were required to delay entry into mitosis after HU or IR treatment (de Vries et al., 2005). They showed a Mei-41-Grp-String (CDC25)-Cdk1 mechanism responding to HU as in the S-M checkpoint in mammalian and yeast cells. The IR-induced G2/M

checkpoint however was also dependent on Mei-41 and Grp, in contrast to the situation in mammalian cells where ATM and CHK2 play the main role in maintaining this checkpoint. A genome-wide RNAi screen investigating this ATR-dependent G2/M checkpoint in S2R+ cells also identified the involvement of Mus101 (TOPBP1) and Mus312 (BTBD12) (Kondo and Perrimon, 2011).

1.5 RNA interference

RNA interference (RNAi) is a post-transcriptional gene regulation mechanism that was originally discovered in plants (Napoli et al., 1990) and *Caenorhabditis elegans* (*C. elegans*) (Fire et al., 1998). It is based upon the principle of small silencing RNAs binding to specific mRNAs and reducing the production of the subsequent protein. There are two main small silencing RNAs, microRNAs (miRNAs) and small interfering RNAs (siRNAs) which work through similar but slightly different pathways (see Figure 1-7).

1.5.1 miRNA

The miRNA pathway is an endogenous system involved in regulating many (possibly up to 50%) genes in plants and animals (Krol et al., 2010). Endogenous miRNAs are produced either from transcribed genes (Lee et al., 1993) or the excised introns of other genes (mirtrons) (Rodriguez et al., 2004). Processing of these RNA products by the RNase III enzyme Drosha, produces a ~70 nucleotide long hairpin pre-miRNA (Lee et al., 2002, 2003b). This pre-miRNA is exported from the nucleus by exportin-5, utilising the Ras-related nuclear protein (RAN) gradient (Lund et al., 2004; Yi et al., 2003), and cleaved further by another RNase III enzyme, Dicer (Grishok et al., 2001; Hutvágner et al., 2001). This produces a ~20bp miRNA duplex. One of the strands (often that with a less stable 5' end) is then incorporated into the miRNA-induced silencing complex (miRISC) (Mourelatos et al., 2002). This complex contains argonaute proteins (AGOs) as well as other adaptors, and the incorporated miRNA guides the complex to the target mRNA. Binding to the target mRNA is often at the 3'UTR where complementarity is particularly high in bases 2-8 (seed region) (Lewis et al., 2003).

Once bound to the mRNA, a variety of different outcomes are possible dependent on the thermodynamics, sequence specificity and organism. Translation can be directly inhibited, the mRNA can be de-adenylated, promoting decay or the mRNA can be

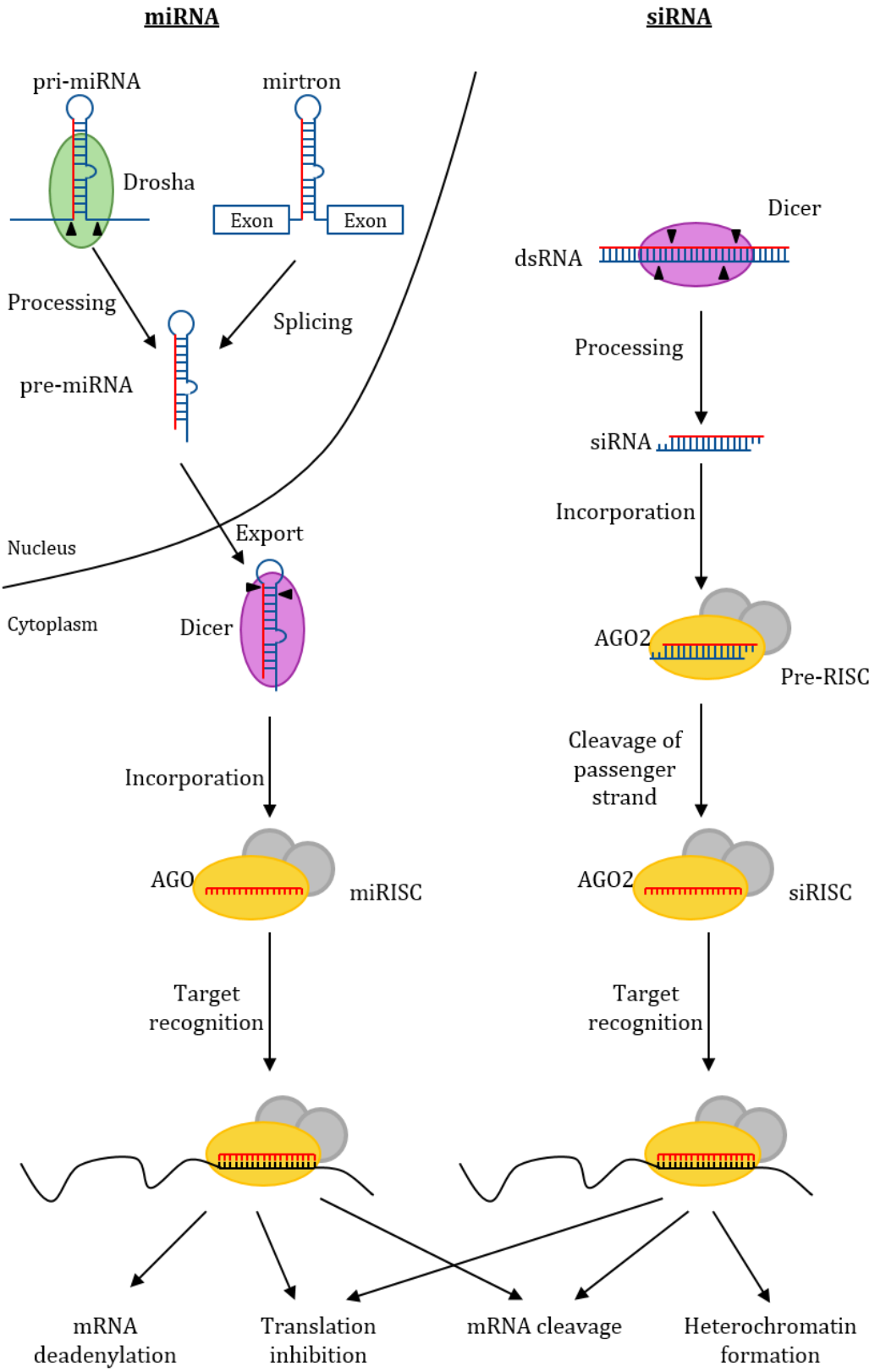

Figure 1-7. RNAi pathways

miRNA and siRNA pathways are similar but have slight differences. See text for details.

directly cleaved and degraded. These all result in a decrease in the production of the target protein (Reviewed in Carthew and Sontheimer, 2009).

1.5.2 siRNA

Gene silencing through siRNAs occurs via a similar mechanism to miRNAs, but details of the process involved differ in their origin. Natural siRNAs are produced from longer double-stranded RNA (dsRNA) molecules which can originate from viruses, repeat-associated transcripts or gene/pseudogene duplexes (Carthew and Sontheimer, 2009). As in the production of miRNA, the dsRNA is processed by Dicer into a ~21 base pair siRNA with two nucleotide 3' overhang. In some organisms (e.g. *Drosophila*) distinct Dicer genes are responsible for siRNA and miRNA production (Lee et al., 2004) while in others , including most mammals, a single Dicer gene is sufficient for both functions.

As with the miRNA pathway, siRNAs are incorporated into a complex with AGO proteins to produce the siRNA-induced silencing complex (siRISC). AGO2 cleaves the passenger strand and the functional siRISC binds to the target mRNA (Rand et al., 2005). If the RNAs bind with near perfect complementarity, AGO2 cleaves the target mRNA (often between the nucleotides that are base-paired to nucleotides 10 and 11 in the siRNA) and degradation by exonucleases occurs (Orban and Izaurralde, 2005). When binding is partial, or the AGO proteins in the siRISC are endonuclease-inactive, other forms of silencing can occur. This includes repression of translation and heterochromatin formation (Carthew and Sontheimer, 2009).

1.5.3 Using RNAi Experimentally

RNAi can be used experimentally to knockdown the expression of a target gene of interest. The miRNA pathway can be used by the addition of small hairpin RNAs (shRNAs), which mimic pre-miRNAs, or by introducing a gene which encodes a miRNA (artificial miRNAs) (Davidson and McCray, 2011).

The siRNA pathway can also, and is more commonly, used experimentally. In *Drosophila* cells, dsRNAs are naturally taken up into cells when they are starved of serum, and these are processed into siRNAs via the cell's natural machinery (Clemens et al., 2000). In mammalian cells, dsRNA induces an interferon response (Reynolds et al., 2006) so siRNA duplexes are directly transfected into the cells where they are incorporated into siRISC complexes (Elbashir et al., 2001).

The siRNA duplexes used in this study are produced by Dharmacon and are one of two types; siGENOME or ON-TARGETplus (OTP). The OTP siRNAs differ from the siGENOME in that they have extra modifications on the passenger strand to prevent incorporation into RISC and on the guide strand seed region to destabilise off-target binding. This results in a decrease in off-target effects. Pooled samples of four different siRNAs all targeting the same gene are also used to decrease off-target effects. (Thermo Fisher Scientific, 2009)

1.5.4 Genome-wide RNAi screening

Due to the specific silencing caused by dsRNA or siRNA in cells, RNAi can be used to discover new genes involved in mechanisms by genome-wide screening. Each gene can be individually knocked down and, by using high-throughput equipment, their effect on the cellular process of interest can be studied. RNAi screens were first performed on *C. elegans* (Gönczy et al., 2000) due to its small genome and the relative ease with which dsRNA could be introduced into this organism. A library of dsRNAs to target most of the *Drosophila* genome was then developed and used to investigate a wide range of cellular processes (Boutros et al., 2004; Foley and O'Farrell, 2004; Müller et al., 2005). More recently siRNA libraries to target the human genome have been developed and used in human cell lines (Whitehurst et al., 2007).

There have been many screens looking for genes involved in cell cycle progression and viability (Boutros et al., 2004; Mukherji et al., 2006; Schlabach et al., 2008) but very few looking for components of specific checkpoints. Kondo and Perrimon reported in 2011 a genome-wide screen in *Drosophila* looking to identify components of the G2/M checkpoint(Kondo and Perrimon, 2011). After the addition of doxorubicin to induce the checkpoint, they calculated the mitotic index (MI) by quantifying the number of phosphorylated histone H3 (phospho-H3) positive cells (a mitotic marker). The screen identified known and novel components of the checkpoint but had to be performed in a sensitised background (all cells were also knocked down with Nbs dsRNA to increase their sensitivity). Another DDR screen was that performed in HeLa cells (Paulsen et al., 2009). Here genes were identified which, when knocked down, caused an increase in H2AX phosphorylation (an early marker of DSBs). This was all performed though in the absence of any artificially applied DNA damaging agents or replication stress and therefore only identified genes that protect cells from endogenous DNA damage.

1.6 Aim

The aim of this work is to use a genome-wide RNAi screen to identify novel components of the S-phase checkpoint. Increasing knowledge of the components and mechanisms of the S-phase checkpoint can help to identify new cancer therapeutic targets.

2. Materials and Methods

2.1 Materials

2.1.1 Solutions

PBS = 137mM NaCl, 2.7mM Na_2HPO_4, 10mM KCl, 2mM KH_2PO_4, pH 7.4

PBT = PBS + 0.05% Tween20

TE = 10mM Tris pH8, 1mM EDTA

TAE = 40mM Tris, 20mM Acetic acid, 1mM EDTA, pH 8

TBS-T = 20mM Tris.HCL pH 7.4, 137mM NaCl, 0.1% Tween

BL buffer = 50mM HEPES, 0.5mM EDTA, 0.36mM Phenyl acetic acid, 0.07mM Oxalic acid, pH 7.8

IFA = 150mM Tris-HCl pH7.6, 500mM NaCl, 0.5% NaN_3, 10% FBS

Lysis buffer = 25mM Tris-Cl pH7.5, 5mM EDTA, 1% Triton-X-100 and 250mM NaCl prepared in advance and stored at room temperature. When required 1mM PMSF and 1x Protease inhibitor cocktail (Roche) was added immediately before use.

SOC media = 2% w/v Tryptone, 0.5% w/v Yeast extract, 8.56mM NaCl, 2.5mM KCl, 10mM $MgCl_2$, 20mM Glucose, pH 7

2.1.2 Primers

Primers were designed in-house using PrimerBLAST (NCBI) and made by Invitrogen.

Table 2-1. Primers

Assay	Primer Name	5'-3' Sequence
PCR	Cact-Fwd-XhoI-PEST (#1)	GATCGACTCGAGGCCGCGGAGCGGAGACCGTAACG
PCR	Cact-Rvs-NheI-UTR-PEST (#2)	GATCGAGCTAGCGCTTTATCTGCAAGTTAATGCCG TGTCAGGCAACTGTCATGGGATTGCC
PCR	Cact-Rvs-PmeI-PEST (#3)	GATCGAGTTTAAACTCAGGCAACTGTCATGGGATT GCC
PCR	TU	TAATACGACTCACTATAGGGTGGCGCCCCTAGATG
PCR	TS1	TAATACGACTCACTATAGGGCGACGCCCGCTGATA

Assay	Primer Name	5'-3' Sequence
PCR	TS3	TAATACGACTCACTATAGGGCGCATGTAGCCTGCC
PCR	TS4	TAATACGACTCACTATAGGGTAGCCTCCCTAGCGC
Sequencing	Fwd Renilla 1	GTTTATTGAATCGGACCCAGG
Sequencing	Fwd Renilla 2	CAACATTATCATGGCCTCGTG
Sequencing	Rvs Renilla UTR	AAGGAGCTGACTGGGTTGAAG
Sequencing	Rvs Renilla CON	GCATTCTAGTTGTGGTTTGTCC
QPCR	Drosophila Histone 3 fwd	CGACTCGTGCAAAGGCGCCA
QPCR	Drosophila Histone 3 rvs	ACGCAAGGCCACGGTTCCAG
QPCR	Drosophila Histone 2B fwd	CTAGTGGAAAGGCAGCCAAG
QPCR	Drosophila Histone 2B rvs	GGATGGACCTGCTTGAGAAC
QPCR	Drosophila Actin fwd	GGCGCAGAGCAAGCGTGGTA
QPCR	Drosophila Actin rvs	GGGTGCCACACGCAGCTCAT
QPCR	Human Histone 3 fwd	GGTAAAGCGCCACGCAAGCA
QPCR	Human Histone 3 rvs	GGCGGTAACGGTGAGGCTTT
QPCR	Human RPL32 fwd	TCTCTTCCTCGGCGCTGCCT
QPCR	Human RPL32 rvs	TCGGTCTGACTGGTGCCGGA
QPCR	Drosophila SLBP fwd	TCCGTGGAGAACACACCGCA
QPCR	Drosophila SLBP rvs	ACTGGAGGCCTCGTCACTGT
QPCR	Renilla fwd	TTATTGAATCGGACCCAGGA
QPCR	Renilla rvs	ACTCGCTCAACGAACGATTT
QPCR	Human GAPDH	GTCTCCTCTGACTTCAACAGCG
QPCR	Human GAPDH	ACCACCCTGTTGCTGTAGCCAA
QPCR	C12orf66 fwd	GCTCGGATGGAGATAGCAGAC
QPCR	C12orf66 rvs	GGACTGAGGATTGGGTGGTG
QPCR	CCDC149 fwd	AAGTCCAGGGCGACAACAAG
QPCR	CCDC149 rvs	CTTCGTCTCCGAGCCTTTGT
QPCR	SCD fwd	GGAGCCACCGCTCTTACAAA
QPCR	SCD rvs	GCCAACCCACGTGAGAGAAG
QPCR	S1PR2 fwd	CCATCGTGCTAGGCGTCTTT
QPCR	S1PR2 rvs	GGAATTCAGGGTGGAGACGG

2.1.3 siRNA

All siRNA came from Dharmacon as one of two types, ON-TARGETplus (OTP) or siGENOME.

Table 2-2. siRNA

siRNA	Type	Sequence/Catalogue number
NT (also called NT 6)	OTP	D-001810-01
CHK1	OTP	AAGAAGCAGUCGCAGUGAAGAUU
NT 1	siGENOME	D-001210-01
NT 2	siGENOME	D-001210-02
NT 3	siGENOME	D-001210-03
NT 4	siGENOME	D-001210-04
NT 5	siGENOME	D-001210-05
NT 7	OTP	D-001810-02
NT 8	OTP	D-001810-03
NT 9	OTP	D-001810-04
NT 10 (pool)	OTP	D-001810-10
NT 11 (RISC free)	siGENOME	D-001220-01
UBB1	OTP	N/A
PLK1	OTP	N/A
ECT2	OTP	N/A
XIAP	OTP	N/A
C12orf66 #1	siGENOME	CCACUUCUAUGAUGACAA
C12orf66 #2	siGENOME	GGACCAGUAUCCAGCUGUA
C12orf66 #3	siGENOME	CAUCUGAUCUGAACAGCUU
C12orf66 #4	siGENOME	AGGCGGUGCUGGAGACGUU
CCDC149 #1	siGENOME	GCACAACUAUUGAGAGAUU
CCDC149 #2	siGENOME	GGAAACAAUCCACGAGAAA
CCDC149 #3	siGENOME	GAUUAAAGCAACUCCAUGA
CCDC149 #4	siGENOME	ACAAAGGCUCGGAGACGAA
SCD #1	siGENOME	GAUAUGCUGUGGUGCUUAA
SCD #2	siGENOME	AGAAUGAUGUCUAUGAAUG
SCD #3	siGENOME	CGACAUUCGCCCUGAUAUA
SCD #4	siGENOME	GGAGUACGCUAGACUUGUC
S1PR2 #1	OTP	UUGCCAAGGUCAAGCUGUA
S1PR2 #2	OTP	CCAACAAGGUCCAGGAACA
S1PR2 #3	OTP	GACAAGAGCUGCCGCAUGC
S1PR2 #4	OTP	GUGACCAUCUUCUCCAUCA

2.1.4 High-throughput equipment

For all experiments using 384-well plates, high-throughput equipment in the Sheffield RNAi screening facility was used. Sterile liquid (e.g. cells, media) was added to wells using a Multidrop Combi (ThermoScientific) and unsterile liquids (e.g. antibodies, PBT) using a Multidrop384 (ThermoScientific). While cells were growing on the plates they were sealed with CO_2 permeable seals using a PlateLoc (Velocity11) plate sealer. The plastic lid was then placed on top and cells were incubated in the appropriate conditions. Plates were also sealed before imaging.

Liquid was aspirated from wells using an ELx405 Select CW (Biotek). Aspiration steps when using S2R+ cells left 25µl in the wells as to not disrupt the cells (except before antibody incubations where 10µl was left). Aspiration steps with human cells only left 10µl as the cells were more adherent. This volume left behind was taken into account when calculating concentrations of solutions and the concentrations described below are the final concentrations.

2.1.5 Graphs and analysis

All Graphs were made using the GraphPad Prism software. Calculations were done using Microsoft Excel.

2.2 General Protocols

2.2.1 DNA Work

2.2.1.1 Processing of Whatman disc

Clone LD10168 containing the *Drosophila cactus* gene came from the Drosophila Genomics Resource Center. DNA was eluted by washing the disc with TE to remove chemicals and then soaking the disc in 50µl TE to elute the DNA. 10µl of this was used for transformation.

2.2.1.2 Transformation

Competent DH5α cells (New England Biolabs) were thawed on ice. 1µg DNA (or 5µl of ligation mix) was added to 20µl of cells and left on ice for 30mins. Cells and DNA were heat shocked at 42^{o}C for 30secs in a water bath and then returned to the ice for 5mins. 200µl room temperature SOC media was added and samples were incubated

at 37°C while shaking, for 1hr. 150µl-200µl of the cell culture was then spread on an agar plate which contained 100µg/ml ampicillin and incubated overnight at 37°C.

2.2.1.3 PCR

PCR amplification of DNA was performed using Phusion polymerase kit (Thermo) as per manufacturer's instructions. Conditions were as Table 2-3 with 1ng of template DNA.

Table 2-3. PCR Conditions

Product	Fwd Primer	Rvs Primer	Annealing Temp.	No. Cycles
UTR-PEST	PCR #1	PCR #2	59°C	35
CON-PEST	PCR #1	PCR #3	60°C	35

2.2.1.4 DNA extraction and purification

Plasmid DNA was extracted from bacterial cultures using Qiagen's Miniprep or Maxiprep as per manufacturer's instructions. DNA was purified after PCR, or enzyme treatment using PCR purification kit (Qiagen) as per manufacturer's instructions.

2.2.1.5 Agarose Gel

Agarose gels were made between 1 and 2%. The required mass of agarose was dissolved in TAE while being heated. Once cooled, but not set, 0.1µl/ml ethidium bromide was added and the gel poured into a Biorad frame. Samples were combined with 5x DNA loading buffer (Bioline) and then loaded and run at 100V until the appropriate bands were in the centre of the gel. Hyperladder I (Bioline) was used to assess the size of bands.

2.2.1.6 Restriction digest

Up to 1µg DNA was digested with 10-20U restriction enzyme(s) (New England Biolabs) in the appropriate buffer at 37°C for 1hr or overnight. If the sample was being used for ligation, the double-digested vectors were treated with 1µl Alkaline Phosphatase to prevent self-ligation.

2.2.1.7 Ligation

Ligation was performed using 10% of purified digested vector DNA (~100ng, 0.025pmol) and 50% of purified insert DNA (~250ng, 2.1pmol). Combined with 1µl T4 DNA ligase (400U) and appropriate buffer, ligation occurred overnight at room temperature. 10% of the ligation was then transformed into competent cells.

2.2.1.8 DNA sequencing

10µl of 100ng/µl plasmid DNA and 10µl 1µM primers were sent to the University of Sheffield Medical School Core Genomic Facility for sequencing. There they were sequenced using an Applied Biosystems 3730 DNA Analyser as per manufacturer's instructions. Results were analysed using ApE - A Plasmid Editor v1.17.

2.2.2 RNA Work

2.2.2.1 RNA extraction

RNA was extracted from cells using one of two methods, Trizol extraction or RNeasy kit extraction.

Trizol extraction: After removing the media and washing the cells with PBS, 1ml of TRI reagent (Sigma) was added to each sample and left for 5mins. Samples were then scraped and transferred to an eppendorf where 200µl chloroform was added. After a brief vortex, samples were left for 5mins at room temperature to allow the layers to separate. The upper layer was then extracted and to it 500µl isopropanol added to precipitate the RNA. After 10mins, the sample was centrifuged at 12000rpm for 10mins and the supernatant removed. After washing the pellet with 70% EtOH, the RNA pellet was resuspended in 20µl H2O.

Kit extraction: RNA was extracted on a column based system using the RNeasy kit (Qiagen) as per manufacturer's instructions. (Only used for Figure 3-4).

2.2.2.2 DNaseI treatment

When histone mRNA was being analysed, RNA samples were DNase treated as normal mRNA specific conditions couldn't be used. When RNA was extracted using Trizol, 4µg of RNA was treated with 1unit of DNaseI for 1hr at 37°C. The reaction was quenched

with 5mM EDTA at 75°C for 10mins. If the RNeasy kit was used, then DNase treatment was performed on the column as per manufacturer's instructions.

2.2.2.3 Reverse transcription

Two methods of reverse transcription were used depending on the target needing to be quantified. If it was histone mRNA, which doesn't have a poly(A) tail, 1µg RNA was reverse transcribed using the Omniscript kit (Qiagen) as per manufacturer's instructions, with 3µl random nonamers (Sigma). If the target wasn't histone mRNA then the High Capacity RNA-to-cDNA kit (Applied Biosystems) was used as per manufacturer's instructions.

2.2.2.4 QPCR

Quantitative PCR (QPC) was carried out using 5µl SYBR Green JumpStart Taq ReadyMix (Sigma), 0.1µl 100µM primers, and roughly 200ng DNA in a well of a 96-well plate (Biorad). Each sample was performed in triplicate due to occasional errors in the machine. Plates were sealed using StarSeal polyolefin film (STARLAB) and then the following reaction carried out on a Bio-Rad C1000 Touch thermal cycler with a CFX96 real-time PCR detection system.

95°C	3min	
95°C	30sec	x 40
62°C	30sec	
	Read	

Melt curve analysis was performed after amplification by increasing the temperature by 0.5°C at a time from 65-95°C and reading the fluroescence.

2.2.2.5 Analysis of QPCR

The results of the QPCR (the Cq values) for each sample was converted into a relative concentration using a standard curve. The standard was made up by combining all samples together and performing 10x serial dilutions. The mean of the triplicate values for each sample was then normalised to the mean of the control target (GAPDH, Actin or RPL32) and, if necessary, this was then normalised to one sample (e.g. 0hrs or NT siRNA).

2.2.2.6 Synthesis of dsRNA

DNA for the equivalent dsRNA was received from the Sheffield RNAi screening facility. This was a PCR product amplified from cDNA using specific primers in Table 2-4 below. The primers were fused to generic t7 primers to aid future steps. To amplify the DNA, 1µl was mixed with 50µl Taq mix, 2µl of fwd and rvs generic T7 primers (see Table 2-1) and 45ul of H_2O and run in the following program:

2mins 94°C
30sec 94°C
1min 57°C } x 35
1min 72°C
2mins 72°C

3µl amplified DNA was then in vitro transcribed into dsRNA using MEGAscript™ T7 High Yield Transcription Kit (Ambion) as per manufacturer's instructions, except that the transcription time was 20hrs and samples were then incubated with DNaseI for 30mins. RNA was precipitated by adding 2.1µl Ammonium acetate and 52.5µl EtOH and samples were frozen from 1hr at -80°C after shaking. Centrifugation at 4000rpm for 50mins then recovered RNA pellets. Pellets were resuspended in 100ul H_2O to give ~1350ng/µl.

Table 2-4. dsRNA synthesis.

Target gene	Forward primer sequence	Forward primer tag	Reverse primer sequence	Reverse primer tag	Amplicon size (bp)
SLBP	AATTACTGTCCTTGGCCGTG	TU	CCCATTCGAGGAACTCAAAA	TS1	357
firefly luciferase (ff)	GGAAGACGCCAAAAAC	TU	CTCTGGCACAAAATCG	TS3	550
Grp	ACGTTCCTATGACCTGGTGG	TU	GAATCGGGTCATTCTCCTCA	TS4	364

2.2.3 Cell Culture

2.2.3.1 Growth conditions

S2R+ cells were cultured in Schneider's *Drosophila* media (Gibco) supplemented with 10% heat-inactivated foetal bovine serum (Sigma Aldrich or Gibco) and 1%

penicillin/streptomycin (Gibco). They were incubated at 25°C and split 1:3-1:5 every three days.

HCT116 cells and HeLa cells were cultured in DMEM (Sigma) supplemented with 10% heat-inactivated foetal bovine serum and occasionally 1% penicillin/streptomycin. They were incubated at 37°C with 5% CO_2 and split 1:10-1:20 approximately every four days.

2.2.3.2 Addition of chemicals

Different chemicals were used as inhibitors or activators during experiments. Many of these were bought as powders and dissolved in water or DMSO as outlined below.

Table 2-5. Chemicals added to cells.

Chemical	Source	Solvent	Stock conc.	Conc. used
Hydroxyurea	Sigma	H_2O	1M	2mM or 10mM
Cycloheximide	Sigma	H_2O	10mg/ml	100µg/ml
Aphidicolin	Fisher	DMSO	30mM	15µM or 60µM
Caffeine	Sigma	H_2O	50mM	5mM
Doxorubicin	Sigma	H_2O	1mM	0.5µM
Nocodazole	Sigma	DMSO	0.5mg/ml	50 or 100ng/ml

When chemicals were added to cells, the chemical was diluted into warmed media at the appropriate concentration and then the existing media was removed from the cells and the chemical solution added gently. When media containing a different chemical was being removed, cells were gently washed in PBS twice, before the new media with chemical was added. Media with the solvent (H_2O or DMSO) was used as a negative control.

2.2.3.3 Transfection of S2R+ cells with dsRNA

Knockdown of target genes in S2R+ cells was carried out by resuspending 2-2.5 $x10^5$ cells in 100µl-500µl serum free media and adding 3.75µg dsRNA for the target gene. The cell-dsRNA mixture was then place in the well of a 24-well plate. After 1hr at 25°C an equal volume of 20% FBS media was added to give a final 10% FBS media. Samples were left for 2-5 days for knockdown to occur.

2.2.3.4 Transfection of S2R+ cells with plasmid DNA

Cells were seeded at $3x10^6$ cells in a 6-well plate the afternoon before transfection. 2µg of plasmid DNA (e.g. 2µg Ren-PEST-UTR or 1µg Ren-PEST-UTR and 1ug pUC19) was transfected using Efffectene (Qiagen) as per manufacturer's instructions. For dual luciferase assays, 1µg of Renilla plasmid, 0.01µg firefly plasmid and 0.99µg pUC19 plasmid were transfected. pUC19 is an empty control plasmid to increase DNA content to 2µg.

2.2.3.5 Transfection of HCT116 cells with siRNA

6-well plate format: Cells were seeded in antibiotic-free media in a 6-well plate at $2.5x10^5$ cells per well 24hrs before transfection. Transfection was performed using Dharmafect1 as per manufacturer's instructions. Briefly, siRNA was diluted to 300nM in DMEM and separately Dharmafect1 diluted to 24µl/ml in DMEM. The two solutions were mixed and left for 30mins before antibiotic-free media was added and the combination applied to cells.

384-well plate format: 5µl 150nM siRNA was added to each well of a sterile 384-well ViewPlate (Perkin Elmer). 1.2% Dharmafect 1 (ThermoScientific) was diluted in DMEM and 5mins after mixing, 5µl of this solution was added to each well. siRNA and transfection reagents were left for 30mins at room temperature to allow complexes to form. While this was incubating, cells were trypsinised off tissue culture flasks and resuspended in antibiotic-free media at the density required. 15µl of cells was then added to each well and the plate sealed. Plates were left at room temperature for 30mins after transfection and then incubated at 37^oC for the required time.

2.2.4 Protein extraction and Analysis

2.2.4.1 S2R+ cell lysis

Cells in 6-well dishes were washed twice in PBS and then 100ul lysis buffer added for 10mins on ice. Samples were then centrifuged at 14000rpm for 10mins at 4°C and the supernatant kept.

2.2.4.2 HCT116 cell lysis

Cells were washed twice with ice cold PBS and then 100ul lysis buffer added (for 6-well plate wells; scaled appropriately for other size wells). Samples were scraped

from the wells and the lysate transferred to an eppendorf. After three freeze thaw cycles (dry ice to 37°C), samples were centrifuged at 13000rpm for 1min at 4°C and the supernatant kept.

2.2.4.3 SDS-PAGE

Resolving gels were typically 12% acrylamide, 375mM Tris (pH8.8), 0.1% SDS, 0.1% ammonium persulphate and 0.04% TEMED. Stacking gels were 5% acrylamide, 125mM Tris (pH6.8), 0.1% SDS, 0.1% ammonium persulphase, 0.1% TEMED. Gels were cast using Biorad Mini-PROTEAN casting system.

Before loading, the protein concentration of samples was measured using a Bradford assay and then an equal mass of protein was prepared for loading. Preparation included adding an equal volume (to the volume of sample) of 2x sample buffer (100mM Tris pH6.8, 4% SDS, 20% glycerol, 200mM DTT and 0.02% bromophenol blue), heating samples at 95°C for 10mins and then centrifuging briefly.

Gels were typically run at 150V in a gel running buffer (25mM Tris pH 8.3, 192mM glycine, 0.1% (w/v) SDS) for 1-2hrs depending on the size of proteins being studied. Molecular weight ladders (ColorPlus Prestained Protein Ladder Broad Range, New England Biolabs) were run alongside lysates to assess the size of bands produced.

2.2.4.4 Western Blotting

In order to detect specific proteins on a membrane, proteins were transferred from the gel onto a nitrocellulose membrane at 100V for 1hr in 25mM Tris, 192mM glycine and 20% methanol.

Once transferred, membranes were blocked for an hour in 5% milk in TBS-T. Membranes were then incubated with primary antibodies (see Table 2-6) in 5% milk-TBS-T overnight at 4°C. After washing 3x for 10mins in TBS-T, membranes were incubated for 1hr at room temperature in the relevant secondary HRP-conjugated antibody at 1:10,000 in 5% milk TBS-T. After this, membranes were again washed 3x for 10mins in TBS-T and then Amersham ECL, Amersham ECL Prime or Amersham ECL Select Western Blotting Detection Reagent (GE Healthcare) was added as per manufacturer's instructions. Bands were imaged by either exposing the membranes to photographic film (Fujifilm RX NIF), which was developed using an Optimax 2010 X-ray film processor or by detecting the chemiluminescence with a UVIPROchemi

camera (Uvitec). (In most instances film was used except where camera use is stated). The intensity of bands was then quantified using UVISoft UVIBand software; if film was used for developing, they were first scanned into digital format.

Table 2-6. Antibodies used in Western blotting.

Antibody	Source	Dilution
Anti-Renilla	Medical & Biological Laboratories	1:1000
Anti-α-Tubulin	Sigma Aldrich	1:2000
Anti-CHK1	In house	1:500
Anti-Nucleolin	Santa Cruz Biotech	1:5000
Anti-CCDC149	Sigma Aldrich	1:5000
Anti-SCD	Abcam	1:5000
Anti-CDK1	Cell Signaling	1:1000
Anti-Phospho-CDK1 (Tyr15)	Cell Signaling	1:500
Anti-Cyclin B1	Cell Signaling	1:500

2.2.4.5 Luciferase assay

Luciferase assays were performed on cells that roughly 8hrs after transfection were seeded into a 96-well plate at $8x10^4$ cells/ml. 3days later the assay was performed. Two difference luciferase assay methods were used. Either the dual-luciferase kit (promega) used as per manufacturer's instruction or an in-house kit with the following protocol. Media was removed from the cells and 20µl BL-lysis buffer added (0.35% triton in BL buffer). 30µl firefly luciferase substrate (42mM DTT, 3.3mM ATP, 0.1mM AMP, 0.46mM D-luciferin in BL buffer) was then added and light levels read on a Varioskan plate reader for 250ms. Immediately afterwards (without removing the firefly substrate), 30µl of Renilla substrate (42mM DTT, 3.3mM ATP, 0.1mM AMP, 0.003mM Coelenterazine in BL buffer) was added and light measured with a 480nm filter for 250ms. Luciferase values from the Promega kits was read using the same protocol.

Renilla luciferase values were normalised to firefly values to account for cell number variation. This resulted in an RL:FL ratio.

2.2.5 Imaging cells

2.2.5.1 Imaging cells on microscope slide

Images were captured on a DeltaVision microscope (Applied Precision) using a 40x objective and deconvolved by in built software. Analysis of replication patterns was performed by eye using ImageJ software. All images within an experiment were acquired at the same exposure and analysed at the same brightness/contrast.

2.2.5.2 Imaging cells on 384-well plate

Images of cells were captured using an ImageXpress Micro microscope (Molecular Devices). For the replication assay, 9 images were taken per well, 500µm apart, with a 20x objective. The DAPI channel was exposed for 16ms and the green and red channels for 2000ms. For the S-M checkpoint assay a 20x objective was used for S2R+ cells and a 10x objective for human cells. Four sites, 500µm apart per well were imaged. The DAPI channel was exposed for 200ms and the green channel for 1500ms. For screening multiple plates, an Automate.it Scara robot (PAA) was used to put the plates in and out of the microscope to decrease the time needed for acquiring.

2.2.5.3 Analysis of images on 384-well plate

Images from the ImageXpress Micro microscope were analysed on the MetaXpress software (Molecular devices). The multi-wavelength cell scoring application was used to quantify the images. For the replication assay, DAPI (blue) staining was used to identify the nuclei of cells and then the average intensity of the green (CldU) and red (IdU) stain in the nuclei was determined. For the S-M checkpoint assay, DAPI staining was again used to identify the nuclei of each cell. The green (phospho-H3) stain was then thresholded and if a cell had above a certain number of pixels that crossed the threshold, the cell was counted as mitotic. The number of mitotic cells was divided by the total number of cells (from the DAPI stain) and a MI was calculated.

2.2.6 Analysis of high-throughput data

2.2.6.1 Normalisation of screen data

In order to analyse the data from the screens data was normalised using the cellHTS2 program (Boutros et al., 2006). Data was $\log_2$ transformed and then divided by the

median of the sample data (no controls) of that plate. Results were converted into z-scores by subtracting the median of all plates of that replicate and dividing by the median absolute deviation (also of all plates of that replicate).

2.2.6.2 Analysis of protein interactions

To analyse known interactions between hit genes, the STRING (Search Tool for the Retrieval of Interacting Genes/proteins) was used (www.string-db.org).

2.3 Experiment protocols

2.3.1 Histone mRNA decay assay

In order to evaluate histone mRNA levels after replication stress, S2R+ cells were seeded at $1.1x10^6$ cells per well of a 6-well plate 24hrs before 10mM HU was added. HU was added to samples in reverse so that even with incubation times varying from 30mins to 15hrs, all samples were harvested at the same time. When the assay was performed in HeLa cells, they were seeded at $2x10^5$ and treated with 5mM HU. When cells were harvested, the RNA was extracted and the concentration measured on a Nanodrop ND-1000 spectrophotometer. DNaseI treatment then occurred to remove genomic DNA and then the RNA was converted into DNA by reverse transcription. A subset of each sample was then taken for the standard curve and the other samples diluted 1 in 10. QPCR of the cDNA was then performed using control gene targets as well as histone mRNA targets. Values were analysed and histone levels calculated as a fold change compared to the untreated (0hr) sample.

2.3.2 Creation of Ren-PEST-UTR and Ren-PEST-CON

In order to clone the PEST sequence of the *Drosophila* cactus protein into the Renilla-histone constructs, the cactus cDNA was eluted from a Whatman disc and transformed into bacteria. It was extracted by mini-prep and the PEST region was amplified up using PCR. Two products were made using different primers: one to insert into Ren-UTR (with histone 3' UTR) and one into Ren-CON (no histone 3'UTR). Once amplified (and checked on an agarose gel), the DNA was purified and digested with XhoI and NheI (Ren-UTR) or Xho1 and PmeI (Ren-CON). The vectors were also digested. After a further purification, inserts and vectors were ligated and transformed into bacteria again. DNA was then extracted by miniprep and sent for

sequencing. Two forward primers and one reverse primer for each construct were used to confirm the correct sequencing.

2.3.3 Measuring the half-life of Renilla

In order to measure the half-life of the Renilla protein with and without the PEST sequence, S2R+ cells were seeded at $3x10^6$ cells per well and 16hrs later transfected with 2µg Ren-PEST-UTR (2 wells) or 2µg Ren-UTR (2 wells). Three days after transfection H_2O or 100µg/ml cycloheximide (CHX) was added and immediately the cells resuspended and 300µl removed. The remaining cells were incubated until later time points, when again the cells were resuspended and a further 300µl removed. Once the cells were removed, they were centrifuged for 3mins at 9000rpm and then lysed with 100µl lysis buffer after washing with PBS. The protein concentration was then calculated and 10µg loaded onto an SDS gel. After western blotting, bands were visualised using a camera and quantified. Exponential analysis of the values was done using GraphPad prism software by fitting the equation:

$$y = (y0 - P)*e^{(-Kx)} + P$$

Where y0 = the y value at time 0 (100%); P = the plateau level which is the amount of signal at time infinity; K = the rate constant; x and y values correspond to graph axis.

To measure the half-life of the protein via its luciferase activity, a similar assay was performed, but a plasmid encoding firefly was also transfected. Cells were then seeded into a 96-well plate and 1µl CHX stock added to each well in reverse time points so that they were all harvested at the same time. A luciferase assay was then performed and Renilla results normalised to the firefly values. Exponential analysis was done using GraphPad prism software fitting the equation above.

2.3.4 Dual-pulse replication assay

2.3.4.1 Microscope slide format

Sterile 13mm coverslips were placed in wells of a 24-well plate and $4\text{-}8x10^5$ cells were seeded 16hrs before pulsing. Cells were pulsed with 30µM 5-chloro-2'-deoxyuridine (CldU, Sigma) for 30mins. This was washed off with PBS and cells treated with 15µM Aph or DMSO (control) for different periods of time. After washing again, cells were pulsed for a second time with 30µM 5-iodo-2'-deoxyuridine (IdU, Sigma) for 30 or

60mins. This was washed off, cells fixed in 70% ice cold ethanol for 15mins and this washed out with PBS.

To permeabilise the membranes to the antibodies, samples were treated with 1.7N hydrochloric acid for 30min. After washing to return the pH back to 7, samples were blocked in 0.2% gelatin in PBT for 1hr. The same blocking buffer was used to dilute the primary antibodies, rat anti-BrdU (Abcam) 1:250 and mouse anti-BrdU (Becton Dickenson) 1:15. The antibodies both recognise 5-bromo-2'-deoxyuridine (BrdU) but one cross reacts with CldU (rat anti-BrdU) and the other IdU (mouse anti-BrdU) (Aten et al., 1992). Coverslips were incubated upturned on primary antibody solution for 1hr in a wet chamber. To reduce cross reactivity between antibodies, samples were washed with a high salt buffer (500mM NaCl, 36mM Tris-HCl, pH 8) for 10mins and then washed twice in PBT. Conjugated secondary antibodies (donkey anti-rat FITC and goat anti-mouse TRITC (Jackson laboratories)) were used at a 1 in 100 dilution and incubated with samples for 1hr in the dark. After washing with PBT, nuclei were stained with 2µg/ml DAPI and washed again before mounting the ProLong Gold onto microscope slides.

2.3.4.2 384-well plate format

As above but with some variation. Cells were seeded into a subset of wells of a 384-well plate at $5x10^4$ cells in 50µl per well. 24hrs later media was removed and 30µM CldU added for 15mins. After washing with PBS, cells were treated +/- 15µM Aph and +/- 5mM caffeine for 6hrs. Once this was washed out cells, were incubated for 60mins in normal media to allow replication to recover. Cells were then pulsed with 30µM IdU for 30mins, washed and fixed in 70% ethanol.

Staining of the cells was as the slide format with a working volume of 60µl per well. 20µl primary antibody mix (rat anti-BrdU 1:500, mouse anti-BrdU 1:25) was used and 30µl secondary antibody mix (anti-mouse AlexaFluor 647 1:500 and anti-rat AlexaFluor 488 1:500 (Invitrogen)) and incubated for an hour each. After DAPI staining for 5mins cells were washed and left in 50µl PBT for imaging.

2.3.5 S-M Checkpoint assay

2.3.5.1 In S2R+ cells

Cells were seeded into a 384-well plate at $2x10^4$ cells per well in 50µl volume two days before treatment. Media was then removed and 30µl inhibitors were added in reverse time order (30hrs first, 4hrs last) so that all were completed at the same time. Aph was used at 15µM and 60µM, HU at 10mM, doxorubicin at 0.5µM and caffeine at 5mM. After treatment the media was aspirated and 4% PFA added for 10mins to fix the cells. After washing with PBT, cells were blocked in 0.2% gelatine (in PBT) for 30mins and then incubated overnight in primary antibody mix (PhosphoDetect™ Anti-Histone H3 (Calbiochem) used at 1 in 2000 in 0.2% gelatin/PBT). Cells were washed with PBT and then incubated for an hour with anti-rabbit AlexaFluor 488 (Invitrogen) used at 1 in 1000. After washing, cells were incubated with 2µg/ml DAPI, washed again and imaged.

2.3.5.2 In Human cells

The S-M checkpoint in human cells was performed multiple times with slight variations. Table 2-7 shows the details for each individual experiment. In brief, human cells were either seeded directly onto a 384-well plate or added during the siRNA transfection protocol. After allowing cells to settle or be knocked down, 25µl 4mM HU (or 30µM Aph or 1µM doxorubicin) was added on top of the existing media to activate the checkpoint and give a final concentration of 2mM (15µM Aph and 0.5µM doxorubicin). After a period of time, media and inhibitors were aspirated off and 50µl cold, 4% PFA was added for 10mins. Wells were then washed twice by removing media and adding 50µl PBT for 3mins. After removing the second wash, 50µl 0.2% gelatin was added for 30mins to block protein binding sites. After removing this, 20µl primary antibody mix was added (Anti-Histone H3 (phospho-S10) – Mitosis Marker (Abcam) diluted in 0.2% gelatin/PBT) and incubated with cells overnight (~16hrs). In the morning, cells were washed twice with PBT and incubated for an hour with 20µl anti-rabbit AlexaFluor 488 (Invitrogen) also diluted in 0.2% gelatin/PBT. After washing cells twice more following this incubation, 30µl 2µg/ml DAPI (in 0.2% gelatin/PBT) was added for 2mins. After a final two washes, the last 50µl PBT was left on the plates and they were sealed for imaging.

Table 2-7. S-M Checkpoint conditions in HCT116 cells.

Experiment	Cells/well	Seeding - HU (hrs)	HU - fix (hrs)	Primary antibody conc.	Secondary antibody conc.
2 cell lines (Figure 5-1)	$1x10^4$	6 or 24	24 or 6	1:2000	1:1000
HU timing optimisation (Figure 5-2B)	$5x10^3$	6-51	2-48	1:2000	1:1000
Antibody optimisation (Figure 5-2C)	$2.5x10^3$	30	24	1:500-1:4000	1:250-1:2000
Knockdown timing optimisation (Figure 5-2E)	$1.8\text{-}5x10^3$	7-55	24	1:500	1:500
Seeding density optimisation (Figure 5-2F)	$0.75\text{-}2.5x10^3$	48	24	1:500	1:1000
Control plate (Figure 5-3)	$2.5x10^3$	30	24	1:2000	1:1000
Kinome-Phosphatome (Figure 5-4)	$1.75x10^3$	48	24	1:500	1:1000
Genome-wide screen (Figure 6-1)	$1.75x10^3$ (batch 3 $2x10^3$)	48	24	1:500	1:1000

2.3.6 Flow cytometry to identify premature mitosis

Cells were seeded at $1.5x10^6$ cells in a 100mm dish and after 24hrs transfected with siRNA as described in section 2.2.3.5 – 6 well plate format. 28hrs later cells were trypsinised, antibiotic-free media added and split in half into two 100mm dishes. After being allowed to settle for 20hrs, the media was removed and 2mM HU (in media with antibiotics) was added to half of the dishes (one per knockdown) and the others had normal media (with antibiotics) added 5hrs later, media was removed and to the HU-treated samples, media with 2mM HU and 100ng/ml nocodazole was added. To the untreated samples, media with 0.02% DMSO was added. One dish was also just treated with 100ng/ml nocodazole for 19hrs as a positive control for identifying mitotic cells.

After all the above treatments, cells were ethanol fixed as follows. Cells were washed with PBS and then trypsinised to detach from the culture dish. 9ml IFA was added (to 1ml trypsinised cells) and cells centrifuged at 1000rpm for 5mins. The cell pellet was resuspended in 500µl supernatant and 4.5ml ice cold 70% ethanol added dropwise whilst shaking the cells gently over a vortexer. The cells were left on ice for 30mins and then centrifuged, resuspended and ethanol added as before. After a final 30mins on ice, samples were stored at -20°C for up to four days.

To stain the fixed cells, samples were centrifuged at 1000rpm for 5mins at 4°C, supernatant removed and 10ml ice cold PBS added. Samples were centrifuged as before and 2ml ice cold permeabilisation buffer (0.5% BSA, 0.25% Triton X-100 in PBS) added to the pellet. After resuspension and incubation on ice for 15mins, samples were centrifuged again and supernatant removed. They were then incubated with 100µl of primary antibody mix (1 in 200 dilution of anti-phospho histone H3 (Abcam) in permeabilisation buffer) at room temperature for 30mins followed by a further 30mins on ice. Samples were then washed twice with 0.25% Triton X-100 in PBS by adding 1ml, centrifuging at 2200rpm for 5mins at 4°C and removing the supernatant. After this, cells were incubated for 30mins in the dark with the secondary antibody, anti-rabbit AlexaFluor 488 (Invitrogen), at a dilution of 1:100 in 1% BSA in PBS. The secondary antibody was washed out by adding 1ml PBS and centrifuging for 2200rpm for 5mins at 4°C and removing the supernatant. Finally, 205µl of 25µg/ml RNaseI and 20µg/ml propidium iodide in PBS was added to the samples and incubated on ice for at least 30mins to stain the DNA.

To examine the cells, a BD Biosciences LSR II flow cytometer was used and then the data were analysed using the FloJo program.

3. Histone mRNA decay in *Drosophila* cells

3.1 Introduction

Histone mRNA levels dramatically fall after replication stress (Borun et al., 1975; Heintz et al., 1983). While there is significant understanding of the mechanism by which histone mRNA is degraded at the end of S-phase, relatively little is known about the components that work to trigger this decay after replication stalling. To try to develop an RNAi screen to investigate this mechanism a robust assay, amenable to high-throughput analysis is required. I set out to develop this using a luciferase reporter in Drosophila S2R+ cells.

Histone mRNA decay upon treatment with the ribonucleotide reductase inhibitor, HU, has been shown previously in mammalian cells (Sittman et al., 1983b) and yeast (Herrero and Moreno, 2011) but not in *Drosophila*. Therefore the starting place for the investigation was to determine whether *Drosophila* S2R+ cells respond similarly.

3.2 Results

3.2.1 Histone mRNA decay

Previously histone mRNA decay has been extensively studied using northern blotting, but as this is not easily converted into a high-throughput format, I developed a method using QPCR. In brief, RNA was extracted, DNase treated and then reverse transcribed using random nonamers as primers to produce cDNA of the entire RNA of the cells including the histone mRNA. (Usual oligo-dT primers could not be used due to histone mRNAs not having a poly(A) tail). With specific histone primers the relative quantity of histone cDNA could then be assessed by QPCR.

Drosophila S2R+ cells were treated with 10mM HU for up to 15hrs. It can be seen in Figure 3-1A and B that replication stress-induced histone mRNA decay occurs in S2R+ cells, as both histone 3 and histone 2B mRNA levels fall after 2hrs HU treatment to 50% of untreated levels. Interestingly, the levels rise again after longer treatment, possibly due to some form of checkpoint override.

Both the rate and the extent of histone mRNA decay observed in *Drosophila* S2R+ were significantly lower than that reported in mammalian cells (Müller et al., 2007).

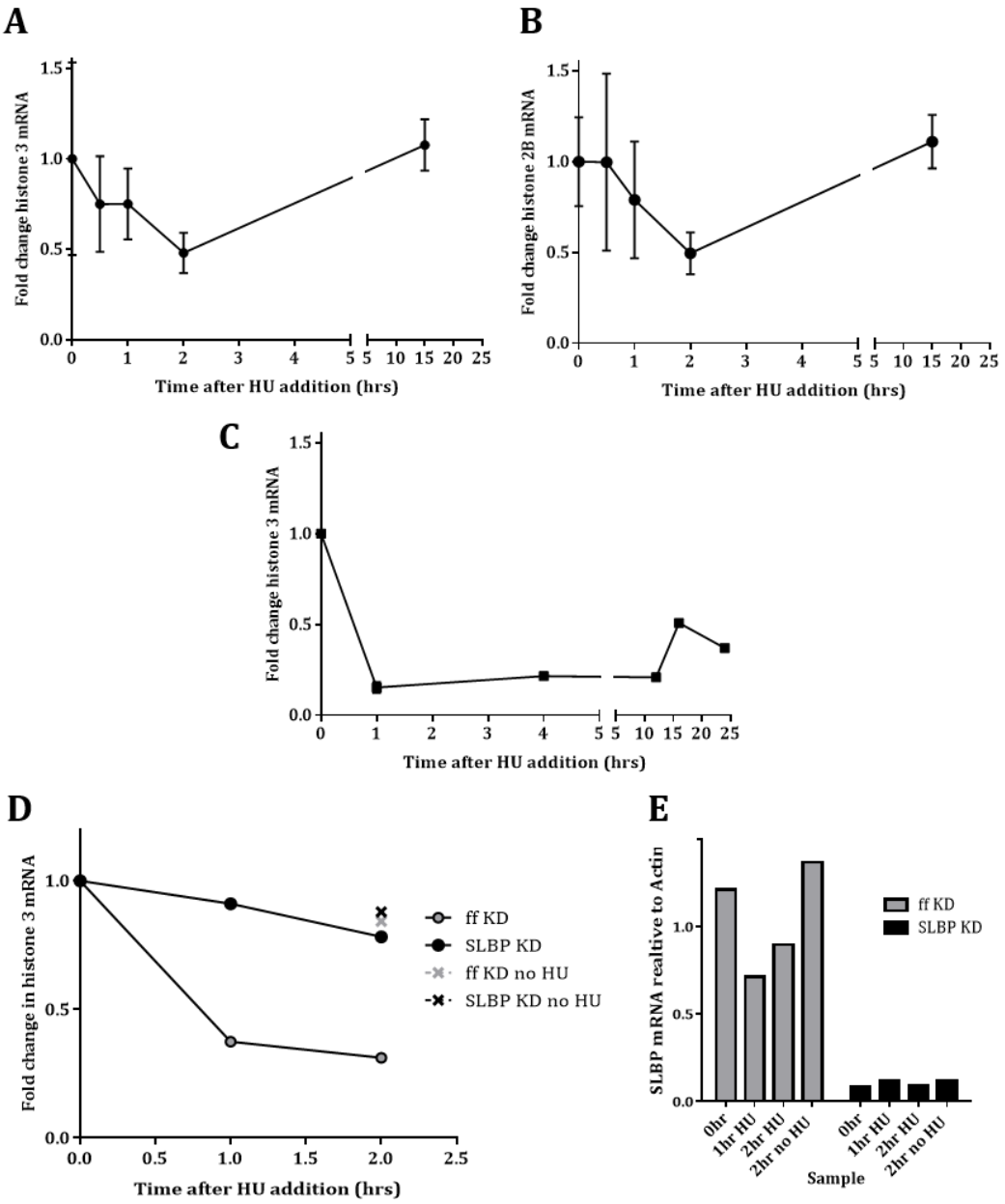

Figure 3-1. Histone mRNA decay in S2R+ and HeLa cells.

A. S2R+ cells were treated with 10mM HU for the indicated periods and RNA levels were quantified by QPCR. Histone 3 mRNA levels were normalised to the loading control actin and the 0hr sample. Error bars = SD n=3. **B.** As A but with Histone 2B mRNA levels measured. **C.** HeLa cells were treated with 2mM HU for various time periods and histone 3 mRNA quantified as in A. Loading control was RPL32. (Experiment performed by Vicky Gotham) n=1. **D.** S2R+ cells were transfected with dsRNA targeting SLBP or firefly (ff, negative control). After 72hrs cells were treated with 10mM HU for the indicated periods of time (cross for samples not treated with HU). RNA levels quantified as in A. N=1 **E.** SLBP mRNA levels of samples in D, quantified in the same manner as histone mRNA levels.

In order to confirm that this was not simply due to some artefact associated with the QPCR methodology adopted here, histone mRNA levels were also examined in HeLa cells following hydroxyurea treatment (Figure 3–1C). In HeLa cells after 1hr HU treatment, histone mRNA levels were reduced to 15%, in contrast to the 75% in S2R+ cells. In HeLa cells prolonged exposure to hydroxyurea also resulted in an increase in histone mRNA levels, although, the levels did not return to 100% as was observed in S2R+ cells.

Histone mRNA decay in S2R+ cells is, nonetheless, dependent on SLBP as it is in mammalian cells (Sullivan et al., 2009). Efficient knockdown of SLBP at the mRNA level (Figure 3-1E), eradicated the HU dependent decay of histone mRNA (Figure 3-1D). Therefore even though decay doesn't occur as effectively as in mammalian cells, S2R+ cells do reduce histone mRNA levels in response to replication stress, in a manner which is dependent on SLBP, suggesting that these cells could be used as a system for a genome-wide screen with histone mRNA decay as the endpoint.

3.2.2 Creation of destabilised luciferase histone mRNA reporter

In order to create a reporter molecule, amenable to high-throughput screening, I set out to build a luciferase-based system in which luciferase mRNA would be engineered to behave analogously to histone mRNA in response to replication stress. Thus, a Renilla luciferase construct with the *Drosophila* histone3 3'untranslated region (UTR) stem-loop (Ren-UTR) was created (a kind gift of Debbie Sutton, Smythe Lab, University of Sheffield). As the stem-loop is the only cis element required for decay (Pandey and Marzluff, 1987) this luciferase construct would be expected to be degraded in a manner similar to histone mRNA. A control plasmid without the histone 3' UTR was also generated (Ren-CON) for reference purposes.

In an attempt to improve the responsiveness of luciferase protein levels to rapid changes in its cognate mRNA levels, both constructs were modified to incorporate amino acid sequences known to promote protein destabilisation. PEST sequences are proline, glutamine, serine and threonine rich and are signals for fast proteolysis (Rechsteiner, 1990; Rogers et al., 1986). The PEST sequence from mouse ornithine decarboxylase is often used to destabilise proteins in mammalian cells, but a destabilised *Drosophila* protein with an endogenous *Drosophila* PEST sequence had not previously been constructed. The PEST sequence from the C-terminal of the

Drosophila Cactus protein was chosen as it controls the signal-independent degradation of Cactus and when deleted the protein is three times more stable (Belvin et al., 1995). It was cloned into the C-terminus of Renilla luciferase upstream of the stop codon to create plasmids Ren-PEST-UTR and Ren-PEST-CON (Figure 3-2).

To confirm the destabilisation of the Renilla protein by the Cactus-derived PEST sequence, cycloheximide (CHX), which inhibits translation, was added to cells transfected 72h previously with either the Ren-PEST-UTR or Ren-UTR plasmids. Levels of Renilla protein remaining after CHX treatment were determined by immunoblotting (Figure 3-3A). A dramatic decay, dependent on the presence of the PEST sequence, was observed. Exponential analysis of the intensity of the bands (Figure 3-3B) calculated a half-life of 1.7hrs for Ren-PEST-UTR compared with over 24hrs for Ren-UTR.

Similar results were also achieved when the Renilla luciferase activity was measured after CHX addition (Figure 3-3C). The half-lives for both Renilla constructs were shorter than with immunoblot analysis, with Ren-PEST-UTR having a half-life of 0.7hrs and Ren-UTR 3.5hrs. These data indicate that Renilla luciferase may be functionally less stable than firefly luciferase (used to normalise) resulting in a shorter half-life. In conclusion the PEST sequence significantly destabilises the Renilla protein making it a more suitable reporter for histone mRNA decay.

3.2.3 Luciferase mRNA decay

To confirm the functionality of the stem-loop in the Renilla construct, Ren-PEST-UTR and Ren-PEST-CON (as a control) were transfected into S2R+ cells and histone and Renilla mRNA levels measured after HU addition. As can be seen in Figure 3-4A when the stem-loop is present in the 3'UTR, the Renilla mRNA levels fall after HU addition, similar to that observed with histone mRNA. The levels do rise slightly following 2hrs HU treatment, possibly due to high levels of transcription from the actin promoter, used in this system. Figure 3-4B shows that without the stem-loop (Ren-PEST-CON) HU-induced decay is not observed, confirming the necessity of the stem-loop in conferring instability in mRNAs in response to replication stress.

3.2.4 Luciferase protein levels and activity

The final test of the Renilla reporter was to see if the decrease in Renilla mRNA after replication stress caused a decrease in protein levels and subsequently a decrease in

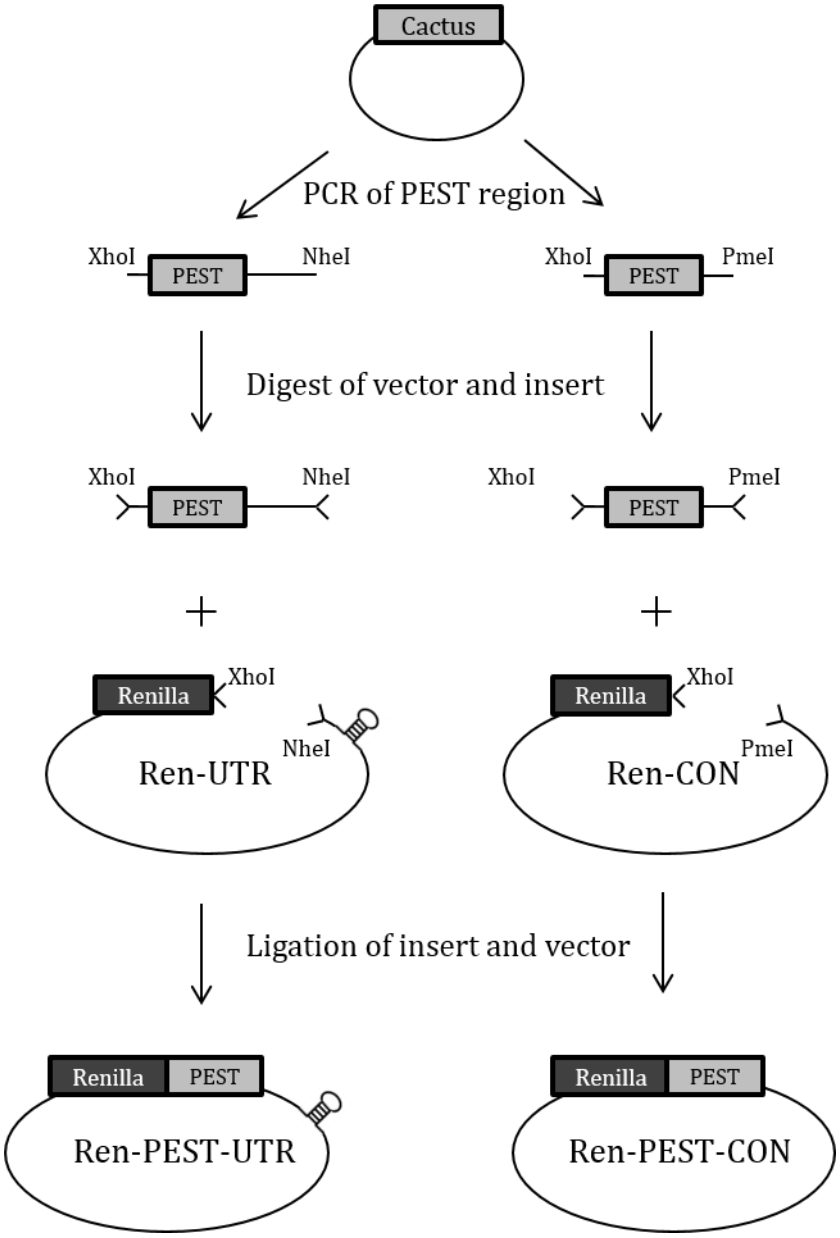

Figure 3-2. Strategy for the creation of Ren-PEST-UTR and Ren-PEST-CON.

Drosophila PEST region was amplified from Cactus cDNA, digested and inserted into Renilla luciferase constructs with and without histone 3' UTR (drawn as stem-loop). Details in materials and methods.

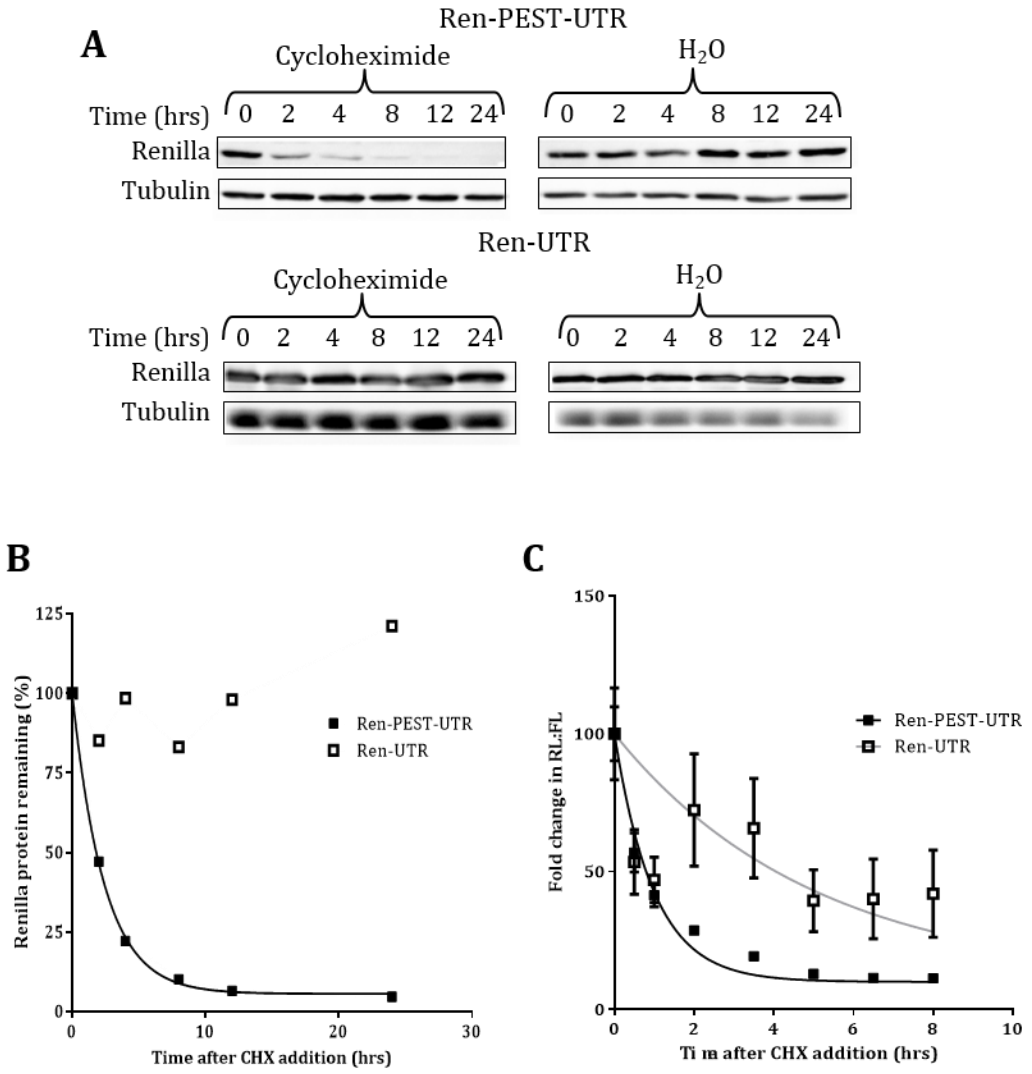

Figure 3-3. Renilla luciferase is destabilised by the addition of a PEST sequence.

A. S2R+ cells were transfected with Ren-PEST-UTR or Ren-UTR and after 3 days 100ug/ml CHX (or H_2O as a control) was added. After indicated periods of time, cells were lysed and Renilla and tubulin (loading control) levels were determined by immunoblotting. Bands were visualised using the camera. Renilla band ran at ~38kDa with PEST and ~32kDa without. Tubulin band ran at 50kDa. **B.** Quantification of bands from A (left-hand panels). Renilla intensity was normalised to the tubulin intensity and 0hr sample. Exponential analysis calculated half-life of Ren-PEST-UTR as 1.7hrs. **C.** S2R+ cells transfected as in A but also with firefly plasmid. CHX was added and luciferase activity measured after lysis. Renilla luciferase values (RL) were normalised to firefly luciferase values (FL). Exponential lines plotted and half-lives of Renilla activity 0.7hrs for Ren-PEST-UTR and 3.5hrs for Ren-UTR. Error bars = SEM of three replicates.

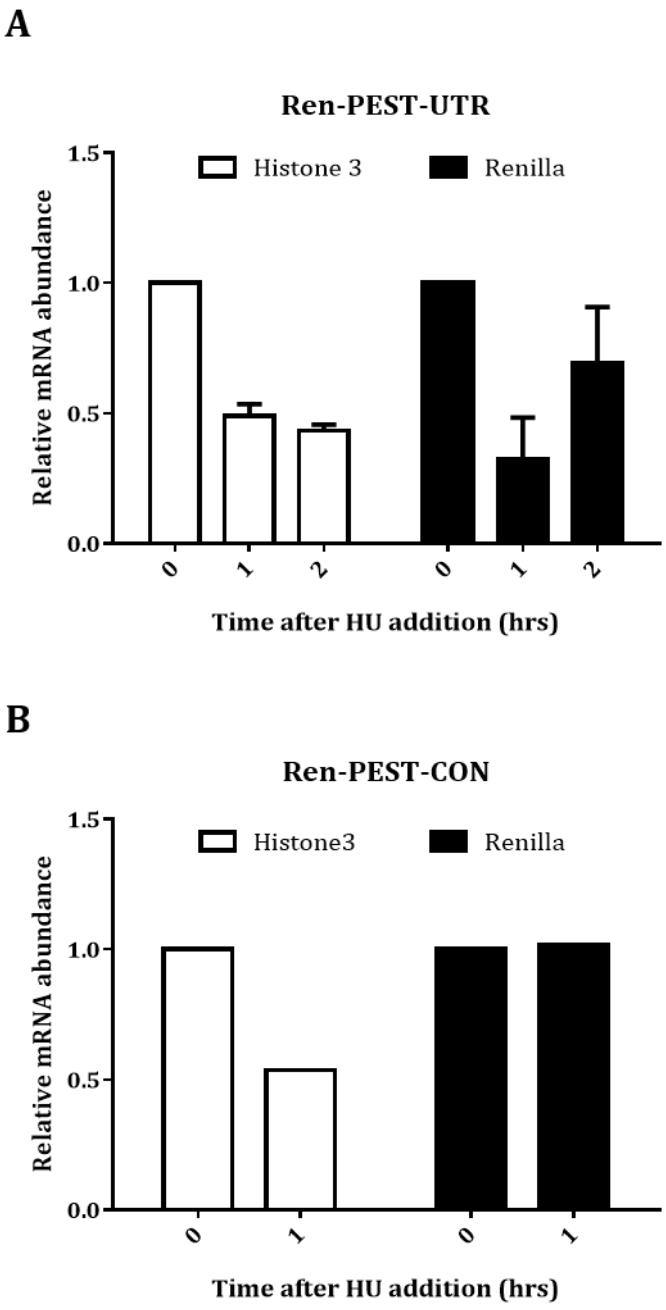

Figure 3-4. Addition of the stem-loop causes replication dependent decay of Renilla mRNA.

S2R+ cells were transfected with either Ren-PEST-UTR **(A)** or Ren-PEST-CON **(B)** and after 2 days 10mM HU was added for 0-2hrs. RNA was extracted using the RNeasy kit (Qiagen). Histone and Renilla RNA levels were normalised to actin mRNA levels and the 0hr sample. A n=2, error bars show sd. B n=1.

luciferase activity. S2R+ cells were transfected with Ren-PEST-UTR and after two days cells were treated with HU (Figure 3-5). The left hand panel of Figure 3-5A shows that the Renilla protein levels don't decrease upon treatment of S2R+ cells with 10mM HU for up to 12hrs. I repeated the experiment exposing cells to prolonged HU exposure (right hand panel), however, no decrease was observed even after 24hrs HU treatment.

The same result was also observed when measuring the luciferase activity of the Renilla reporter. Figure 3-5B shows a slight decrease in Renilla activity in the Ren-PEST-UTR transfected cells after 2hrs of HU treatment but the same decrease is seen with the addition of H_2O and with the Ren-PEST-CON construct. The Ren-PEST-UTR construct gave significantly lower Renilla/Firefly luciferase ratios compared to Ren-PEST-CON indicating that the expression level of renilla, in which the 3'UTR contains a histone mRNA derived stem loop, is substantially reduced. This implies that the stem-loop confers a reduction in mRNA levels and presumably as a consequence, reduces protein and luciferase activity, but there is no effect of replication stress on luciferase activity.

3.3 Conclusions

The inability of the protein levels and activity of the luciferase reporter to respond to replication stress means it cannot be used as a reporter for histone mRNA decay. This is likely to be due to a combination of many reasons that include the inefficiency of histone mRNA decay in S2R+ cells, the recovery of histone and renilla mRNA after longer periods of replication stress and the half-life of the renilla protein.

Histone mRNA decay occurs in S2R+ cells but not to such a dramatic extent as in mammalian cells. This may be due to the fact that these cells are derived from a late embryonic stage where the histone levels have only just started to be cell cycle regulated, after previously being mass produced and supplemented with maternal histone mRNA (Anderson and Lengyel, 1980). There may also be other mechanisms to regulate histone levels in *Drosophila,* with the consequence that regulation at the mRNA level is not so tightly controlled.

The observation that there is a recovery in histone mRNA levels after prolonged replication stress is unexpected. The recovery, observed in both S2R+ cells and HeLa cells implies that it may be conserved across evolution in metazoans. It is known that after prolonged exposure to DNA damage, yeast have a mechanism to adapt and over-

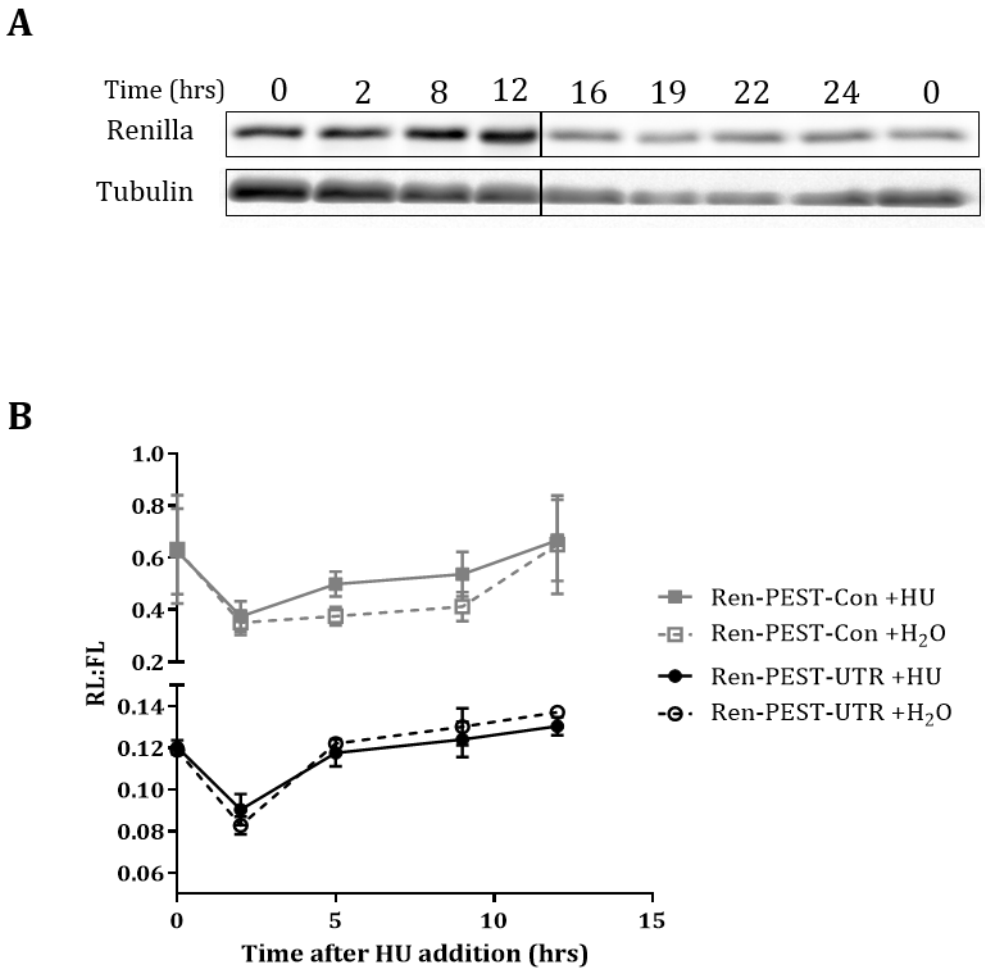

Figure 3-5. Addition of the stem-loop doesn't cause replication dependent decay of Renilla protein or activity.

A. S2R+ cells were transfected with 1ug Ren-PEST-UTR and after 2 days 10mM HU added for indicated time periods. Cells were lysed and Renilla and tubulin levels visualised via western blotting. The boxes separate two different experiments each with their own 0hrs time point. All samples ran on the same gel. Renilla ran at ~38kDa and tubulin at ~50kDa. **B.** S2R+ cells were transfected with either Ren-PEST-UTR or Ren-PEST-CON along with firefly luciferase and after 3 days 10mM HU or H_2O was added for 0-12hrs. Luciferase levels were assayed using the dual-luciferase kit (Promega). Error bars = standard deviation for 5 technical replicates on one 96-well plate.

.

ride the G2/M checkpoint (Toczyski et al., 1997), however a similar response in other organisms has not been observed. It may be that there is an additional layer of complexity associated with the S-phase checkpoint, comprising a mechanism that is activated to inhibit the S-phase checkpoint after prolonged stress, to encourage the cell to attempt the completion of S-phase. An alternative explanation is that the initial checkpoint signalling mechanism becomes attenuated with time, resulting in eventual cell cycle progression.

This increase in mRNA levels occurs even quicker with the Renilla reporter. This may be due to the fact that the renilla gene is under the control of the Drosophila actin promoter which gives a high level of expression. It is conceivable that the capacity of the histone mRNA decay pathway is limited and cannot respond proportionately to the relatively high levels of mRNA generated in this artificial system.

The cactus PEST sequence added to the Renilla gene caused a dramatic decrease in protein half-life. This is the first time that an endogenous *Drosophila* sequence has been used to destabilise a protein. The half-life decreased to about 1.5hrs from 24hrs but this may still not be short enough to be able to report histone mRNA decay.

4. Other S-phase checkpoint responses in *Drosophila* cells

4.1 Introduction

There are many outcomes from activation of the S-phase checkpoint, other than histone mRNA decay, so I sought to investigate whether these could be used for an RNAi screen in S2R+ cells.

Activation of the S-phase checkpoint by replication stress also causes inhibition of late origin firing and stabilisation of the active replisomes. Eukaryotic chromosomes are replicated from multiple origins which are programmed to initiate replication in a precise temporal sequence throughout S-phase (Diffley, 1998; Gilbert, 2002; Ma et al., 1998). The spatial pattern of sites of active replication indicates their temporal position within S-phase, allowing the dynamics of groups of co-ordinately replicating chromosomal domains to be monitored (Feijoo et al., 2001). As replication occurs in distinct patterns during different phases of S-phase (O'Keefe et al., 1992) the functionality of this aspect of the S-phase checkpoint can be monitored using a dual-pulse replication assay (Aten et al., 1992; Dimitrova and Gilbert, 2000; Feijoo et al., 2001).

Briefly this involves pulsing asynchronous cells with a thymidine analogue (e.g. 5-chloro-2'-deoxyuridine (CldU)) which is incorporated into actively replicating DNA. Cells are then treated with a replication inhibitor to activate the checkpoint. After a period of time has elapsed, the inhibitor is removed, and after recovering, cells are pulsed with a different thymidine analogue (e.g. 5-iodo-2'-deoxyuridine (IdU)) to mark the newly replicating regions. The two thymidine analogues can be identified and distinguished from one another by analogue-specific antibodies (Aten et al., 1992) and these may be imaged by fluorescent microscopy. If the checkpoint is functional, then replication forks should be reversibly arrested in the presence of the replication inhibitor and later origins be prevented from firing. Therefore, following removal of the inhibitor, the spatio-temporal location and patterns of each analogue should overlap (Dimitrova and Gilbert, 2000; Feijoo et al., 2001).

Replication stress also activates the S-M checkpoint which prevents cells entering mitosis when replication isn't complete. This can be measured by quantifying cells positive for phosphorylated histone H3 serine10 (phospho-H3), a marker of mitosis

(Gurley et al., 1974; Hendzel et al., 1997; Shoemaker and Chalkley, 1978), after replication stress. The S-M checkpoint has been previously been well studied in yeast and to some extent in mammalian cells but I sought to see if it was also a functional checkpoint in *Drosophila* S2R+ cells.

4.2 Results

4.2.1 Dual Pulse replication assay in S2R+ cells

4.2.1.1 Replication Patterns in S2R+ cells

Replication patterns in many cell types progress from a speckled wide-spread 'early' pattern to a distinct 'late' pattern comprising a small number of large puncta (O'Keefe et al., 1992) during S-phase, reflecting the progressive activation of multiple origins of replication as discussed previously. I wanted to establish whether replication origin firing in Drosophila S2R+ cells could be monitored using this approach. Synchronised cells are primarily used to observe the replication pattern throughout S-phase (O'Keefe et al., 1992) though cell cycle synchronisation can be challenging in *Drosophila* cells (Rizzino and Blumenthal, 1978). I therefore used a dual pulse protocol utilising thymidine analogues to characterise patterns of replication throughout S-phase. Cells were pulsed with CldU to identify those initially in S-phase and then, after differing periods of time in media, pulsed with a second analogue (IdU) to visualise cells in S-phase at the later time point.

By studying and quantifying the patterns of the IdU incorporation in cells that had not previously incorporated CldU, I initially established the spatio-temporal order of replication patterns in S2R+ cells. The patterns that were observed at early time points consisted of small speckles across the euchromatic compartment of the nucleus. With increasing time, this pattern progressively decreased while there was significant labelling of the perinuclear region and nucleolar periphery. Later, patterns comprising small numbers of large puncta increased significantly. These data, which are consistent with those obtained in other metazoan cells (O'Keefe et al., 1992) enabled me to define the replication patterns during different stages of S2R+ S-phase (see Figure 4-1).

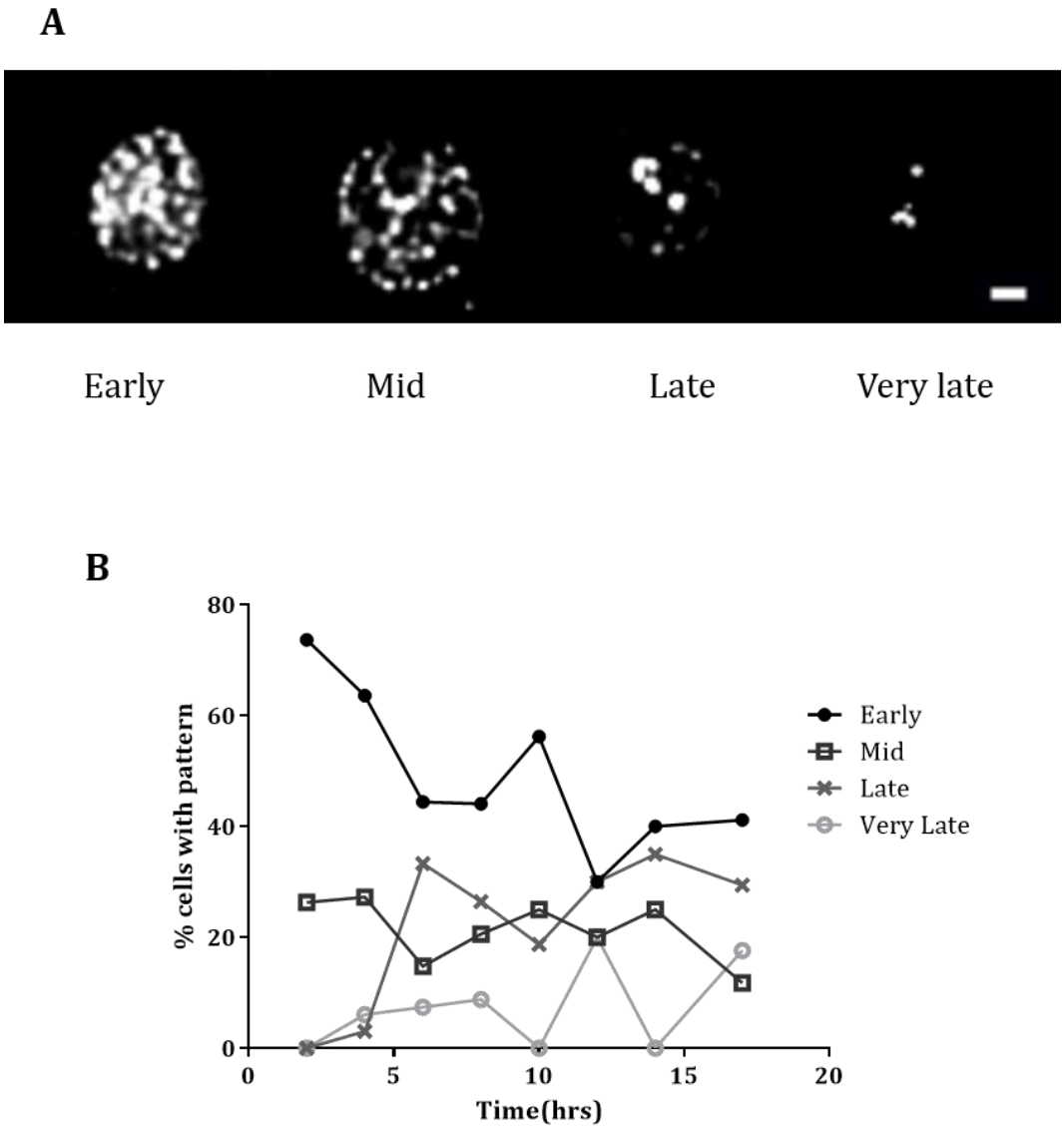

Figure 4-1. Replication patterns in S2R+ cells.

S2R+ cells were seeded at $8x10^5$ cells per well of a 24 well plate and were pulsed with CldU for 30mins, washed and incubated in normal media for 0-17hrs. Cells were then pulsed with IdU for 30mins and cells were fixed and stained as described in materials and methods. **A.** The different patterns were categorised upon their timing that they appeared in the IdU+ CldU- population (cells who entered into S-phase between the two pulses). Figures show IdU staining. Scale bar = 1μm **B.** Quantification of the % of CldU negative cells that showed the IdU patterns. Between 10 and 34 IdU+ CldU- cells were analysed per condition.

4.2.1.2 S-phase checkpoint replication effects in S2R+ cells

When the S-phase checkpoint is activated by addition of a replication inhibitor for various time periods after the first thymidine analogue pulse, and washed out prior to the second, it is expected that the same pattern of incorporation would be observed with each analogue with a significant degree of co-localisation. As shown in Figure 4-2, when cells are treated with 15μM Aph between pulses, a high percentage of cells display the same replication pattern with each analogue (see Figure 4-2A), although the degree of co-localisation was variable and lower than expected. Nonetheless, the pattern obtained contrasted with cells incubated in mock-treated media, where cells continued to progress through S-phase between pulses, resulting in non-co-localised distinct pattern types in these cells (Figure 4-2B).

These results are similar to those observed previously in mammalian cells (Dimitrova and Gilbert, 2000; Feijoo et al., 2001; Müller et al., 2007) although, here, the ability of the checkpoint to facilitate resumption of replication at the same location appeared to be limited in the Drosophila S2R+ cell system. The error bars shown in Figure 4-2C indicate the large variation between three separate experiments performed in the same way. The data also show that, even at the shortest periods of replication arrest tested (about two hours), only approximately 40% of doubly-labelled cells retained the same replication pattern. This is in contrast to observations in mammalian cells which shows 100% efficiency even after 12hrs Aph (Müller et al., 2007). This apparent difference was not due to an insufficient concentration of Aph used in these experiments (which would enable cells to progress, however slowly, through S-phase) as even 1μM Aph completely inhibits DNA replication in S2R+ cells (data not shown).

There was also a decrease in the proportion of cells that resumed replication in the same spatial location 8hrs after the replication inhibitor had been washed away. This could have been due to cells not being able to recover from prolonged replication inhibition, or alternatively, that the cells have progressed into a later cell cycle stage and are no longer in S-phase, (16% of cells with an early CldU pattern had a late IdU pattern after 8hrs Aph, whereas the rest have no IdU staining (data not shown)). Either way, these data imply that the ability of the S-phase checkpoint to stabilise arrested replication forks and suppress initiation of replication at late origins is significantly limited in S2R+ cells.

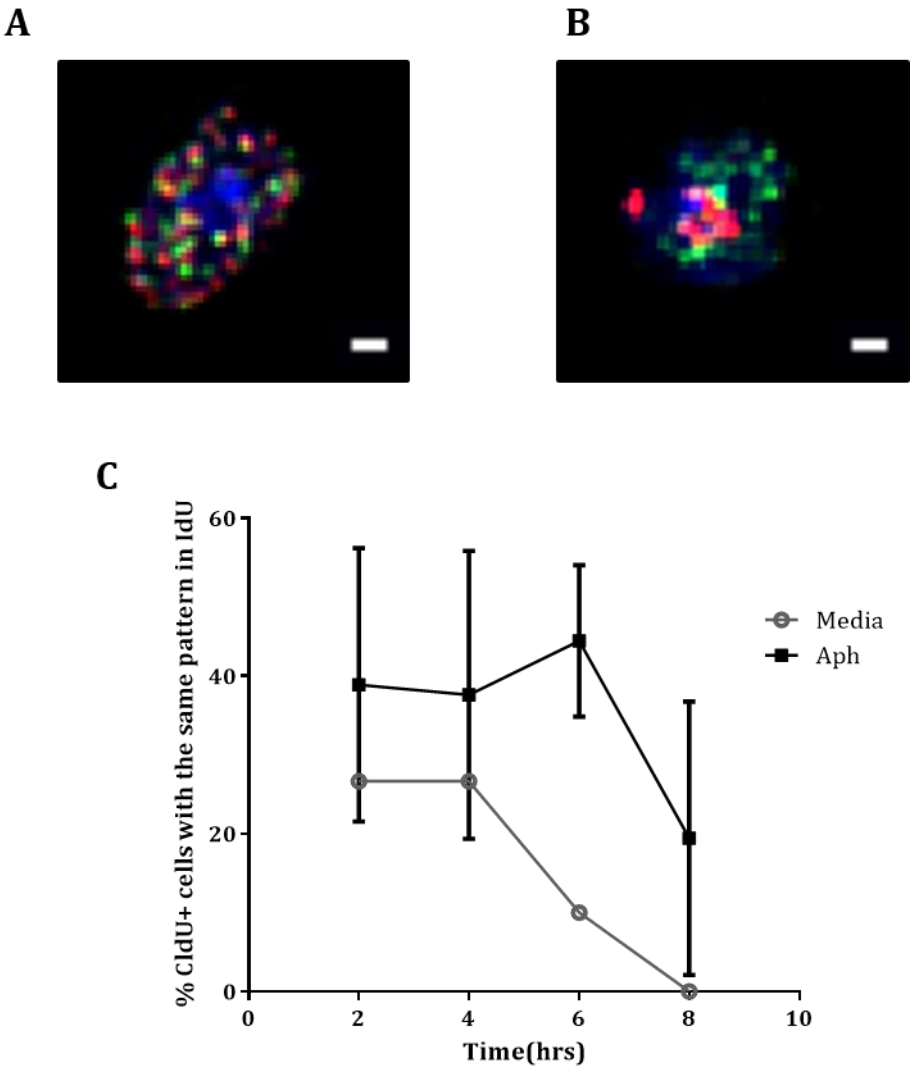

Figure 4-2. Replication stress causes stalling of S-phase progression.

S2R+ cells were pulsed with CldU for 30mins, treated with 15μM Aph or media (control) for 2-8hrs and then pulsed with IdU for 60mins. **A.** Example cell treated with Aph for 4hrs showing early pattern of replication for both CldU (green) and IdU (red) with DAPI staining the nuclei (blue). Scale bar = 1μm. **B.** Example cell treated with media for 4hrs between pulses showing early pattern with CldU (green) and late pattern with IdU (red). Scale bar = 1μm. **C.** Quantification of the percentage of CldU positive cells that have the same pattern with the two analogues. Experiment was performed using 3 separate coverslips per time point for Aph treated samples (error bars show sd) and one coverslip for media treated. Each coverslip was imaged 5 times and at all stained cells were counted (between 5 and 23 cells per coverslip).

4.2.1.3 Inhibiting the S-phase checkpoint in S2R+ cells

The replication effects of the S-phase checkpoint have been shown in mammalian cells to be dependent on the activity of CHK1 and sensitive to caffeine (Feijoo et al., 2001 and Dimitrova and Gilbert, 2000). Despite the apparent limited functionality of this checkpoint in S2R+ cells, I wanted to investigate whether this was the same in S2R+ cells.

In an attempt to interfere with the function of the CHK1 homolog (Grp) in *Drosophila*, a dsRNA interference approach was utilised. Figure 4-3A shows that there was a very strong knockdown of Grp mRNA five days after incubation with dsRNA. Unfortunately, antibodies were not available to determine whether the persistent knockdown of Grp mRNA resulted in significant loss of protein. Analysis in the pulse replication assay indicated that, as observed previously, the addition of Aph did interfere with the replication timing programme (Figure 4-3B). In this experiment a strong inhibition of replication progression was seen with Aph treatment. The cause of this much higher percentage of pattern co-localisation (~85% of Aph treated cells after firefly dsRNA have the same CldU and IdU pattern) compared with the previous experiments (~40% Aph treated cells have the same CldU and IdU pattern, Figure 4.2C) is unknown. It is possible that the knockdown process even with control dsRNA has an effect on the checkpoint. However, by comparing Grp dsRNA to the firefly control, it can be seen that Grp knockdown had little or no effect on the ability of these cells to stabilise arrested replication forks and suppress initiation of replication at late origins.

Inhibition of the checkpoint was also attempted using caffeine. It has been previously shown in S2R+ cells that 5mM caffeine inhibits the G2/M checkpoint (supplemental material of Kondo and Perrimon, 2011). This concentration was therefore used to assess the effect of caffeine on the ability of these cells to stabilise arrested replication forks and suppress initiation of replication at late origins when exposed to replication stress. Unlike the previous experiments which were undertaken using a microscope slide format (see section 2.3.4.1), the assay was performed in 384-well plate format, to enable more cells to be analysed and to facilitate quantification of resultant data (see section 2.3.4.2). In this format precise patterns could not be distinguished but the levels of incorporation of CldU (green average intensity) and IdU (Red average intensity) were measured for each well and plotted against each other. Figure 4-4A and B shows that the addition of Aph between pulses caused an increase in cells

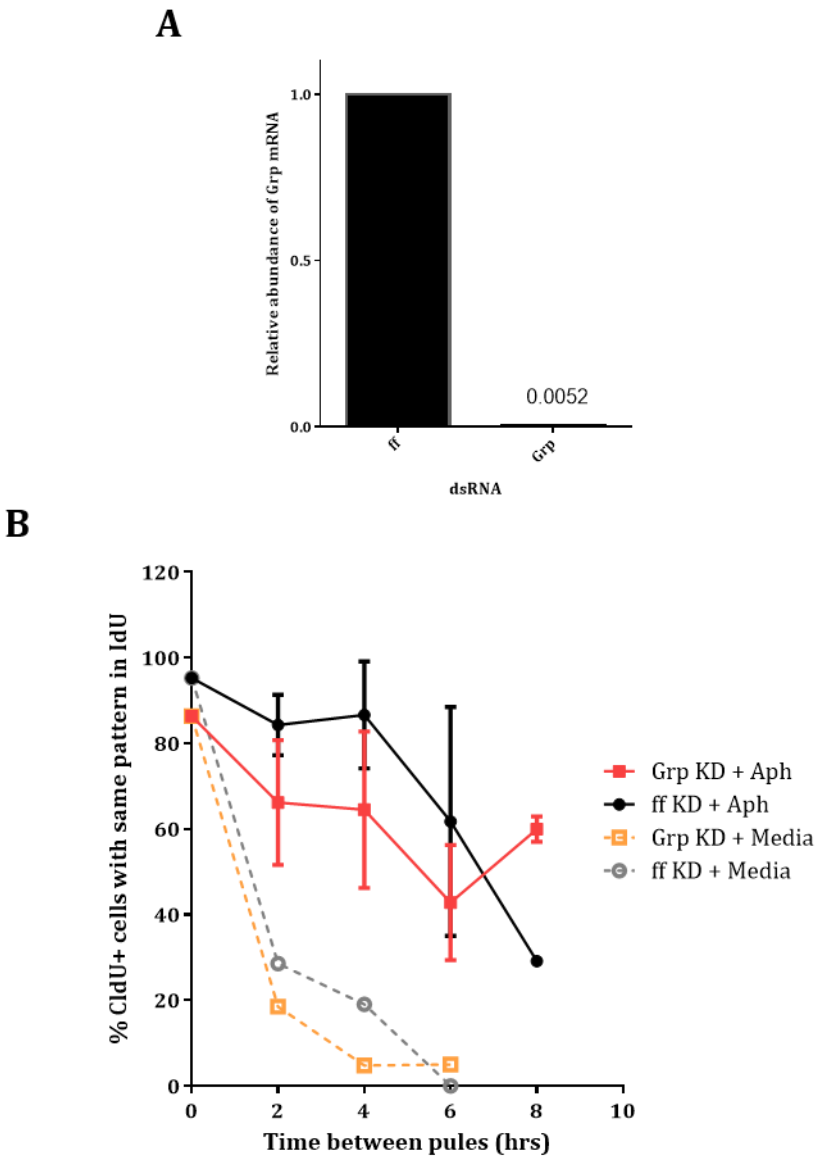

Figure 4-3. Knockdown of Grp has only a slight effect on the replication checkpoint.

A. QPCR results of Grp mRNA levels showing strong knockdown after 5 days incubation with dsRNA. ff = firefly control dsRNA **B.** 4 days after knockdown cells were seeded on cover slips and a dual-pulse replication assay performed. (IdU-60mins). Quantification of the percentage of CldU positive cells that had the same pattern with IdU. Experiment was performed using 2 separate coverslips per condition for Aph treated samples (error bars show sd) and one coverslip for media treated conditions. Each coverslip was imaged 4 times and at all stained cells were counted (between 4 and 23 cells per coverslip).

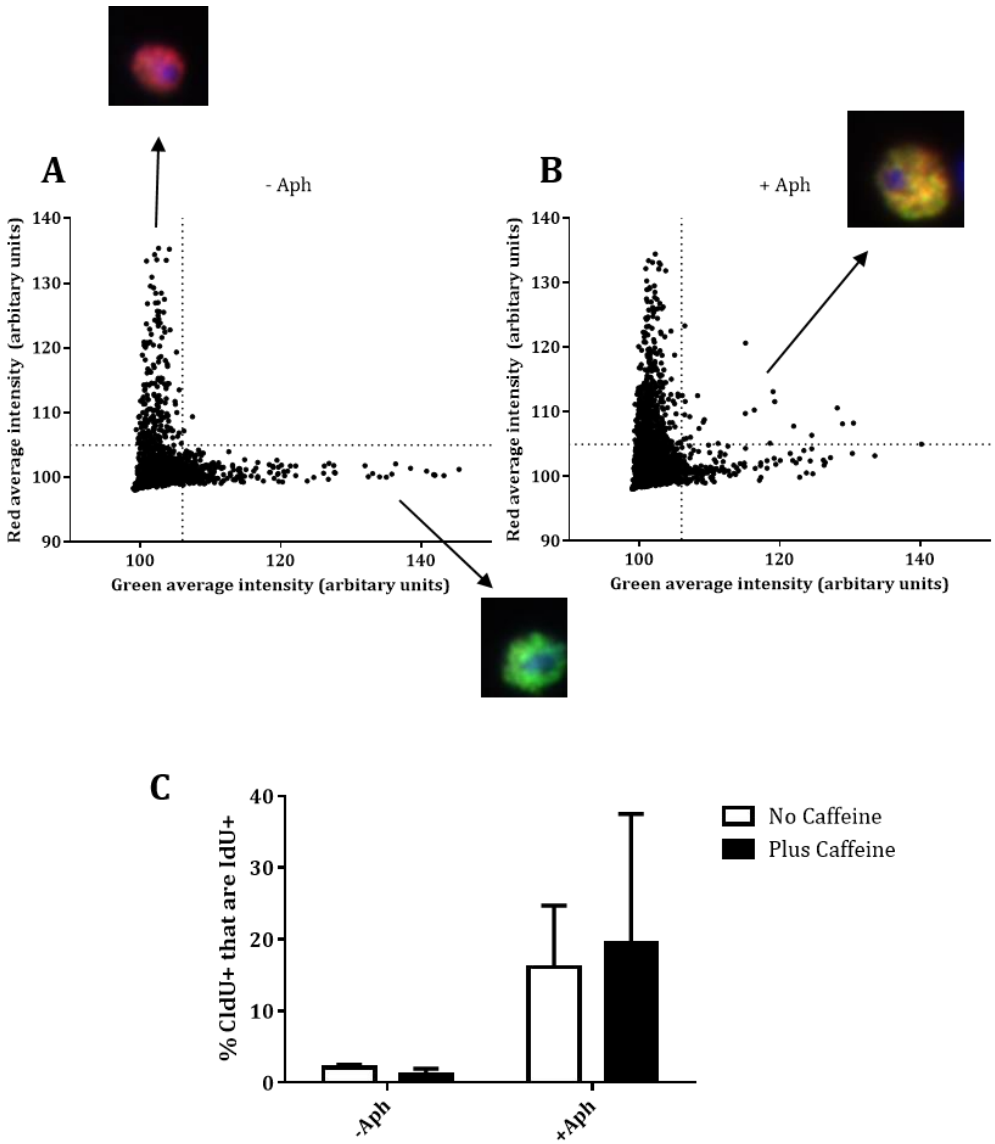

Figure 4-4. Caffeine doesn't override the replication checkpoint in S2R+ cells.

Dual-pulse replication assay in 384-well plate format with 4 wells per condition. Each well was imaged at 9 sites giving an average of 1500 cells imaged per well. **A+B.** Analysis was performed on each cell's green (CldU) and red (IdU) intensity. Cells over dotted line threshold counted as positive, see representative images. **A.** 6hrs of media with DMSO between pulses. **B.** 6hrs of 15μM Aph between pulses. **C.** Quantification of the percentage of CldU+ cells that were also IdU+ after 6hrs +/- 15μM Aph and +/- caffeine. N=4 error bars = sd

positive for CldU and IdU (compare top right segments). Quantification of the percentage of CldU positive cells which were also IdU positive (Figure 4-4C) showed that the addition of 5mM caffeine, in combination with Aph, didn't have any effect on the checkpoint, although again there was substantial variation between replicates.

4.2.2 S-M checkpoint in S2R+ cells

In order to investigate the S-M checkpoint in *Drosophila,* S2R+ cells were treated with compounds that induce replication stress (Aph or HU) or, for comparison (Kondo and Perrimon, 2011), DNA damage (doxorubicin), in the presence or absence of the checkpoint abrogator, caffeine. The mitotic index (MI) was then measured by determining the fraction of total cells expressing the mitotic marker phospho-H3, using a phospho-specific antibody as described in materials and methods. The replication stress compounds were expected to activate the S-M checkpoint whereas the DNA damage compound would activate the G2/M checkpoint. Both of these checkpoints are known to be inhibited by caffeine in various model cell systems (Lau and Pardee, 1982; Schlegel and Pardee, 1986).

Figure 4-5 shows that the MI in untreated cells is approximately 1.5-2.0%. Interestingly, the addition of caffeine alone to otherwise untreated cells resulted in a slight, rapid (within 4hrs) increase in MI which reduced over prolonged exposure, suggesting that even in the absence of exogenously induced DNA damage, a caffeine-sensitive mechanism regulates the G2-M transition in these cells. Doxorubicin treatment resulted in a rapid (within 4hrs) reduction in MI, to < 0.5% which persisted for up to 16hrs, consistent with the known role of doxorubicin in inducing G2 delay via activation of the G2-M checkpoint in these cells (Kondo and Perrimon, 2011). There was an increase in MI in doxorubicin-treated cells after prolonged treatment, which may reflect a lack of stability of this compound over time (Mayer et al., 2001; Rochard et al., 1992). Also, as expected, treatment of cells with the combination of doxorubicin and caffeine resulted in a dramatic increase (to ~4%) in MI, as reported previously (Kondo and Perrimon, 2011) and consistent with a role for caffeine-sensitive elements in the G2-M checkpoint in this system.

Unsurprisingly, the introduction of replication stress (Aph or HU) caused relatively little change in MI after 4hrs treatment, unlike DNA damage induced by doxorubicin. This is because the S-M checkpoint only prevents cells in S-phase from entering mitosis, so those in G2 at the time of treatment are still able to progress into mitosis.

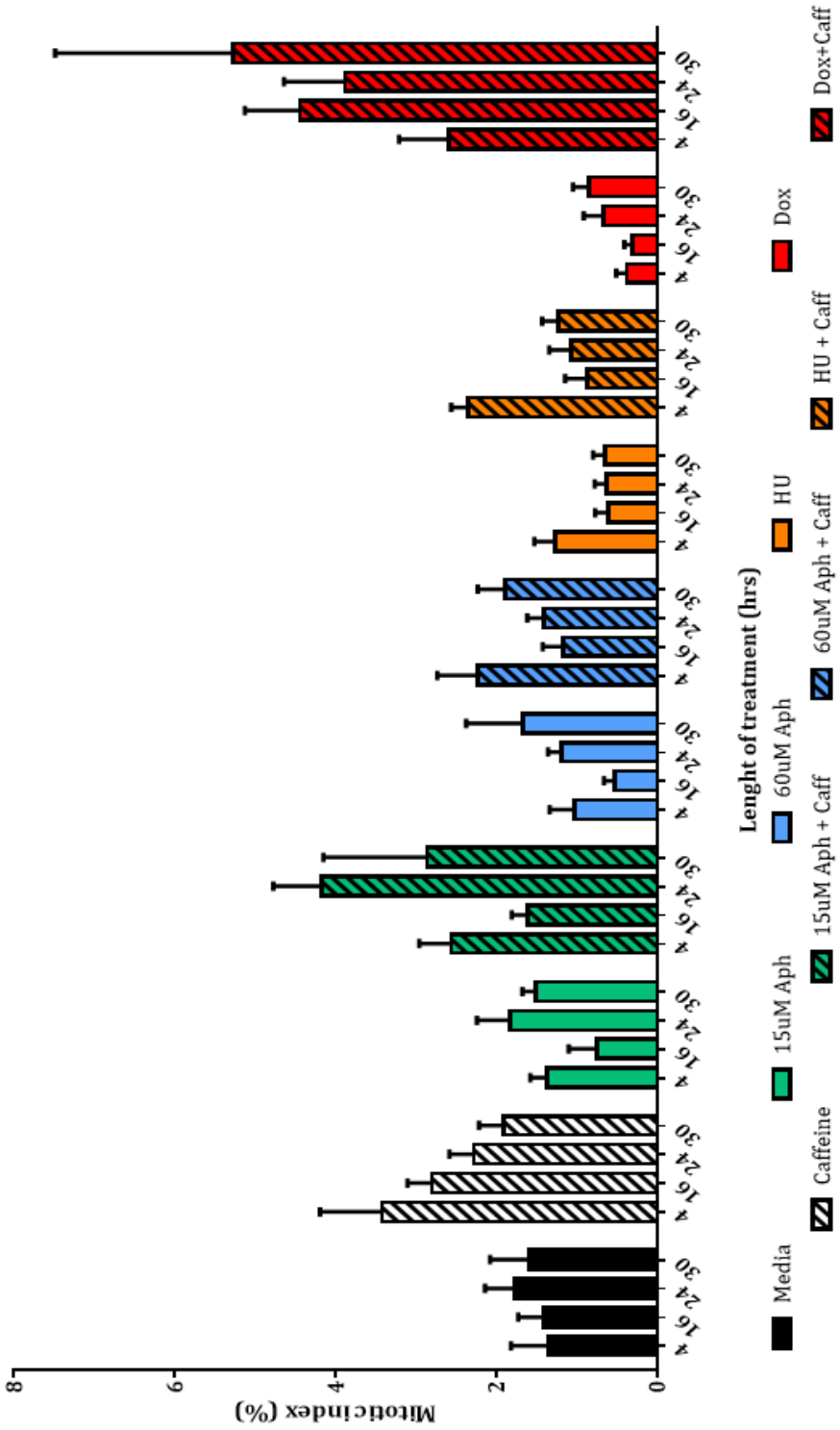

Figure 4-5. S-M checkpoint in S2R+ cells.

After treatment with different inhibitors (15µM and 60µM Aph and 10mM HU or 0.5µM doxorubicin) +/- 5mM caffeine for the indicated times, the MI was measured by quantifying the number of phospho-H3 positive cells. N=8. Error bars = sd.

After 16hrs or more exposure to the replication inhibitor HU, the MI was found to decrease to ~0.7%. This is about a 50% decrease from untreated levels, and is weaker than seen in previous work using related cells. (In Drosophila S2 de Vries et al., (2005) showed a 75% decrease in MI after 15hrs exposure to 10mM HU).

In contrast, the replication inhibitor Aph only transiently reduced the MI (after 16hrs of treatment) as this effect was not observed after longer exposure to Aph. This apparent lack of an ability to block mitotic entry in the presence of an incompletely replicated genome did not appear to be due to insufficient amounts of Aph or inactivation over time, as higher concentrations of Aph (60μM) were no more effective. Treatment with caffeine in addition to exposure to 15μM Aph did result in higher overall MI values, (ranging from 1.5 -4%) across all time-points examined, suggesting that caffeine does have an effect on either the timing of entry into, or the duration of, M phase under these conditions. This effect of caffeine was much reduced when cells were exposed to 60μM Aph.

Where cells were treated with HU for 16 hrs or longer, the addition of caffeine had almost no effect on observed MI. Taken together these data suggest that the ability of caffeine to override the S-M checkpoint may depend on the nature (Aph versus HU) and perhaps, the extent of, the mechanism by which replication stress is imposed. The absence of any significant increase in MI in HU plus caffeine treated cells implies that a caffeine-insensitive pathway contributes to a HU-induced S-M checkpoint in these cells.

These results imply that the S-M checkpoint in S2R+ cells may operate differently and be more complex than some model mammalian cell types (Rodríguez-Bravo et al., 2006), particularly in response to Aph.

4.3 Conclusions

The work described in this and the previous chapter investigated a number of previously described endpoints arising from a checkpoint activated following imposition of replication stress.

The effects of the S-phase checkpoint on replisome stability and suppression of late origin firing in S2R+ cells appear to be less coherent when compared to previous work in mammalian systems, at least using the analysis utilised here. The reasons for this are unknown. One possibility is that the occurrence of complete replication arrest is

a non-physiological situation, and therefore this particular metazoan cell type has not evolved the type of robust response, observed in other systems. Another is that the spatio-temporal regulation of replication origin firing and the assumptions that underpin the dual-pulse assay may not be applicable to this cell type.

The observed slight decrease in MI in response to HU and lack of long-lasting MI decrease in response to Aph (the S-M checkpoint) is also surprising. The response to delay mitosis when replication is incomplete has been shown to be conserved from yeast to humans (Cliby et al., 1998; Enoch et al., 1992). It is conceivable that the effects of individual replication inhibitors as well as caffeine may have additional impact on these cells which might make interpretation of the data more difficult, such as additional effects on cell cycle phase duration.

All of the S-phase checkpoint responses studied here appear to be relatively transient and "overridden" after extended periods of replication stress. "Leaky" checkpoints have also been observed in studies with *Drosophila* embryos. Sibon et al. reported that injection of embryos with Aph (which cannot be subsequently removed) did suppress the onset of mitosis, however embryos did ultimately undergo M phase. The average delay was 22mins with a large variance between embryos (Sibon et al., 1997). S2R+ cells are an incompletely-characterised cell type derived from a later stage embryo than this, and it is conceivable that similar 'leakiness' in checkpoint operation occurs in this cell line.

The underlying causes of the high degree of variability between experiments described in this chapter are unknown. While they may be due to technical error, treatment of cells with a DNA damaging agent did significantly reduce the population MI and this was robustly overridden by the co-addition of caffeine, suggesting that the fundamental basis of the assay system was reasonable. Nonetheless, the primary aim of this work was to undertake a genome-wide screen for novel checkpoint components, rather than to undertake a detailed analysis of the replication checkpoint in an incompletely characterised Drosophila cell line. Therefore it was decided that S2R+ cells were not an appropriate cell line to use for an RNAi screen of the S-phase checkpoint. Consequently other cell lines were investigated to find a more robust system for analysis.

5. S-M checkpoint assay optimisation in a human cell line

5.1 Introduction

As the S-phase checkpoint is well studied and robust in mammalian cells, I looked to mammals to choose a cell type in which to perform our screen. Due to the recent availability of the human siRNA library and the obvious medical application, I chose to focus on human cell lines. Work by the Agell group has shown that different cell lines have different responses to S-M checkpoint inhibitors; in particular, non-transformed and cancer cell lines behave differently (Florensa et al., 2003). They showed that there was more redundancy and complexity in non-transformed cell lines whereas cancer cell lines (e.g. HCT116 and HeLa cells) had a simpler mechanism which was easier to inhibit (Rodríguez-Bravo et al., 2007). Due to the nature of the RNAi screen I wanted to perform, which only eliminates one gene at a time, I needed a system with little redundancy, so HeLa and HCT116 tumour human cell lines were chosen. These cell lines were also much easier to handle and use in a high-throughput manner than non-transformed cell lines.

Due to its relative simplicity, potential for robustness and the ability to perform it in 384-well plates, the S-M checkpoint assay was chosen to be used for the screen.

5.2 Results

5.2.1 S-M checkpoint in human cell lines

In order to assess the S-M checkpoint in human cancer cell lines to see if they were suitable for a genome-wide screen, I performed a similar assay to that undertaken using S2R+ cells described in the previous chapter, but instead using the HCT116 colon carcinoma cell line and HeLa cervical cancer cell line (cell lines used in Rodríguez-Bravo et al., 2007). Figure 5-1 shows that mitotic cells were easily identified using the phospho-H3 antibody, and that in both cell lines treatment with 2mM HU or 15μM Aph caused a decrease in the MI after 6 and 24hrs, implying activation of the S-M checkpoint. This response was more persistent, initiated quicker and gave a greater reduction in MI than the response observed in S2R+ cells.

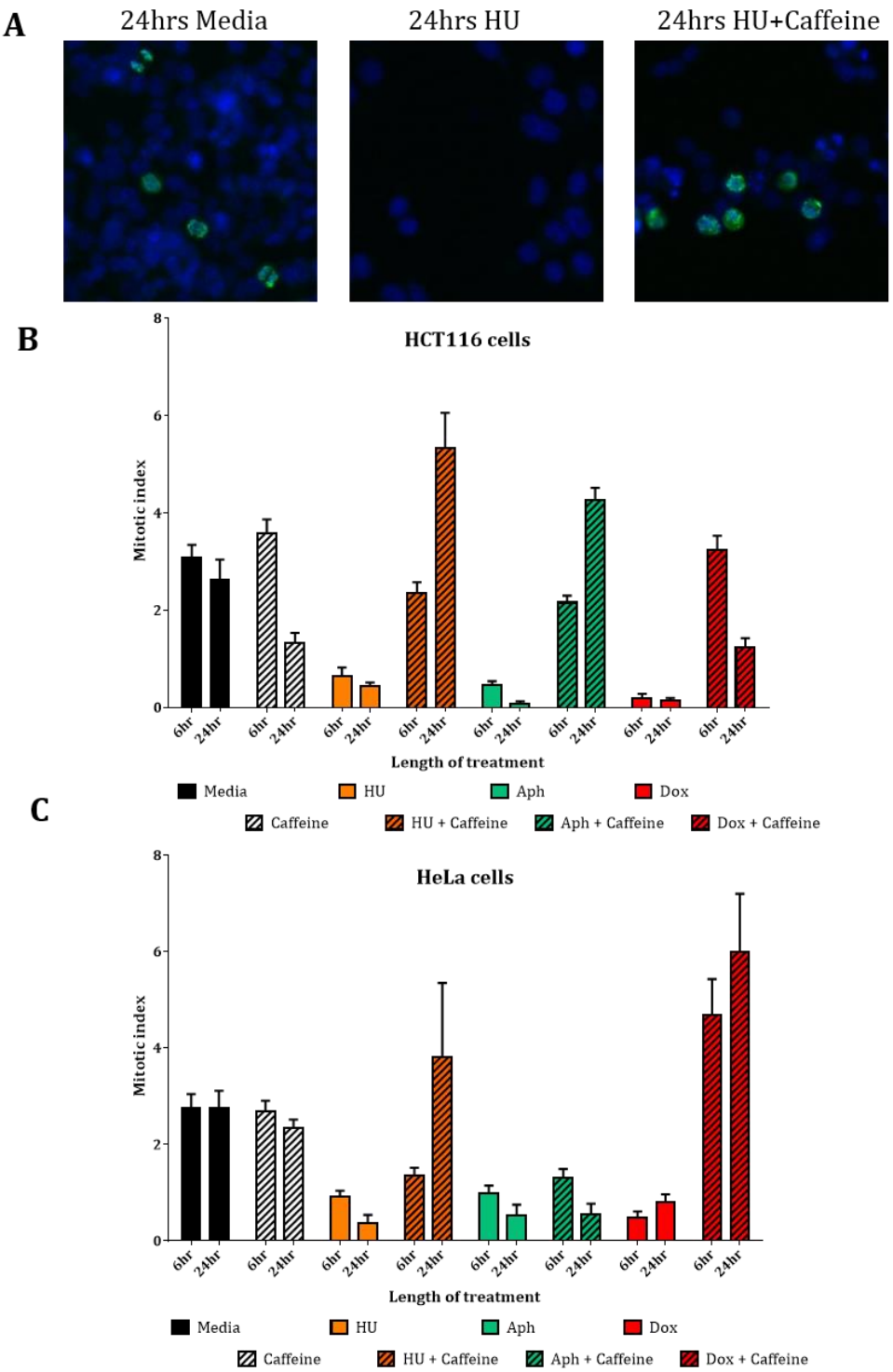

Figure 5-1. S-M checkpoint in human cell lines.

A. Representative images of HCT116 cells stained with anti-phospho-H3 antibody (green) and DNA stain DAPI (blue). Left-hand panel: asynchronous HCT116 cells; middle panel: HCT116 cells treated for 24 h with 2mM HU; right-hand panel: HCT116 cells treated for 24 h with 2mM HU plus 5mM caffeine. Treatment with 2mM HU decreases the percentage of mitotic cells and treatment with 2mM HU and caffeine causes an increase. **B.** HCT116 cells treated with replication inhibitors (2mM HU or 15μM Aph) or 0.5μM doxorubicin +/- 5mM caffeine for 6 or 24hrs. MI measured by determining the fraction of cells displaying phospho-H3 staining as a proportion of the total cells present as measured by DAPI staining. N=8. Error bars = SD **C.** HeLa cells treated as for HCT116 cells in **B.**

Previous work has shown that the activation of the S-M checkpoint with HU in HCT116 cells, but not HeLa cells, can be inhibited by caffeine (Florensa et al., 2003 Rodríguez-Bravo et al., 2006). In contrast to this, I saw an inhibition of the checkpoint in both cell lines treated with HU, and a caffeine-insensitive response in HeLa cells only when treated with Aph. This contrast with published results may be due to experimental differences, including the fact that in this experiment caffeine was added at the same time as the replication inhibitors whereas in previous studies it was only added for the last 10hrs of the 25hr HU treatment.

As a control, cells were also treated with the DNA damaging agent doxorubicin, which activates the G2/M checkpoint. In both cell lines, doxorubicin, caused a large decrease in MI and as expected, the decrease was inhibited by caffeine (van Vugt et al., 2010).

These observations show that the S-M checkpoint in human cell lines is much more robust than in *Drosophila* S2R+ cells and that in HCT116 cells in particular the checkpoint was strongly abrogated by caffeine. Due to the simplicity of the S-M checkpoint in HCT116 cells, this cell line was chosen to carry out further optimisation of the assay for an RNAi screen.

5.2.2 Optimisation of conditions for screening

In order to perform a genome-wide RNAi screen, the conditions for each step in the S-M checkpoint assay (Figure 5-2A) had to be optimised to ensure the largest difference between hits that gave a positive outcome and negative results. Therefore, optimisation of each step was undertaken either using caffeine treatment or CHK1 siRNA as a positive control, compare to untreated or non-targetting siRNA as negative controls. As discussed above, CHK1 has been shown previously to be involved in the S-M checkpoint.

Firstly, the length of time that cells were exposed to HU was optimised to maximise the decrease in observed MI. Figure 5-2B shows that the MI started falling after 2hrs HU treatment and reached the lowest value after 24hrs. At longer time points (e.g. 48hrs) the MI started to rise again but this was mainly due to a decrease in overall cell number which meant that even though the number of mitotic cells was the same, the percentage was higher. Addition of caffeine together with HU induced a similar decrease in MI for the first 8hrs, but at longer time points the checkpoint was inhibited, as shown by a significant increase in MI, which peaked at ~6%. This value is higher than the normal MI but similar to that previously reported when the

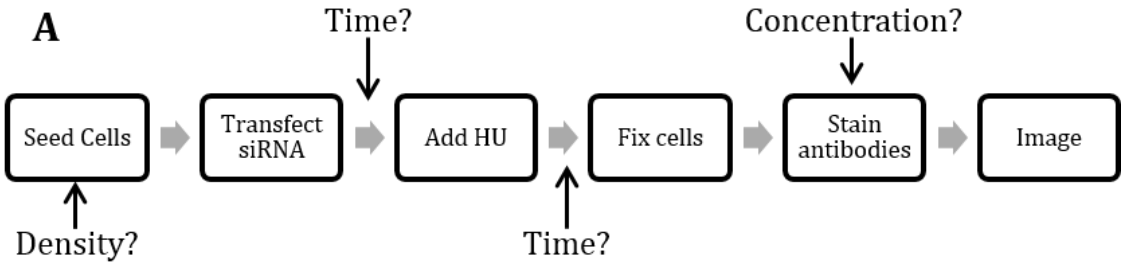
A
Time?
Concentration?
Seed Cells
Transfect siRNA
Add HU
Fix cells
Stain antibodies
Image
Density?
Time?

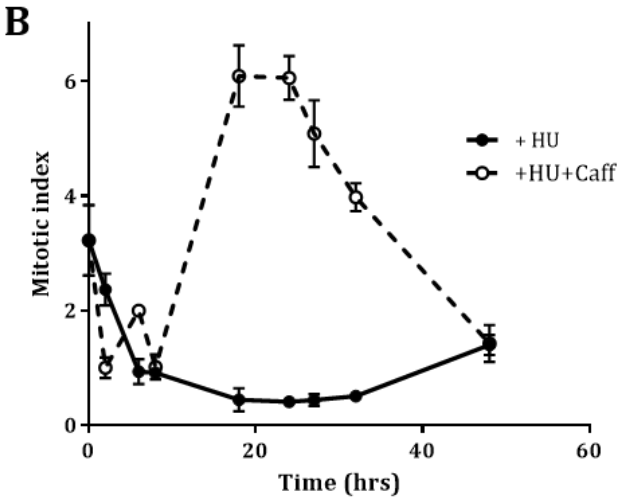
B
Mitotic index
Time (hrs)
+ HU
+HU+Caff

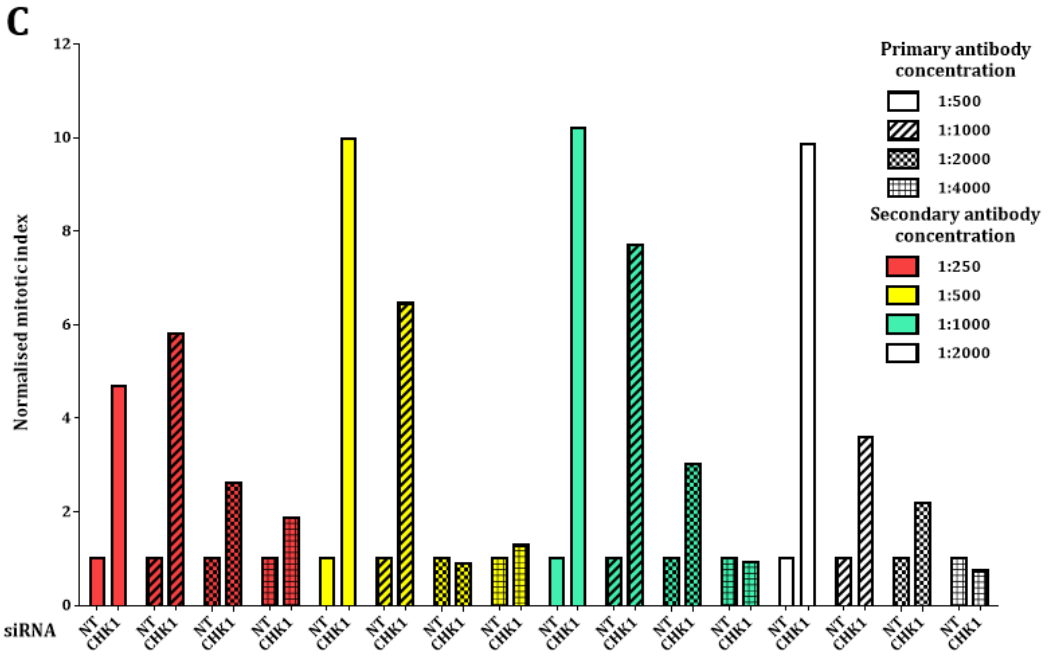
C
Normalised mitotic index
siRNA
NT
CHK1
Primary antibody concentration
1:500
1:1000
1:2000
1:4000
Secondary antibody concentration
1:250
1:500
1:1000
1:2000

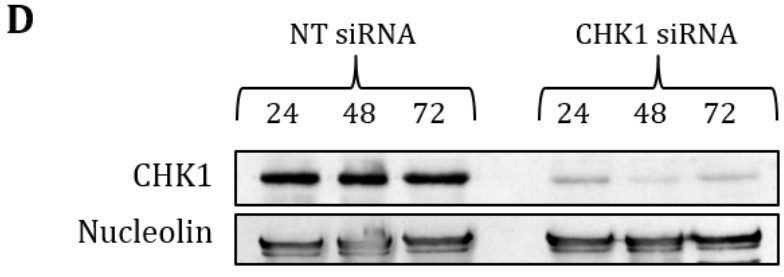
D
NT siRNA
CHK1 siRNA
24
48
72
24
48
72
CHK1
Nucleolin

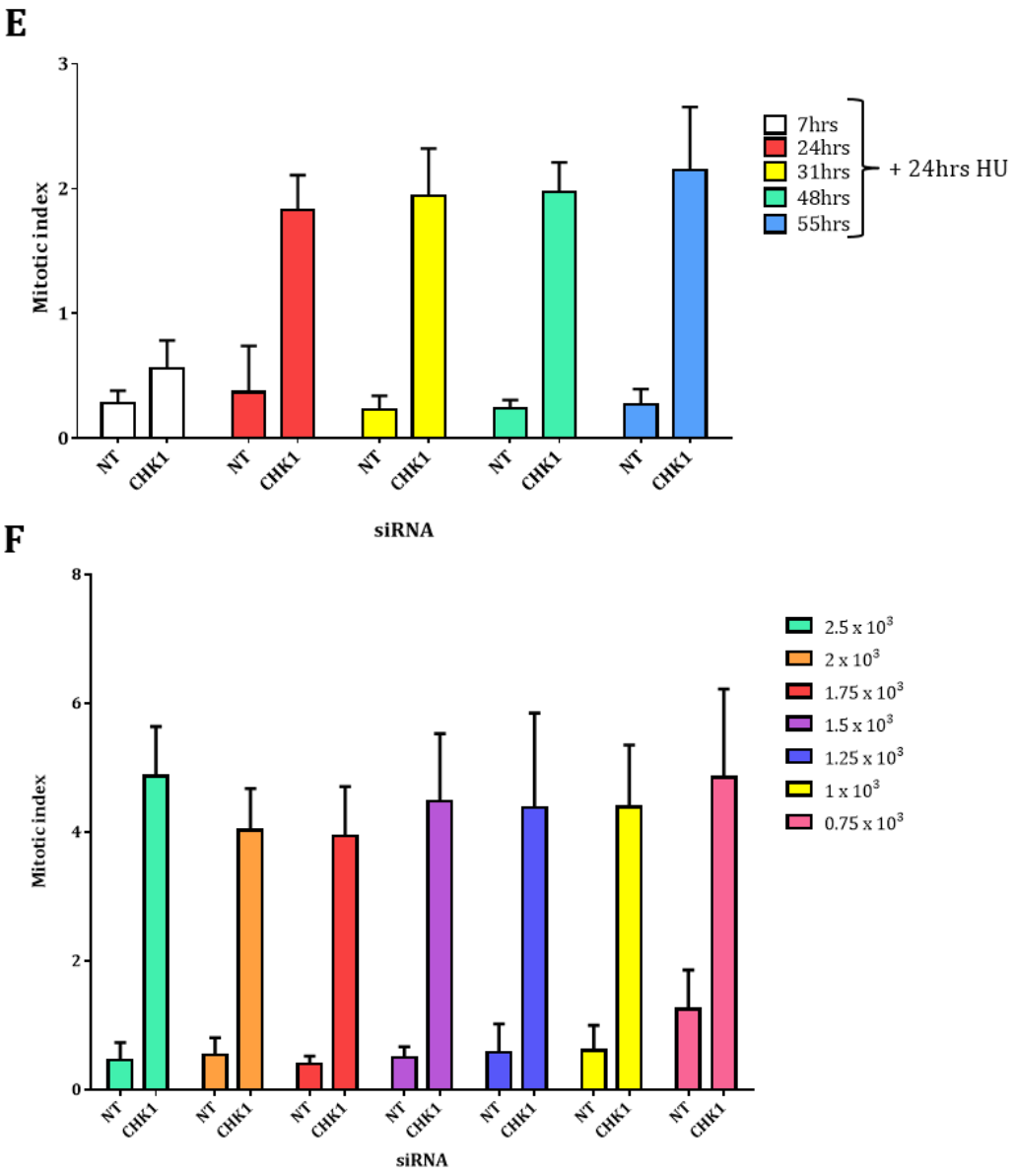

Figure 5-2. Optimisation of S-M checkpoint assay in HCT116 cells.

A. Outline of S-M checkpoint assay and identification of steps that required optimisation. **B.** Optimisation of HU treatment time. MI versus length of treatment with HU. Cells incubated with 2mM HU or 2mM HU + 5mM caffeine for different periods of time. N = 4. Error bars = sd. **C.** Optimisation of antibody concentration. MI normalised to NT MI for different combinations of primary and secondary antibodies. Primary antibody concentration indicated by pattern and secondary antibody concentration by fill colour. N = 4. Error bars = sd. **D.** Western blot showing optimisation of knockdown time. In 6-well plate cells transfected with NT or CHK1 siRNA for the indicated times and then treated with 2mM HU for 24hrs. Cells lysed and 20µg run on an SDS gel. CHK1 band at ~50kDa and Nucleolin at ~100kDa. **E.** Optimisation of knockdown time. Cells seeded and transfected at different time points and densities in 384-well plate. N = 8. Error bars = sd. **F.** Optimisation of cell seeding density. Cells were seeded in a 384-well plate at different densities and transfected with CHK1 or NT siRNA. S-M checkpoint assay then performed. N = 8. Error bars = sd. Details of conditions for each experiment in Table 2-7.

checkpoint is abrogated (Florensa et al., 2003; Rodríguez-Bravo et al., 2006). It presumably reflects an increase in the overall time these cells spend in mitosis, due to the fact that their <4n DNA content will trigger the spindle checkpoint. As the biggest difference observed between HU-treated and HU + caffeine-treated cells was observed at 24h, this time point was chosen for the screen.

Next, it was necessary to determine the concentration of phospho-H3 antibody and secondary antibody sufficient to provide a robust signal to background ratio in untreated compared to checkpoint compromised cells. To do this, I compared the MI in cells treated with NT siRNA versus cells treated with Chk1 siRNA, as Chk1 has been shown previously to be a critical component of the S-M checkpoint (Kumagai et al., 1998; Zachos et al., 2005). Figure 5-2C shows that in general higher concentrations of the primary antibody, but a mid-range concentration of the secondary antibody gave the largest signal to noise ratio in siRNA-transfected HU-treated cells. Therefore, the primary antibody was used at a 1 in 500 dilution and the secondary at 1 in 1000 for the screen.

The length of time required to knockdown genes was harder to determine as different proteins and mRNAs have different half-lives, and therefore would need different lengths of time to achieve knockdown. For CHK1, I observed a strong and persistent knockdown at the protein level, lasting from 24-72 hrs (Figure 5-2D), and a large difference between the MI of cells treated with NT and CHK1 siRNA (Figure 5-2E) at time periods greater than 24hrs (with an additional 24hrs with HU). In order to take into account the fact that other proteins may have a longer half-life, I decided to use a knockdown time of 48hrs before adding HU.

The final component of the assay optimisation was to determine the cell seeding density. Using all the previously optimised conditions, the assay was performed after seeding cells at a range of densities. Figure 5-2F shows that there was limited effect on the MI of CHK1-depleted cells with different cell densities, but when cells were seeded at a low density, the NT transfected cells had a higher MI. Based on these results, I chose a cell density of 1.75×10^3 cells per well to use in the screen.

5.2.3 Assay Plate

In order to assess the assay on a full 384-well plate and to identify positive and negative controls for the screen, a trial analysis using an initial, defined 'assay plate' was undertaken. The trial comprised one 384-well plate, 320 wells of which

contained pooled ON-TARGETplus (OTP) siRNAs generated to knockdown 320 random kinases. There were 64 spaces on the plate to which 16 other siRNAs were added. These additional siRNAs included 11 different non-targeting (NT) siRNAs, four 'death' siRNAs and CHK1 siRNA. Different NT siRNAs were assessed as it is known that they can generate variable levels of false positive signal which may be dependent on the assay and cell line (Brown, S. pers. comm.). I aimed to find the NT siRNA which resulted in the lowest MI after HU treatment.

In order to identify a suitable transfection control, four 'death' siRNAs, XIAP, PLK1, ECT2 and UBB1 were used to identify a gene, knockdown of which caused cell death upon transfection. In screens of this nature, the transfection of "death" siRNAs into one well of each plate is undertaken and resultant low cell number in that well indicates that transfection on that plate was successful. XIAP is an apoptotic suppressor protein which inhibits multiple caspases and prevents cell death (Holcik et al., 2001). Knockdown of XIAP thus induces cell death. PLK1 a key component of mitotic regulation, contributing to CDK1/cyclin B1 activation and centrosome maturation (Lane and Nigg, 1996; Lindqvist et al., 2009). Knockdown of PLK1 causes a mitotic cell cycle arrest and subsequent cell death (Lan et al., 2010). ECT2 is a guanine nucleotide exchange factor required for cytokinesis which is regulated by PLK1 (Cook et al., 2011; Niiya et al., 2006). The interference of cytokinesis caused by ECT2 knockdown induces cell death. UBB1 is ubiquitin B and plays a role in many aspects of cell function. Knockdown of UBB1 has been shown to decrease cell viability but the exact mechanism of this is unknown (Oh et al., 2013). Though these 'death' siRNAs are expected to cause cell death upon transfection in all cells, there is variability between cell types (Brown, S. pers. comm.). Therefore all four "death" siRNAs were assessed to find one that could function as a transfection control in the screen in HCT116 cells.

Figure 5-3A shows that the mean MI for the plate was less than 1% (left-hand bar). Low MIs were also achieved for most of the non-targeting siRNAs, though MIs were lower for the OTP NT siRNAs (NT6-10) than the siGENOME ones (NT 1-5). This is presumably because the OTP siRNAs have been optimised to decrease off-target effects. NT 6 was chosen as the negative control for all further studies; this siRNA had also been used in previous experiments.

High mitotic indices were seen for CHK1 siRNA and caffeine-treated cells as observed previously, but a high MI was also observed with UBB1 and PLK1 knockdown. These

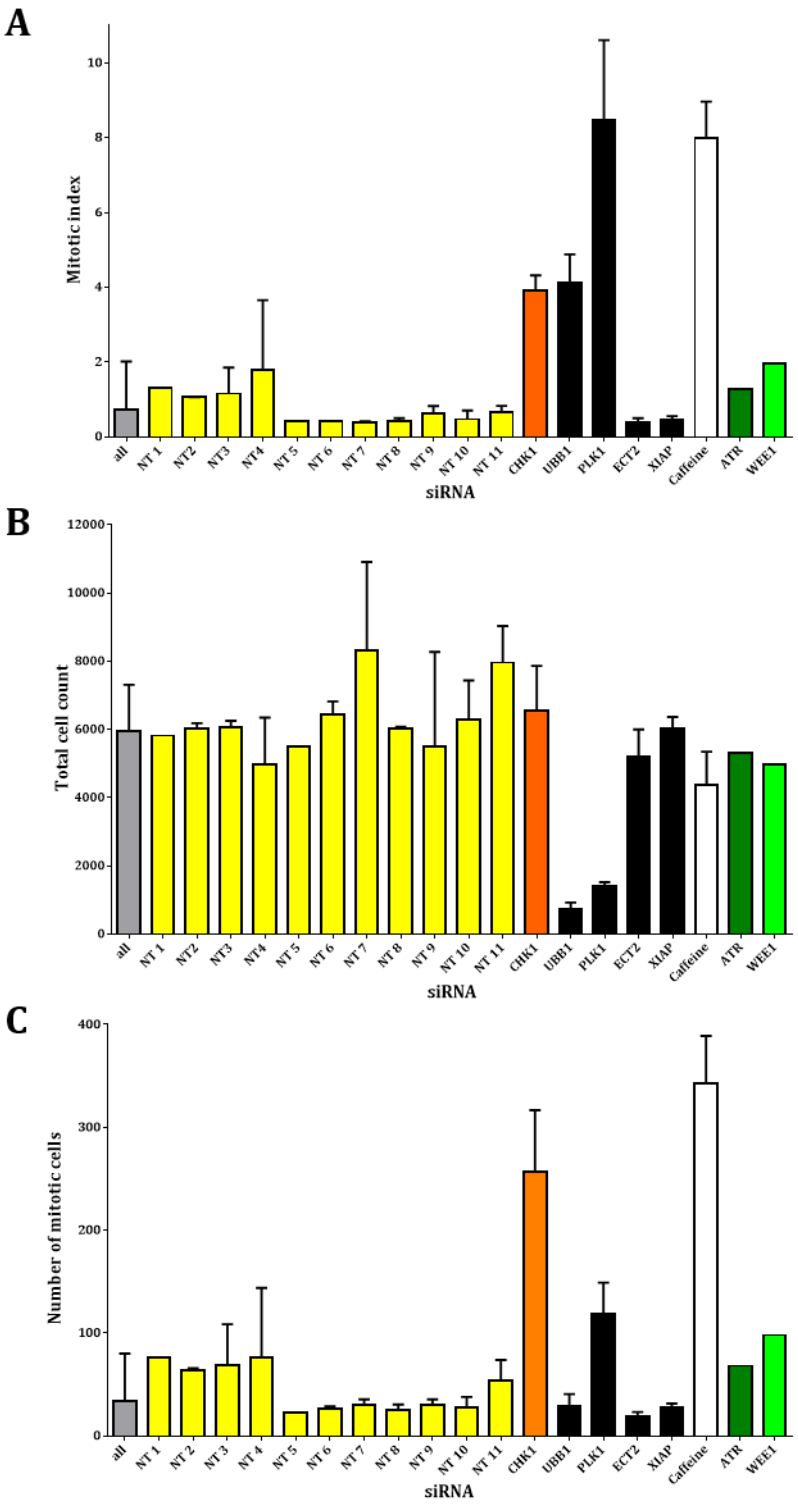

Figure 5-3. Assay plate controls for S-M checkpoint screen.

A. MI of cells in 384-well plate subjected to the optimised protocol outlined in Fig. 5-2A. Where multiple wells had the same siRNA mean and sd shown. Grey = all wells on the plate. Yellow = non-targeting siRNA. Black = death controls. Green = Positive results on plate **B.** As A but cell count shown. **C.** As A but number of mitotic cells shown.

"death" inducing siRNAs caused a dramatic decrease in cell number as expected (see Figure 5-3B) unlike transfection of XIAP and ECT2 siRNA which caused no deviation from the cell number seen with non-targeting siRNA. The high MI observed after UBB1 knockdown is likely to be due to the fact there were very few cells remaining and a few of these were in mitosis (Figure 5-3C). The high MI for PLK1 is likely to be due to the fact that there was a high percentage of mitotic cells (Figure 5-3C). This is due to the PLK1's role in mitotic control (Nigg, 2001). As it effectively killed cells and did not induce a high number of cells in mitosis UBB1 siRNA was chosen as the transfection control for further studies.

When analysing the data from the random kinases on the rest of the plate it was observed that ATR and WEE1 knockdown resulted in a higher MI than average. As the roles of these protein in the S-M checkpoint and G2/M checkpoint are well established (Enoch et al., 1992; Nghiem et al., 2001), siRNAs against ATR and WEE1 were chosen as additional positive controls in subsequent screening development.

5.2.4 Kinome-Phosphatome screen

In order to assess the reproducibility of the assay and to practice performing it with multiple plates, a small subset screen was performed targeting all of the known kinases (kinome) and phosphatases (phosphatome) in the human genome. Four 384-well plates contained the library and the assay was carried out in triplicate for each plate. Each plate contained 320 siRNAs to screen and 6 controls added to 16 wells (see Figure 5-4A for plate layout). UBB1 siRNA was the transfection control, NT6 siRNA (now called NT) the negative control and CHK1 siRNA the positive control. ATR and WEE1 siRNA were added as further positive controls after their identification in the assay plate, though it is of note that the siRNA used as controls was siGENOME siRNA and not OTP as used on the rest of the assay plate. CDK5R1 siRNA was also used as it has been reported to affect apoptosis after S-phase checkpoint activation (Van Hateran, N. and Brown S. pers. comms.).

The plates were screened using the conditions in Table 2-7 and the data analysed. Figure 5-4B shows that although most of the plates had a low median score (below 1%) there was some variation between plates. To remove this variation from the analysis, results were normalised and converted into z-scores (see section 2.2.6.1) in which the median of each plate has the value of zero (Figure 5-4C). Due to the logarithmic nature of the z-score calculation, the wells that had no mitotic cells were

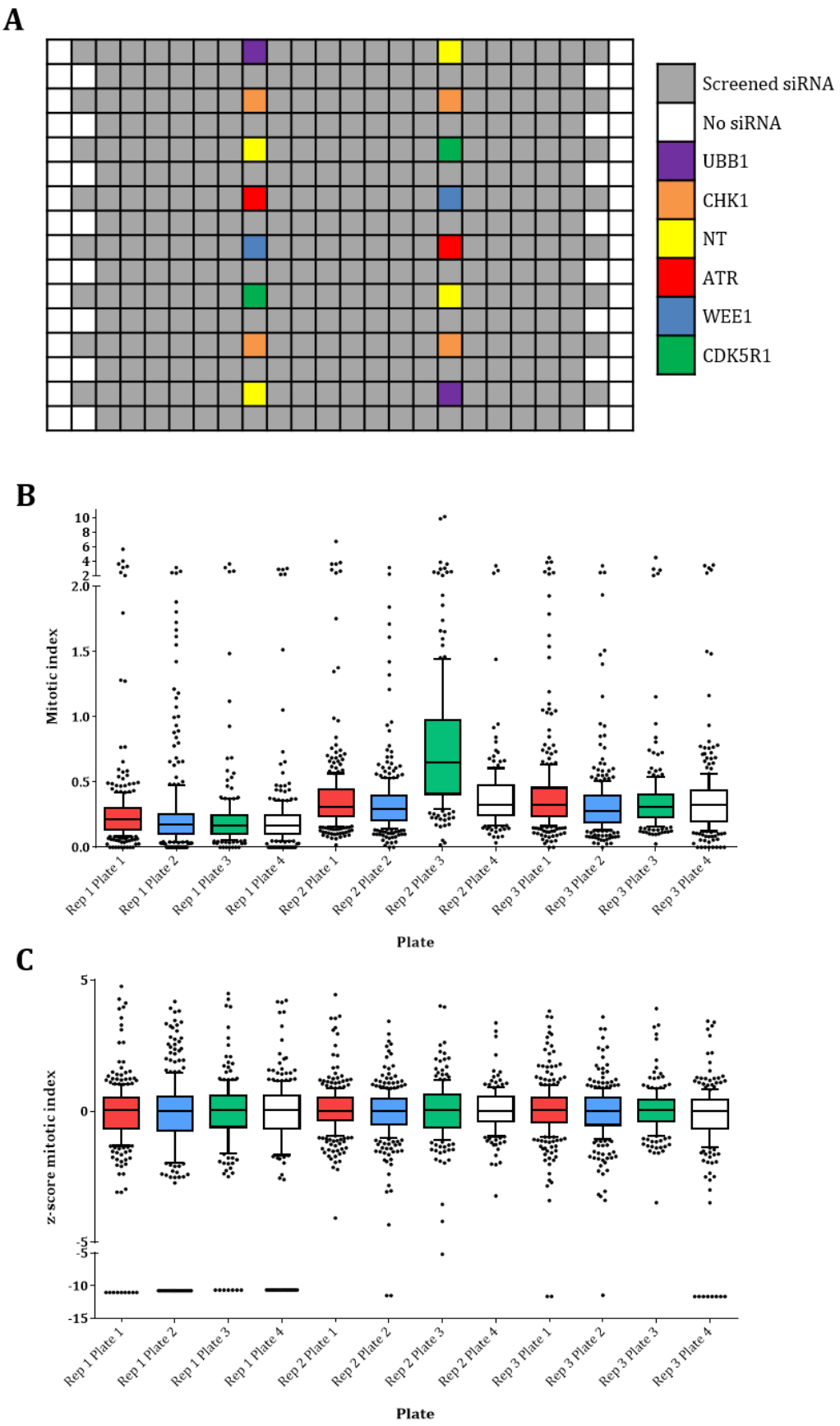
A
Screened siRNA
No siRNA
UBB1
CHK1
NT
ATR
WEE1
CDK5R1
B
Mitotic index
Rep 1 Plate 1
Rep 1 Plate 2
Rep 1 Plate 3
Rep 1 Plate 4
Rep 2 Plate 1
Rep 2 Plate 2
Rep 2 Plate 3
Rep 2 Plate 4
Rep 3 Plate 1
Rep 3 Plate 2
Rep 3 Plate 3
Rep 3 Plate 4
Plate
C
z-score mitotic index
Plate

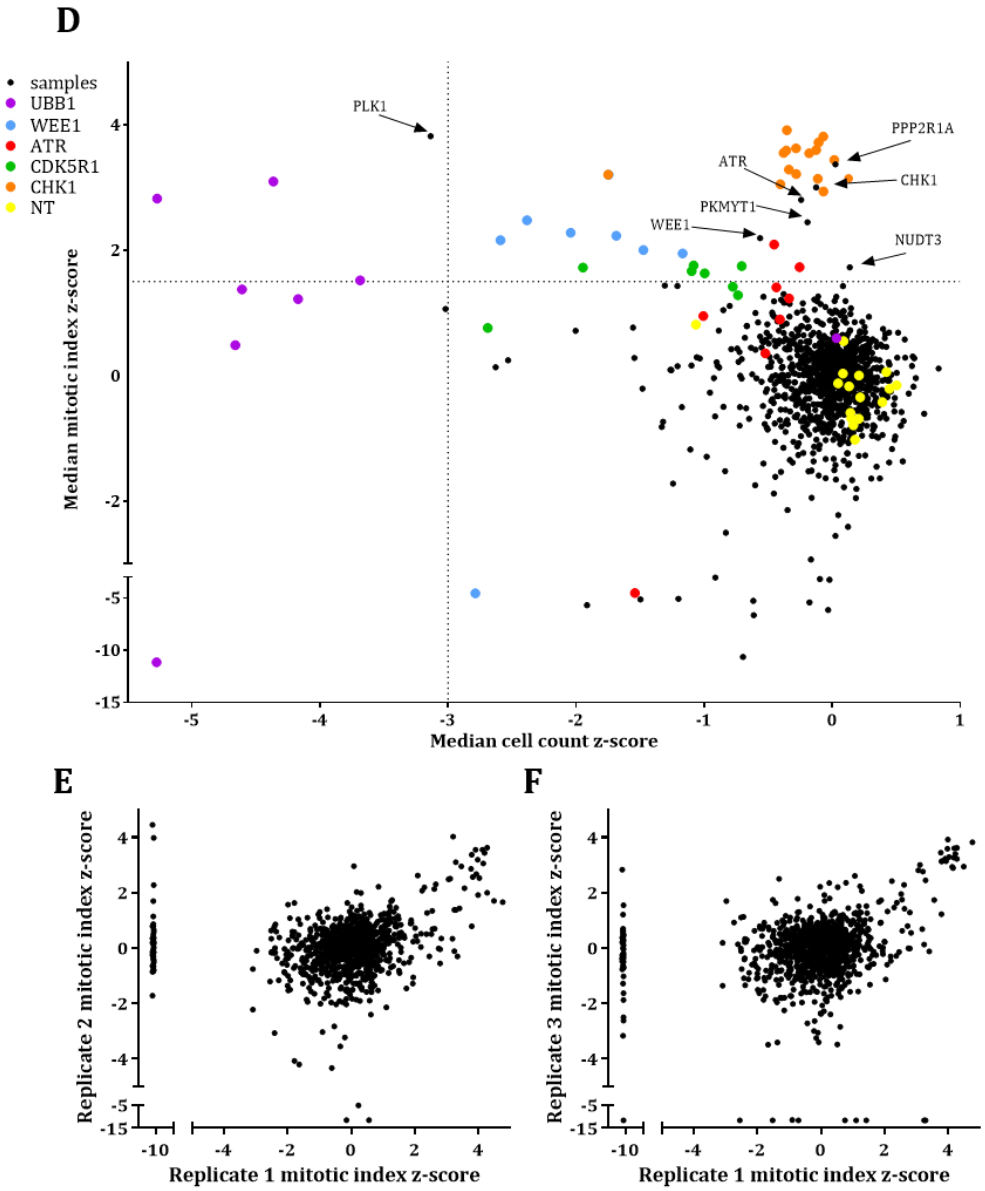

Figure 5-4. Kinome-Phosphatome screen results.

A. Layout of the 384-well plate used for kinome-phosphatome screen (and genome-wide screen). **B.** MI values obtained from kinome-phosphatome screen. Each bar is one of the 12 plates. Box represents 25th-75th percentile with line at the median. Whiskers extend to 10th and 90th percentile with outliers as dots. **C.** MI z-score obtained for the 12 plates. Box plots as in B. **D.** Median MI z-score versus median cell count z-score. Controls in colour. Dotted lines represent thresholds. **E.** MI z-scores for replicate 1 plotted against MI z-scores for replicate 2. **F.** As E but with replicates 1 and 3.

given very strongly negative z-scores (bottom axis of Figure 5-4C). As these results are not of interest it did not affect the analysis.

Figure 5-4D shows a plot of the median z-score of the cell count versus the median z-score of the MI. The dotted lines segregate the plot into four areas. The left hand top and bottom segments have a low cell count presumably because the siRNAs cause cell death (e.g. UBB1 and PLK1 siRNA) and these are excluded from further study (even if they had a high MI). The samples of interest are those in the top right segment where knockdown causes an increase in MI without substantial cell death. In this segment are the known components ATR, CHK1, WEE1 and PKMYT1 as well as PPP2R1A (a regulatory subunit of protein phosphatase 2 involved in mitotic exit (Wurzenberger and Gerlich, 2011)) and NUDT3 (Diphosphoinositol Polyphosphate Phosphohydrolase 1 which is involved in nucleoside phosphate metabolic pathways (Safrany et al., 1998). The majority of the positive controls were also in this segment, although the MI resulting from ATR knockdown was lower than expected. This is most likely due to siGENOME ATR siRNA not being as effective as the OTP siRNA in knocking down ATR protein expression as the OTP siRNA in the samples gave a high MI.

The reproducibility of the assay was moderately strong as shown in the scatter plots in Figure 5-4E and F. The majority of the data clustered around the median but strong hits (above two z-scores) were reproducible across the three replicates.

5.3 Conclusions

The S-M checkpoint in HCT116 cells has been shown to be robust, reliable and dependent on many of the known checkpoint components. Therefore optimising and preparing for a high-throughput screen has been possible.

The sensitivity of the checkpoint to caffeine in HCT116 cells indicates that many of the pathways in other cell types (e.g. MAPKs) may be non-functional in these cells. Although this means that components of the S-M checkpoint in these pathways will not be identified in the screen, it does decrease the redundancy in the system. Therefore it increases the likelihood that knockdown of a component will affect the checkpoint and thus be identified. The involvement of identified components can then be assessed in other cell lines at a later stage. It was interesting to note that different results to those previously published were observed in caffeine-treated HeLa cells treated with HU or Aph. Previously it has been reported that after treatment with HU

for 25hrs combined with caffeine for the final 10hrs, the MI in HeLa cell populations remains low (Florensa et al., 2003), suggesting that caffeine is unable to abrogate the S-M checkpoint in this cell line. In contrast to that report, I observed an increase in MI in HeLa cells treated with HU and caffeine compared to HU alone; however treatment with Aph and caffeine did not increase the MI compared to the value obtained after treatment with Aph alone. The reasons for the discrepancy with the observations of Florensa et al., (2003) are unknown. One possibility is that the different modes of action of these replication inhibitors have different effects on checkpoint activation. Therefore the timing of checkpoint inhibition with caffeine may affect checkpoint abrogation differently.

The conditions for the screen were all optimised using CHK1 knockdown or caffeine treatment as positive controls. It follows that conditions may not be optimal for other genes that may be involved in the checkpoint, and therefore they may not be discovered during the screen. Although I have tried to allow for this by extending knockdown time by 24hrs, it is possible that but ultimately some checkpoint genes may not be identified.

Interestingly, even with optimised conditions CHK1 knockdown caused the MI to rise only to ~5%. This is a significant increase from 0.5% (NT average) but nevertheless, it means that 95% of cells are not in mitosis even after depletion of this key checkpoint protein. The stage of the cell cycle at which cells are in when they are treated with HU is likely to be a dominant factor in this; cells in G2, M or G1 phase may stall at the G1/S boundary by activation of the G1/S checkpoint. However, the percentage of cells in S-phase is higher than 5% and so one would expect a higher percentage than 5% to be in mitosis following S-phase arrest and subsequent checkpoint abrogation; therefore there may be other reasons for the low percentage of mitotic cells seen in the assay.

Variation in the efficiency of transfection such that some cells take up less CHK1 siRNA and the protein is not knocked down as strongly, may contribute to a lower MI than expected. However, a similar MI was also seen in cells treated with caffeine. Stress inflicted on the cells during the assay process may increase the cell cycle time and affect the S-phase population. Another factor is that cells may undergo mitotic catastrophe after loss of the checkpoint and not be visible when the cells are imaged.

The identification of the known checkpoint components ATR and WEE1 in this initial assay plate trial, increased confidence that this assay had the potential to identify novel components of the S-M checkpoint.

6. Genome-wide screening and Secondary screening

6.1 Introduction

Genome-wide RNAi screens are carried in a high-throughput manner to identify components of a mechanism. Our human siRNA screen targeted 18,104 different genes with pooled OTP siRNAs. These were arrayed on 58 x 384-well plates also containing control siRNAs. A balance must be made in the execution and analysis of a screen to attempt to eliminate both false positives and false negatives. In this screen, I erred more on the side of eliminating false positives, meaning that some true positive components won't be identified. This does not undermine the overall aim which was to undertake a screen to identify novel, rather than all, components of the S-phase checkpoint.

Secondary screens are required to confirm the validity of the hits that emerge from a primary screen. These may use different siRNAs and distinct assay conditions to increase confidence in the hits.

6.2 Results

6.2.1 Genome-wide screening

The genome-wide RNAi screen was carried out in duplicate, in batches of ~20 plates at a time (a third of the genome). The assay was performed as described for the kinome-phosphatome screen, including the same principles of plate layout (Figure 5-4A). As in the kinome-phosphatome screen, the MI and total cell count were normalised to the plate median to reduce experimental variation (Boutros et al., 2006) and gives rise to z-scores. Figure 6-1A shows the MI z-score for all samples on each plate. Once normalised, the data are reasonably consistent across the batches and plates. The two exceptions are the replicates of plate 39 (marked with arrows). Due to a high number of wells having no mitotic cells on these plates, the median was 0 and therefore the normalisation process was not functional and this plate was eliminated from further analysis.

Figure 6-1B shows the MI z-score against the cell count z-score for each gene screened (mean result of two replicates shown). These data indicated that knockdowns of

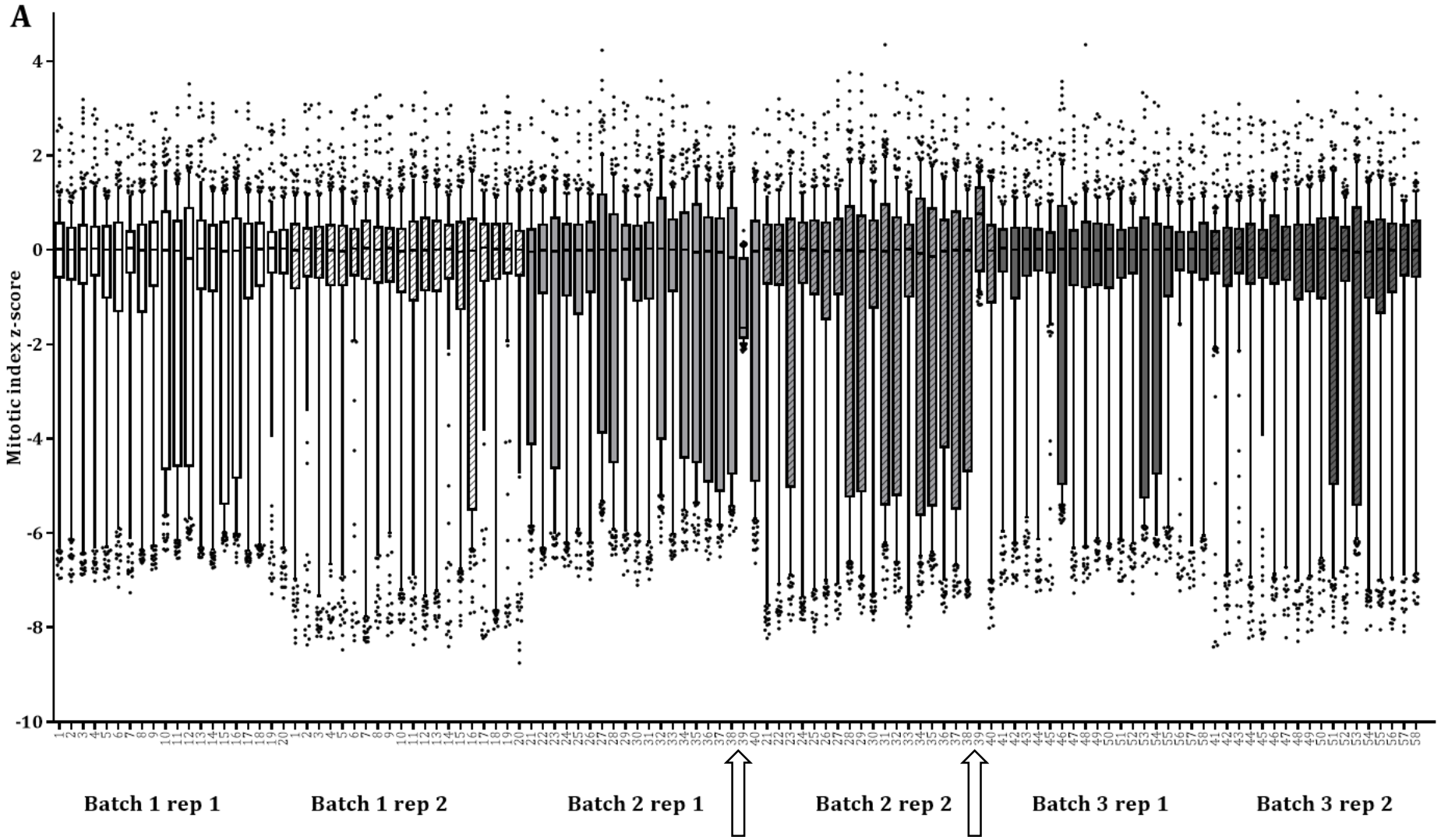
A
Mitotic index z-score
4
2
0
-2
-4
-6
-8
-10
Batch 1 rep 1
Batch 1 rep 2
Batch 2 rep 1
Batch 2 rep 2
Batch 3 rep 1
Batch 3 rep 2

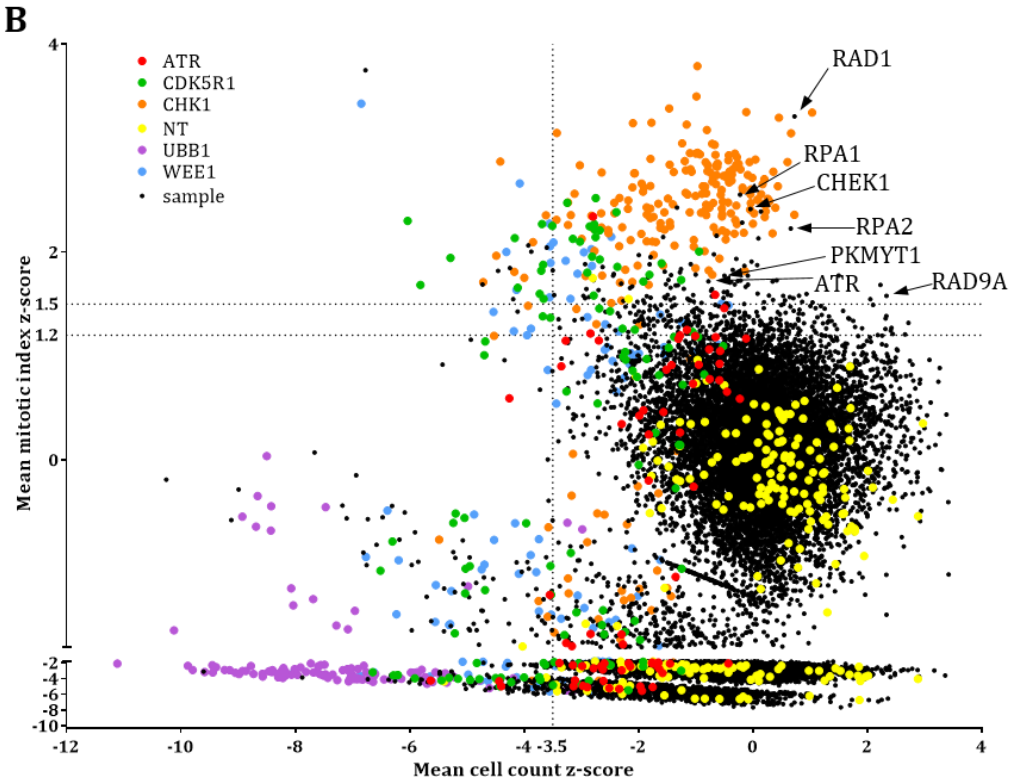

Figure 6-1. Genome-wide RNAi screen of S-M checkpoint.

A. Distribution of the normalised MI across all 116 plates screened. Each box represents the 25th-75th percentile of the plate with the median marked as a line. The whiskers extend to the 5th and 95th percentiles and data outlying this range are marked as dots. Plate 39 from both replicates are marked with arrows as they gave skewed results and so were excluded from analysis. **B.** Mean MI z-score vs mean cell count z-score of the controls and all samples for the genome-wide screen. Dotted lines represent thresholds used in hit evaluation. Results of known checkpoint components are highlighted.

control genes had the expected outcomes. The presence of UBB1 siRNA resulted in cell death (average cell count z-score -7.2), CHK1 siRNA resulted in an increase in MI without impacting dramatically on cell death (average MI z-score 1.9 and cell count z-score -1.4), and the NT siRNA gave an average MI and cell count (~0). As in the kinome-phosphatome screen, other controls, ATR, WEE1 and CDK5R1, resulted in a slight increase in MI but did cause a degree of cell death, as might be expected.

6.2.2 Hits

The samples of most interest were those in which both replicates had a MI z-score above 1.2 and a mean cell count z-score above -3.5 (MI in wells where the extent of cell death was very high was unreliable). This threshold was chosen as it included known components of the checkpoint (see those labelled in Figure 6-1B) and emphasised reproducibility across the two replicates. The 127 genes that crossed this threshold and are listed in table 6-1 and table 6-2 with their mean MI and cell count z-scores shown. Figure 6-2 shows a map of the known interactions and associations between these identified genes (93 genes have no interaction with any other and are not shown). From this figure, it can be seen that many of the known components involved in ATR activation were hits (ATR, RPA1, RPA2, RAD1, RAD9 and RFC4) as well as CHK1 and some replication components (RCF4, LIG1 and CDC6). There are many other replication components but these may not have been identified due to their knockdown strongly effecting viability or their lack of function in the checkpoint. Identification of checkpoint and replication components provided validation for the screen. Figure 6-2 also shows that knockdown of a number of genes known to be involved in the regulation of mitotic progression were identified in the first round of this screen. The identification of such genes is expected as the elimination of positive regulators of mitotic progression would be expected to increase the MI independently of the checkpoint.

6.2.3 Secondary screening

In order to further validate the hits, 100 were chosen to be taken forward for secondary screening. This included 71 of the 127 hits that crossed the initial threshold (table 6-1) and were those that gave the highest, most reproducible MI, with little cell death. Of the 56 over the threshold that weren't taken forward (table 6-2), 11 were those already known to be involved in the checkpoint or those known to be involved in mitosis. These were not taken forward as the aim of the screen was to identify novel

Gene Name	Mean MI z-score	Mean cell count z-score	Gene Name	Mean MI z-score	Mean cell count z-score
RPA1	2.552	-0.226	KLRA1	1.628	-0.734
CDC6	2.391	0.138	GAL3ST3	1.582	0.280
PPP1CA	2.283	-0.190	PHF1	1.580	0.805
RPA2	2.227	0.660	CR2	1.567	-2.868
CHRNE	2.158	-0.639	LIG1	1.561	-1.789
SFRP5	1.979	-0.684	RGS2	1.557	0.707
TAGAP	1.971	-1.997	SERTAD3	1.556	-1.525
SLC46A1	1.952	-1.792	NRN1L	1.553	-1.145
AQP3	1.908	-0.027	WIBG	1.540	0.349
GSTM1	1.904	-1.594	C12orf66	1.540	-1.122
ARRDC5	1.885	-1.090	EFCAB5	1.536	0.560
CELA1	1.883	-1.808	RASAL1	1.534	-1.094
AMAC1	1.875	0.073	PCSK2	1.519	0.191
OVCH1	1.867	-0.152	DYNC1I2	1.507	-0.463
ACRV1	1.837	-1.259	KIF4A	1.502	0.535
RALB	1.829	-0.354	TNIP1	1.501	-0.154
LARP4B	1.788	-1.801	CCDC149	1.461	1.092
IMPA1	1.779	-1.434	WARS	1.452	-1.680
CCT6A	1.774	1.499	MARK3	1.440	-0.936
XDH	1.773	-0.092	BCKDHB	1.431	-1.996
TUBB7P	1.772	-2.444	CCDC78	1.429	-0.319
TTC1	1.756	-1.835	TGM7	1.422	-1.914
RFC4	1.733	-1.479	FAM83A	1.419	-0.142
PIGF	1.729	0.413	NR1H4	1.387	-1.478
TMPRSS7	1.727	-0.217	KDM3A	1.386	-0.950
S1PR2	1.721	-0.264	DNM1L	1.386	0.082
ATP10D	1.721	-0.480	ANKMY2	1.384	-0.631
FUT2	1.717	0.341	KIF19	1.364	-0.736
EIF2C4	1.690	-1.522	PAPSS2	1.359	0.311
APOC3	1.684	2.228	BARX1	1.358	0.787
ITGB5	1.681	-1.314	SCARF2	1.353	-1.988
DYNC1LI2	1.680	-1.352	RPESP	1.328	-0.358
CARD17	1.666	-0.129	ZP1	1.322	-0.359
OR4E2	1.646	-1.210	OSBPL5	1.314	1.223
HERC6	1.644	-0.718	HSPB1	1.313	-0.443
FKBP10	1.634	-2.702			

Table 6-1. Genes that crossed the initial threshold and were taken forward for secondary screening.

127 genes scored an MI z-score above 1.2 in both replicates and had a mean cell count z-score above -3.5 (initial threshold). The 71 genes shown here are those that were taken forward for secondary screening.

Gene Name	Mean MI z-score	Mean cell count z-score	Gene Name	Mean MI z-score	Mean cell count z-score	Gene Name	Mean MI z-score	Mean cell count z-score	Evidence of involvement
DNAJC13	1.884	-2.934	ASH1L	1.390	-0.159				Checkpoint (Nghiem et al., 2001)
HEATR7B2	1.856	-2.629	MRPL46	1.386	-1.949	ATR	1.719	-0.780	
RBP1	1.813	-1.545	SLC44A3	1.384	-0.501				Checkpoint (Zachos et al., 2005)
SNTG2	1.805	-1.278	NPEPPS	1.380	1.327	CHK1	2.414	-0.044	
MLLT11	1.790	-2.433	ADAM19	1.376	-1.009				Checkpoint (Rhind and Russell, 2011)
GJB1	1.696	-2.305	CCT5	1.365	1.665	PKMYT1	1.774	-0.498	
LSP1	1.689	-0.319	CD1E	1.364	-0.225				Checkpoint (Zhang et al., 2011)
ABHD12B	1.645	-2.912	RPP30	1.358	-1.258	RAD1	3.306	0.725	
WNT10B	1.589	-1.491	IL9R	1.358	1.682				Checkpoint (Delacroiz et al., 2007)
HILPDA	1.567	0.645	KIAA0409	1.346	-1.566	RAD9A	1.579	2.332	
PFDN4	1.559	-0.515	SCML1	1.327	-0.551				Mitosis (Kramer et al., 1988)
C15orf39	1.542	-2.617	CMTM3	1.326	1.075	ANAPC2	2.133	0.094	
PAFAH1B1	1.492	2.100	C12orf60	1.322	-1.170				Mitosis (Chang and Barford, 2014)
TMEM67	1.474	-2.229	SESN2	1.308	-1.103	CDC16	2.428	-1.328	
LIPF	1.461	-0.984	VPS11	1.306	0.479				Mitosis (Chang and Barford, 2014)
NUDT13	1.460	0.190	DECR2	1.299	0.131	CDC26	1.934	-0.293	
PAGE5	1.456	1.254	ASF1B	1.296	-0.230				Mitosis (McEwen et al., 2001)
OR52B6	1.435	1.574	SLC16A1	1.292	-0.149	CENPE	2.145	-1.572	
ENDOU	1.423	0.431	SPRR1B	1.292	-0.377				Mitosis (Daum et al., 2009)
CLEC18B	1.421	-0.890	TAS1R3	1.291	0.484	SKA3	1.712	-0.381	
BAZ1B	1.417	-1.039	TPSG1	1.281	1.783				Mitosis (Garnett et al., 2009)
NAT8	1.408	0.799	PHF21A	1.266	0.308	UBE2S	1.688	-0.087	
OR4K13	1.396	-0.326							

Table 6-2. Genes that crossed the initial threshold but were not taken forward

127 genes scored an MI z-score above 1.2 in both replicates and had a mean cell count z-score above -3.5 (initial threshold). The 56 genes shown here are those that were not taken forward for secondary screening. 11 of these were due to known involvement in the checkpoint or mitosis (see right-hand side of table). The remaining 45 were not included due to low cell numbers or low reproducibility between replicates.

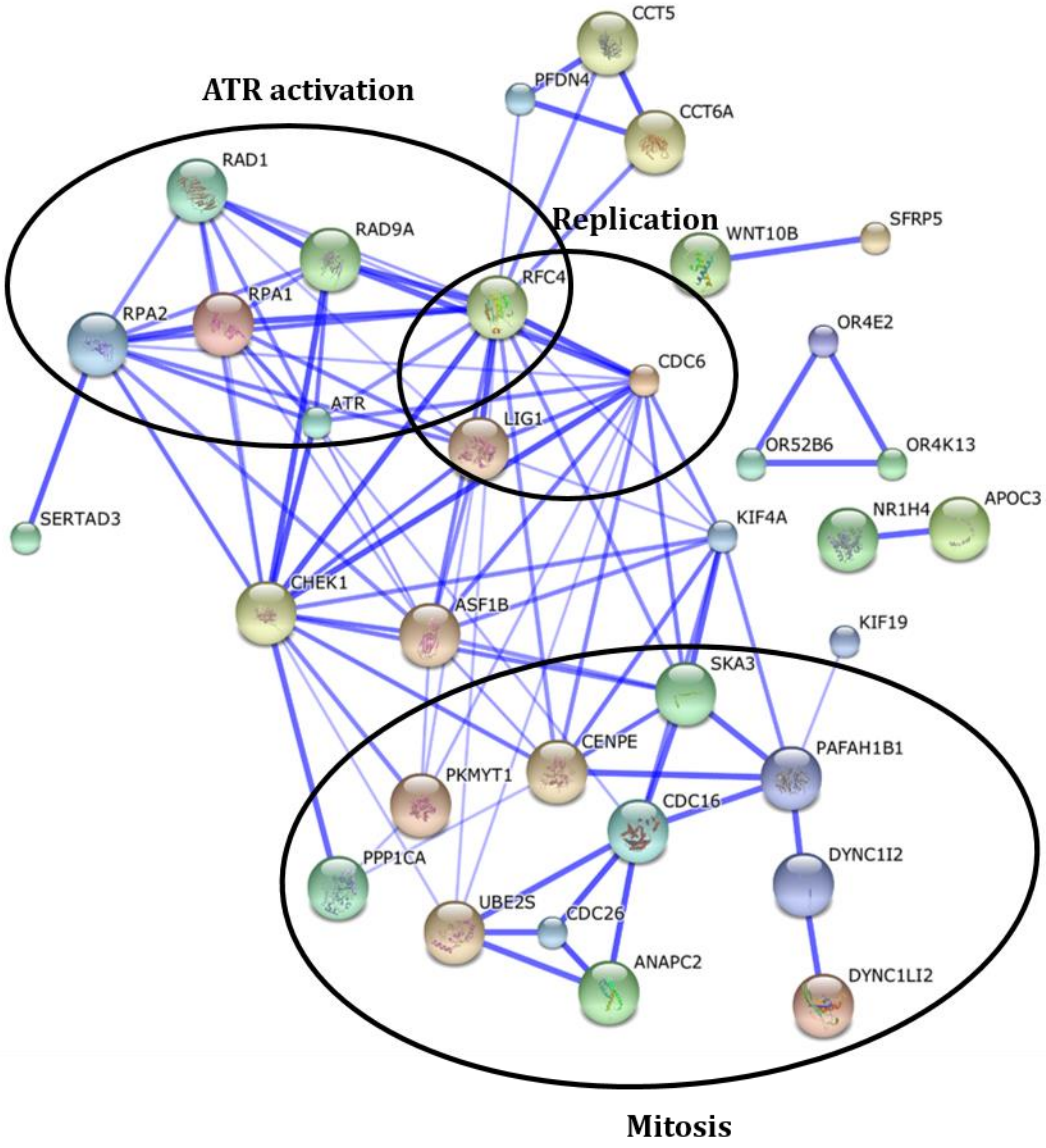

Figure 6-2. Hits from the genome-wide RNAi screen.

Interactions and associations of proteins that crossed the threshold. Only those that have an interaction with others are shown. The darker the blue line the more evidence for the interaction. Three main pathways are highlighted: those known to be involved in ATR activation, replication and mitosis.

components. RPA1 was included to act as a further positive control as its function in ATR activation is well documented (Zou and Elledge, 2003). CDC6's homolog Cdc18 has been found to have a role in the S-M checkpoint in yeast (Fersht et al., 2007)and the human protein has been shown to be involved in CHK1 activation and mitosis (Clay-Farrace et al., 2003; Lau et al., 2006). Therefore CDC6, which had a high MI z-score average of 2.3, was also taken forward as a highly probable component of the checkpoint.

A further 29 genes were chosen from hits that had one replicate with a MI z-score over 1.45 and the other under 1.2, but had a link to cancer or the cell cycle in the literature (Table 6-3).

In order to validate the 100 hits, they were screened in three further assays: one a repeat of the genome-wide screen, one utilising Aph, instead of HU, as the replication stress activator and one without any replication stress. All of these were performed using pooled siGENOME siRNA instead of the OTP siRNA used in the genome-wide screen which had different sequences. This was advantageous as off-target effects from siRNA sequences can be decreased, resulting in the potential identification of false positives. These pooled siRNAs were added to 384-well plates so that each plate contained two replicates of each hit, 8 wells with CHK1 siRNA, two wells with UBB1 siRNA and 32 wells with NT siRNA. Two plates were used for each secondary screen giving four replicates of each hit.

6.2.3.1 HU secondary screen

The first secondary screen was done to reproduce the original results with exactly the same assay conditions (except using siGENOME siRNA). Surprisingly, this secondary analysis generated a low frequency of hits which had a MI above one (Figure 6-3A). This could be due to some hits being false positives in the original screen, or the siGENOME siRNA being not as effective at inducing knockdown of the target protein below its critical effector concentration under the screening conditions used. Nonetheless, a number of hits gave a significant (p value <0.001 in two-tailed unpaired t-test) increase in MI compared to the NT siRNA. These were divided into strong and weak hits based on whether their mean MI was above or below one (Figure 6-3B).

Gene Name	Rep1 MI z-score	Rep 2 MI z-score	Mean MI z-score	Mean cell count z-score
C10ORF53	1.035	1.458	1.246	1.071
CARTPT	0.284	2.206	1.245	0.569
CAV2	1.120	1.508	1.314	-1.910
CD46	1.664	1.167	1.415	-2.148
CPNE9	1.192	1.494	1.343	-1.424
DNAJB12	1.922	0.868	1.395	1.202
DYNLRB1	1.187	2.014	1.600	0.081
E2F7	1.701	0.833	1.267	1.905
EGLN3	2.120	0.925	1.522	0.859
ERBB4	1.794	1.193	1.494	-0.493
ESCO2	1.766	1.066	1.416	-0.416
GSK3B	1.143	1.465	1.304	-1.912
KRT72	1.044	1.633	1.339	1.751
NCF4	1.803	0.856	1.329	-1.121
NME3	0.941	1.550	1.246	-0.004
NUDT9	2.541	0.696	1.619	-0.451
PDX1	1.062	1.969	1.515	1.042
PPP2R1A	1.995	0.667	1.331	-1.469
PPP2R5A	2.270	1.037	1.654	-2.151
PPP4R1	2.011	0.655	1.333	1.320
RBBP9	1.640	1.052	1.346	-0.151
SCAMP2	1.112	1.769	1.440	-1.807
SCD	0.893	1.689	1.291	-2.510
SFMBT2	1.982	1.131	1.556	-2.935
TNK1	1.856	1.125	1.491	0.494
VRK3	0.975	2.108	1.541	-1.444
WBP1	1.065	1.587	1.326	-1.023
XPC	1.106	2.046	1.576	-0.720
ZNF438	0.590	1.890	1.240	-0.821

Table 6-3. Weaker hits selected for secondary screening.

29 weaker hits in the primary scree were selected for secondary screening if they had one replicate with a MI z-score over 1.45 and the other under 1.2, and had a link to cancer or the cell cycle in the literature.

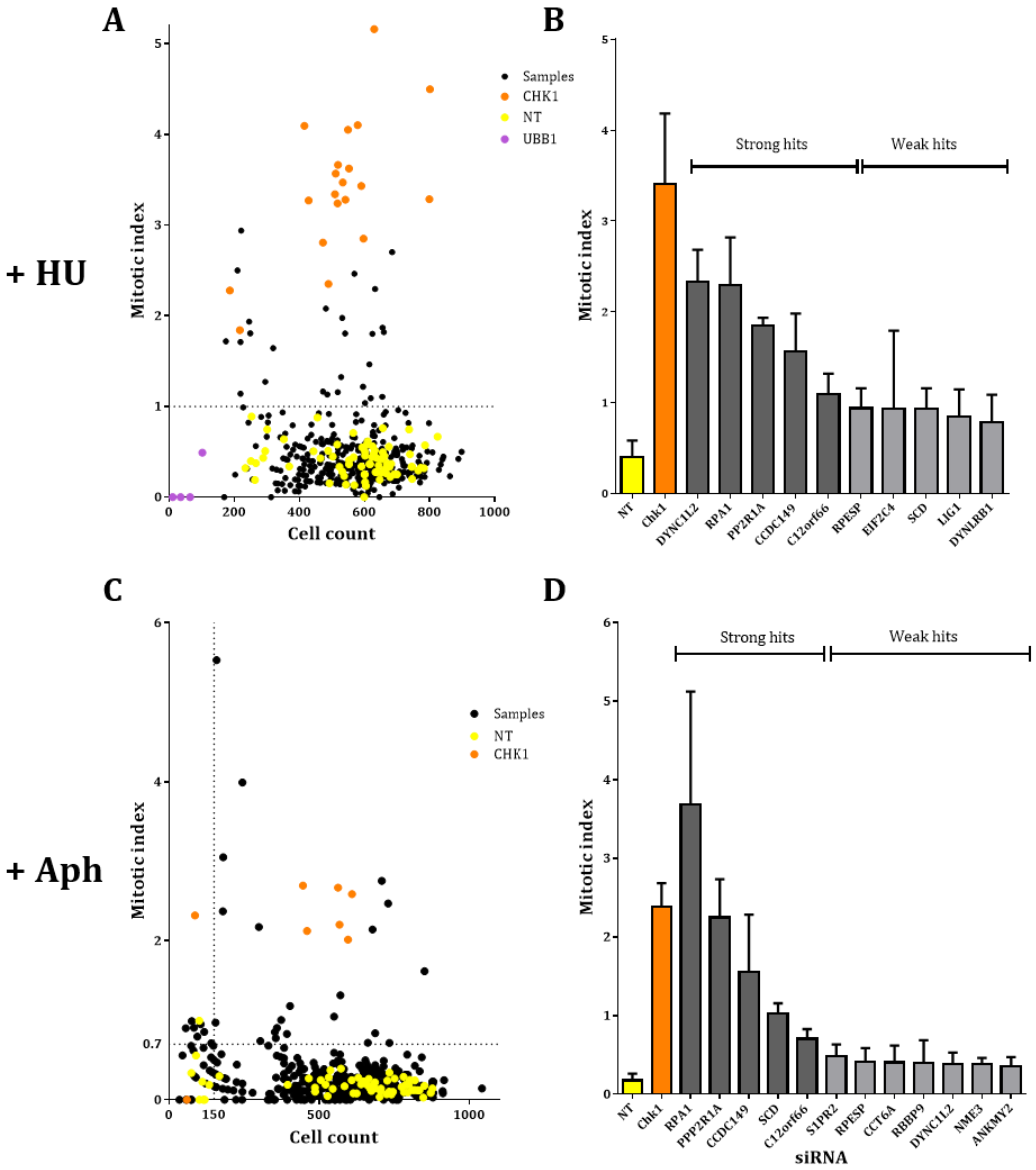

Figure 6-3. Secondary screening.

A. MI vs cell count for each individual well on the two secondary screening plates after S-M checkpoint assay with 2mM HU. **B.** Hits that had a significant difference from the NT samples ($p<0.001$ two tailed t-test). Hits with a mean MI over 1 were classified as strong. Bars represent the mean + sd **C.** As A but with 15μM Aph instead of HU. Dotted vertical line represents the cut off for those with a low cell count that were excluded. **D.** Hits that had a significant increase in MI compare to the NT samples ($p<0.001$ two-tailed t-test). Hits with a mean MI of over 0.7 were classified as strong and those less than 0.7 weak. Bars represent the mean + sd.

6.2.3.2 Aph secondary screen

The second secondary screen utilised 15μM Aph, instead of HU, to attempt to identify those hits that were responsive to replication stress generally and not specific to HU. Similarly to the first secondary screen, Figure 6-3C shows that there were few hits with a MI higher than the NT siRNA samples. There were also a few wells that had very low cell counts (generally found on the edge of the plates) and so these were removed from the analysis. The samples that showed a significant difference from the NT siRNA ($p<0.001$ two tailed unpaired t-test) are shown in Figure 6-3D, again split into strong (mean MI over 0.7) and weak hits. Encouragingly many of the hits (particularly the strong ones) were the same as those identified in the HU secondary screen.

6.2.3.3 No replication stress secondary screen

The final secondary screen was performed in the same manner as the previous two but with no replication stress added. This was to exclude hits that affected the MI independently of replication stress. Five hits gave an increased MI: DYNC1I2, CCT6A, EIF2C4, PPP2R1A and DYNLRB1 (data not shown). PPP2RA is a structural scaffold protein which forms part of PP2A. This heterotrimeric phosphatase controls multiple functions in mitosis, including playing a key role in mitotic exit (Schmitz et al., 2010; Wurzenberger and Gerlich, 2011). DYNC1L2 and DYNLRB1 are components of the Dynein motor protein complex. This plays a role in chromosome movement and spindle formation during mitosis and knockdown of components are known to affect mitotic progression (Raaijmakers et al., 2013). CCT6A is a subunit of the Chaperonin Containing TCP (CCT) complex, which is involved in protein folding. Though not directly involved in mitosis the CCT complex is known to associate with PLK1 and CDC20, an activator of the Anaphase Promoting Complex/Cyclosome (APC/C) (Camasses et al., 2003; Liu et al., 2005). Possibly due to this protein folding functions knockdown of CCT components has been shown to cause a G2/M arrest (Liu et al., 2005). EIF2C4/AGO4 is an argonaute protein involved in RNAi. The reasons as to why its knockdown increases the MI is unknown, but it is known to play a role in meiosis and a similar mechanism may apply in mitosis (Modzelewski et al., 2012). These genes, whilst involved in the process, were excluded from further analysis as mitotic genes were not the primary focus of this work.

6.2.3.4 Conclusions from the secondary screens

A summary of the results from the primary and secondary screens is shown in a Venn diagram in Figure 6-4A (mitotic genes from the third secondary screen are excluded). Even with a low number of genes being classified as hits in the secondary screens, there were 10 genes that performed well in both secondary assays. Table 6-4 shows how they performed in the different screens. The strongest overlap between the screens comes from the genes that were classified as strong hits in the secondary screens (Figure 6-4A see strong overlap of dark green and blue circles). That these genes showed strong effects in repeated and independent analyses adds more weight to the notion that these genes play a role in the S-M checkpoint.

In order to investigate some of the hits further a smaller number were chosen to take forward. The strongest hit in the secondary screens was RPA1 which is already known to be involved in ATR activation (Fanning et al., 2006), so this wasn't investigated further. The other top six hits are shown in Figure 6-4B where their responses in all the screens are compared. Four out of these six were chosen for further validation. The role of LIG1 was not investigated further due to its known involvement in replication and, consequently checkpoint activation. Because RPESP knockdown showed a slight increase in MI even when cells had not been previously treated with replication inhibitors, this potential hit was not pursued.

C12orf66 was chosen as it was a strong hit in all the screens though nothing is known of its function. CCDC149 is also relatively unknown and gave a strong response in the secondary screens. SCD was weak in the primary screen and the HU secondary screen but a strong response was observed when Aph was used to impose replication stress. S1PR2 was the final hit chosen for further investigation due to its strong response in the original screen and known link to cell proliferation (Kluk and Hla, 2002) even though it had a weaker response in the secondary screens.

6.3 Conclusions

In conclusion, a genome-wide RNAi screen has been performed to identify components of the S-M checkpoint. The screen was validated by the identification of many known components, CHK1, ATR, RAD1, RAD9A, RPA1, RPA2 and RFC4 (Canman, 2001). Other components, known to be involved in the checkpoint, were

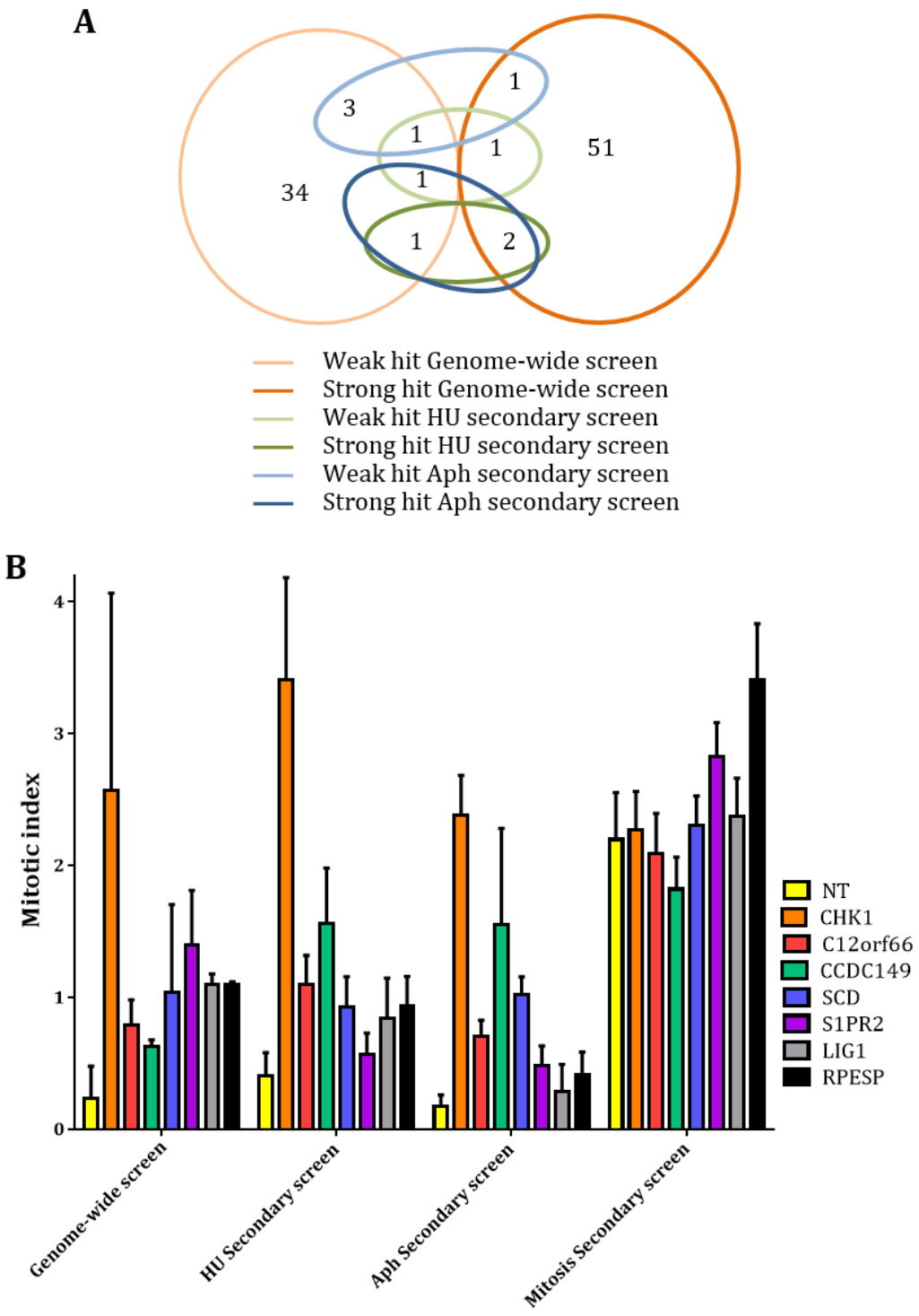

Figure 6-4. Summary of hits performance in primary and secondary screens.

A. Venn diagram (circles not to scale) of the strong (darker) and weak (lighter) hits from the three screens. Strong hits in from the genome-wide screen defined as those with mean MI z-score over 1.5. 5 Mitotic hits are excluded. **B.** MI of the 6 top hits in all 4 (original and 3 secondary) screens. Bar = mean + sd

	Genome-wide	HU Secondary	Aph Secondary
RPA1	Strong	Strong	Strong
C12orf66	Strong	Strong	Strong
CCDC149	Weak	Strong	Strong
SCD	Weak	Weak	Strong
S1PR2	Strong	None	Weak
RPESP	Weak	Weak	Weak
LIG1	Strong	Weak	None
ANKMY2	Weak	None	Weak
RBBP9	Weak	None	Weak
NME3	Weak	None	Weak

Table 6-4. Summary of hits from primary and secondary screens.

The 10 hits from the secondary screens with their result from the three screens. In the genome-wide screen strong hits classified as having a mean MI z-score over 1.5. In the HU secondary screen strong hits classified as having a mean MI over 1. In the Aph secondary screen strong hits classified as having a mean MI over 0.7.

not identified in the screening process (see Figure 6-5). There are several reasons for this, which may also apply to other false negative results.

Firstly only positive regulators of the checkpoint would be identified in the assay that was performed. The MI could only rise in comparison to the negative controls, meaning that the knockdown of any gene that increased the activity of the checkpoint could not be identified. For example, knockdown of CDC25A, B and C, CDK1 and cyclin B1 are all expected to decrease the MI in untreated cells but after treatment with replication stress would behave as control cells.

ATRIP, the key interacting partner of ATR, was not identified because targeting constructs for this gene have not been validated and therefore are not included in the available siRNA dataset. The analysis undertaken here involved targeting 18,104 genes, and thus approximately 2,000 genes were not screened. Once reagents are available for the remaining genes they can be investigated in the future.

Somewhat surprisingly, other genes, which are known to play key roles in the ATR activation, such as HUS1, Claspin, RAD17, and TOPBP1 (Delacroix et al., 2007; Kumagai and Dunphy, 2000; Lee and Dunphy, 2010) were not revealed in this screen. They may not have been identified due to insufficient knockdown of the protein by the siRNA protocol. This may be due to a long protein half-life or the ineffectiveness of the siRNA. They may also not be identified if there is redundancy in those elements of the system leading from detection of replication stress to the execution point of mitotic delay. It follows that knockdown of some of these components may have had other effects on aspects of checkpoint signalling and the DNA damage response, but these were not detected here. For example, if there was a way for the checkpoint signalling components to be activated independently of some upstream element (even if not to 100% of the optimal level) a significant effect from their knockdown might not necessarily be observed.

Some genes which are known to have a role in the wider DDR, BRCA2, NBS1 and WEE1, gave a relatively high response in one replicate but no response in another. This is a problem with only performing the screen in duplicate. Ineffectiveness of the assay in one well (due to edge effects, multidrop error or other reasons) results in two different results and inability to determine which is the true result.

There were 100 genes that produced an increase in the MI in the primary screen that were further validated in three secondary screens with siGENOME siRNA. There was

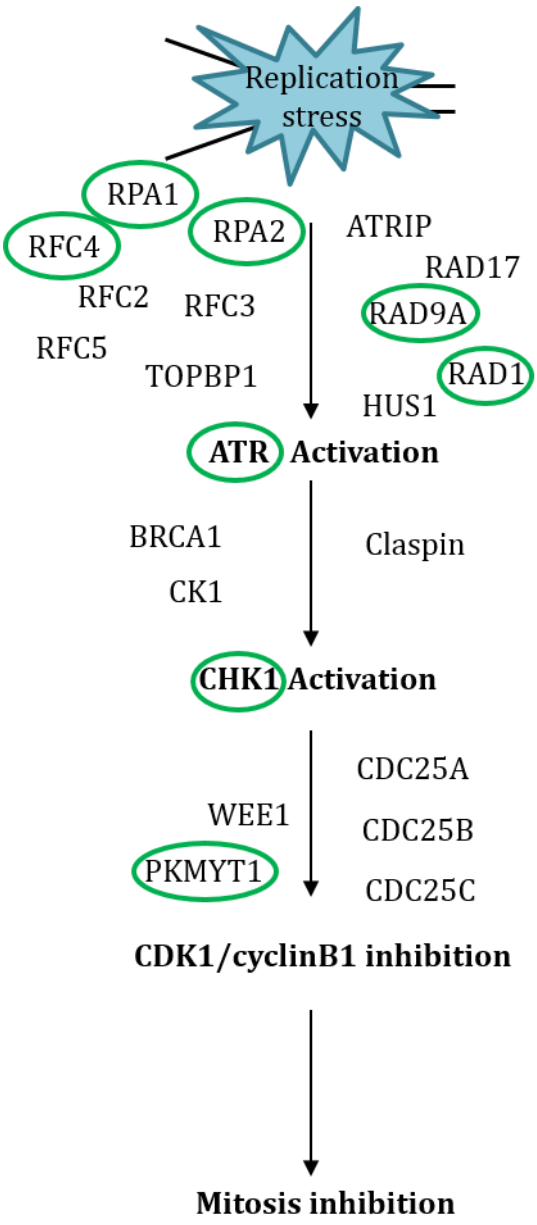

Figure 6-5. Identified components in the S-M checkpoint.

An outline of the S-M checkpoint with components identified in the genome-wide screen encircled in green. Unidentified components exist throughout the pathway.

a very low retention rate in the secondary screens, with only 10 of the 100 performing well, with one of the positive controls CDC6 not having an effect. This is most likely due to the change in type of siRNA from OTP to siGENOME. siGENOME siRNA doesn't have the further modifications that OTP siRNA has and is also designed to target a different sequence (Thermo Fisher Scientific, 2009). Even if knockdown of the mRNA did occur with the siGENOME siRNA it may not be as effective and still leave enough protein present to function in the checkpoint. Further work is needed to verify that this is the cause of low retention by analysing the protein levels of the primary hits after knockdown with each type of siRNA.

Four hits have been chosen to be taken forward that did give a response in the secondary screens. Although many other novel components may have been omitted during this analysis, the identification of these four is a positive outcome. Further screening and validation will be required to robustly identify all components of the S-phase checkpoint.

7. Validation of hits

7.1 Introduction

The four hits identified in the screen were of great interest, so further investigation into their role in the S-phase checkpoint was necessary. To initiate this a literature search was performed to evaluate what was already known about these genes.

Chromosome 12 open reading frame 66 (C12orf66), also known as FLJ32549 and UPF0536, is a 36kbp gene which encodes a 445aa protein of unknown function. It is over 96% conserved in mice and nearly 80% in zebrafish. Little is known about its function, but it has been shown to have increased expression in breast cancers that have invaded into the lymph nodes, indicating poor prognosis (Kim et al., 2011). It was also found in a genome-wide RNAi screen in U2OS cells (a human osteosarcoma cell line) to play a role in homologous recombination (Adamson et al., 2012). These few results are encouraging and suggest that C12orf66 may play a role in the DDR and cancer progression.

Coiled-coil domain containing protein 149 (CCDC149) is also a relatively unknown gene. It encodes a 4079bp mRNA made up of 13 exons which are translated into a 53kDa protein with an uncharacterised coiled-coil domain. Coiled-coil domains are versatile elements which are found in many proteins including structural proteins and transcription factors (Burkhard et al., 2001). CCDC149 has been identified as a ubiquitinated protein in Fanconi anemia bone marrow cells (Vanderwerf et al., 2009) and the region of chromosome 4 where the gene is located has been shown to be linked to bipolar disorder and schizophrenia (Christoforou et al., 2007).

Stearoyl-CoA desaturase (SCD/SCD1) is an endoplasmic-reticulum based enzyme involved in fatty acid metabolism which converts saturated stearoyl-CoA into monounsaturated oleoyl-CoA. This production is vital in the synthesis of phospholipids, triacylglycerols and cholesterol esters, all of which are required for cell membranes, signalling pathways and energy storage. Due to the requirement for fatty acids during cell proliferation, SCD is tightly regulated, and its expression increases upon mitogen stimulation. SCD is also highly expressed in many types of cancer cells, and linked to diabetes and obesity (Igal, 2010)

Sphingosine-1-phosphate receptor 2 (S1PR2/EDG5) is a small G-protein coupled receptor (GPCR) which is expressed in a wide range of cells and tissues (Kluk and Hla,

2002). Activation of the receptor by sphingosine-1-phosphate (S1P), causes a range of different signals which can affect migration, membrane ruffling, stress fibre formation and cell proliferation (Kluk and Hla, 2002). Levels of S1P are also known to be increased greatly in ovarian cancer cells (Wang et al., 2008) and deletion of S1PR2 in mice causes neuronal dysfunction (MacLennan et al., 2001).

These genes have no prior known link to the S-M checkpoint or any other DDR components and therefore to further validate their role and to investigate their function, further experiments were required. In order to do this, the siRNA type that gave the strongest phenotype was chosen to use for further investigation (Figure 6-4B). This was siGENOME siRNA (as used in the secondary screens) for C12orf66, CCDC149 and SCD and OTP siRNA (as used in the original screen) siRNA for S1PR2.

7.2 Results

7.2.1 Confirmation of knockdown

In a first step toward validation of the hits, it was necessary to confirm that transfection with the pooled siRNA caused knockdown of predicted target genes. As antibodies to some of the hits were unavailable, knockdown could only be confirmed at the mRNA level. Figure 7-1 shows that a strong knockdown of each mRNA was observed 72hrs after transfection with the pooled siRNA. This is suggestive that levels of the cognate protein in each case were also significantly reduced at this time point (though that may not be the case if any gene product has a significantly long half-life).

7.2.2 Deconvolution of siRNAs

The principles by which an siRNA efficiently brings about knockdown remain incomplete despite considerable progress (Pei and Tuschl, 2006). Distinct siRNAs targeting the same gene may result in different knockdown efficiencies. As a consequence, the large genome libraries utilised in the primary and secondary screen described here utilise a combination of four different sequences for each gene target (siRNA pools) in order to maximise the likelihood of efficient knockdown. This ensures that should one siRNA fail to reduce expression, the redundancy provided by the presence of other siRNAs will still result in knockdown, although possibly with decreased efficiency. The use of pooled siRNA also decreases the chance of off-target effects (Dharmacon, 2014). It was decided to deconvolve the pooled siRNA sets against the hits outlined above, into their individual siRNAs, and to assess each one's

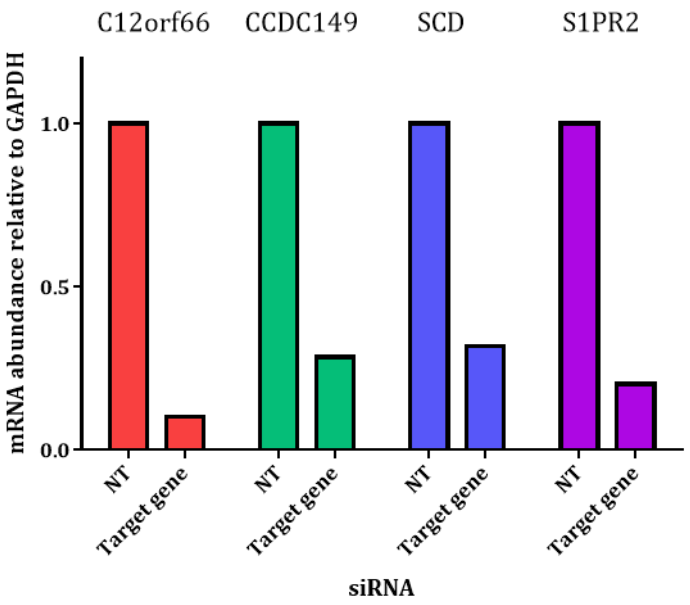

Figure 7-1. mRNA levels after hit gene knockdown with pooled siRNA

Expression of the indicated genes were knocked down using pooled siRNA (or NT as control) for 72hrs. RNA was extracted and levels quantified by QPCR for each target gene in the knocked down and control sample. Levels were normalised to GAPDH and fold change to NT sample calculated. N=1.

ability to knockdown expression of its predicted cognate gene. By doing this, the single siRNA that gave the best knockdown could be identified.

Knockdown was first evaluated by measuring relative mRNA levels, as shown in Figure 7-2. Not unexpectedly, the efficiency of knockdown as measured by q-PCR varied across each set of siRNAs. In general, as expected, each siRNA pool resulted in a knockdown efficiency compatible with the notion that, in the pools, each active component was present at reduced concentration, compared to experiments involving each unique siRNA.

Knockdown at the protein level was then confirmed for CCDC149 and SCD for which antibodies were available. Figure 7-3A shows that CCDC149 protein levels were significantly reduced from cells exposed to all cognate siRNAs in agreement with the mRNA data. SCD protein levels were found to decrease considerably with siRNA #1 and #3 and moderately with #4 but no knockdown was observed with #2 (Figure 7-3B). These data are not completely consistent with the mRNA data in which SCD mRNA was unaffected by siRNA #1. The reasons for these discrepancies are not clear. One possibility is the presence of well-to-well variation in the transfection efficiency. Another possibility is that the distinct chemistries associated with individual siRNAs may affect protein levels through different mechanisms, for example mRNA degradation or translation inhibition (Carthew and Sontheimer, 2009).

Finally, to identify individual mRNAs for further investigation, the individual siRNAs were also assessed in the S-M checkpoint assay. Figure 7-4A shows that again there was a range of effects from the different siRNAs and in general the pooled siRNAs resulted in phenotypes consistent with the combined effects of each. In the case of C12orf66, siRNA #2 gave the highest MI which was consistent with it giving the best knockdown at the mRNA level. This siRNA was chosen for further work. In the case of CCDC149, no increase in MI was observed with siRNA #2 although a modest knockdown had been observed at the protein level. But siRNA #3 did give a high MI and produced a moderate knockdown at the mRNA and protein level, so this was subsequently used. The SCD S-M checkpoint results were also broadly consistent with SCD protein levels, with no effect with siRNA #2 but a strong checkpoint abrogation with siRNA #3 and the pooled siRNA. Therefore siRNA #3 was used in subsequent experiments.

In Figure 7-4A, knockdown with S1PR2 siRNAs did not cause an effect on the S-M checkpoint. This result was concluded to be an anomaly as even the pooled siRNA,

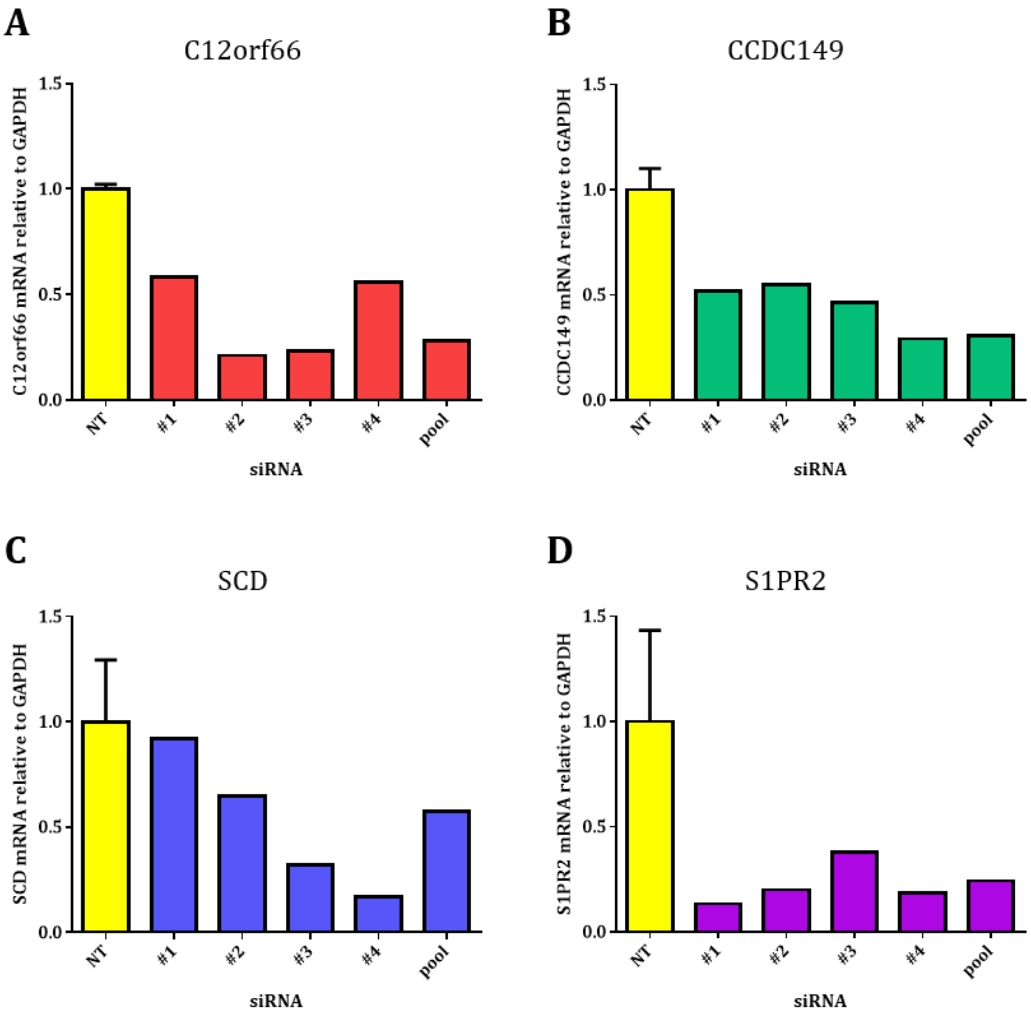

Figure 7-2. mRNA levels after knockdown of hits with deconvolved siRNA.

Genes were knocked down using individual siRNAs for 72hrs. RNA was extracted and levels quantified by QPCR for each target gene in the knocked down and control samples. Levels were normalised to GAPDH and fold change to the average of the two NT sample calculated. For NT N=2, for other samples N=1. **A** = C12orf66, **B** = CCDC149, **C** = SCD, **D** = S1PR2.

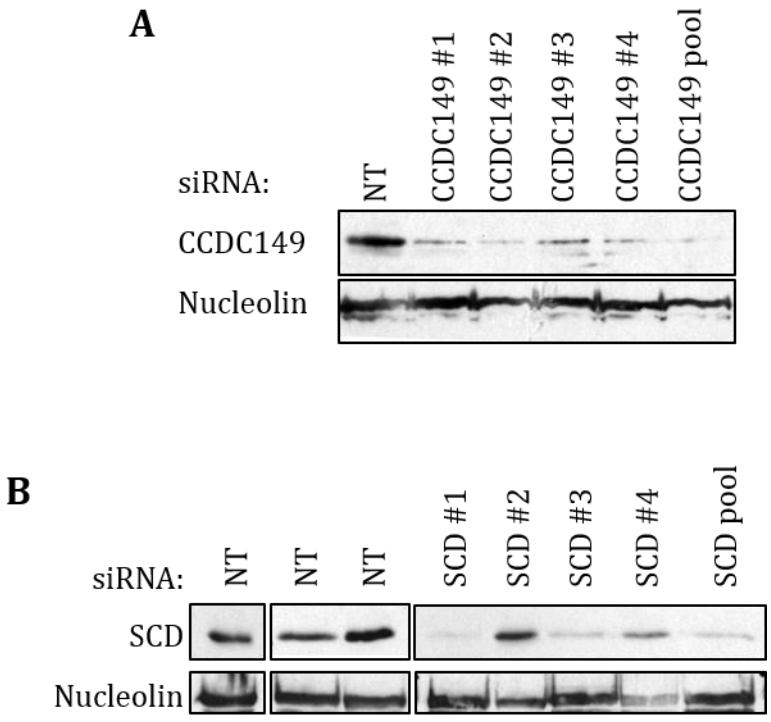

Figure 7-3. Protein levels after knockdown of hits.

A. Cells were transfected with siRNA either to individual CCDC149 siRNAs, a pool of all 4 siRNA or NT (control). After 72hrs cells were lysed and 60µg electrophoresed on a 10% SDS-gel. After western blotting levels of CCDC149 and Nucleolin (loading control) were detected by photographic film. CCDC149 band at ~50kDa and Nucleolin at ~80kDa. **B.** As A but 50µg loaded, SCD detected and 3 NT samples used as controls. Boxes represent where unnecessary bands were cropped out but all bands are from the same experiment and were developed for the same length of time, therefore comparable intensities. SCD ran at ~32kDa and Nucleolin ~80kDa.

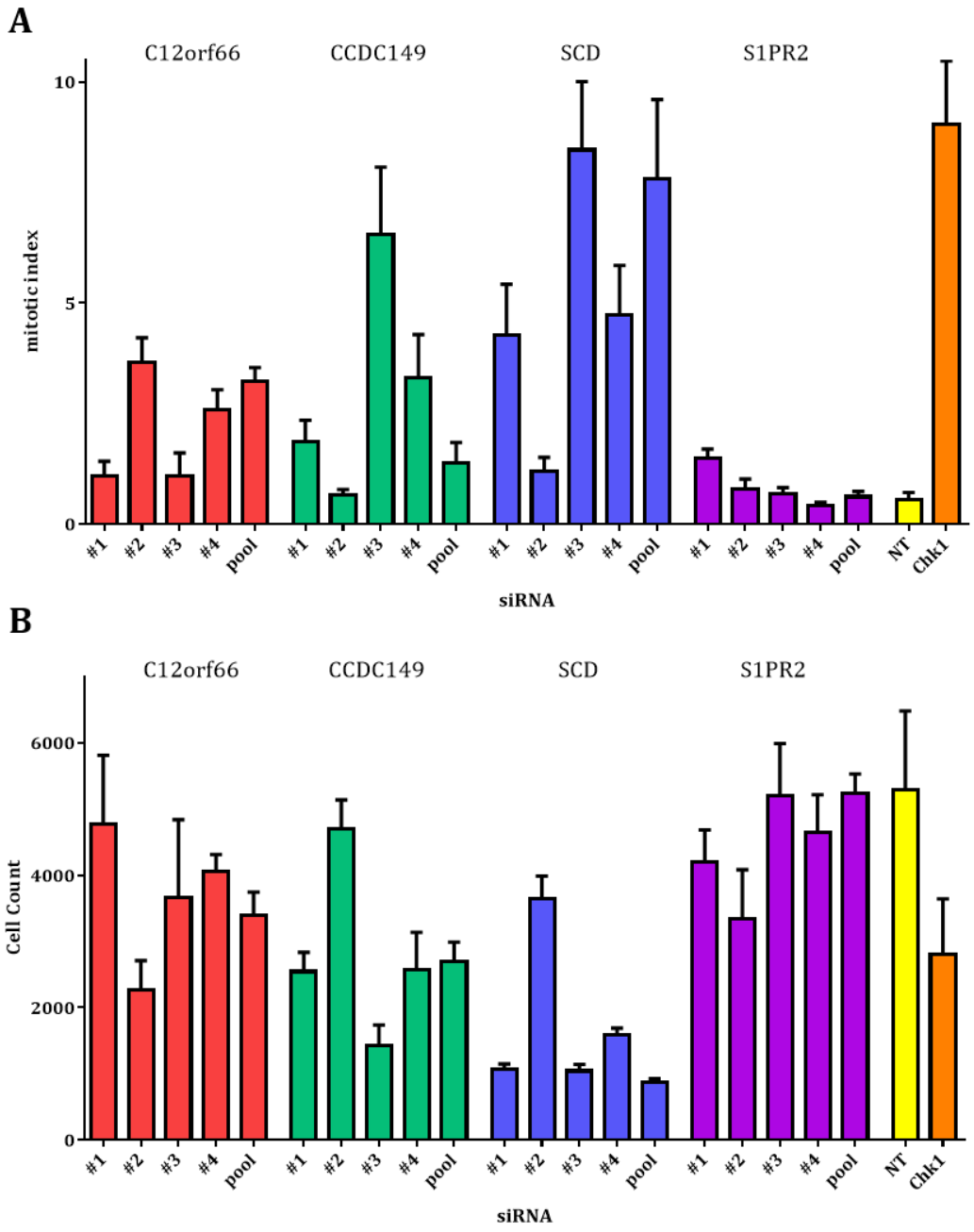

Figure 7-4. Effect of knockdown with deconvolved siRNAs on S-M checkpoint assay.

Cell population were transfected with individual or pooled siRNA to the hits or NT or CHK1 (controls). MI was measured after 24hrs HU treatment as in screen. MI (A) and cell count (B) show variation between individual siRNAs.

which had previously given an increase in MI, did not differ from the NT result. This is most likely due to inefficient knockdown of S1PR2, as a limited effect of cell count was also observed compared to the other knockdowns (Figure 7-4B). This could be caused by edge effects on the assay plate as the S1PR2 knockdowns were the closest to the edge, and it has been observed previously that the cells populations located at plate edges are affected by different incubation conditions. siRNA #1 was chosen to take forward as it gave a slight increase in MI in the S-M checkpoint assay and gave a strong knockdown at the mRNA level. A repeat of the S-M checkpoint assay is required though to confirm that this individual siRNA affects the S-M checkpoint.

7.2.3 Further investigation of role of hits in S-M checkpoint

7.2.3.1 Premature mitosis

To further investigate the role of the four proteins described above, I used siRNA induced knockdown, using the chosen individual siRNAs, to directly investigate the effect on premature mitosis. To do this, cells were treated with HU to activate the S-M checkpoint and then, after 5hrs, nocodazole (a microtubule polymerisation inhibitor that arrests cells in pro-metaphase) was added to trap cells in mitosis and prevent their loss through mitotic catastrophe. (See experiment timeline in Figure 7-5A). Cells were fixed and stained with anti-phospho-H3 as a marker for mitosis and propidium iodine to indicate DNA content respectively.

Figure 7-5B shows that, utilising the protocol outlined in Figure 7-5A, cells treated with HU and nocodazole, following transfection with NT siRNA, displayed the same proportion of 4N mitotic cells as asynchronous cells, similarly transfected. Unexpectedly, the MI was not low as it was in the S-M checkpoint experiments in which cells were exposed solely to HU, indicating that, in these experimental conditions, insufficient time had elapsed between the addition of HU and before the addition of nocodazole. Therefore mitotic cells that had a DNA content of 4N were likely to be those that were in G2 at the time of HU addition and not of particular interest in the analysis. Future experiments with a longer delay (or no nocodazole) would hopefully be able to reproduce the MI observed in the S-M checkpoint assay.

Nonetheless, there was still a noticeable effect when the S-M checkpoint was inhibited. Transfection with CHK1 siRNA and treatment of cells with HU and nocodazole caused a large percentage of cells to enter mitosis prematurely, indicated by those with a DNA content <4N (Figure 7-5B and D).

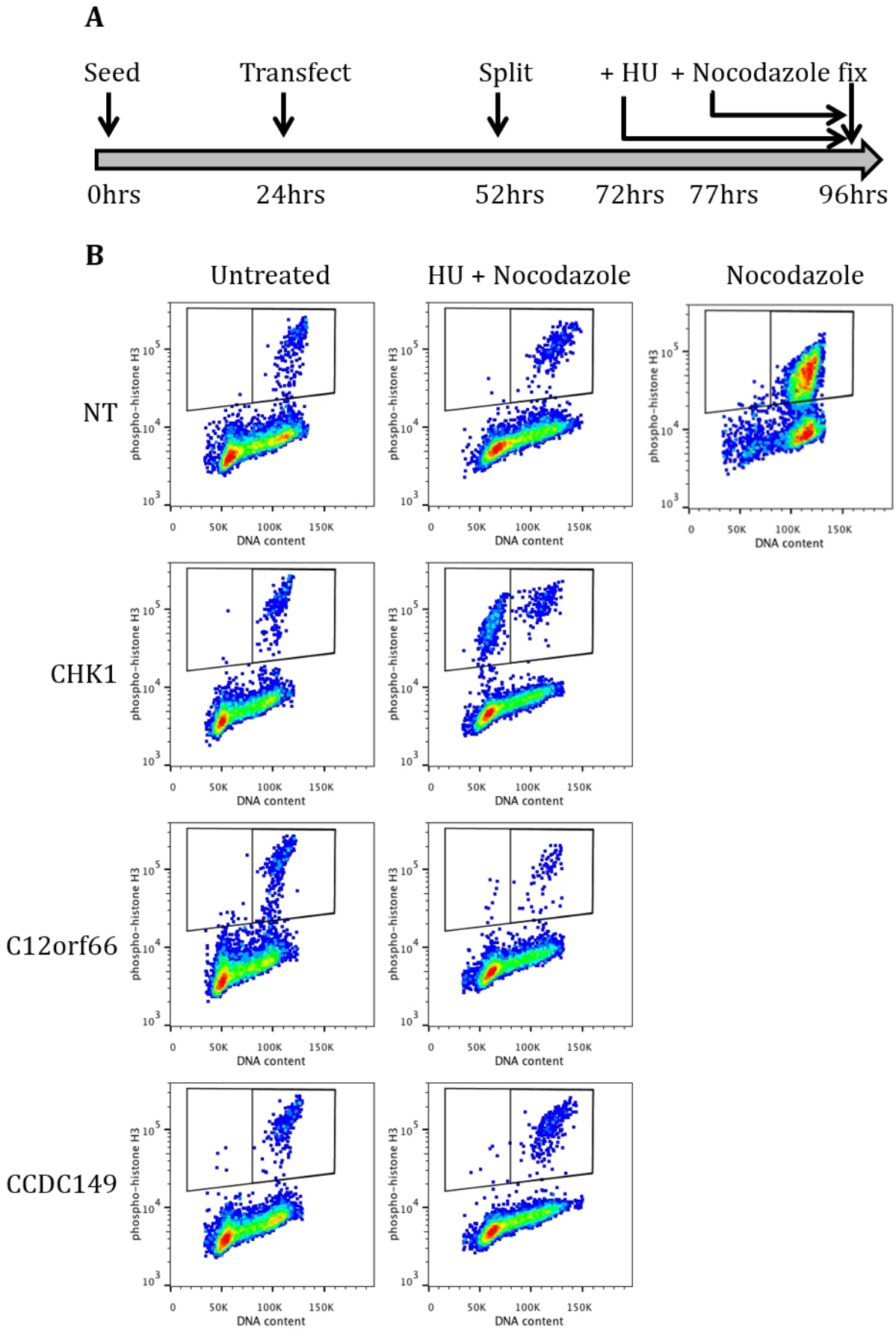
A
Seed
Transfect
Split
+ HU
+ Nocodazole fix
0hrs
24hrs
52hrs
72hrs
77hrs
96hrs
B
Untreated
HU + Nocodazole
Nocodazole
NT
CHK1
C12orf66
CCDC149
phospho-histone H3
DNA content
0
50K
100K
150K

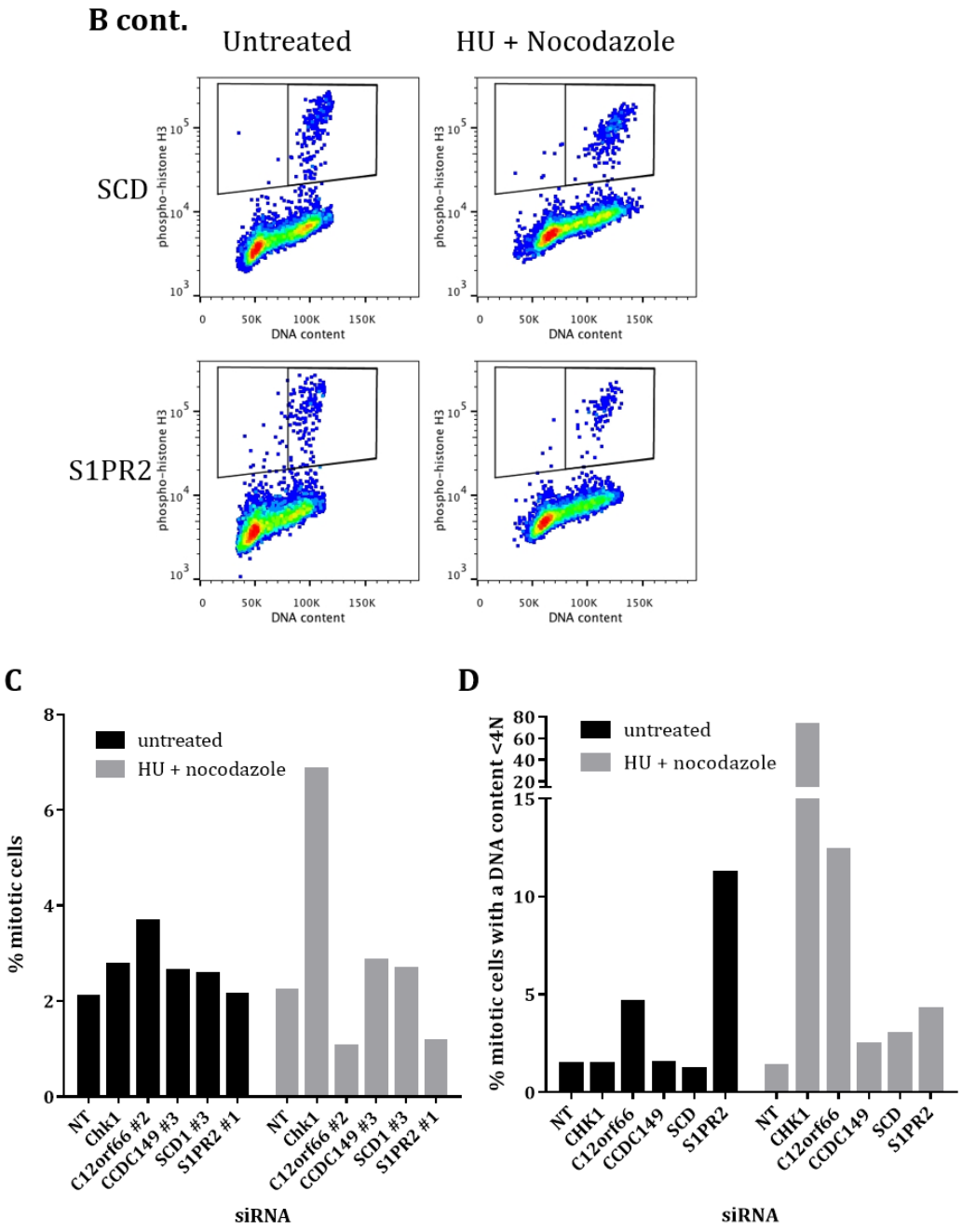

Figure 7-5. Effect of knockdown of hits on premature mitosis.

A. Timeline of assay before flow cytometry. Cells were knocked down with individual siRNAs to the hits or NT or CHK1 (controls). After transfection dishes were split in to two dishes. One was then left untreated and the other treated with 2mM HU for 24hrs and 100ng/ml nocodazole for the last 19hrs of the HU treatment. **B.** After protocol in A, samples were stained with anti-phospho-H3 and propidium iodide and flow cytometry used to identify mitotic cells. Two boxes at the top of each graph indicated the mitotic cells with the left hand side DNA content <4N and the right at 4N **C.** Quantification of the percentage of all cells that are phospho-H3 positive and therefore mitotic. **D.** Quantification of the percentage of all mitotic cells that have a DNA content less than 4N.

Knockdown with C12orf66 siRNA also resulted in an effect on mitosis with a strong decrease in the percentage of mitotic cells after HU and nocodazole treatment (Figure 7-5C). Looking into the cells that are mitotic it can be seen that C12orf66 knockdown gives an elevated percentage with a <4N DNA content compared to the NT siRNA control, although the effect is not as striking as that observed following CHK1 knockdown (see Figure 7-5D). This increase in <4N mitotic cells is also seen to a lesser extent in the untreated sample but here the mitotic index isn't low.

An increase in the percentage of mitotic cells with <4N DNA content was also observed with in untreated cells with S1PR2 knockdown (Figure 7-5D). This effect is lessened in HU and nocodazole treated cells where the mitotic index decreases (Figure 7-5C). This may suggest a role for S1PR2 in cell cycle progression which changes under conditions of replication stress.

Knockdown of CCDC149 and SCD only had a few cells entering mitosis prematurely after HU and nocodazole treatment but had no substantial difference from the NT control in untreated samples.

7.2.3.2 CDK1 and Cyclin B1

The end point of the S-M checkpoint, which causes the delay into mitosis, is the prevention of the activation of CDK1-cyclinB1 complex (Rhind and Russell, 1998). I therefore investigated whether knockdown of any of the four gene products described above had an effect on CDK1 or cyclin B1 levels or phosphorylation.

Cell populations were treated with the relevant optimised siRNA as above, together with NT and CHK1 siRNA as controls, and either left untreated, or treated for 24hrs with HU with nocodazole added for the final 16hrs. Figure 7-6A shows that levels of cyclin B1 (which are known to increase up to early mitosis) are higher in HU + nocodazole treated cells than untreated (compare the NT samples). This is in agreement with previous work that showed that S-phase arrested HCT116 cells continue to accumulate cyclin B1 during S-phase arrest (unlike other cell lines) (Florensa et al., 2003). It is possible that some G2/M cells remained present in this population following addition of nocodazole. In contrast, the cyclin B1 levels did not increase in cells containing reduced levels of CCDC149 or SCD. This is different from cells knocked down with CHK1, C12orf66 or S1PR2 which behave as the NT sample.

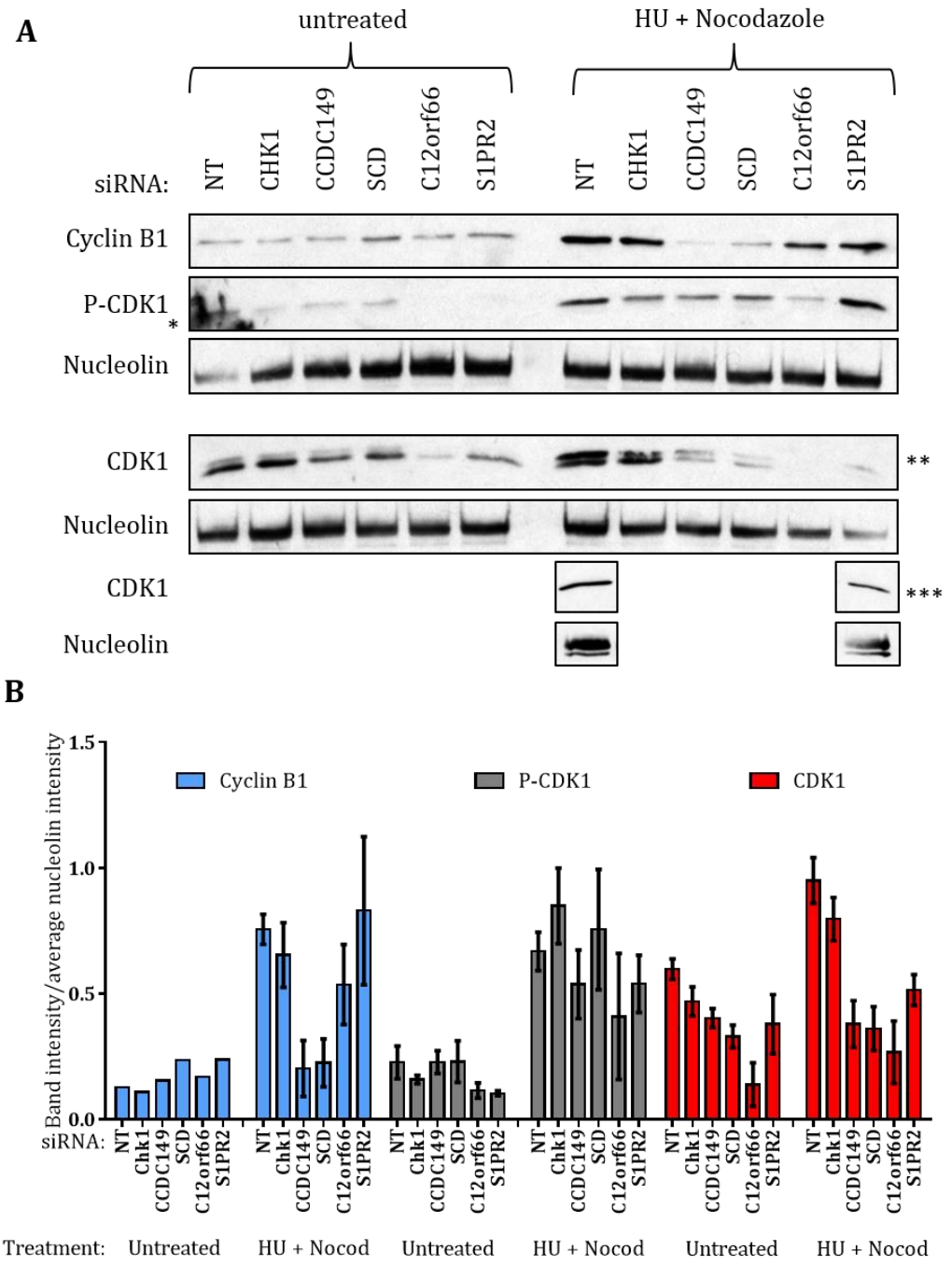

Figure 7-6. Knockdown of hits affects CDK1/cyclin B1.

A. Cells were either untreated or treated with 2mM HU for 24hrs and 50ng/ml nocodazole for the last 16hours. Cells were lysed, 15µg run on a gel and blotted for the above proteins. Nucleolin loading control for the samples above it. P-Cdc2 = Cdc2 phosphorylated at tyrosine 15. * indicates a mark on the blot not related to the protein. ** indicates band which was stronger when re-run, see ***. CyclinB1 ran at ~49kDa, P-CDK1 and CDK1 at ~27kDa and Nucleolin at ~80kDa. **B.** Quantification of repeats of the above experiment. Band intensity for each target protein was quantified and then divided by the average intensity of all the Nucleolin bands on that blot. N = 1 untreated Cyclin B1. N = 2 for treated Cyclin B1. N = 4-5 for P-CDK1 and CDK1 with NT, CHK1, CCDC149 or SCD siRNA. N = 2-3 for P-CDK1 and CDK1 with C12orf66 or S1PR2 siRNA. Error bars = SEM.

The overall levels of CDK1 were analysed in the same experiment. Treatment with HU is expected to activate the S/M checkpoint and induce increased levels of CDK1 phosphorylated at Y15. This was observed in the samples from cells exposed to NTsiRNA, where there was an increase in the ratio of phospho- (upper band) to dephospho (lower band) CDK1 in immunoblots probed with anti-CDK1 antibodies. An increase in phosphorylated CDK1 was also observed using a Y15 phospho-CDK1 specific antibody after treatment with HU and nocodazole (Figure 7-6A).

Knockdown of CHK1 shows a slight decrease in phospho-CDK1 after treatment in Figure 7-6A but this was not reproduced in other replicates (see quantification of five replicates in Figure 7-6B). This lack of dephosphorylation, though in contrast to the current model, agrees with previous work that shows CHK1-/- DT40 cells undergoing premature mitosis after Aph addition but still containing phospho-CDK1 (Zachos et al., 2005). Knockdown of CHK1 has no effect on CDK1 levels.

Knockdown of CCDC149 or SCD caused little effect on untreated cells but appeared to induce a decrease in CDK1 levels in HU and nocodazole treated cells relative to similarly treated cells exposed to NT siRNA. The phosphorylated levels of CDK1 only decrease slightly, indicating that the reduction is primarily due to a decrease in unphosphorylated CDK1. These results were confirmed in five experiments quantified in Figure 7-6B.

Knockdown of C12orf66 causes a substantial decrease in CDK1 levels in both untreated and treated conditions. Phospho-CDK1 levels are also low but this is likely to be due to the relatively low expression levels of the total protein.

With knockdown of S1PR2, untreated levels of CDK1 were slightly lower than the NT control. When treated with HU and nocodazole though, the levels of phosphorylated CDK1 were less than the NT control. In the image in Figure 7-6A, the overall CDK1 levels for this sample appeared drastically low but this was later explained as poor antibody binding as when the samples were re-run the band was only slightly fainter than NT (see bottom boxes in Figure 7-6A). The medium effect of S1PR2 knockdown on CDK1 levels was also confirmed in two further repeats of the experiment (Figure 7-6B) where the levels were only slightly less than the NT samples.

7.3 Conclusions

The siRNA pools, to the four hits that I identified in the screen, were confirmed to cause a knockdown of their target mRNAs. Deconvolution of the pools into their four individual siRNAs showed a range of effects on mRNA levels, protein levels and assay results.

Interestingly, the effects of the siRNA on mRNA levels didn't always correlate with the amount of knockdown seen at the protein level. With the SCD siRNAs strong knockdown at the mRNA level was only seen with siRNA #3 and #4. But at the protein level a strong decrease in SCD was seen with #1 and #3 and a moderate effect with #4. Therefore siRNA #1 is most likely targeting the translation efficiency of the SCD mRNA without effecting the mRNA stability. In contrast with this, the four CCDC149 siRNAs all caused a moderate decrease in mRNA levels and a strong knockdown at the protein level. With the availability of robust antibodies to C12orf66 and S1PR2 hopefully their effects on protein knockdown can be assessed in the future.

There is also not always a direct correlation between protein/mRNA knockdown and effectiveness in the S-M checkpoint assay. Even though knockdown at the protein and mRNA level had been consistent for all four CCDC149 siRNAs, a dramatic difference was seen in the S-M checkpoint with #2 giving no effect and #3 a very high MI. This may be due to inefficient knockdown in the S-M checkpoint assay or indicating that the effect on the S-M checkpoint assay is due to an off-target effect and not loss of CCDC149. As an effect on the assay is also seen with siRNA #1 and #4, I assume it is not an off-target effect but further work is necessary to prove this.

The strength of S1PR2 as a hit still needs to be verified as very little effect was seen on the S-M checkpoint assay with the individual siRNAs. As explained previously this may be due to experimental error or may indicate the true result. It is of note that S1PR2 gave a stronger response in the original genome wide screen than it did in the two secondary screens and therefore OTP siRNA was used in the individual siRNA experiments. In the assays looking into premature mitosis and CDK1/Cyclin B1 little effect was seen with S1PR2. This may be due to a lack of protein knockdown or confirming that S1PR2 is not involved in effecting mitosis. Although an increase in the percentage of mitotic cells with a DNA content <4N when cells are untreated indicates otherwise.

The results of the experiments investigating the function of the other hits checkpoint, showed some distinct differences. Knockdown of C12orf66 caused an increase in the percentage of mitotic cells with a DNA content <4N before, and more prominently, after checkpoint activation. It had no effect on cyclin B1 levels though does decrease CDK1 levels with and without replication stress.

CCDC149 and SCD knockdown had little effect on the cell cycle and premature mitosis but did cause a significant decrease in cyclin B1 levels after checkpoint activation. In these conditions knockdown of these hits also caused a decrease in unphosphorylated CDK1. Of note too is the observation that SCD protein levels decrease slightly with CCDC149 knockdown but rise after HU and nocodazole treatment (data not shown) indicating a further link between these genes.

It is interesting that knockdown of C12orf66, CCDC149 and SCD all caused a decrease in CDK1 levels after HU and nocodazole treatment, even though after only HU treatment they have an increase in cells entering mitosis. As the percentage of cells that do enter mitosis is still relatively low (2%) it may be that the CDK1 levels are high enough in these cells to activate mitosis. The mechanism by which these knockdowns effect CDK1 levels is unknown. CDK1 levels in HCT116 cells have also been shown to decrease after prolonged exposure to IR (Badie et al., 2000). In this case the mechanism is via a decrease in transcription. p53 has been shown to be a transcriptional repressor of CDK1 when the transcription factor NF-Y is present (Yun et al., 1999). It may be of interest that SCD expression is also activated by NF-Y (Tabor et al., 1999).

In conclusion I am still far from understanding the function of these four proteins in the S-phase checkpoint. But it is clear that these proteins play a role as their knockdown affects mitotic components in a replication stress-dependent manner. Further work is needed to determine how these proteins play their part.

8. Discussion and Future Perspectives

8.1 Introduction

The S-phase checkpoint's function is to protect cells from the difficulties that occur from having unreplicated DNA. Key components of the pathway have been discovered through genetic screens in yeast but there is much more complexity in higher eukaryotes. This work aimed to identify novel components of the S-phase checkpoint, by performing an RNAi screen. Initially, assays assessing histone mRNA decay, the stabilisation of the replisome, the inhibition of late origin firing and the S-M checkpoint were developed for *Drosophila* tissue culture cells. All the checkpoint responses were unreliable and therefore an S-M checkpoint assay was developed in the human colon carcinoma cell line, HCT116.

This assay was used for an RNAi screen, performed in duplicate across the majority of the genome. After secondary screening, four genes were identified that decreased the function of the S-M checkpoint when they were knocked down. Surprisingly some of these genes also decreased the levels of the key mitotic kinase CDK1/cyclin B1. On the surface this appears to contradict their checkpoint function but does confirm their role in mitotic regulation.

This work has produced as many questions as it has answers and some of these are discussed below. These also identify future experiments which would help to further our understanding of the S-phase checkpoint.

8.2 How do *Drosophila* culture cells survive with a weak checkpoint?

The S-phase checkpoint has mainly been previously studied in yeast, *Xenopus* and mammalian systems. In this investigation, I sought to use *Drosophila* S2R+ cells due to the ease of RNAi and their decreased redundancy. During assay development I discovered that when activated by HU or Aph, the checkpoint does not give a lasting, reliable effect in my hands. Histone mRNA levels only decreased to 50% after 2hrs of HU (unlike the 10% seen in HeLa cells), and levels returned to normal after 15hrs HU. Treatment of cells with Aph prevented origin firing and stabilised replication forks for up to 6hrs but only in 40% of cells and after 8hrs this was diminished further. The

S-M checkpoint was also ineffective with only a 50% reduction in mitotic cells after 24hrs HU and no reduction seen with 24hrs Aph treatment.

Previous work in early embryos has also shown the checkpoints to be 'leaky' and not long lasting (Fasulo et al., 2012; Sibon et al., 1997; Song, 2005). There is limited work investigating the S-phase checkpoint in *Drosophila* tissue culture cells but Vries et al. did show a 65% decrease in the MI after 15hrs HU in S2 cells (similar to S2R+)(de Vries et al., 2005). However, later time points were not investigated in this work and so the robustness of the checkpoint cannot be compared. The inhibition of late origin firing is more conserved in *Drosophila*, with the checkpoint response being observed after G2-synchronised Kc cells (another embryonic cell line) were released into HU containing media (Macalpine et al., 2004). There has been more work investigating the G2/M checkpoint in *Drosophila*, which appears to be quite robust with a conserved mechanism similar to that in mammalian cells (Kondo and Perrimon, 2011; Siudeja et al., 2011).

It is of note that synchronisation of many *Drosophila* tissue culture cells is challenging with many cell cycle inhibitors, e.g. nocodazole (Follmer and Francis, 2012; Rizzino and Blumenthal, 1978). This indicates further that the cell cycle checkpoints, which are the target of many synchronisation protocols, in these cells are not resilient as in other cell types.

Checkpoints exist to protect cells from DNA damage and replication stress. So how can *Drosophila* cells survive without robust checkpoints? It may be that components in the checkpoint pathways have been lost in S2R+ cells and that the responses are fully functional in the whole organism or other cell types. Further work investigating the S-phase checkpoint in other *Drosophila* cell lines would been needed to confirm this.

It may be the case that *Drosophila* do not have long lasting, robust checkpoints as they do not need them. Total inhibition of replication for 24hrs (as achieved by the addition of HU or Aph) is likely to be a rare occurrence in the natural environment of the whole organism. More likely is the failure of replication at a few replication forks or a brief lack of some replication components. Therefore the checkpoint mechanism may not have evolved to cope with extended, wide-spread replication stress, resulting in an inefficient checkpoint responses. Assessing the checkpoint response after different types and concentrations of DNA damaging agents and replication inhibitors is needed to investigate this situation further.

8.3 Mitotic regulation

The initiation of mitosis is dependent primarily on the activation of CDK1/cyclin B1. This kinase phosphorylates multiple targets involved in mitosis including nuclear envelope breakdown, chromosome condensation and centromere separation (Nigg, 2001). In order to prevent premature activation of CDK1/cyclin B1, the complex is regulated in two main mechanisms. Firstly, during interphase CDK1 is inhibited by phosphorylation on Y15 and T14 by WEE1 and PKMYT1 (McGowan and Russell, 1993; Mueller et al., 1995). At the G2/M boundary the activities of WEE1 and PKMYT1 are decreased and that of the CDC25 phosphatases are increased resulting in unphosphorylated Y15 and T14. Secondly, during interphase cyclin B1 is located in the cytoplasm due to high levels of nuclear export and ubiquitination-dependent degradation of nuclear cyclin B1 (Bassermann et al., 2005; Pines and Hunter, 1991; Toyoshima et al., 1998). At mitotic entry the cyclin is phosphorylated, encouraging its nuclear localisation by decreasing nuclear export (Hagting et al., 1999). The nuclear ubiquitin ligase is also inhibited increasing the nuclear accumulation (Bassermann et al., 2005).

8.3.1 How do cells enter mitosis with high CDK1 phosphorylation?

The current theory of the S-M checkpoint is that when it is activated, entry into mitosis is inhibited by preventing the loss of the inhibitory phosphorylations on CDK1. This is predicted to occur by CHK1 inhibiting CDC25C and activating WEE1. This has been reported in fission yeast, *Xenopus* and some mammalian cell culture lines (Blasina et al., 1997; Peng et al., 1997; Rhind and Russell, 1998; Smythe and Newport, 1992; Zeng et al., 1998).

Therefore inhibitors of the checkpoint are expected to decrease CDK1's inhibitory phosphorylation and increase CDK1/cyclin B1 activity. This has been shown in *Xenopus* with the addition of caffeine or okadaic acid in the presence of Aph (Smythe and Newport, 1992). I have also seen a decrease in CDK1 phosphorylation when HCT116 cells are treated with HU and caffeine compared to HU alone (data not shown).

In contrast to this, a loss of CDK1 phosphorylation has not been seen when the checkpoint is inhibited by loss of CHK1. DT40 cells (chicken) with CHK1 knocked out

and treated with Aph showed signs of premature mitosis and increased CDK1 activity but still displayed high levels of Y15 phosphorylation (Zachos et al., 2005). In this work I show that knockdown of known and discovered checkpoint components - CHK1, C12orf66, CCDC149, SCD and S1PR2 - also do not have a strong effect on CDK1 Y15 phosphorylation after HU. Similar results are also seen by Zuazua-Villar et al. who used thymidine to inhibit replication in HCT116 cells with CHK1 knocked down (Zuazua-Villar et al., 2014).

How are these cells entering mitosis when inhibitory phosphorylation is high? There are many ideas as to how this might occur. In the Zachos et al. study they saw that the CDK1 activity remained high and it would be interesting to see if the same was true of the checkpoint knockdowns in HCT116 cells. If this was the case, then perhaps the sub-population of CDK1 that is not phosphorylated (see lower band of CDK1 in Figure 7-6), is able to activate mitosis. There may be a further regulatory mechanism preventing this unphosphorylated CDK1 from initiating mitosis in interphase cells which is inhibited by the knockdown of checkpoint components.

8.3.2 How do cells enter mitosis with low cyclin B1 levels?

Also in contrast to the current S-M checkpoint theory, is the observation that knockdown of CCDC149 or SCD and treatment with HU, which leads to an increased MI, leads to low cyclin B1 levels. How are the cells entering mitosis without high levels of cyclin B1 levels? It may be that there is sufficient cyclin B1 in the nucleus to allow mitotic entry Fractionation of the cell lysate or immunofluorescence would be interesting to see where they cyclin B1 is located. A similar result was reported by Rodriguez et al. when non-transformed rat cells (NRK) were treated with HU, a CHK1 inhibitor, and a p38 inhibitor. Under these conditions, the S-M checkpoint was inhibited and cells entered mitosis but cyclin B1 levels remained low (Rodríguez-Bravo et al., 2007).

It may also be the case that other cyclins are activating CDK1. Although the knockout of cyclin B1 is embryonic lethal in mice (Brandeis et al., 1998), when it is knocked down in HeLa cells (to <5% of normal levels) mitosis can still occur (Soni et al., 2008). It is only when both cyclin B2 and cyclin B1 are knocked down that mitosis is prevented. Therefore it may be that cyclin B2 is activating CDK1 in HCT116 cells and it would be interesting to see what effect knockdown of CCDC149 or SCD have on cyclin B2 levels and localisation.

8.3.3 How does knockdown of CCDC149 or SCD decrease cyclin B1 levels?

The low levels of cyclin B1 seen after CCDC149 or SCD knocked down cells are treated with HU and nocodazole may either be caused by a decrease in cyclin B1 production (transcription or translation) or an increase in cyclin B1 degradation.

Cyclin B1 is transcribed during S-phase and G2 and is regulated by many transcription factors. The promoter sequence contains binding sites for NF-Y, E2Fs, B-MYB, p300 and FOXM1 (Porter and Donoghue, 2003). Many of these are also required for CDK1 and CCDC25C transcription (Fung and Poon, 2005). The SCD gene also contains a NF-Y binding element in its promoter and it may be through this transcription factor that a decrease in cyclin B1 is achieved (Tabor et al., 1999). In order to investigate this further the activity of the cyclin B1 promoter needs to be assessed by placing it upstream of a reporter gene and assessing expression after knockdown of the checkpoint genes.

Cyclin B1 is ubiquitinated from metaphase to early S-phase by the Anaphase Promoting Complex/Cyclosome (APC/C) which results in its degradation (Peters, 2006). An increase in APC/C activity could result in decreased levels of cyclin B1. The APC/C is activated by CDK1 and PLK1 in early mitosis and inactivated by a combination of different mechanisms during the G1/S transistion (e.g. E2F activation of APC/C inhibitor EMI1 and APC/C's own degradation of E2 ubiquitin-conjugating enzyme UBCH10) (Golan et al., 2002; Hsu et al., 2002; Rape and Kirschner, 2004). Analysis of the levels and phosphorylation states of the APC/C components and cofactors could determine whether APC/C activity is upregulated or misregulated after knockdown of CCDC149 or SCD causing loss of cyclin B1.

8.3.4 How do cells enter mitosis with low CDK1 levels?

A decrease in total CDK1 levels was seen when the checkpoint was activated after CCDC149, SCD or C12orf66 knockdown. Again this is in contrast to the current S-M checkpoint theory and seems to contradict the increase in MI seen. Entry into mitosis with low CDK1 may be possible due to the large amount of feedback in the system. Active CDK1/cyclin B1 inhibits WEE1 and PKMYT1 activity and promotes CDC25 activity further reinforcing its own activation. It is also involved in the activation of

PLK1 which activates multiple targets including CDC25C, cyclin B1 and the mitotic transcription factor FOXM1 (reviewed Lindqvist et al., 2009).

It may also be the case that CDK1 activation is not necessary for phosphorylation of histone H3 (the marker used for mitosis in this study). Zuazua-Villar et al. recently showed that cells that entered mitosis prematurely, after treatment with thymidine and CHK1 siRNA, had an increase in active Aurora B but inhibitory phosphorylations on CDK1. Aurora B is the kinase that phosphorylates histone H3 (Murnion et al., 2001) and they proposed that CHK1 is involved in inactivating Aurora B after replication stress independently of CDK1 (Zuazua-Villar et al., 2014). In order to determine whether low levels of CDK1 are sufficient for mitosis or whether an alternative mechanism to promote phospho-H3 occurs, it would be necessary to assess the CDK1/cyclin B1 activity. If this could be performed specifically in the cells that were positive for phospho-H3 after HU and CCDC149, SCD or C12orf66 knockdown then this would help us to understand the system better.

8.3.5 How does knockdown of CCDC149, SCD or C12orf66 decrease CDK1 levels?

However these cells enter mitosis with low CDK1 levels it is also of interest as to how the decrease is achieved. Low levels are seen after checkpoint activation with CCDC149 and SCD knockdown but both before and after checkpoint activation with C12orf66 knockdown. Interestingly this decrease is not seen with CHK1 knockdown suggesting that these checkpoint components are not downstream of CHK1.

CDK1 total levels normally remain fairly constant throughout the cell cycle. Activation of the G2/M checkpoint can cause a decrease in CDK1 in a p53-dependent manner (Taylor et al., 1999). The CCAAT boxes in the promoter are crucial for this as is the binding to the transcription factor NF-Y (Yun et al., 1999). A decrease in expression of CDK1 is seen in HCT116 cells treated with the topoisomerase II inhibitor, doxorubicin, and this is dependent on DNA methyl transferase 1 indicating repression via DNA methylation may be involved (Le Gac et al., 2006). It is possible that knockdown of CCDC149, SCD and C12orf66 results in activation of this repression pathway. Further work investigating the CDK1 promoter activity and the effect of removing p53 on CDK1 levels would hopefully shed more light on this.

8.4 What function are the hits playing in the S-phase checkpoint?

The four genes discovered in the screen have no previously known connection to the S-phase checkpoint. Therefore further work is necessary to fully understand their functions in this mechanism though some conjectures can be made.

8.4.1 C12orf66

C12orf66 is a relatively unknown gene that is well conserved in vertebrates but not in lower organisms (Geer et al., 2010). An x-ray structure of the C-terminal 320 amino acids of the mouse homolog has been published (PBDI: 2gnx, Phillips Jr et al.). The human protein has 94% identity to the mouse region crystallised and therefore is likely to have a similar structure. This structure contains a β-sheet made of five antiparallel strands and 17 alpha helices but no strong homology to other known protein structures. Therefore the function of this protein is still unknown.

A small section of the human protein (amino acids 132-210) shows some modelled structural similarity to the *Salmo salar* (Atlantic salmon) p38α (Arnold et al., 2009). This covers only a small section of the protein and the sequence identity is only 34% but further investigation may lead to a stronger link. p38α has previously been shown to be necessary for the S-M checkpoint in non-transformed rodent cells (Llopis et al., 2012; Rodríguez-Bravo et al., 2007) and it is possible that C12orf66 may be able to perform a similar role due to its similar structure. Further work investigating the structure of C12orf66 is necessary to validate this.

One theory of the possible role of C12orf66 is that it is involved in the early signalling of DNA damage and replication stress. This would explain its role in the S-M checkpoint and in homologous recombination (Adamson et al., 2012). This may also explain the increased expression in cancer (Kim et al., 2011), in which the cells may up-regulate checkpoint components to protect themselves from DNA damage. A role in DNA damage signalling would also explain why C12orf66 knocked down cells show a normal cell cycle profile and MI when not subjected to any DNA damage or replication stress agents. This theory does not explain the observation that CDK1 levels are dramatically decreased in untreated and HU and nocodazole treated cells when C12orf66 is knocked down. This may be due to a separate function of the protein or an off target effect of the siRNA.

In order to investigate this theory further it would be interesting to see the effect that knockdown of C12orf66 has on other DNA damage effects like the G2/M checkpoint and DNA repair. Further light may also be shed by identifying interacting proteins by mass spectrometry and investigating its DNA binding ability via an electrophorectic mobility shift assay (EMSA).

8.4.2 CCDC149

Little is known about CCDC149. Its potential coiled-coil domains could indicate a function in interacting with DNA so experiments investigating this (e.g. EMSA) would be useful. Previous studies have found it able to bind prions and amyloid-β (Oláh et al., 2011; Satoh et al., 2009) as well as be ubiquitinated in Fanconi anemia cells (Vanderwerf et al., 2009). Our study has found that knockdown of CCDC149 overrides the S-M checkpoint as well as causing a decrease in CDK1 and cyclin B1 after HU and nocodazole treatment. Interestingly the *Drosophila* homolog of CCDC149, CG14868 has been found to interact with *Drosophila* cyclin B in a yeast two hybrid screen (Giot et al., 2003).

Cyclin B1 levels do not accumulate in non-transformed rat kidney (NRK) cells after replication stress but do in HCT116 cells (Florensa et al., 2003). Knockdown of CCDC149 prevents this accumulation in HCT116 cells and therefore it is possible that CCDC149 is functioning in HCT116 cells to inhibit the mechanism that results in low cyclin B1. This inhibition may be through CCDC149's interaction with cyclin B1, if this is conserved in humans. CCDC149 expression may be lower in NRK cells explaining why they do not accumulate cyclin B1 after replication stress. In order to investigate this theory CCDC149's interaction with cyclin B1 would need to be confirmed and the expression of CCDC149 in different cell lines.

This function does not fully explain CCDC149's role in the S-M checkpoint or how it affects CDK1 levels. As the cyclin B1 regulation is replication-stress dependent and linked to the S-M checkpoint, CCDC149 knockdown may affect the S-M checkpoint through effects on this pathway or it may be have a separate function. Further work into assessing the state of CDC25 and CHK1 after checkpoint activation may help to identify if the core S-M checkpoint pathway is affected by CCDC149 knockdown.

8.4.3 SCD

Stearoyl CoA desaturase is a primary component of the fatty acid synthesis pathway and is highly regulated. SCD is over expressed in many cancers (Li et al., 1994; Yahagi et al., 2005) and involved in diabetes and obesity (Chow et al., 2013; García-Serrano et al., 2011) and therefore many studies have been performed to understand its function. Studies show that the inhibition of SCD through RNAi or chemical inhibitors decreases proliferation and tumour formation in cancer cells (Morgan-Lappe et al., 2007; Scaglia and Igal, 2005; Scaglia et al., 2009). This effect may be via signalling to AKT and glycogen synthase kinase-3β (GSK-3β), whose activities have been seen to decrease and increase, respectively, after SCD knockdown (Scaglia and Igal, 2008). GSK-3β has many targets including cyclin D1 and Cdc25A (Diehl et al., 1998; Kang et al., 2008). Phosphorylation of these by GSK-3β targets them for ubiquitination and subsequent degradation. Perhaps it is via this pathway that knockdown of SCD also causes degradation of cyclin B1 and CDK1 and inhibits the S-M checkpoint.

In order to investigate the function of SCD further it would be interesting to see if the same results are seen with a chemical inhibitor of SCD (CVT-11127) as with RNAi. It would also be of interest to assess the expression levels of SCD in HCT116 cells and other cells lines and compare this to the effect that SCD inhibition has on the S-M checkpoint in each cell lines. SCD may be over expressed in HCT116 cells meaning that its function in the S-M checkpoint is specific to this cell line.

8.4.4 S1PR2

Sphingosine-1-phosphate receptor 2 is a GPCR which, when activated, can cause a wide range of effects. It has shown to be primarily anti-proliferative, resulting in a decrease in AKT signalling when it interacts with $G_{12/13}$ (Sanchez et al., 2007). In contrast, in prostate cancer cells it can interact with G_i resulting in an increase in AKT signalling (Beckham et al., 2013). AKT is a pro-proliferation and anti-apoptotic kinase which phosphorylates multiple targets involved in cell cycle regulation (Xu et al., 2012). These include activation of CDC25B and inhibition of WEE1, PKMYT1 and CDK2 to encourage the G2/M transition (Baldin et al., 2003; Katayama et al., 2005; Maddika et al., 2008; Okumura et al., 2002). Overexpression of AKT can also abrogate the G2 checkpoint and CHK1 activation by directly phosphorylating CHK1 and TOPBP1 (Kandel et al., 2002; King et al., 2004; Liu et al., 2006).

Inhibition of the S-M checkpoint after knockdown of S1PR2 (or SCD) may be the result of increased activation of AKT. Inappropriate phosphorylation of CHK1 or TOPBP1 may lead to the inability of the checkpoint mechanism to function or phosphorylation of WEE1, PKMYT1 or CDC25B may lead to a strong mitotic signal that overrides the checkpoint. Knockdown of S1PR2 has previously been shown to cause an increase in γH2AX (DNA damage marker) which may result from checkpoint inhibition (Paulsen et al., 2009). Further study of AKT phosphorylation after S1PR2 knockdown and replication stress would confirm or deny this theory.

S1PR2 may also not be a component of the S-M checkpoint but affect general mitotic levels. An initial strong effect in the assay was seen in the genome-wide screen which used OTP siRNA. A more diminished effect was seen in the secondary assays when the siGENOME siRNA was used indicating that either this siRNA may not result in a strong knockdown of the protein or that the OTP siRNA may cause off-target effects that impact the checkpoint. Unfortunately siGENOME siRNA was also used to assess the MI with no replication stress. In these conditions no deviation from the control was seen (Figure 6-4B) but no investigation into S1PR2 mRNA or protein levels was performed to confirm knockdown. Therefor it may be that the siGENOME siRNA for S1PR2 does not cause knockdown and that if the OTP siRNA had been used an increase in MI would be seen in untreated cells. This expectation is confirmed by the result of the flow cytometry where, with OTP siRNA, an increase in mitotic cells with a DNA content of less than 4N is seen in untreated cells (Figure 7-5B). Unlike the other hits, knockdown of S1PR2 did not affect cyclin B1 or CDK1 levels.

8.5 What other information can be obtained from the genome-wide RNAi screening data?

The aim of the genome-wide screen was to identify novel components of the S-phase checkpoint. This was achieved and the hits have been discussed above. There is still a huge amount of knowledge which can be extracted from the screen data though. Of particular interest is the other 96 genes which were taken forward for secondary screening but no result was seen with the siGENOME siRNA. Some of these may have been false positives in the original screen, but others may have not been knocked down successfully with the siGENOME siRNA. It would be of great interest to assess their function further and to confirm or deny their knockdown. Even one of the positive control genes (CDC6) did not give a positive result in the secondary screens further indicating that the siGENOME siRNA was not always effective.

It would also be interesting to follow up those genes whose knockdown resulted in low cell numbers in the screen. It would be useful to identify if any of them only caused cell death when HU was present as this may indicate a role in the replication stress response.

8.6 Final conclusions

The aim of this work was to identify novel components of the S-phase checkpoint which could become potential therapeutic targets for cancer. A genome-wide RNAi screen was performed using an S-M checkpoint assay and four novels genes were identified. Two of these are relatively unknown, C12orf66 and CCDC149, and two have a previous known function in cell proliferation but not in checkpoint response, SCD and S1PR2. The effect of their knockdown on the mitotic initiator CDK1/cyclin B1 has been investigated confirming their role in mitotic regulation after replication stress. Further work assessing the impact of these genes on different pathways and in different cell lines is necessary to elucidate their full function in the checkpoint.

9. Bibliography

Abbas, T., and Dutta, A. (2009). P21 in Cancer: Intricate Networks and Multiple Activities. Nat. Rev. Cancer *9*, 400–414.

Adamson, B., Smogorzewska, A., Sigoillot, F.D., King, R.W., and Elledge, S.J. (2012). A genome-wide homologous recombination screen identifies the RNA-binding protein RBMX as a component of the DNA-damage response. Nat. Cell Biol. *14*, 318–328.

Agami, R., and Bernards, R. (2000). Distinct initiation and maintenance mechanisms cooperate to induce G1 cell cycle arrest in response to DNA damage. Cell *102*, 55–66.

Alberts, B., Johnson, A., Lewis, J., Raff, M., Roberts, K., and Walter, P. (2008). The Cell Cycle. In Molecular Biology of the Cell, (Garland Science, Taylor & Francis Group), pp. 1053–1114.

Al-Khodairy, F., and Carr, A.M. (1992). DNA repair mutants defining G2 checkpoint pathways in Schizosaccharomyces pombe. EMBO J. *11*, 1343–1350.

Allen, C., Ashley, A.K., Hromas, R., and Nickoloff, J. a (2011). More forks on the road to replication stress recovery. J. Mol. Cell Biol. *3*, 4–12.

Anderson, K., and Lengyel, J. (1980). Changing rates of histone mRNA synthesis and turnover in Drosophila embryos. Cell *21*, 717–727.

Appella, E., and Anderson, C.W. (2001). Post-translational modifications and activation of p53 by genotoxic stresses. Eur. J. Biochem. *268*, 2764–2772.

Arnold, K., Kiefer, F., Kopp, J., Battey, J.N.D., Podvinec, M., Westbrook, J.D., Berman, H.M., Bordoli, L., and Schwede, T. (2009). The Protein Model Portal. J. Struct. Funct. Genomics *10*, 1–8.

Aten, J. a, Bakker, P.J., Stap, J., Boschman, G. a, and Veenhof, C.H. (1992). DNA double labelling with IdUrd and CldUrd for spatial and temporal analysis of cell proliferation and DNA replication. Histochem. J. *24*, 251–259.

Badie, C., Itzhaki, J.E., Sullivan, M.J., Carpenter, A.J., and Porter, A.C.G. (2000). Repression of CDK1 and Other Genes with CDE and CHR Promoter Elements during DNA Damage-Induced G 2 / M Arrest in Human Cells. Mol. Cell. Biol. *20*, 2358–2366.

Bakkenist, C.J., and Kastan, M.B. (2003). DNA damage activates ATM through intermolecular autophosphorylation and dimer dissociation. Nature *421*, 499–506.

Baldin, V., Theis-Febvre, N., Benne, C., Froment, C., Cazales, M., Burlet-Schiltz, O., and Ducommun, B. (2003). PKB/Akt phosphorylates the CDC25B phosphatase and regulates its intracellular localisation. Biol. Cell *95*, 547–554.

Ball, H.L., Ehrhardt, M.R., Mordes, D. a, Glick, G.G., Chazin, W.J., and Cortez, D. (2007). Function of a conserved checkpoint recruitment domain in ATRIP proteins. Mol. Cell. Biol. *27*, 3367–3377.

Banin, S., Moyal, L., Shieh, S.-Y., Taya, Y., Anderson, C.W., Chessa, L., Smorodinsky, N.I., Prives, C., Reiss, Y., Shiloh, Y., et al. (1998). Enhanced Phosphorytation of p53 by ATM in Response to DNA Damage. Science *281*, 1674–1677.

Bartek, J., Lukas, C., and Lukas, J. (2004). Checking on DNA damage in S phase. Nat. Rev. Mol. Cell Biol. *5*, 792–804.

Bassermann, F., von Klitzing, C., Münch, S., Bai, R.-Y., Kawaguchi, H., Morris, S.W., Peschel, C., and Duyster, J. (2005). NIPA defines an SCF-type mammalian E3 ligase that regulates mitotic entry. Cell *122*, 45–57.

Baumbach, L.L., Marashi, F., Plumb, M., Stein, G., and Stein, J. (1984). Inhibition of DNA replication coordinately reduces cellular levels of core and H1 histone mRNAs: requirement for protein synthesis. Biochemistry *23*, 1618–1625.

Beckham, T.H., Cheng, J.C., Lu, P., Shao, Y., Troyer, D., Lance, R., Marrison, S.T., Norris, J.S., and Liu, X. (2013). Acid ceramidase induces sphingosine kinase 1/S1P receptor 2-mediated activation of oncogenic Akt signaling. Oncogenesis *2*, e49.

Bell, S.P., and Dutta, A. (2002). DNA replication in eukaryotic cells. Annu. Rev. Biochem. *71*, 333–374.

Belvin, M.P., Jin, Y., and Anderson, K. V (1995). Cactus protein degradation mediates Drosophila dorsal-ventral signaling. Genes Dev *9*, 783–793.

Bensimon, A., Schmidt, A., Ziv, Y., Elkon, R., Wang, S.Y., Chen, D.J., Aebersold, R., and Shiloh, Y. (2010). ATM-dependent and -independent dynamics of the nuclear phosphoproteome after DNA damage. Sci. Signal. *3*, rs3.

Bermudez, V.P., Lindsey-Boltz, L. a, Cesare, A.J., Maniwa, Y., Griffith, J.D., Hurwitz, J., and Sancar, A. (2003). Loading of the human 9-1-1 checkpoint complex onto DNA by the checkpoint clamp loader hRad17-replication factor C complex in vitro. Proc. Natl. Acad. Sci. U.S.A. *100*, 1633–1638.

Birnstiel, M.L., Busslinger, M., and Strub, K. (1985). Transcription termination and 3' processing: the end is in site! Cell *41*, 349–359.

Blagosklonny, M. V, and Pardee, A.B. (2002). The restriction point of the cell cycle. Cell Cycle *1*, 103–110.

Blasina, a, Paegle, E.S., and McGowan, C.H. (1997). The role of inhibitory phosphorylation of CDC2 following DNA replication block and radiation-induced damage in human cells. Mol. Biol. Cell *8*, 1013–1023.

Blasina, A., Price, B.D., Turenne, G. a, and McGowan, C.H. (1999). Caffeine inhibits the checkpoint kinase ATM. Curr. Biol. *9*, 1135–1138.

Bonner, W.M., Wu, R.S., Panusz, H.T., and Muneses, C. (1988). Kinetics of accumulation and depletion of soluble newly synthesized histone in the reciprocal regulation of histone and DNA synthesis. Biochemistry *27*, 6542–6550.

Boos, D., Sanchez-Pulido, L., Rappas, M., Pearl, L.H., Oliver, A.W., Ponting, C.P., and Diffley, J.F.X. (2011). Regulation of DNA replication through Sld3-Dpb11 interaction is conserved from yeast to humans. Curr. Biol. *21*, 1152–1157.

Borun, T.W., Gabrielli, F., Ajiro, K., Zweidler, a, and Baglioni, C. (1975). Further evidence of transcriptional and translational control of histone messenger RNA during the HeLa S3 cycle. Cell *4*, 59–67.

Boutros, M., Kiger, A., Armknecht, S., Kerr, K., Hild, M., Koch, B., Haas, S.A., Heidelberg Fly Array Consortium, Paro, R., and Perrimon, N. (2004). Genome-wide RNAi analysis of growth and viability in Drosophila cells. Science *303*, 832–835.

Boutros, M., Brás, L., and Huber, W. (2006). Analysis of cell-based RNAi screens. Genome Biol. *7*, 66.

Brandeis, M., Rosewell, I., Carrington, M., Crompton, T., Jacobs, M. a, Kirk, J., Gannon, J., and Hunt, T. (1998). Cyclin B2-null mice develop normally and are fertile whereas cyclin B1-null mice die in utero. Proc. Natl. Acad. Sci. U.S.A. *95*, 4344–4349.

Brodsky, M., Sekelsky, J., Tsang, G., Hawley, R.S., and Rubin, G.M. (2000). mus304 encodes a novel DNA damage checkpoint protein required during Drosophila development. Genes Dev. *14*, 666–678.

Brown, E.J., and Baltimore, D. (2000). ATR disruption leads to chromosomal fragmentation and early embryonic lethality. Genes Dev. *14*, 397–402.

Brown, E.J., and Baltimore, D. (2003). Essential and dispensable roles of ATR in cell cycle arrest and genome maintenance. Genes Dev. *17*, 615–628.

Burkhard, P., Stetefeld, J., and Strelkov, S. V (2001). Coiled coils: a highly versatile protein folding motif. Trends Cell Biol. *11*, 82–88.

Burma, S., Chen, B.P., Murphy, M., Kurimasa, a, and Chen, D.J. (2001). ATM phosphorylates histone H2AX in response to DNA double-strand breaks. J. Biol. Chem. *276*, 42462–42467.

Busino, L., Donzelli, M., Chiesa, M., Guardavaccaro, D., Ganoth, D., Dorrello, N.V., Hershko, A., Pagano, M., and Draetta, G.F. (2003). Degradation of Cdc25A by b -TrCP during S phase and in response to DNA damage. Nature *426*, 87–91.

Camasses, A., Bogdanova, A., Shevchenko, A., and Zachariae, W. (2003). The CCT Chaperonin Promotes Activation of the Anaphase-Promoting Complex through the Generation of Functional Cdc20. Mol. Cell *12*, 87–100.

Canman, C.E. (2001). Replication checkpoint: preventing mitotic catastrophe. Curr. Biol. *11*, R121–R124.

Canman, C.E., Lim, D., Cimprich, K.A., Taya, Y., Tamai, K., Sakaguchi, K., Appella, E., Kastan, M.B., and Siliciano, J.D. (1998). Activation of the ATM Kinase by Ionizing Radiation and Phosphorylation of p53. Science *281*, 1677–1679.

Carney, J.P., Maser, R.S., Olivares, H., Davis, E.M., Le Beau, M., Yates, J.R., Hays, L., Morgan, W.F., and Petrini, J.H. (1998). The hMre11/hRad50 protein complex and Nijmegen breakage syndrome: linkage of double-strand break repair to the cellular DNA damage response. Cell *93*, 477–486.

Carthew, R.W., and Sontheimer, E.J. (2009). Origins and Mechanisms of miRNAs and siRNAs. Cell *136*, 642–655.

Chang, L., and Barford, D. (2014). Insights into the anaphase-promoting complex: a molecular machine that regulates mitosis. Curr. Opin. Struct. Biol. *29C*, 1–9.

Chen, T., Stephens, P.A., Middleton, F.K., and Curtin, N.J. (2012). Targeting the S and G2 checkpoint to treat cancer. Drug Discov. Today *17*, 194–202.

Cheng, S.C., Hilton, B.D., Roman, J.M., and Dipple, A. (1989). DNA adducts from carcinogenic and noncarcinogenic enantiomers of benzo pyrenedihydrodiol epoxide. Chem. Res. Toxicol. *2*, 334–340.

Chini, C.C.S., and Chen, J. (2003). Human claspin is required for replication checkpoint control. J. Biol. Chem. *278*, 30057–30062.

Chow, L.S., Li, S., Eberly, L.E., Seaquist, E.R., Eckfeldt, J.H., Hoogeveen, R.C., Couper, D.J., Steffen, L.M., and Pankow, J.S. (2013). Estimated plasma stearoyl co-A desaturase-1 activity and risk of incident diabetes: the Atherosclerosis Risk in Communities (ARIC) study. Metabolism. *62*, 100–108.

Christoforou, a, Le Hellard, S., Thomson, P. a, Morris, S.W., Tenesa, a, Pickard, B.S., Wray, N.R., Muir, W.J., Blackwood, D.H., Porteous, D.J., et al. (2007). Association analysis of the chromosome 4p15-p16 candidate region for bipolar disorder and schizophrenia. Mol. Psychiatry *12*, 1011–1025.

Cimprich, K. a, and Cortez, D. (2008). ATR: an essential regulator of genome integrity. Nat. Rev. Mol. Cell Biol. *9*, 616–627.

Clay-Farrace, L., Pelizon, C., Santamaria, D., Pines, J., and Laskey, R.A. (2003). Human replication protein Cdc6 prevents mitosis through a checkpoint mechanism that implicates Chk1. EMBO J. *22*, 704–712.

Clemens, J.C., Worby, C. a, Simonson-Leff, N., Muda, M., Maehama, T., Hemmings, B. a, and Dixon, J.E. (2000). Use of double-stranded RNA interference in Drosophila cell lines to dissect signal transduction pathways. Proc. Natl. Acad. Sci. U.S.A. *97*, 6499–6503.

Cliby, W. a, Roberts, C.J., Cimprich, K. a, Stringer, C.M., Lamb, J.R., Schreiber, S.L., and Friend, S.H. (1998). Overexpression of a kinase-inactive ATR protein causes sensitivity to DNA-damaging agents and defects in cell cycle checkpoints. EMBO J. *17*, 159–169.

Cobb, J., Schleker, T., Rojas, V., Bjergbaek, L., Tercero, J.A., and Gasser, S.M. (2005). Replisome instability, fork collapse, and gross chromosomal rearrangements arise synergistically from Mec1 kinase and RecQ helicase mutations. Genes … *19*, 3055–3069.

Cobb, J. a, Bjergbaek, L., Shimada, K., Frei, C., and Gasser, S.M. (2003). DNA polymerase stabilization at stalled replication forks requires Mec1 and the RecQ helicase Sgs1. EMBO J. *22*, 4325–4336.

Cook, D.R., Solski, P. a, Bultman, S.J., Kauselmann, G., Schoor, M., Kuehn, R., Friedman, L.S., Cowley, D.O., Van Dyke, T., Yeh, J.J., et al. (2011). The ect2 rho Guanine nucleotide exchange factor is essential for early mouse development and normal cell cytokinesis and migration. Genes Cancer *2*, 932–942.

Cortez, D., Guntuku, S., Qin, J., and Elledge, S.J. (2001). ATR and ATRIP: Partners in Checkpoint Signaling. Science *294*, 1713–1716.

Cortez, D., Glick, G., and Elledge, S.J. (2004). Minichromosome maintenance proteins are direct targets of the ATM and ATR checkpoint kinases. Proc. Natl. Acad. Sci. U.S.A. *101*, 10078–10083.

Costanzo, V., Robertson, K., Ying, C.Y., Kim, E., Avvedimento, E., Gottesman, M., Grieco, D., and Gautier, J. (2000). Reconstitution of an ATM-dependent checkpoint that inhibits chromosomal DNA replication following DNA damage. Mol. Cell *6*, 649–659.

Costanzo, V., Shechter, D., Lupardus, P.J., Cimprich, K. a, Gottesman, M., and Gautier, J. (2003). An ATR- and Cdc7-dependent DNA damage checkpoint that inhibits initiation of DNA replication. Mol. Cell *11*, 203–213.

Daum, J.R., Wren, J.D., Daniel, J.J., Sivakumar, S., McAvoy, J.N., Potapova, T.A., and Gorbsky, G.J. (2009). Ska3 is required for spindle checkpoint silencing and the maintenance of chromosome cohesion in mitosis. Curr. Biol. *19*, 1467–1472.

Davidson, B.L., and McCray, P.B. (2011). Current prospects for RNA interference-based therapies. Nat. Rev. Genet. *12*, 329–340.

Delacroix, S., Wagner, J.M., Kobayashi, M., Yamamoto, K., and Karnitz, L.M. (2007). The Rad9–Hus1–Rad1 (9–1–1) clamp activates checkpoint signaling via TopBP1. Genes Dev. *1*, 1472–1477.

DeLisle, A.J., Graves, R.A., Marzluff, W.F., and Johnson, L.F. (1983). Regulation of histone mRNA production and stability in serum-stimulated mouse 3T6 fibroblasts. Mol. Cell. Biol. *3*, 1920–1929.

Demidova, A.R., Aau, M.Y., Zhuang, L., and Yu, Q. (2009). Dual regulation of Cdc25A by Chk1 and p53-ATF3 in DNA replication checkpoint control. J. Biol. Chem. *284*, 4132–4139.

Dharmacon (2014). Off-target Effects: Disturbing the Silence of RNA interference (RNAi). http://dharmacon.gelifesciences.com/uploadedFiles/Resources/off-Target-Tech-Review.pdf Accessed 19/09/14.

Diehl, J. a., Cheng, M., Roussel, M.F., and Sherr, C.J. (1998). Glycogen synthase kinase-3beta regulates cyclin D1 proteolysis and subcellular localization. Genes Dev. *12*, 3499–3511.

Diffley, J.F.X. (1998). Replication control : Choreographing replication origins. Curr. Biol. *8*, 771–773.

Dimitrova, D.S., and Gilbert, D.M. (2000). Temporally coordinated assembly and disassembly of replication factories in the absence of DNA synthesis. Nat. Cell Biol. *2*, 686–694.

Dolganov, G., Maser, R., Novikov, A., Tosto, L., Chong, S., Bressan, D.A., and Petrini, J.H. (1996). Human Rad50 is physically associated with human Mre11: identification of a conserved multiprotein complex implicated in recombinational DNA repair. Mol. Cell. Biol. *16*, 4832.

Donzelli, M., and Draetta, G.F. (2003). Regulating mammalian checkpoints through Cdc25 inactivation. EMBO Rep. *4*, 671–677.

Elbashir, S.M., Harborth, J., Lendeckel, W., Yalcin, a, Weber, K., and Tuschl, T. (2001). Duplexes of 21-nucleotide RNAs mediate RNA interference in cultured mammalian cells. Nature *411*, 494–498.

Ellison, V., and Stillman, B. (2003). Biochemical characterization of DNA damage checkpoint complexes: clamp loader and clamp complexes with specificity for 5' recessed DNA. PLoS Biol. *1*, E33.

Enoch, T., Carr, a M., and Nurse, P. (1992). Fission yeast genes involved in coupling mitosis to completion of DNA replication. Genes Dev. *6*, 2035–2046.

Eriksson, P.R., Mendiratta, G., McLaughlin, N.B., Wolfsberg, T.G., Marino-Ramirez, L., Pompa, T.A., Jainerin, M., Landsman, D., Shen, C.-H., and Clark, D.J. (2005). Global Regulation by the

Yeast Spt10 Protein Is Mediated through Chromatin Structure and the Histone Upstream Activating Sequence Elements. Mol. Cell. Biol. *25*, 9127–9137.

Falck, J., Mailand, N., Syljuåsen, R.G., Bartek, J., and Lukas, J. (2001). The ATM-Chk2-Cdc25A checkpoint pathway guards against radioresistant DNA synthesis. Nature *410*, 842–847.

Falck, J., Coates, J., and Jackson, S.P. (2005). Conserved modes of recruitment of ATM, ATR and DNA-PKcs to sites of DNA damage. Nature *434*, 605–611.

Fanning, E., Klimovich, V., and Nager, A.R. (2006). A dynamic model for replication protein A (RPA) function in DNA processing pathways. Nucleic Acids Res. *34*, 4126–4137.

Fasulo, B., Koyama, C., Yu, K.R., Homola, E.M., Hsieh, T.S., Campbell, S.D., and Sullivan, W. (2012). Chk1 and Wee1 kinases coordinate DNA replication, chromosome condensation, and anaphase entry. Mol. Biol. Cell *23*, 1047–1057.

Feijoo, C., Hall-Jackson, C., Wu, R., Jenkins, D., Leitch, J., Gilbert, D.M., and Smythe, C. (2001). Activation of mammalian Chk1 during DNA replication arrest: a role for Chk1 in the intra-S phase checkpoint monitoring replication origin firing. J. Cell. Biol. *154*, 913–923.

Fersht, N., Hermand, D., Hayles, J., and Nurse, P. (2007). Cdc18/CDC6 activates the Rad3-dependent checkpoint in the fission yeast. Nucleic Acids Res. *35*, 5323–5337.

Fire, A., Xu, S., Montgomery, M., Kostas, S., Driver, S., and Mello, C. (1998). Potent and specific genetic interference by double-stranded RNA in Caenorhabditis elegans. Nature *391*, 806–811.

Florensa, R., Bachs, O., and Agell, N. (2003). ATM/ATR-independent inhibition of cyclin B accumulation in response to hydroxyurea in nontransformed cell lines is altered in tumour cell lines. Oncogene *22*, 8283–8292.

Fogarty, P., Campbell, S.D., Abu-Shumays, R., Phalle, B.S., Yu, K.R., Uy, G.L., Goldberg, M.L., and Sullivan, W. (1997). The Drosophila grapes gene is related to checkpoint gene chk1/rad27 and is required for late syncytial division fidelity. Curr. Biol. *7*, 418–426.

Foley, E., and O'Farrell, P.H. (2004). Functional dissection of an innate immune response by a genome-wide RNAi screen. PLoS Biol. *2*, E203.

Follmer, N.E., and Francis, N.J. (2012). Preparation of Drosophila tissue culture cells from different stages of the cell cycle for chromatin immunoprecipitation using centrifugal counterflow elutriation and fluorescence-activated cell sorting. Methods Enzymol. *513*, 251–269.

Friesner, J., Liu, B., Culligan, K., and Britt, A.B. (2005). Ionizing radiation–dependent γ-H2AX focus formation requires ataxia telangiectasia mutated and ataxia telangiectasia mutated and Rad3-related. Mol. Biol. Cell *16*, 2566–2576.

Fung, T.K., and Poon, R.Y.C. (2005). A roller coaster ride with the mitotic cyclins. Semin. Cell Dev. Biol. *16*, 335–342.

Le Gac, G., Estève, P.-O., Ferec, C., and Pradhan, S. (2006). DNA damage-induced down-regulation of human Cdc25C and Cdc2 is mediated by cooperation between p53 and maintenance DNA (cytosine-5) methyltransferase 1. J. Biol. Chem. *281*, 24161–24170.

García-Serrano, S., Moreno-Santos, I., Garrido-Sánchez, L., Gutierrez-Repiso, C., García-Almeida, J.M., García-Arnés, J., Rivas-Marín, J., Gallego-Perales, J.L., García-Escobar, E., Rojo-

Martinez, G., et al. (2011). Stearoyl-CoA desaturase-1 is associated with insulin resistance in morbidly obese subjects. Mol. Med. *17*, 273–280.

Garnett, M.J., Mansfeld, J., Godwin, C., Matsusaka, T., Wu, J., Russell, P., Pines, J., and Venkitaraman, A.R. (2009). UBE2S elongates ubiquitin chains on APC/C substrates to promote mitotic exit. Nat. Cell Biol. *11*, 1363–1369.

Gatei, M., Sloper, K., Sorensen, C., Syljuäsen, R., Falck, J., Hobson, K., Savage, K., Lukas, J., Zhou, B.-B., Bartek, J., et al. (2003). Ataxia-telangiectasia-mutated (ATM) and NBS1-dependent phosphorylation of Chk1 on Ser-317 in response to ionizing radiation. J. Biol. Chem. *278*, 14806–14811.

Gautier, J., Solomon, M.J., Booher, R.N., Bazan, J.F., and Kirschner, M.W. (1991). cdc25 is a specific tyrosine phosphatase that directly activates p34cdc2. Cell *67*, 197.

Geer, L.Y., Marchler-Bauer, A., Geer, R.C., Han, L., He, J., He, S., Liu, C., Shi, W., and Bryant, S.H. (2010). The NCBI BioSystems database. Nucleic Acids Res. *38*, D492–D496.

Gilbert, D.M. (2002). Replication timing and transcriptional control: beyond cause and effect. Curr. Opin. Cell Biol. *14*, 377–383.

Giot, L., Bader, J.S., Brouwer, C., Chaudhuri, a, Kuang, B., Li, Y., Hao, Y.L., Ooi, C.E., Godwin, B., Vitols, E., et al. (2003). A protein interaction map of Drosophila melanogaster. Science *302*, 1727–1736.

Golan, A., Yudkovsky, Y., and Hershko, A. (2002). The cyclin-ubiquitin ligase activity of cyclosome/APC is jointly activated by protein kinases Cdk1-cyclin B and Plk. J. Biol. Chem. *277*, 15552–15557.

Gönczy, P., Echeverri, C., Oegema, K., Coulson, a, Jones, S.J., Copley, R.R., Duperon, J., Oegema, J., Brehm, M., Cassin, E., et al. (2000). Functional genomic analysis of cell division in C. elegans using RNAi of genes on chromosome III. Nature *408*, 331–336.

Gould, K.L., and Nurse, P. (1989). Tyrosine phosphorylation of the fission yeast cdc2+ protein kinase regulates entry into mitosis. Nature *342*, 39–25.

Graves, R. a, and Marzluff, W.F. (1984). Rapid reversible changes in the rate of histone gene transcription and histone mRNA levels in mouse myeloma cells. Mol. Cell. Biol. *4*, 351–357.

Graves, P.R., Lovly, C.M., Uy, G.L., and Piwnica-Worms, H. (2001). Localization of human Cdc25C is regulated both by nuclear export and 14-3-3 protein binding. Oncogene *20*, 1839–1851.

Graves, R. a, Pandey, N.B., Chodchoy, N., and Marzluff, W.F. (1987). Translation is required for regulation of histone mRNA degradation. Cell *48*, 615–626.

Grishok, a, Pasquinelli, a E., Conte, D., Li, N., Parrish, S., Ha, I., Baillie, D.L., Fire, a, Ruvkun, G., and Mello, C.C. (2001). Genes and mechanisms related to RNA interference regulate expression of the small temporal RNAs that control C. elegans developmental timing. Cell *106*, 23–34.

Gunjan, A., and Verreault, A. (2003). A Rad53 Kinase-Dependent Surveillance Mechanism that Regulates Histone Protein Levels in S. cerevisiae. Cell *115*, 537–549.

Guo, Z., Kumagai, A., Wang, S.X., and Dunphy, W.G. (2000). Requirement for Atr in phosphorylation of Chk1 and cell cycle regulation in response to DNA replication blocks and UV-damaged DNA in Xenopus egg extracts. Genes Dev. *14*, 2745–2756.

Gurley, L.R., Walters, R.A., and Tobey, R.A. (1974). Cell Cycle-specific changes in histone phosphorylation associated with cell proliferation and chromosoe condensation. J. Cell Biol. *60*, 356–364.

Hagting, a, Karlsson, C., Clute, P., Jackman, M., and Pines, J. (1998). MPF localization is controlled by nuclear export. EMBO J. *17*, 4127–4138.

Hagting, a, Jackman, M., Simpson, K., and Pines, J. (1999). Translocation of cyclin B1 to the nucleus at prophase requires a phosphorylation-dependent nuclear import signal. Curr. Biol. *9*, 680–689.

Hall-Jackson, C.A., Cross, D.A.E., Morrice, N., and Smythe, C. (1999). ATR is a caffeine-sensitive , DNA-activated protein kinase with a substrate specificity distinct from DNA-PK. Oncogene *18*, 6707–6713.

Hanahan, D., and Weinberg, R. (2000). The hallmarks of cancer. Cell *100*, 57–70.

Hartwell, L.H. (1971). Genetic Control of the Cell Division Cycle in Yeast II. Genes Controlling DNA Replication and its Intiation. J. Mol. Biol. *59*, 183–194.

Hartwell, L.H., and Weinert, T.A. (1989). Checkpoints: Controls That Ensure Order of Cell Cycle Events. Science *246*, 629–634.

Heffernan, T.P., Unsal-Kaçmaz, K., Heinloth, A.N., Simpson, D. a, Paules, R.S., Sancar, A., Cordeiro-Stone, M., and Kaufmann, W.K. (2007). Cdc7-Dbf4 and the human S checkpoint response to UVC. J. Biol. Chem. *282*, 9458–9468.

Heintz, N., Sive, H.L., and Roeder, R.G. (1983). Regulation of human histone gene expression: kinetics of accumulation and changes in the rate of synthesis and in the half-lives of individual histone mRNAs during the HeLa cell cycle. Mol. Cell. Biol. *3*, 539–550.

Hendzel, M.J., Wei, Y., Mancini, M. a, Van Hooser, a, Ranalli, T., Brinkley, B.R., Bazett-Jones, D.P., and Allis, C.D. (1997). Mitosis-specific phosphorylation of histone H3 initiates primarily within pericentromeric heterochromatin during G2 and spreads in an ordered fashion coincident with mitotic chromosome condensation. Chromosoma *106*, 348–360.

Hentschel, C.C., and Birnstiel, M.L. (1981). The organization and expression of histone gene families. Cell *25*, 301–313.

Herrero, A.B., and Moreno, S. (2011). Lsm1 promotes genomic stability by controlling histone mRNA decay. EMBO J. *30*, 2008–2018.

Holcik, M., Gibson, H., and Korneluk, R.G. (2001). XIAP: apoptotic brake and promising therapeutic target. Apoptosis *6*, 253–261.

Hsu, J.Y., Reimann, J.D.R., Sørensen, C.S., Lukas, J., and Jackson, P.K. (2002). E2F-dependent accumulation of hEmi1 regulates S phase entry by inhibiting APC(Cdh1). Nat. Cell Biol. *4*, 358–366.

Hutvágner, G., McLachlan, J., Pasquinelli, a E., Bálint, E., Tuschl, T., and Zamore, P.D. (2001). A cellular function for the RNA-interference enzyme Dicer in the maturation of the let-7 small temporal RNA. Science *293*, 834–838.

Igal, R.A. (2010). Stearoyl-CoA desaturase-1: a novel key player in the mechanisms of cell proliferation, programmed cell death and transformation to cancer. Carcinogenesis *31*, 1509–1515.

Ishimi, Y., Komamura-Kohno, Y., Kwon, H.-J., Yamada, K., and Nakanishi, M. (2003). Identification of MCM4 as a target of the DNA replication block checkpoint system. J. Biol. Chem. *278*, 24644–24650.

Jares, P., Donaldson, a, and Blow, J.J. (2000). The Cdc7/Dbf4 protein kinase: target of the S phase checkpoint? EMBO Rep. *1*, 319–322.

Jazayeri, A., Falck, J., Lukas, C., Bartek, J., Smith, G.C.M., Lukas, J., and Jackson, S.P. (2006). ATM- and cell cycle-dependent regulation of ATR in response to DNA double-strand breaks. Nat. Cell Biol. *8*, 37–45.

Jena, N.R. (2012). DNA damage by reactive species: Mechanisms, mutation and repair. J. Biosci. *37*, 503–517.

Jin, J., Shirogane, T., Xu, L., Nalepa, G., Qin, J., Elledge, S.J., and Harper, J.W. (2003). SCFbeta-TRCP links Chk1 signaling to degradation of the Cdc25A protein phosphatase. Genes Dev. *17*, 3062–3074.

Jin, J., Ang, X.L., Ye, X., Livingstone, M., and Harper, J.W. (2008). Differential roles for checkpoint kinases in DNA damage-dependent degradation of the Cdc25A protein phosphatase. J. Biol. Chem. *283*, 19322–19328.

Kandel, E.S., Skeen, J., Majewski, N., Cristofano, A. Di, Pandolfi, P.P., Feliciano, C.S., Gartel, A., and Hay, N. (2002). Activation of Akt / Protein Kinase B Overcomes a G 2 / M Cell Cycle Checkpoint Induced by DNA Damage. Mol. Cell. Biol. *22*, 7831.

Kang, T., Wei, Y., Honaker, Y., Yamaguchi, H., Appella, E., Hung, M.-C., and Piwnica-Worms, H. (2008). GSK-3 beta targets Cdc25A for ubiquitin-mediated proteolysis, and GSK-3 beta inactivation correlates with Cdc25A overproduction in human cancers. Cancer Cell *13*, 36–47.

Kastan, M.B., and Bartek, J. (2004). Cell-cycle checkpoints and cancer. Nature *432*, 316–323.

Katayama, K., Fujita, N., and Tsuruo, T. (2005). Akt/Protein Kinase B-Dependent Phosphorylation and Inactivation of WEE1Hu Promote Cell Cycle Progression at G2/M Transition. Mol. Cell. Biol. *25*, 5725–5737.

Katou, Y., Kanoh, Y., Bando, M., Noguchi, H., Tanaka, H., Ashikari, T., Sugimoto, K., and Shirahige, K. (2003). S-phase checkpoint proteins Tof1 and Mrc1 form a stable replication-pausing complex. Nature *424*, 1078–1083.

Kaygun, H., and Marzluff, W.F. (2005a). Translation termination is involved in histone mRNA degradation when DNA replication is inhibited. Mol. Cell. Biol. *25*, 6879–6888.

Kaygun, H., and Marzluff, W.F. (2005b). Regulated degradation of replication-dependent histone mRNAs requires both ATR and Upf1. Nat. Struct. Mol. Biol. *12*, 794–800.

Kim, S., Nam, H., and Lee, D. (2011). Exploring molecular links between lymph node invasion and cancer prognosis in human breast cancer. BMC Syst. Biol. *5 Suppl 2*, S4.

Kim, S.-T., Xu, B., and Kastan, M.B. (2002). Involvement of the cohesin protein, Smc1, in Atm-dependent and independent responses to DNA damage. Genes Dev. *16*, 560–570.

King, F.W., Skeen, J., Hay, N., and Shtivelman, E. (2004). Inhibition of Chk1 by Activated PKB/Akt. Cell Cycle *3*, 634–637.

De Klein, A., Muijtjens, M., van Os, R., Verhoeven, Y., Smit, B., Carr, A.M., Lehmann, A.R., and Hoeijmakers, J.H.J. (2000). Targeted disruption of the cell-cycle checkpoint gene ATR leads to early embryonic lethality in mice. Curr. Biol. *10*, 479–482.

Kluk, M.J., and Hla, T. (2002). Signaling of sphingosine-1-phosphate via the S1P/EDG-family of G-protein-coupled receptors. Biochim. Biophys. Acta *1582*, 72–80.

Kondo, S., and Perrimon, N. (2011). A Genome-Wide RNAi Screen Identifies Core Components of the G2-M DNA Damage Checkpoint. Sci. Signal. *4*, rs1.

Kozlov, S. V, Graham, M.E., Peng, C., Chen, P., Robinson, P.J., and Lavin, M.F. (2006). Involvement of novel autophosphorylation sites in ATM activation. EMBO J. *25*, 3504–3514.

Kramer, K.M., Fesquet, D., Johnson, a L., and Johnston, L.H. (1998). Budding yeast RSI1/APC2, a novel gene necessary for initiation of anaphase, encodes an APC subunit. EMBO J. *17*, 498–506.

Krause, S.A., Loupart, M., Vass, S., Schoenfelder, S., Harrison, S., and Heck, M.M.S. (2001). Loss of Cell Cycle Checkpoint Control in Drosophila Rfc4 Mutants. Mol. Cell. Biol. *21*, 5156–5168.

Krol, J., Loedige, I., and Filipowicz, W. (2010). The widespread regulation of microRNA biogenesis, function and decay. Nat. Rev. Genet. *11*, 597–610.

Kumagai, a, and Dunphy, W.G. (1991). The cdc25 protein controls tyrosine dephosphorylation of the cdc2 protein in a cell-free system. Cell *64*, 903–914.

Kumagai, A., and Dunphy, W.G. (2000). Claspin, a Novel Protein Required for the Activation of Chk1 during a DNA Replication Checkpoint Response in Xenopus Egg Extracts. Mol. Cell *6*, 839–849.

Kumagai, a, Guo, Z., Emami, K.H., Wang, S.X., and Dunphy, W.G. (1998). The Xenopus Chk1 protein kinase mediates a caffeine-sensitive pathway of checkpoint control in cell-free extracts. J. Cell Biol. *142*, 1559–1569.

Kumagai, A., Lee, J., Yoo, H.Y., and Dunphy, W.G. (2006). TopBP1 activates the ATR-ATRIP complex. Cell *124*, 943–955.

Kumagai, A., Shevchenko, A., Shevchenko, A., and Dunphy, W.G. (2010). Treslin collaborates with TopBP1 in triggering the initiation of DNA replication. Cell *140*, 349–359.

Lan, H., Zhu, J., Ai, Q., Yang, Z., Ji, Y., Hong, S., Song, F., and Bu, Y. (2010). Rapid functional screening of effective siRNAs against Plk1 and its growth inhibitory effects in laryngeal carcinoma cells. BMB Rep. *43*, 818–823.

Lane, H. a, and Nigg, E. a (1996). Antibody microinjection reveals an essential role for human polo-like kinase 1 (Plk1) in the functional maturation of mitotic centrosomes. J. Cell Biol. *135*, 1701–1713.

Lange, T. de (2009). How telomeres solve the end-protection problem. Science *326*, 948–952.

Lau, C.C., and Pardee, a B. (1982). Mechanism by which caffeine potentiates lethality of nitrogen mustard. Proc. Natl. Acad. Sci. U.S.A. *79*, 2942–2946.

Lau, E., Zhu, C., Abraham, R.T., and Jiang, W. (2006). The functional role of Cdc6 in S-G2/M in mammalian cells. EMBO Rep. *7*, 425–430.

Lee, J., and Dunphy, W. (2010). Rad17 plays a central role in establishment of the interaction between TopBP1 and the Rad9-Hus1-Rad1 complex at stalled replication forks. Mol. Biol. Cell *21*, 926–935.

Lee, J.-H., and Paull, T.T. (2004). Direct activation of the ATM protein kinase by the Mre11/Rad50/Nbs1 complex. Science *304*, 93–96.

Lee, M.G., and Nurse, P. (1987). Complementation used to clone a human homologue of the fission yeast cell cycle control gene cdc2. Nature *327*, 31–35.

Lee, A.Y.-L., Chiba, T., Truong, L.N., Cheng, A.N., Do, J., Cho, M.J., Chen, L., and Wu, X. (2012a). Dbf4 is direct downstream target of ataxia telangiectasia mutated (ATM) and ataxia telangiectasia and Rad3-related (ATR) protein to regulate intra-S-phase checkpoint. J. Biol. Chem. *287*, 2531–2543.

Lee, E.-M., Trinh, T.T.B., Shim, H.J., Park, S.-Y., Nguyen, T.T.T., Kim, M.-J., and Song, Y.-H. (2012b). Drosophila Claspin is required for the G2 arrest that is induced by DNA replication stress but not by DNA double-strand breaks. DNA Repair *11*, 741–752.

Lee, J., Kumagai, a, and Dunphy, W.G. (2001). Positive regulation of Wee1 by Chk1 and 14-3-3 proteins. Mol. Biol. Cell *12*, 551–563.

Lee, J., Kumagai, A., and Dunphy, W.G. (2003a). Claspin, a Chk1-regulatory protein, monitors DNA replication on chromatin independently of RPA, ATR, and Rad17. Mol. Cell *11*, 329–340.

Lee, J., Kumagai, A., and Dunphy, W.G. (2007). The Rad9-Hus1-Rad1 checkpoint clamp regulates interaction of TopBP1 with ATR. J. Biol. Chem. *282*, 28036–28044.

Lee, J.-H., Goodarzi, A. a, Jeggo, P. a, and Paull, T.T. (2010). 53BP1 promotes ATM activity through direct interactions with the MRN complex. EMBO J. *29*, 574–585.

Lee, R.C., Feinbaum, R.L., and Ambros, V. (1993). The C. elegans heterochronic gene lin-4 encodes small RNAs with antisense complementarity to lin-14. Cell *75*, 843–854.

Lee, Y., Jeon, K., Lee, J.-T., Kim, S., and Kim, V.N. (2002). MicroRNA maturation: stepwise processing and subcellular localization. EMBO J. *21*, 4663–4670.

Lee, Y., Ahn, C., Han, J., Choi, H., Kim, J., Yim, J., Lee, J., Provost, P., Rådmark, O., Kim, S., et al. (2003b). The nuclear RNase III Drosha initiates microRNA processing. Nature *425*, 415–419.

Lee, Y.S., Nakahara, K., Pham, J.W., Kim, K., He, Z., Sontheimer, E.J., and Carthew, R.W. (2004). Distinct roles for Drosophila Dicer-1 and Dicer-2 in the siRNA/miRNA silencing pathways. Cell *117*, 69–81.

Lemaire, M., Froment, C., and Boutros, R. (2006). Report CDC25B Phosphorylation by p38 and MK-2. Cell Cycle *5*, 1649–1653.

Lewis, B.P., Shih, I., Jones-Rhoades, M.W., Bartel, D.P., and Burge, C.B. (2003). Prediction of mammalian microRNA targets. Cell *115*, 787–798.

Li, J., Ding, S.F., Habib, N.A., Fermor, B.F., Wood, C.B., and Gilmour, R.S. (1994). Partial characterization of a cDNA for human stearoyl-CoA desaturase and changes in its mRNA expression in some normal and malignant tissues. Int. J. Cancer *57*, 348–352.

Li, J., Meyer, a N., and Donoghue, D.J. (1995). Requirement for phosphorylation of cyclin B1 for Xenopus oocyte maturation. Mol. Biol. Cell *6*, 1111–1124.

Lin, S.-Y., Li, K., Stewart, G.S., and Elledge, S.J. (2004). Human Claspin works with BRCA1 to both positively and negatively regulate cell proliferation. Proc. Natl. Acad. Sci. U.S.A. *101*, 6484–6489.

Lindqvist, A., Rodríguez-Bravo, V., and Medema, R.H. (2009). The decision to enter mitosis: feedback and redundancy in the mitotic entry network. J. Cell Biol. *185*, 193–202.

Liu, F., Stanton, J., Wu, Z., and Piwnica-Worms, H. (1997). The human Myt1 kinase preferentially phosphorylates Cdc2 on threonine 14 and localizes to the endoplasmic reticulum and Golgi complex. Mol. Cell. Biol. *17*, 571–583.

Liu, K., Paik, J.C., Wang, B., Lin, F.-T., and Lin, W.-C. (2006). Regulation of TopBP1 oligomerization by Akt/PKB for cell survival. EMBO J. *25*, 4795–4807.

Liu, Q., Guntuku, S., Cui, X., Matsuoka, S., Cortez, D., Tamai, K., Luo, G., Carattini-rivera, S., Demayo, F., Bradley, A., et al. (2000). Chk1 is an essential kinase that is regulated by Atr and required for the G 2 / M DNA damage checkpoint. Genes Dev. *14*, 1448–1459.

Liu, S., Shiotani, B., Lahiri, M., Maréchal, A., Tse, A., Leung, C.C.Y., Glover, J.N.M., Yang, X.H., and Zou, L. (2011). ATR autophosphorylation as a molecular switch for checkpoint activation. Mol. Cell *43*, 192–202.

Liu, X., Lin, C., Lei, M., Yan, S., Zhou, T., and Erikson, R.L. (2005). CCT Chaperonin Complex Is Required for the Biogenesis of Functional Plk1 CCT Chaperonin Complex Is Required for the Biogenesis of Functional Plk1. Mol. Cell. Biol. *25*, 4993–5010.

Llopis, A., Salvador, N., Ercilla, A., Guaita-Esteruelas, S., Barrantes, I.D.B., Gupta, J., Gaestel, M., Davis, R.J., Nebreda, A.R., and Agell, N. (2012). The stress-activated protein kinases p38α/β and JNK1/2 cooperate with Chk1 to inhibit mitotic entry upon DNA replication arrest. Cell Cycle *11*, 3627–3637.

Lomax, M.E., Folkes, L.K., and O'Neill, P. (2013). Biological consequences of radiation-induced DNA damage: relevance to radiotherapy. Clin. Oncol. (R. Coll. Radiol). *25*, 578–585.

Lopez-Mosqueda, J., Maas, N.L., Jonsson, Z.O., Defazio-Eli, L.G., Wohlschlegel, J., and Toczyski, D.P. (2010). Damage-induced phosphorylation of Sld3 is important to block late origin firing. Nature *467*, 479–483.

Lucca, C., Vanoli, F., Cotta-Ramusino, C., Pellicioli, A., Liberi, G., Haber, J., and Foiani, M. (2004). Checkpoint-mediated control of replisome-fork association and signalling in response to replication pausing. Oncogene *23*, 1206–1213.

Lukas, J., Lukas, C., and Bartek, J. (2004). Mammalian cell cycle checkpoints: signalling pathways and their organization in space and time. DNA Repair *3*, 997–1007.

Lund, E., Güttinger, S., Calado, A., Dahlberg, J.E., and Kutay, U. (2004). Nuclear export of microRNA precursors. Science *303*, 95–98.

Ma, H., Samarabandu, J., Devdhar, R.S., Acharya, R., Cheng, P.C., Meng, C., and Berezney, R. (1998). Spatial and temporal dynamics of DNA replication sites in mammalian cells. J. Cell Biol. *143*, 1415–1425.

Ma, T., Van Tine, B.A., Wei, Y., Garrett, M.D., Nelson, D., Adams, P.D., Wang, J., Qin, J., Chow, L.T., and Harper, J.W. (2000). Cell cycle-regulated phosphorylation of p220NPAT by cyclin E/Cdk2 in Cajal bodies promotes histone gene transcription. Genes Dev. *14*, 2298–2313.

Macalpine, D.M., Rodríguez, H.K., and Bell, S.P. (2004). Coordination of replication and transcription along a Drosophila chromosome. Genes Dev. *18*, 3094–3105.

MacLennan, a J., Carney, P.R., Zhu, W.J., Chaves, a H., Garcia, J., Grimes, J.R., Anderson, K.J., Roper, S.N., and Lee, N. (2001). An essential role for the H218/AGR16/Edg-5/LP(B2) sphingosine 1-phosphate receptor in neuronal excitability. Eur. J. Neurosci. *14*, 203–209.

Maddika, S., Ande, S.R., Wiechec, E., Hansen, L.L., Wesselborg, S., and Los, M. (2008). Akt-mediated phosphorylation of CDK2 regulates its dual role in cell cycle progression and apoptosis. J. Cell Sci. *121*, 979–988.

Mailand, N., Falck, J., Lukas, C., Syljuåsen, R.G., Welcker, M., Bartek, J., and Lukas, J. (2000). Rapid Destruction of Human Cdc25A in Response to DNA Damage. Science *288*, 1425–1429.

Manke, I. a, Nguyen, A., Lim, D., Stewart, M.Q., Elia, A.E.H., and Yaffe, M.B. (2005). MAPKAP kinase-2 is a cell cycle checkpoint kinase that regulates the G2/M transition and S phase progression in response to UV irradiation. Mol. Cell *17*, 37–48.

Massagué, J. (2004). G1 cell-cycle control and cancer. Nature *432*, 298–306.

Matsuoka, S., Huang, M., and Elledge, S.J. (1998). Linkage of ATM to Cell Cycle Regulation by the Chk2 Protein Kinase. Science *282*, 1893–1897.

Matsuoka, S., Rotman, G., Ogawa, A., Shiloh, Y., Tamai, K., and Elledge, S.J. (2000). Ataxia telangiectasia-mutated phosphorylates Chk2 in vivo and in vitro. Proc. Natl. Acad. Sci. U.S.A. *97*, 10389–10394.

Matsuoka, S., Ballif, B., Smogorzewska, A., McDonald, E.R.I., Hurov, K.E., Luo, J., Bakalarski, C.E., Zhao, Z., Solimini, N., Lerenthal, Y., et al. (2007). ATM and ATR substrate analysis reveals extensive protein networks responsive to DNA damage. Science *316*, 1160–1166.

Mayer, M., Weickum, R., Solimando, D.J., Fileta, B., Abdel-Rahim, M., and Fant, G. (2001). Stability of cisplatin, doxorubicin and mitomycin combined with loversol for chemoembolization. Ann. Pharmacother. *25*, 1548–1551.

Maynard, S., Schurman, S.H., Harboe, C., de Souza-Pinto, N.C., and Bohr, V. a (2009). Base excision repair of oxidative DNA damage and association with cancer and aging. Carcinogenesis *30*, 2–10.

McEwen, B.F., Chan, G.K., Zubrowski, B., Savoian, M.S., Sauer, M.T., and Yen, T.J. (2001). CENP-E is essential for reliable bioriented spindle attachment, but chromosome alignment can be achieved via redundant mechanisms in mammalian cells. Mol. Biol. Cell *12*, 2776–2789.

McGowan, C.H., and Russell, P. (1993). Human Wee1 kinase inhibits cell division by phosphorylating p34cdc2 exclusively on Tyr15. EMBO J. *12*, 75–85.

McGowan, C.H., and Russell, P. (1995). Cell cycle regulation of human WEE1. EMBO J. *14*, 2166–2175.

Meeks-Wagner, D., and Hartwell, L.H. (1986). Normal stoichiometry of histone dimer sets is necessary for high fidelity of mitotic chromosome transmission. Cell *44*, 43–52.

Melixetian, M., Klein, D.K., Sørensen, C.S., and Helin, K. (2009). NEK11 regulates CDC25A degradation and the IR-induced G2/M checkpoint. Nat. Cell Biol. *11*, 1247–1253.

Meng, Z., Capalbo, L., Glover, D.M., and Dunphy, W.G. (2011). Role for casein kinase 1 in the phosphorylation of Claspin on critical residues necessary for the activation of Chk1. Mol. Biol. Cell *22*, 2834–2847.

Merrick, C.J., Jackson, D., and Diffley, J.F.X. (2004). Visualization of altered replication dynamics after DNA damage in human cells. J. Biol. Chem. *279*, 20067–20075.

Michel, B., Ehrlich, S.D., and Uzest, M. (1997). DNA double-strand breaks caused by replication arrest. EMBO J. *16*, 430–438.

Mirzoeva, O., and Petrini, J. (2001). DNA damage-dependent nuclear dynamics of the Mre11 complex. Mol. Cell. Biol. *21*, 281–288.

Modzelewski, A., Holmes, R., Hilz, S., Grimson, A., and Cohen, P.E. (2012). AGO4 regulates entry into meiosis and influences silencing of sex chromosomes in the male mouse germline. Dev. Cell *23*, 251–264.

Molinari, M., Mercurio, C., Dominguez, J., Goubin, F., and Draetta, G.F. (2000). Human Cdc25 A inactivation in response to S phase inhibition and its role in preventing premature mitosis. EMBO Rep. *1*, 71–79.

Moll, U., and Petrenko, O. (2003). The MDM2-p53 interaction. Mol. Cancer Res. *1*, 1001–1008.

Mordes, D. a, Glick, G.G., Zhao, R., and Cortez, D. (2008). TopBP1 activates ATR through ATRIP and a PIKK regulatory domain. Genes Dev. *22*, 1478–1489.

Morgan-Lappe, S.E., Tucker, L. a, Huang, X., Zhang, Q., Sarthy, A. V, Zakula, D., Vernetti, L., Schurdak, M., Wang, J., and Fesik, S.W. (2007). Identification of Ras-related nuclear protein, targeting protein for xenopus kinesin-like protein 2, and stearoyl-CoA desaturase 1 as promising cancer targets from an RNAi-based screen. Cancer Res. *67*, 4390–4398.

Mourelatos, Z., Dostie, J., Paushkin, S., Sharma, A., Charroux, B., Abel, L., Rappsilber, J., Mann, M., and Dreyfuss, G. (2002). miRNPs: a novel class of ribonucleoproteins containing numerous microRNAs. Genes Dev. *16*, 720–728.

Mu, J.-J., Wang, Y., Luo, H., Leng, M., Zhang, J., Yang, T., Besusso, D., Jung, S.Y., and Qin, J. (2007). A proteomic analysis of ataxia telangiectasia-mutated (ATM)/ATM-Rad3-related (ATR) substrates identifies the ubiquitin-proteasome system as a regulator for DNA damage checkpoints. J. Biol. Chem. *282*, 17330–17334.

Mueller, P., Coleman, T., Kumagai, A., and Dunphy, W. (1995). Myt1: a membrane-associated inhibitory kinase that phosphorylates Cdc2 on both threonine-14 and tyrosine-15. Science *270*, 86–90.

Mukherji, M., Bell, R., Supekova, L., Wang, Y., Orth, A.P., Batalov, S., Miraglia, L., Huesken, D., Lange, J., Martin, C., et al. (2006). Genome-wide functional analysis of human cell-cycle regulators. Proc. Natl. Acad. Sci. U.S.A. *103*, 14819–14824.

Mullen, T.E., and Marzluff, W.F. (2008). Degradation of histone mRNA requires oligouridylation followed by decapping and simultaneous degradation of the mRNA both 5’ to 3' and 3' to 5'. Genes Dev. *22*, 50–65.

Müller, B., Blackburn, J., Feijoo, C., Zhao, X., and Smythe, C. (2007). DNA-activated protein kinase functions in a newly observed S phase checkpoint that links histone mRNA abundance with DNA replication. J. Cell Biol. *179*, 1385–1398.

Müller, P., Kuttenkeuler, D., Gesellchen, V., Zeidler, M.P., and Boutros, M. (2005). Identification of JAK/STAT signalling components by genome-wide RNA interference. Nature *436*, 871–875.

Murakami, H., and Okayama, J. (1995). A kinase from fission yeast responsible for blocking mitosis in S-phase. Nature *374*, 817–819.

Murnion, M.E., Adams, R.R., Callister, D.M., Allis, C.D., Earnshaw, W.C., and Swedlow, J.R. (2001). Chromatin-associated protein phosphatase 1 regulates aurora-B and histone H3 phosphorylation. J. Biol. Chem. *276*, 26656–26665.

Nakagawa, K., Taya, Y., Tamai, K., and Yamaizumi, M. (1999). Requirement of ATM in phosphorylation of the human p53 protein at serine 15 following DNA double-strand breaks. Mol. Cell. Biol. *19*, 2828–2834.

Nam, E. a, and Cortez, D. (2011). ATR signalling: more than meeting at the fork. Biochem. J. *436*, 527–536.

Napoli, C., Lemieux, C., and Jorgensen, R. (1990). Introduction of a Chimeric Chalcone Synthase Gene into Petunia Results in Reversible Co-Suppression of Homologous Genes in trans. Plant Cell *2*, 279–289.

Nelson, D.M., Ye, X., Hall, C., Santos, H., Ma, T., Kao, G.D., Yen, T.J., Harper, J.W., and Adams, P.D. (2002). Coupling of DNA Synthesis and Histone Synthesis in S Phase Independent of Cyclin/cdk2 Activity. Mol. Cell. Biol. *22*, 7459–7472.

Nghiem, P., Park, P.K., Kim, Y., Vaziri, C., and Schreiber, S.L. (2001). ATR inhibition selectively sensitizes G1 checkpoint-deficient cells to lethal premature chromatin condensation. Proc. Natl. Acad. Sci. U.S.A. *98*, 9092–9097.

Nigg, E. a (2001). Mitotic kinases as regulators of cell division and its checkpoints. Nat. Rev. Mol. Cell Biol. *2*, 21–32.

Niiya, F., Tatsumoto, T., Lee, K.S., and Miki, T. (2006). Phosphorylation of the cytokinesis regulator ECT2 at G2/M phase stimulates association of the mitotic kinase Plk1 and accumulation of GTP-bound RhoA. Oncogene *25*, 827–837.

Norbury, C., Blow, J., and Nurse, P. (1991). Regulatory phosphorylation of the p34cdc2 protein kinase in vertebrates. EMBO J. *10*, 3321–3329.

O'Keefe, R.T., Henderson, S.C., and Spector, D.L. (1992). Dynamic organization of DNA replication in mammalian cell nuclei: spatially and temporally defined replication of chromosome-specific alpha-satellite DNA sequences. J. Cell Biol. *116*, 1095–1110.

Oh, C., Park, S., Lee, E.K., and Yoo, Y.J. (2013). Downregulation of ubiquitin level via knockdown of polyubiquitin gene Ubb as potential cancer therapeutic intervention. Sci. Rep. *3*, 2623.

Okumura, E., Fukuhara, T., Yoshida, H., Hanada Si, S., Kozutsumi, R., Mori, M., Tachibana, K., and Kishimoto, T. (2002). Akt inhibits Myt1 in the signalling pathway that leads to meiotic G2/M-phase transition. Nat. Cell Biol. *4*, 111–116.

Oláh, J., Vincze, O., Virók, D., Simon, D., Bozsó, Z., Tõkési, N., Horváth, I., Hlavanda, E., Kovács, J., Magyar, A., et al. (2011). Interactions of pathological hallmark proteins: tubulin polymerization promoting protein/p25, beta-amyloid, and alpha-synuclein. J. Biol. Chem. *286*, 34088–34100.

Orban, T., and Izaurralde, E. (2005). Decay of mRNAs targeted by RISC requires XRN1, the Ski complex, and the exosome. RNA *11*, 459–469.

Pabla, N., Huang, S., Mi, Q.-S., Daniel, R., and Dong, Z. (2008). ATR-Chk2 signaling in p53 activation and DNA damage response during cisplatin-induced apoptosis. J. Biol. Chem. *283*, 6572–6583.

Pacek, M., and Walter, J.C. (2004). A requirement for MCM7 and Cdc45 in chromosome unwinding during eukaryotic DNA replication. EMBO J. *23*, 3667–3676.

Painter, R.B., and Young, B.R. (1980). Radiosensitivity in ataxia-telangiectasia: a new explanation. Proc. Natl. Acad. Sci. U.S.A. *77*, 7315–7317.

Pandey, N.B., and Marzluff, W.F. (1987). The stem-loop structure at the 3' end of histone mRNA is necessary and sufficient for regulation of histone mRNA stability. Mol. Cell. Biol. *7*, 4557–4559.

Papamichos-Chronakis, M., and Peterson, C.L. (2008). The Ino80 chromatin-remodeling enzyme regulates replisome function and stability. Nat. Struct. Mol. Biol. *15*, 338–345.

Parker, L.L., and Piwnica-Worms, H. (1992). Inactivation of the p34cdc2-cyclin B complex by the human WEE1 tyrosine kinase. Science *257*, 1955–1957.

Parrilla-Castellar, E.R., and Karnitz, L.M. (2003). Cut5 is required for the binding of Atr and DNA polymerase alpha to genotoxin-damaged chromatin. J. Biol. Chem. *278*, 45507–45511.

Paulsen, R.D., Soni, D. V, Wollman, R., Hahn, A.T., Yee, M.-C., Guan, A., Hesley, J. a, Miller, S.C., Cromwell, E.F., Solow-Cordero, D.E., et al. (2009). A genome-wide siRNA screen reveals diverse cellular processes and pathways that mediate genome stability. Mol. Cell *35*, 228–239.

Pei, Y., and Tuschl, T. (2006). On the art of identifying effective and specific siRNAs. Nat. Methods *3*, 670–676.

Peng, C.-Y., Graves, P.R., Thoma, R.S., Wu, Z., Shaw, A.S., and Piwnica-Worms, H. (1997). Mitotic and G2 Checkpoint Control: Regulation of 14-3-3 Protein Binding by Phosphorylation of Cdc25C on Serine-216. Science *277*, 1501–1505.

Peters, J.-M. (2006). The anaphase promoting complex/cyclosome: a machine designed to destroy. Nat. Rev. Mol. Cell Biol. *7*, 644–656.

Phillips Jr, G.N., McCoy, J.G., Bitto, E., Wesenberg, G.E., and Bingman, C.A. PDI: 2gnx X-ray stricture of a hypothetical protein from Mous Mm.209172. Cent. Eukaryot. Struct. Genomics.

Pines, J., and Hunter, T. (1989). Isolation of a human cyclin cDNA: evidence for cyclin mRNA and protein regulation in the cell cycle and for interaction with p34cdc2. Cell *58*, 833–846.

Pines, J., and Hunter, T. (1991). Human cyclins A and B1 are differentially located in the cell and undergo cell cycle-dependent nuclear transport. J. Cell Biol. *115*, 1–17.

Poirier, M.C. (2004). Chemical-induced DNA damage and human cancer risk. Nat. Rev. Cancer *4*, 630–637.

Poon, R.Y.C., Jiang, W., Toyoshima, H., and Hunter, T. (1996). Cyclin-dependent Kinases Are Inactivated by a Combination of p21 and Thr-14/Tyr-15 Phosphorylation after UV-induced DNA Damage. J. Biol. Chem. *271*, 13283–13291.

Porter, L. a, and Donoghue, D.J. (2003). Cyclin B1 and CDK1: nuclear localization and upstream regulators. Prog. Cell Cycle Res. *5*, 335–347.

Raaijmakers, J. a, Tanenbaum, M.E., and Medema, R.H. (2013). Systematic dissection of dynein regulators in mitosis. J. Cell Biol. *201*, 201–215.

Rand, T. a, Petersen, S., Du, F., and Wang, X. (2005). Argonaute2 cleaves the anti-guide strand of siRNA during RISC activation. Cell *123*, 621–629.

Rao, P.N., and Johnson, R.T. (1970). Mammalian Cell Fusion: Studies on the Regulation of DNA Synthesis and Mitosis. Nature *225*, 159–164.

Rape, M., and Kirschner, M.W. (2004). Autonomous regulation of the anaphase-promoting complex couples mitosis to S-phase entry. Nature *432*, 588–595.

Rechsteiner, M. (1990). PEST sequences are signals for rapid intracellular proteolysis. Semin. Cell Biol. *1*, 433–440.

Reynolds, A., Anderson, E.M., Vermeulen, A., Fedorov, Y., Robinson, K., Leake, D., Karpilow, J. on, Marshall, W.S., and Khvorova, A. (2006). Induction of the interferon response by siRNA is cell type– and duplex length –dependent. RNA *12*, 988–993.

Rhind, N., and Russell, P. (1998). Tyrosine phosphorylation of cdc2 is required for the replication checkpoint in Schizosaccharomyces pombe. Mol. Cell. Biol. *18*, 3782–3787.

Rizzino, A., and Blumenthal, A. (1978). Synchronization of Drosophila cells in culture. In Vitro *14*, 437–442.

Rochard, E., Barthes, D., and Courtois, P. (1992). Stability of flurouracil, cytarabine, or doxorubicin hydrochloride in ethylene vinlacetate portable infusion pump reservoirs. Am. J. Heal. Pharm. *49*, 619–623.

Rodriguez, A., Griffiths-Jones, S., Ashurst, J.L., and Bradley, A. (2004). Identification of Mammalian microRNA Host Genes and Transcription Units. Genome Res. *14*, 1902–1910.

Rodríguez-Bravo, V., Guaita-Esteruelas, S., Florensa, R., Bachs, O., and Agell, N. (2006). Chk1- and claspin-dependent but ATR/ATM- and Rad17-independent DNA replication checkpoint response in HeLa cells. Cancer Res. *66*, 8672–8679.

Rodríguez-Bravo, V., Guaita-Esteruelas, S., Salvador, N., Bachs, O., and Agell, N. (2007). Different S/M checkpoint responses of tumor and non tumor cell lines to DNA replication inhibition. Cancer Res. *67*, 11648–11656.

Rogers, S., Wells, R., and Rechsteiner, M. (1986). Amino acid sequences common to rapidly degraded proteins: the PEST hypothesis. Science *234*, 364–368.

Roshak, a K., Capper, E. a, Imburgia, C., Fornwald, J., Scott, G., and Marshall, L. a (2000). The human polo-like kinase, PLK, regulates cdc2/cyclin B through phosphorylation and activation of the cdc25C phosphatase. Cell. Signal. *12*, 405–411.

Safrany, S.T., Caffrey, J.J., Yang, X., Bembenek, M.E., Moyer, M.B., Burkhart, W.A., and Shears, S.B. (1998). A novel context for the " MutT " module , a guardian of cell integrity , in a diphosphoinositol polyphosphate phosphohydrolase. EMBO J. *17*, 6599–6607.

Sanchez, T., Skoura, A., Wu, M.T., Casserly, B., Harrington, E.O., and Hla, T. (2007). Induction of vascular permeability by the sphingosine-1-phosphate receptor-2 (S1P2R) and its downstream effectors ROCK and PTEN. Arterioscler. Thromb. Vasc. Biol. *27*, 1312–1318.

Sanchez, Y., Wong, C., Thoma, R.S., Richman, R., Wu, Z., Piwnica-Worms, H., and Elledge, S.J. (1997). Conservation of the Chk1 Checkpoint Pathway in Mammals: Linkage of DNA Damage to Cdk Regulation Through Cdc25. Science *277*, 1497–1501.

Sanchez-Pulido, L., Diffley, J.F.X., and Ponting, C.P. (2010). Homology explains the functional similarities of Treslin/Ticrr and Sld3. Curr. Biol. *20*, R509–R510.

Sansam, C.L., Cruz, N.M., Danielian, P.S., Amsterdam, A., Lau, M.L., Hopkins, N., and Lees, J. a (2010). A vertebrate gene, ticrr, is an essential checkpoint and replication regulator. Genes Dev. *24*, 183–194.

Santocanale, C., and Diffley, J.F. (1998). A Mec1- and Rad53-dependent checkpoint controls late-firing origins of DNA replication. Nature *395*, 615–618.

Sarkaria, J.N., Busby, E.C., Tibbetts, R.S., Roos, P., Taya, Y., Karnitz, L.M., and Abraham, R.T. (1999). Inhibition of ATM and ATR kinase activities by the radiosensitizing agent, caffeine. Cancer Res. *59*, 4375–4382.

Sato, K., Sundaramoorthy, E., Rajendra, E., Hattori, H., Jeyasekharan, A.D., Ayoub, N., Schiess, R., Aebersold, R., Nishikawa, H., Sedukhina, A.S., et al. (2012). A DNA-damage selective role for BRCA1 E3 ligase in claspin ubiquitylation, CHK1 activation, and DNA repair. Curr. Biol. *22*, 1659–1666.

Satoh, J., Obayashi, S., Misawa, T., Sumiyoshi, K., Oosumi, K., and Tabunoki, H. (2009). Protein microarray analysis identifies human cellular prion protein interactors. Neuropathol. Appl. Neurobiol. *35*, 16–35.

Scaglia, N., and Igal, R.A. (2005). Stearoyl-CoA desaturase is involved in the control of proliferation, anchorage-independent growth, and survival in human transformed cells. J. Biol. Chem. *280*, 25339–25349.

Scaglia, N., and Igal, R.A. (2008). Inhibition of Stearoyl-CoA Desaturase 1 expression in human lung adenocarcinoma cells impairs tumorigenesis. Int. J. Oncol. *33*, 839–850.

Scaglia, N., Chisholm, J.W., and Igal, R.A. (2009). Inhibition of stearoylCoA desaturase-1 inactivates acetyl-CoA carboxylase and impairs proliferation in cancer cells: role of AMPK. PLoS One *4*, e6812.

Schlabach, M., Luo, J., Solimini, N., Hu, G., and Xu, Q. (2008). Cancer proliferation gene discovery through functional genomics. Science *319*, 620–624.

Schlegel, R., and Pardee, a B. (1986). Caffeine-induced uncoupling of mitosis from the completion of DNA replication in mammalian cells. Science *232*, 1264–1266.

Schmitz, M.H. a, Held, M., Janssens, V., Hutchins, J.R. a, Hudecz, O., Ivanova, E., Goris, J., Trinkle-Mulcahy, L., Lamond, A.I., Poser, I., et al. (2010). Live-cell imaging RNAi screen identifies PP2A-B55alpha and importin-beta1 as key mitotic exit regulators in human cells. Nat. Cell Biol. *12*, 886–893.

Segurado, M., and Diffley, J.F.X. (2008). Separate roles for the DNA damage checkpoint protein kinases in stabilizing DNA replication forks. Genes Dev. *22*, 1816–1827.

Shi, Y., Dodson, G.E., Mukhopadhyay, P.S., Shanware, N.P., Trinh, A.T., and Tibbetts, R.S. (2007). Identification of carboxyl-terminal MCM3 phosphorylation sites using polyreactive phosphospecific antibodies. J. Biol. Chem. *282*, 9236–9243.

Shimada, K., Oma, Y., Schleker, T., Kugou, K., Ohta, K., Harata, M., and Gasser, S.M. (2008). Ino80 chromatin remodeling complex promotes recovery of stalled replication forks. Curr. Biol. *18*, 566–575.

Shoemaker, C., and Chalkley, R. (1978). An H3 histone-specific kinase isolated from bovine thymus chromatin. J. Biol. Chem. *253*, 5802–5807.

Sibon, O.C., Stevenson, V. a, and Theurkauf, W.E. (1997). DNA-replication checkpoint control at the Drosophila midblastula transition. Nature *388*, 93–97.

Sinha, R.P., and Häder, D.-P. (2002). UV-induced DNA damage and repair: a review. Photochem. Photobiol. Sci. *1*, 225–236.

Sittman, D.B., Graves, R. a, and Marzluff, W.F. (1983a). Histone mRNA concentrations are regulated at the level of transcription and mRNA degradation. Proc. Natl. Acad. Sci. U.S.A. *80*, 1849–1853.

Sittman, D.B., Graves, R.A., and Marzluff, W.F. (1983b). Histone mRNA concentrations are regulated at the level of transcription and mRNA degradation. Proc. Natl. Acad. Sci. U.S.A. *80*, 1849–1853.

Siudeja, K., Jong, J. De, and Sibon, O.C.M. (2011). Studying Cell Cycle Checkpoints Using Drosophila Cultured Cells. Cell Cycle Checkpoints, Methods Mol. Biol. *782*, 59–73.

Smith, J., Tho, L.M., Xu, N., and Gillespie, D.A. (2010). The ATM-Chk2 and ATR-Chk1 pathways in DNA damage signaling and cancer. Adv. Cancer Res. *108*, 73–112.

Smythe, C., and Newport, J.W. (1992). Coupling of mitosis to the completion of S phase in Xenopus occurs via modulation of the tyrosine kinase that phosphorylates p34cdc2. Cell *68*, 787–797.

Song, Y. (2005). Drosophila melanogaster: a Model for the Study of DNA Damage Checkpoint Response. Mol. Cells *19*, 167–179.

Soni, D. V, Sramkoski, R.M., Lam, M., Stefan, T., and Jacobberger, J.W. (2008). Cyclin B1 is rate limiting but not essential for mitotic entry and progression in mammalian somatic cells. Cell Cycle *7*, 1285–1300.

Steinmann, K.E., Belinsky, G.S., Lee, D., and Schlegel, R. (1991). Chemically induced premature mitosis: differential response in rodent and human cells and the relationship to cyclin B synthesis and p34cdc2/cyclin B complex formation. Proc. Natl. Acad. Sci. U.S.A. *88*, 6843–6847.

Stewart, G.S., Wang, B., Bignell, C.R., Taylor, a M.R., and Elledge, S.J. (2003). MDC1 is a mediator of the mammalian DNA damage checkpoint. Nature *421*, 961–966.

Stiff, T., Walker, S. a, Cerosaletti, K., Goodarzi, A. a, Petermann, E., Concannon, P., O'Driscoll, M., and Jeggo, P. a (2006). ATR-dependent phosphorylation and activation of ATM in response to UV treatment or replication fork stalling. EMBO J. *25*, 5775–5782.

Stokes, M.P., Rush, J., Macneill, J., Ren, J.M., Sprott, K., Nardone, J., Yang, V., Beausoleil, S. a, Gygi, S.P., Livingstone, M., et al. (2007). Profiling of UV-induced ATM/ATR signaling pathways. Proc. Natl. Acad. Sci. U.S.A. *104*, 19855–19860.

Stracker, T.H., and Petrini, J.H.J. (2011). The MRE11 complex: starting from the ends. Nat. Rev. Mol. Cell Biol. *12*, 90–103.

Strausfeld, U., Labbé, J.C., Fesquet, D., Cavadore, J.C., Picard, A., Sadhu, K., Russell, P., and Dorée, M. (1991). Dephosphorylation and activation of a p34cdc2/cyclin B complex in vitro by human CDC25 protein. Nature *351*, 242–245.

Su, T., and Jaklevic, B. (2001). DNA damage leads to a Cyclin A–dependent delay in metaphase-anaphase transition in the Drosophila gastrula. Curr. Biol. *11*, 8–17.

Su, T.T., Walker, J., and Stumpff, J. (2000). Activating the DNA damage checkpoint in a developmental context. Curr. Biol. *10*, 119–126.

Su, W., Slepenkov, S. V, Slevin, M.K., Lyons, S.M., Ziemniak, M., Kowalska, J., Darzynkiewicz, E., Jemielity, J., Marzluff, W.F., and Rhoads, R.E. (2013). mRNAs containing the histone 3' stem-loop are degraded primarily by decapping mediated by oligouridylation of the 3' end. RNA *19*, 1–16.

Sullivan, K.D., Mullen, T.E., Marzluff, W.F., and Wagner, E.J. (2009). Knockdown of SLBP results in nuclear retention of histone mRNA. RNA *15*, 459–472.

Sun, Y., Xu, Y., Roy, K., and Price, B.D. (2007). DNA damage-induced acetylation of lysine 3016 of ATM activates ATM kinase activity. Mol. Cell. Biol. *27*, 8502–8509.

Tabor, D.E., Kim, J.B., Spiegelman, B.M., and Edwards, P. a. (1999). Identification of Conserved cis-Elements and Transcription Factors Required for Sterol-regulated Transcription of Stearoyl-CoA Desaturase 1 and 2. J. Biol. Chem. *274*, 20603–20610.

Tam, S.W., Belinsky, G.S., and Schlegel, R. (1995). Premature expression of cyclin B sensitizes human HT1080 cells to caffeine-induced premature mitosis. J. Cell. Biochem. *59*, 339–349.

Taylor, W.R., and Stark, G.R. (2001). Regulation of the G2/M transition by p53. Oncogene *20*, 1803–1815.

Taylor, W.R., DePrimo, S.E., Agarwal, a, Agarwal, M.L., Schönthal, a H., Katula, K.S., and Stark, G.R. (1999). Mechanisms of G2 arrest in response to overexpression of p53. Mol. Biol. Cell *10*, 3607–3622.

Tercero, A., Longhese, M.P., and Diffley, J.F.X. (2003). A Central Role for DNA Replication Forks in Checkpoint Activation and Response. Mol. Cell *11*, 1323–1336.

Thermo Fisher Scientific (2009). Thermo Scientific Dharmacon ON-TARGET plus siRNA: The Standard for siRNA Specificity http://dharmacon.gelifesciences.com/uploadedfiles/resources/ontargetplus-brochure.pdf accessed 13/09/2014.

Toczyski, D.P., Galgoczy, D.J., and Hartwell, L.H. (1997). CDC5 and CKII control adaptation to the yeast DNA damage checkpoint. Cell *90*, 1097–1106.

Tomimatsu, N., Mukherjee, B., and Burma, S. (2009). Distinct roles of ATR and DNA-PKcs in triggering DNA damage responses in ATM-deficient cells. EMBO Rep. *10*, 629–635.

Toyoshima, F., Moriguchi, T., Wada, a, Fukuda, M., and Nishida, E. (1998). Nuclear export of cyclin B1 and its possible role in the DNA damage-induced G2 checkpoint. EMBO J. *17*, 2728–2735.

Trenz, K., Smith, E., Smith, S., and Costanzo, V. (2006). ATM and ATR promote Mre11 dependent restart of collapsed replication forks and prevent accumulation of DNA breaks. EMBO J. *25*, 1764–1774.

Tsvetkov, L., and Stern, D. (2005). Phosphorylation of Plk1 at S137 and T210 is Inhibited in Response to DNA Damage. Cell Cycle *4*, 166–171.

Uziel, T., Lerenthal, Y., Moyal, L., Andegeko, Y., Mittelman, L., and Shiloh, Y. (2003). Requirement of the MRN complex for ATM activation by DNA damage. EMBO J. *22*, 5612–5621.

Vanderwerf, S.M., Svahn, J., Olson, S., Rathbun, R.K., Harrington, C., Yates, J., Keeble, W., Anderson, D.C., Anur, P., Pereira, N.F., et al. (2009). TLR8-dependent TNF-alpha overexpression in Fanconi anemia group C cells. Blood *114*, 5290–5298.

Veatch, W., and Okada, S. (1969). Radiation-induced breaks of DNA in cultured mammalian cells. Biophys. J. *9*, 330–346.

De Vries, H.I., Uyetake, L., Lemstra, W., Brunsting, J.F., Su, T.T., Kampinga, H.H., and Sibon, O.C.M. (2005). Grp/DChk1 is required for G2-M checkpoint activation in Drosophila S2 cells, whereas Dmnk/DChk2 is dispensable. J. Cell Sci. *118*, 1833–1842.

Van Vugt, M.A.T.M., Gardino, A.K., Linding, R., Ostheimer, G.J., Reinhardt, H.C., Ong, S.-E., Tan, C.S., Miao, H., Keezer, S.M., Li, J., et al. (2010). A Mitotic Phosphorylation Feedback Network Connects Cdk1, Plk1, 53BP1, and Chk2 to Inactivate the G2/M DNA Damage Checkpoint. PLoS Biol. *8*, e1000287.

Walker, M., Black, E.J., Oehler, V., Gillespie, D. a, and Scott, M.T. (2009). Chk1 C-terminal regulatory phosphorylation mediates checkpoint activation by de-repression of Chk1 catalytic activity. Oncogene *28*, 2314–2323.

Walter, J., and Newport, J. (2000). Initiation of eukaryotic DNA replication: origin unwinding and sequential chromatin association of Cdc45, RPA, and DNA polymerase alpha. Mol. Cell *5*, 617–627.

Wang, D., Zhao, Z., Caperell-Grant, A., Yang, G., Mok, S.C., Liu, J., Bigsby, R.M., and Xu, Y. (2008). S1P differentially regulates migration of human ovarian cancer and human ovarian surface epithelial cells. Mol. Cancer Ther. *7*, 1993–2002.

Wang, J., Gong, Z., and Chen, J. (2011). MDC1 collaborates with TopBP1 in DNA replication checkpoint control. J. Cell Biol. *193*, 267–273.

Wang, X., Zou, L., Lu, T., Bao, S., Hurov, K.E., Hittelman, W.N., Elledge, S.J., and Li, L. (2006a). Rad17 phosphorylation is required for claspin recruitment and Chk1 activation in response to replication stress. Mol. Cell *23*, 331–341.

Wang, X., Redpath, J., Fan, S.T., and Stanbridge, E.J. (2006b). ATR dependent activation of Chk2. J. Cell. Physiol. *619*, 613–619.

Weinert, T. a, and Hartwell, L.H. (1988). The RAD9 gene controls the cell cycle response to DNA damage in Saccharomyces cerevisiae. Science *241*, 317–322.

Whitehurst, A.W., Bodemann, B.O., Cardenas, J., Ferguson, D., Girard, L., Peyton, M., Minna, J.D., Michnoff, C., Hao, W., Roth, M.G., et al. (2007). Synthetic lethal screen identification of chemosensitizer loci in cancer cells. Nature *446*, 815–819.

Williams, A.S., Ingledue 3rd, T.C., Kay, B.K., and Marzluff, W.F. (1994). Changes in the stem-loop at the 3' terminus of histone mRNA affects its nucleocytoplasmic transport and cytoplasmic regulation. Nucleic Acids Res. *22*, 4660–4666.

Wu, R.S., and Bonner, W.M. (1981). Separation of basal histone synthesis from S-phase histone synthesis in dividing cells. Cell *27*, 321–330.

Wurzenberger, C., and Gerlich, D.W. (2011). Phosphatases: providing safe passage through mitotic exit. Nat. Rev. Mol. Cell Biol. *12*, 469–482.

Xu, N., Lao, Y., Zhang, Y., and Gillespie, D. a (2012). Akt: a double-edged sword in cell proliferation and genome stability. J. Oncol. *2012*, 951724.

Yahagi, N., Shimano, H., Hasegawa, K., Ohashi, K., Matsuzaka, T., Najima, Y., Sekiya, M., Tomita, S., Okazaki, H., Tamura, Y., et al. (2005). Co-ordinate activation of lipogenic enzymes in hepatocellular carcinoma. Eur. J. Cancer *41*, 1316–1322.

Yamada, M., Watanabe, K., Mistrik, M., Vesela, E., Protivankova, I., Mailand, N., Lee, M., Masai, H., Lukas, J., and Bartek, J. (2013). ATR-Chk1-APC/CCdh1-dependent stabilization of Cdc7-ASK (Dbf4) kinase is required for DNA lesion bypass under replication stress. Genes Dev. *27*, 2459–2472.

Yan, S., and Michael, W.M. (2009a). TopBP1 and DNA polymerase α-mediated recruitment of the 9-1-1 complex to stalled replication forks. Cell Cycle *8*, 2877–2884.

Yan, S., and Michael, W.M. (2009b). TopBP1 and DNA polymerase-alpha directly recruit the 9-1-1 complex to stalled DNA replication forks. J. Cell Biol. *184*, 793–804.

Yang, J., Song, H., Walsh, S., Bardes, E.S., and Kornbluth, S. (2001). Combinatorial control of cyclin B1 nuclear trafficking through phosphorylation at multiple sites. J. Biol. Chem. *276*, 3604–3609.

Yarden, R., Metsuyanim, S., Pickholtz, I., Shabbeer, S., Tellio, H., and Papa, M.Z. (2012). BRCA1-dependent Chk1 phosphorylation triggers partial chromatin disassociation of phosphorylated Chk1 and facilitates S-phase cell cycle arrest. Int. J. Biochem. Cell Biol. *44*, 1761–1769.

Yazdi, P.T., Wang, Y., Zhao, S., Patel, N., Lee, E.Y.-H.P., and Qin, J. (2002). SMC1 is a downstream effector in the ATM/NBS1 branch of the human S-phase checkpoint. Genes Dev. *16*, 571–582.

Ye, X., Franco, A.A., Santos, H., Nelson, D.M., Kaufman, P.D., and Adams, P.D. (2003). Defective S Phase Chromatin Assembly Causes DNA Damage, Activation of the S Phase Checkpoint, and S Phase Arrest. Mol. Cell *11*, 341–351.

Yi, R., Qin, Y., Macara, I.G., and Cullen, B.R. (2003). Exportin-5 mediates the nuclear export of pre-microRNAs and short hairpin RNAs. Genes Dev. *17*, 3011–3016.

Yoo, H.Y., Shevchenko, A., Shevchenko, A., and Dunphy, W.G. (2004). Mcm2 is a direct substrate of ATM and ATR during DNA damage and DNA replication checkpoint responses. J. Biol. Chem. *279*, 53353–53364.

You, Z., Chahwan, C., Bailis, J., Hunter, T., and Russell, P. (2005). ATM activation and its recruitment to damaged DNA require binding to the C terminus of Nbs1. Mol. Cell. Biol. *25*, 5363–5379.

Yun, J., Chae, H.-D., Choy, H.E., Chung, J., Yoo, H.-S., Han, M.-H., and Shin, D.Y. (1999). p53 Negatively Regulates cdc2 Transcription via the CCAAT-binding NF-Y Transcription Factor. J. Biol. Chem. *274*, 29677–29682.

Zachos, G., Rainey, M.D., and Gillespie, D. a F. (2003). Chk1-deficient tumour cells are viable but exhibit multiple checkpoint and survival defects. EMBO J. *22*, 713–723.

Zachos, G., Rainey, M.D., and Gillespie, D.A.F. (2005). Chk1-Dependent S-M Checkpoint Delay in Vertebrate Cells Is Linked to Maintenance of Viable Replication Structures. Mol. Cell. Biol. *25*, 563–574.

Zarubin, T., and Han, J. (2005). Activation and signaling of the p38 MAP kinase pathway. Cell Res. *15*, 11–18.

Zegerman, P., and Diffley, J.F.X. (2010). Checkpoint-dependent inhibition of DNA replication initiation by Sld3 and Dbf4 phosphorylation. Nature *467*, 474–478.

Zeman, M.K., and Cimprich, K. a (2014). Causes and consequences of replication stress. Nat. Cell Biol. *16*, 2–9.

Zeng, Y., Forbes, K.C., Wu, Z., Moreno, S., Piwnica-Worms, H., and Enoch, T. (1998). Replication checkpoint requires phosphorylation of the phosphatase Cdc25 by Cds1 or Chk1. Nature *395*, 507–510.

Zhao, H., and Piwnica-Worms, H. (2001). ATR-Mediated Checkpoint Pathways Regulate Phosphorylation and Activation of Human Chk1. Mol. Cell. Biol. *21*, 4129–4139.

Zhao, H., Watkins, J.L., and Piwnica-Worms, H. (2002). Disruption of the checkpoint kinase 1/cell division cycle 25A pathway abrogates ionizing radiation-induced S and G2 checkpoints. Proc. Natl. Acad. Sci. U.S.A. *99*, 14795–14800.

Zhao, J., Kennedy, B.K., Lawrence, B.D., Barbie, D.A., Matera, A.G., Fletcher, J.A., and Harlow, E. (2000). NPAT links cyclin E-Cdk2 to the regulation of replication-dependent histone gene transcription. Genes Dev. *14*, 2283–2297.

Zhou, B.-B.S., and Bartek, J. (2004). Targeting the checkpoint kinases: chemosensitization versus chemoprotection. Nat. Rev. Cancer *4*, 216–225.

Zhou, B.S., and Elledge, S.J. (2000). The DNA damage response: putting checkpoints in perspective. Nature *408*, 433–439.

Zou, L., and Elledge, S.J. (2003). Sensing DNA damage through ATRIP recognition of RPA-ssDNA complexes. Science *300*, 1542–1548.

Zou, L., Liu, D., and Elledge, S.J. (2003). Replication protein A-mediated recruitment and activation of Rad17 complexes. Proc. Natl. Acad. Sci. U.S.A. *100*, 13827–13832.

Zuazua-Villar, P., Rodriguez, R., Gagou, M.E., Eyers, P. a, and Meuth, M. (2014). DNA replication stress in CHK1-depleted tumour cells triggers premature (S-phase) mitosis through inappropriate activation of Aurora kinase B. Cell Death Dis. *5*, e1253.